FORCED-FLOW ONCE-THROUGH BOILERS

NASA RESEARCH

STONE,
GRAY,
AND
GUTIERREZ

NATIONAL AERONAUTICS AND SPACE ADMINISTRATION
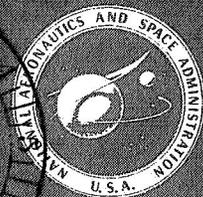
FORCED-FLOW ONCE-THROUGH BOILERS (1961-1971)

NASA RESEARCH

James R. Stone, Vernon H. Gray, and Orlando A. Gutierrez
Lewis Research Center

Prepared at Lewis Research Center

Dedicated to

Vernon H. Gray

1917 - 1975

Foreword

This special publication is a compilation and review of the NASA-sponsored research on forced-flow, once-through boilers for use in spacecraft electrical power generation systems. Emphasis is on the heat-transfer and fluid-flow problems. In addition to space applications, much of the boiler technology presented herein is applicable to such terrestrial and marine uses as vehicular power, electrical power generation, vapor generation, and heating and cooling.

The studies presented herein were performed primarily in the period between 1961 and 1971 The research was done mainly at the Lewis Research Center and has been previously reported in piecemeal fashion. Some of the work was done under contract, and a small but significant amount of the data are presented herein for the first time. A large amount of related work is referenced and commented upon but not discussed in detail. Examples of such related research areas are condensation, cavitation, line and boiler dynamics, the SNAP-8 project (mercury-Rankine cycle), and conventional terrestrial boilers (either supercritical or gravity-assisted liquid-vapor separation types).

The emphasis of this research effort has been to develop the technology for once-through compact boilers with high heat fluxes to generate dry vapor stably, without utilizing gravity for phase separations. Many different approaches to the problem were pursued, primarily experimentally, and several potential solutions were obtained In some areas, tests, analyses, and integration of the results were not completed because of a shift in priorities toward other work.

Following the introduction to this boiler study and a background section that discusses, tutorially, the complex aspects of the boiling process, the text is divided into two parts. Part I presents the numerous boiler configurations that were tested in attempts to obtain good and stable performance. Part II goes into various boiling characteristics, such as stability, initiation of two-phase flow, pressure drop, and heat transfer. Correlations of data for use by designers are also presented whenever they are available. Throughout the text, discussions of tests on alkali metals are interspersed with those on water and other fluids on a phenomenological basis rather than on the basis of temperature level or, even, application. This approach should give a better perspective on the problems that are common to most boilers.

Contents

INTRODUCTION AND BACKGROUND

INTRODUCTION

Forced-flow boiling phenomena must be understood in order for rational designs of Rankine-cycle energy conversion systems to be made. This is especially but not exclusively true for applications in space, where compactness is important. In addition, forced-flow boiling, because of its high heat-transfer coefficients, is also applicable to cooling problems where high heat fluxes are required, such as in cooling nozzles and other surfaces subjected to high-temperature environments.

Future space vehicles may require the capacity to generate relatively large amounts of electric power For large power levels the Rankine-cycle system appears attractive. In this system, power is generated by turboalternators driven by vapor generated in a boiler The vapor is then condensed and the waste heat of condensation is rejected in a radiator. In order to minimize the size and weight of the radiator and to achieve high efficiency in space, boiling temperatures of the order of 1450 K are required. The alkali metals (sodium, potassium, etc.) have been advanced as working and heat-transfer fluids in order to meet the high-temperature (and moderate pressure) requirements. In turn, the need for suitable containment materials for the alkali metals has led to selection of refractory-metal alloys (niobium, tantalum, etc.) for system components. In addition to the high-temperature requirements, the power system must operate unattended for periods in excess of 10 000 hours in a stable and reliable manner under zero-gravity conditions.

For design of a space power system boiler, new information was required in regard to two-phase heat transfer and pressure drop, definitions of various boiling regimes, predictions of critical heat-transfer conditions such as the "boiling crisis" and critical flows, and requirements for thermal and hydraulic stability The available analytical predictions of two-phase heat-transfer and hydraulic performance had limited or uncertain applicability and in most cases required accurate experimental data for their use.

For use in spacecraft Rankine-cycle power systems, the once-through boiler concept was most attractive and was selected for study In this technique, a subcooled liquid is converted into a superheated vapor in one continuous pass through the boiler. This publication summarizes the research on such boilers conducted at the Lewis Research Center and also some closely related work on pressure drop and heat transfer. The major emphasis is on alkali metal heat-exchanger boilers, since space power system boilers will most likely be of this type. NASA has also put considerable effort into the development of mercury boilers for the SNAP-8 program. But little comparison of these data to those for alkali metals and water is made herein because of significant differences in physical properties, especially liquid density and surface tension. Many of the experiments to be described were performed with water, since boiling experiments with liquid metals are difficult and expensive to perform. However, with the exception of liquid thermal conductivity, low-pressure water has boiling properties similar to those of alkali

1

metals; and water itself may be of interest for many terrestrial applications. In addition, experiments made with other fluids, such as the Freons, and numerous analytical studies have contributed to the understanding of forced-flow boiling phenomena and are included. An attempt is made to point out the important results and the problems that remain unsolved. Selected correlations and analyses are given, and a bibliography covering much of the pertinent research in the areas mentioned is included. It is subdivided into various subject categories and includes many publications not cited in the text.

BACKGROUND

During the boiling of a fluid flowing through a channel, several heat-transfer regimes are encountered. A typical case is illustrated in figure 1. The liquid to be vaporized enters the channel and is heated in the liquid phase to the point where bubble nucleation first occurs. Nucleate boiling continues until enough vapor is generated that the resulting increase in velocity is sufficient to suppress nucleation. Beyond this point, heat is added to a thin liquid film and vaporization occurs at the liquid-vapor interface. Throughout these boiling regimes, liquid is being entrained in the vapor core. In spite of any redeposition of liquid from the core to the film, at some point there is no longer sufficient liquid to wet the wall, and the liquid film breaks down, with a large

reduction in heat-transfer coefficient, often more than an order of magnitude. This transition has been variously termed "boiling crisis," "departure from nucleate boiling," "onset of dry-wall boiling," and "burnout," as well as other names. This film breakdown is generally followed by a transitional regime wherein a considerable amount of liquid remains on the wall. Eventually, only a few droplets remain on the wall, and most of the heat added through the wall goes into heating the vapor. It then becomes difficult to vaporize the remaining liquid droplets.

In order to design a forced-flow boiler, it is necessary to be able to predict the heat-transfer and pressure-drop characteristics in each of these regimes. This problem is complicated by the wide variety of possible two-phase flow regimes and by various thermodynamic nonequilibria, such as subcooled boiling in many fluids, liquid bulk superheat in alkali metals, and liquid droplets in superheated vapor. It is also very important that the boiler not interact with other components of the flow system to produce instabilities. The following sections describe these problem areas in more detail.

Stability

The problem of boiler instabilities is quite serious in systems using forced-flow, once-through boilers. Such instabilities lead to poor performance of the system and can even cause failure. Lowdermilk, Lanzo, and Siegel (ref. 1) found that flow oscillations could
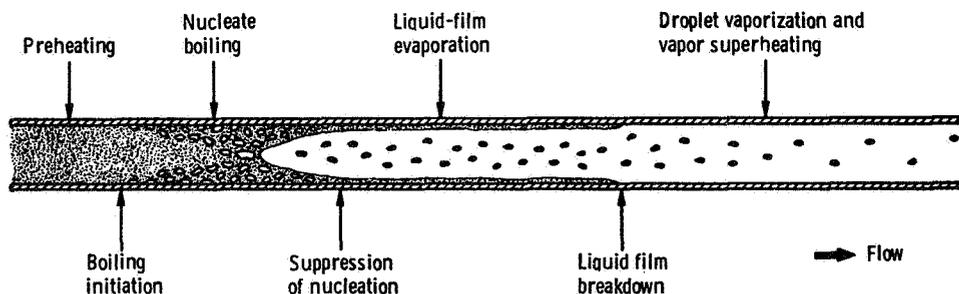

Figure 1. Typical heat-transfer regimes for boiling in flow channel.

cause a large decrease in the heat flux at the boiling crisis. The instability could be prevented by restricting the flow upstream of the test section, thereby decoupling or isolating the boiler from the upstream liquid leg, which can also contain vapor or gas voids. In this regard, they found that a compressible volume upstream of the test section had a destabilizing effect. Similar results were reported by Aladyev, Miropolsky, Doroschchuk, and Styrikovich (ref. 2). Jeglic (ref. 3) noted three types of instability that may occur in two-phase flow: interfacial, flow excursion, and oscillation. One important class of oscillation instability is that due to dynamic coupling of the boiler feed system and the subcooled boiling region. Jeglic and Grace (ref. 4) observed flow oscillations in subcooled boiling; these oscillations were strongly dependent on the thermodynamic conditions existing in the boiler. It has also been reported that restricting the boiler exit has a destabilizing effect. Thus, the boiler feed system, inlet, and exit geometries are all quite important.

The first type of instability to receive much attention with regard to forced-flow boilers was the flow excursion instability, sometimes called the "Ledinegg instability." This problem generally results from improper matching of pump and boiler hydraulic characteristics, as was first reported by Ledinegg (ref. 5). As discussed in reference 3, this instability results in a rapid change of flow rate with time and in a tendency toward finding a stable value corresponding to the pressure drop imposed on the system. This type of instability may be explained with the aid of a typical curve of pressure drop ΔP against boiling fluid flow rate W_b, as shown in figure 2 (from ref. 3). (Symbols are defined in appendix A.) If the operating point is in the negative-slope portion of the boiler pressure-drop curve when the slope of the supply system curve is less steep than the slope of the boiler curve, the system is
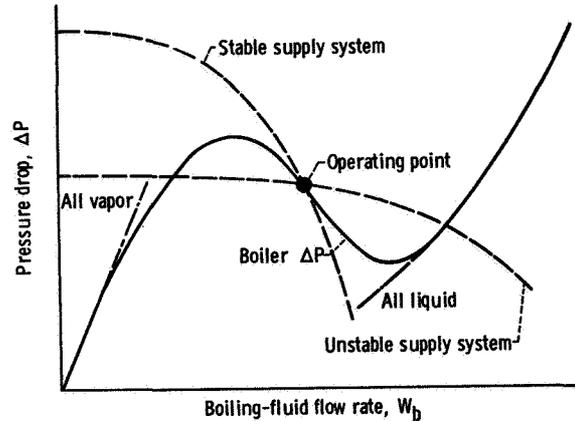

Figure 2. Pressure drop as function of flow rate for typical boiler and supply systems (ref. 3).

unstable. The operating point may jump to one of the other two points of intersection. This type of instability may be avoided by increasing the slope of the supply system curve, that is, by increasing the system pressure drop to steepen the pump characteristic (refs. 3 and 6 to 8).

As research and development of Rankine-cycle power systems continued, other modes of instability were recognized, such as boiler—feed system coupling, excursions caused by the flashing of superheated alkali metals, and interactions of boiler and condenser. Boiler—feed system coupling instabilities occur when the dynamic or time-varying flow resistances of the boiler and its feed system produce, instantaneously, a situation similar to the Ledinegg instability described in the preceding paragraph. However, since this instability is caused by the dynamic flow resistances (generally termed impedances by analogy to electric circuits), it produces oscillations rather than excursions (refs. 9 to 14). The solution to the problem is generally to restrict the flow at the boiler inlet.

The instabilities due to both actions in the condenser and breakdown of liquid superheat are related to the sudden formation or collapse of vapor. The rapid collapse of a vapor void can cause reverse flow downstream

3

of the void and simultaneously increase the flow rate upstream. This obviously can cause instabilities throughout the flow loop. With sudden void formation, as in superheat breakdown, the reverse (or at least reduced) flow occurs upstream of the void and increased flow occurs downstream, but the destabilizing effects are similar

Initiation of Vaporization

In order to initiate vaporization in a liquid, either the pressure must be lowered below saturation pressure or the temperature raised above saturation temperature. Vaporization generally cannot be initiated exactly at saturation conditions because of surface tension effects and the unavailability of nucleating sites. For a spherical vapor bubble of radius r at saturation pressure P_s to grow, the pressure P_l of the surrounding liquid must be less than

$$P_l = P_s - \frac{2\sigma}{r} \qquad (1)$$

where σ is the surface tension. This equation is derived from a force balance on a static, spherical bubble. The nonequilibrium condition required to initiate vaporization can be obtained by different processes, therefore, there are several different ways in which the amount of nonequilibrium can be defined. Such terms as "liquid tension" (ref. 15), "bulk superheat," and "wall superheat" are used.

In boiling initiation studies the superheat terminology is generally used. For nonmetallic liquids the term "wall superheat" is commonly used, since boiling can usually be caused by bringing the liquid in contact with a sufficiently hot surface, even when the bulk temperature of the liquid is less than saturation. Surface boiling with the liquid bulk temperature less than saturation is termed subcooled boiling. Some of the more important studies on the initiation of boiling

in nonmetallic fluids are references 16 to 18, and more are listed in the bibliography under "INITIATION OF VAPORIZATION." The important parameters in determining the wall superheat are heat flux, mass velocity, liquid bulk subcooling, fluid physical properties, and surface condition.

In order to boil the metallic fluids, it is often necessary to raise the liquid bulk temperature considerably above saturation (e.g., refs. 19 and 20); thus, the term bulk superheat $T_l - T_s$ is used. The effects of physical properties and surface condition have been studied in references 19 to 25, Chen (ref. 23) and Holtz (ref. 22) have pointed out the importance of the pressure-temperature history of the fluid and surface. The effects of mass velocity and heat flux or wall temperature have not been resolved at present.

When vaporization is achieved by lowering the pressure of the liquid below saturation, the term "liquid tension" is generally used to describe the nonequilibrium condition before vaporization occurs. The liquid tension is given by $P_s - P_l$. Such terminology has commonly been used in cavitation studies (e.g., refs. 26 to 31). The existence of liquids at pressures below zero absolute has long been known (ref. 15). This phenomenon has been attributed to the considerable magnitude of the intermolecular cohesive forces (ref. 32). Many experimental measurements of these negative absolute pressures appear in the literature, such as references 33 and 34 for water and reference 35 for organic liquids.

Void Fraction

In describing the characteristics of two-phase flows, the relative flow rates and velocities of the two phases must be known. The relation between the flow rate and velocity of each phase is, in turn, related to that fraction of the flow-passage area
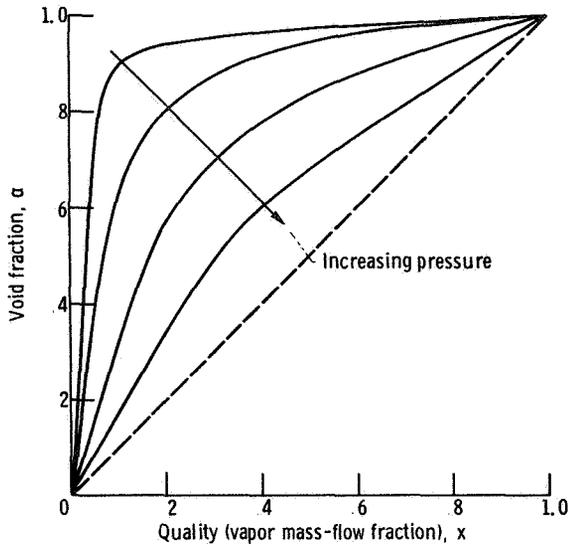
4

Figure 3.   Typical variation of void fraction with quality for various pressure levels.

occupied by each phase. The fraction of the area occupied by the vapor is termed the void fraction α; the liquid fraction is then $1 - \alpha$. The continuity equation relates the void fraction to the densities and velocities of the phases and the quality (vapor mass-flow fraction) x as follows

$$\alpha = \frac{x\left(\dfrac{u_l}{u_g}\right)\left(\dfrac{\rho_l}{\rho_g}\right)}{1 + x\left[\left(\dfrac{u_l}{u_g}\right)\left(\dfrac{\rho_l}{\rho_g}\right) - 1\right]} \qquad (2)$$

Typical variations of void fraction with quality for various pressures are shown in figure 3 in a manner similar to that of reference 36. Considering the effect of pressure, it can be seen that as pressure increases, α approaches x At lower pressures and especially at low qualities, the slip ratio u_g/u_l is a most important parameter but is not generally known. Nonequilibrium is also important, since the quality does not necessarily correspond to that calculated from a heat balance. Thus, because of the analytical complications, there are many empirical

correlations (refs. 37 and 38) and semitheoretical predictions (refs. 39 to 42) of the void fraction.

Flow Patterns

A multitude of flow patterns is conceivable for two phases flowing concurrently, as is the case in a boiler tube. This makes it difficult to develop reliable correlations of two-phase pressure drop, heat-transfer coefficient, and boiling crisis. Some of the flow patterns typically encountered are shown in figure 4. These are only a few, other flow patterns are plug, wave, dispersed, fog, spray-annular, froth, and rivulet. Most flow pattern studies have been with adiabatic, two-component systems (e.g., refs. 43 to 49), although some data exist for diabatic conditions such as those of references
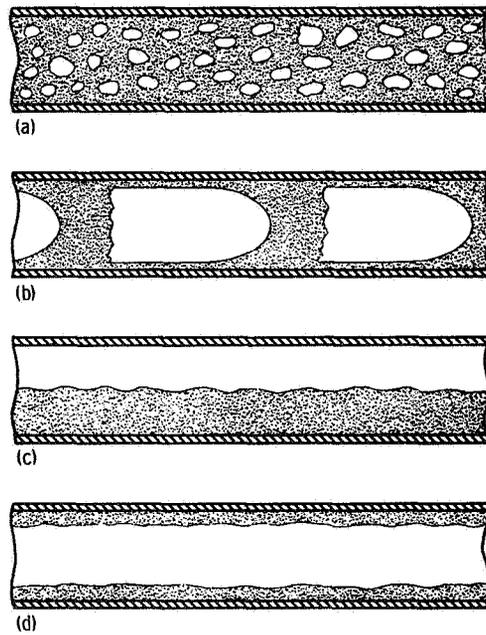
(a) Bubbly flow.

(b) Slug flow.

(c) Stratified flow.

(d) Annular flow.

Figure 4.   Typical two-phase flow patterns.
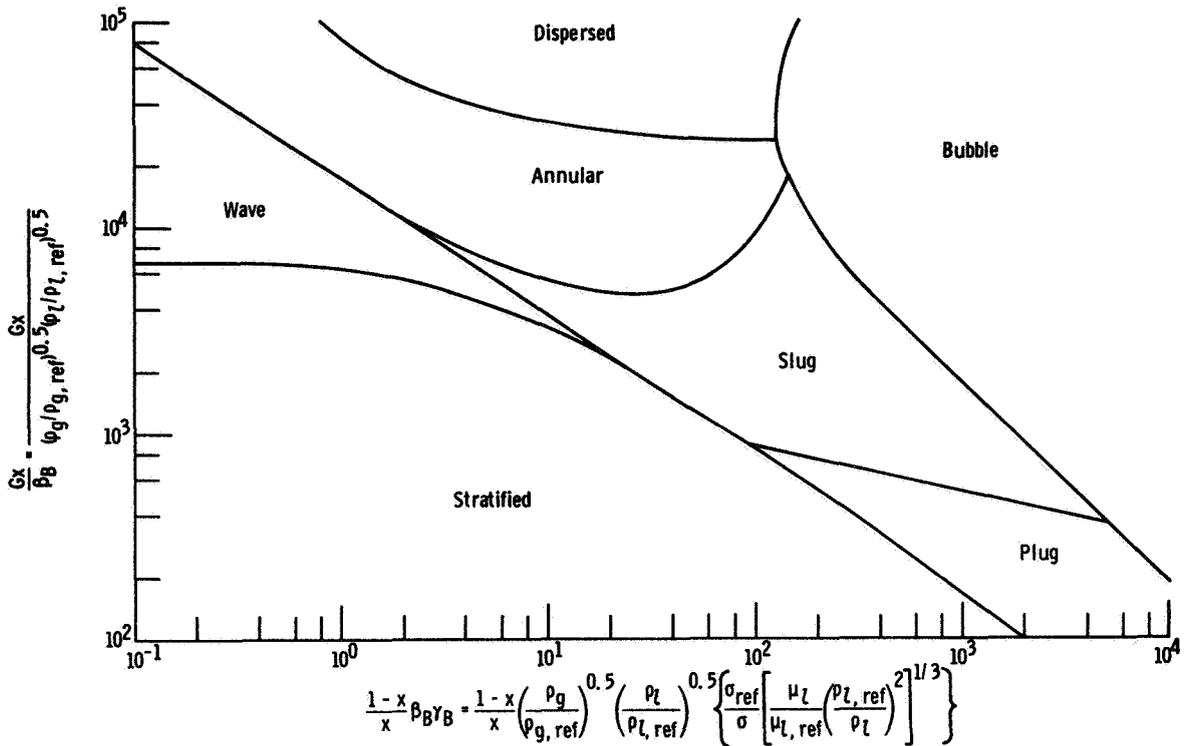
5

Figure 5. - Flow pattern map of Baker (ref. 43); horizontal flow.

Pressure Drop

Knowledge of boiling pressure drop is important in the design of power systems and cooling applications. The pressure drop must be known to determine local saturation temperatures and pumping power requirements. The boiling pressure drop is also an important parameter in the dynamics of the system.

Correlations of boiling pressure drop are numerous. A number of these correlations are based on the early work of Lockhart and Martinelli (ref 58), for example, those of references 36 and 59. Levy (ref 60) has proposed a momentum exchange model, in which he postulates that as void fraction, quality, and densities of the two-phase flow

vary, momentum exchange equalizes the sum of frictional and gravitational head losses for the two phases. Thom (ref. 61) has developed a semiempirical correlation in which momentum, energy, and mass balances are solved, assuming that the slip ratio u_g/u_l is a function of the density ratio ρ_l/ρ_g only, the two-phase friction factor was correlated as a function of quality only

Helical-flow-promoting inserts are often used in forced-flow boilers to improve separation of the phases, to increase heat-transfer coefficients (thereby reducing the required heat-transfer area), and to produce a more stable and reliable system. However, these benefits are accompanied by a larger pressure drop across the boiler than with no inserts. Thus, in order to achieve an optimum design, it is necessary to know the pressure-drop penalties imposed by the helical flow inserts, as well as the performance improvements obtained by their use.

50 to 57. These results are generally presented in terms of flow pattern maps similar to that of Baker (ref 43), which is shown in figure 5.

6

Heat Transfer

Although there have been numerous studies of boiling heat transfer, there is still no generally applicable means of prediction available, particularly for high-density-ratio fluids such as alkali metals and low-pressure water. This is especially true of the subcooled boiling regime, where nonequilibrium effects are important, although the subcooled boiling heat-transfer correlations of references 62 to 65 give reasonable design approximations in many cases. Some correlations proposed for net-quality boiling heat-transfer are given in references 57 and 66 to 73.

Typical variations of the boiling heat-transfer coefficient and quality with axial distance through a boiling heat exchanger are shown in figure 6, the heat-transfer coefficient is normalized to the all-liquid value. Boiling heat-transfer coefficients are much higher than liquid values prior to the boiling crisis and then decrease rapidly with distance, eventually reaching a value of the order of a gas heat-transfer coefficient. For purposes of

discussion, three heat-transfer regimes are defined: the subcooled regime, from the inception of boiling to zero heat-balance quality; net-quality boiling prior to the crisis; and the postcrisis regime. This is, of course, a great oversimplification, and more detail is given where appropriate.

Boiling Crisis: Liquid Film Breakdown

When there is no longer sufficient liquid on the heated wall to maintain a continuous liquid film, the liquid film breaks down and a drastic reduction in the heat-transfer coefficient occurs. This transition has variously been called "the onset of dry-wall boiling," "departure from nucleate boiling," "boiling crisis," or "burnout." The term "boiling crisis" is used in this report for simplicity.

The boiling heat-transfer transition herein called the boiling crisis must be known for both power systems and cooling applications. In heat-exchanger boilers the transition may be accompanied by more than an order-of-magnitude change in heat-transfer coefficient. In cooling applications, physical failure (burnout) of the containment material may occur because excessive wall temperatures are reached. Although the boiling crisis has been the subject of numerous experiments, analyses, and correlations, there remains much uncertainty in predicting the boiling crisis for any particular system. Much of this uncertainty can be attributed to flow system characteristics and instabilities.

Drying of Vapor

In conventional stationary powerplants, generally no attempt is made to vaporize all the incoming liquid, instead the vapor and liquid are separated, and the remaining liquid is recirculated. However, compact systems, such as those for space use, are usually
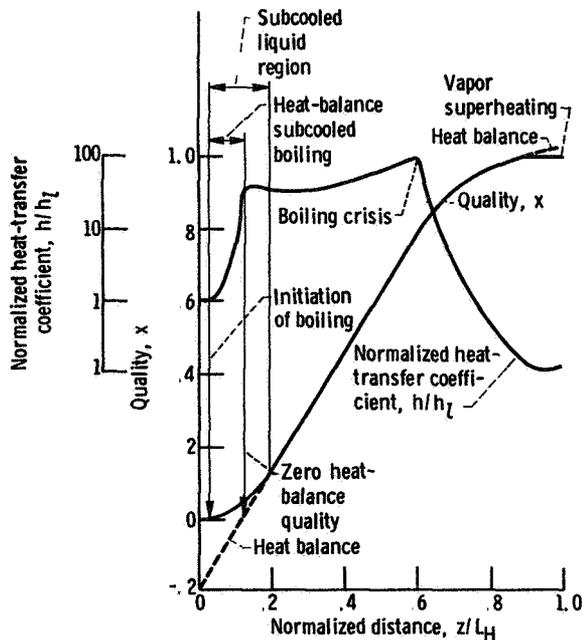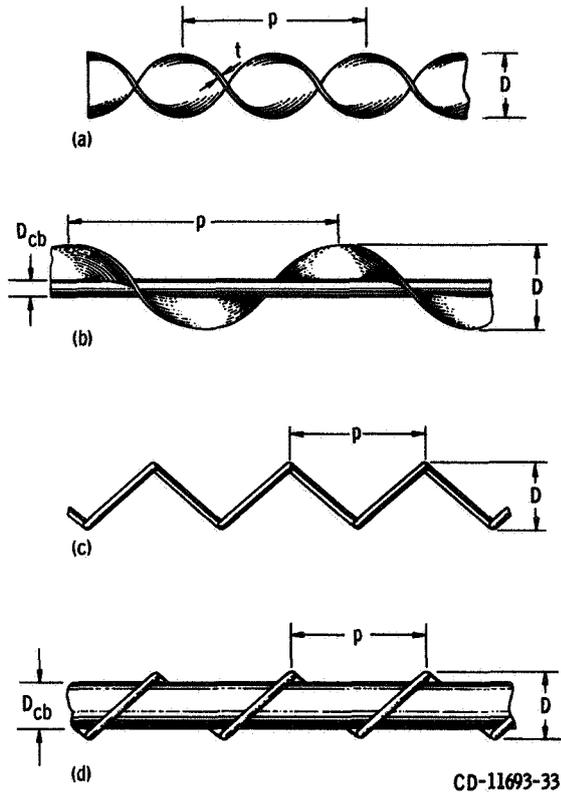

Figure 6. - Typical boiling heat-transfer performance.

7

(a) Twisted-tape insert.

(b) Helical vane insert.

(c) Helical wire insert.

(d) Helical wire insert with plug.
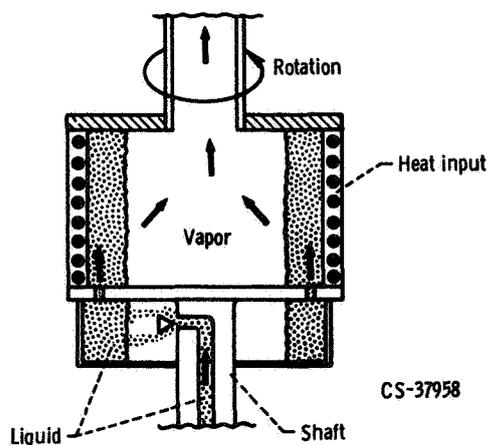
Figure 7. - Types of boiler tube inserts.

Figure 8. - Rotating boiler concept.

designed to vaporize all the incoming liquid. This is the "once-through boiler" concept. In order to dry the vapor, the two-phase mixture is often swirled within the boiler, thus centrifuging the liquid to the heated wall, where it can be vaporized.

This swirl has generally been obtained by means of inserts such as those shown in figure 7, by coiling the tube, or by a combination of inserts and tube coiling. These approaches have resulted in varying degrees of improvement, as for example in the mercury boiler development programs (refs. 74 to 77). Generally, these swirl techniques improve overall performance. But, they increase pressure drop and tend to promote rivulet flow with its associated problems, such as vapor superheat with liquid still present (refs. 74 to 78). Part of the problem may be due to the shear of high-velocity vapor on the liquid, causing the liquid film to be torn apart.

A more novel approach to producing dry vapor is to rotate the boiler, as shown schematically in figure 8. Experiments on such a boiler are reported in references 79 and 80. A rotating boiler has many obvious advantages. It is insensitive to gravity field and orientation. The liquid-vapor interface is rather sharp and stable, yielding a steady flow of both vapor and liquid. Because of the centrifugal action on droplets in the vapor space the exit vapor should have low moisture content (high quality). Heat fluxes considerably higher than for pool boiling at normal earth gravity should be attainable. The use of a rotating boiler, however, requires moving parts and rotating seals. The cyclone boiler concept (fig. 9) represents an attempt to combine the benefits of the rotating boiler with the simplicity of having no moving parts. The liquid or two-phase feed mixture flows into the boiler tangentially and vaporizes because of the pressure drop in such a manner that a vortex flow pattern is established. The liquid is centrifuged to the wall and is then driven toward the apex of the cone by
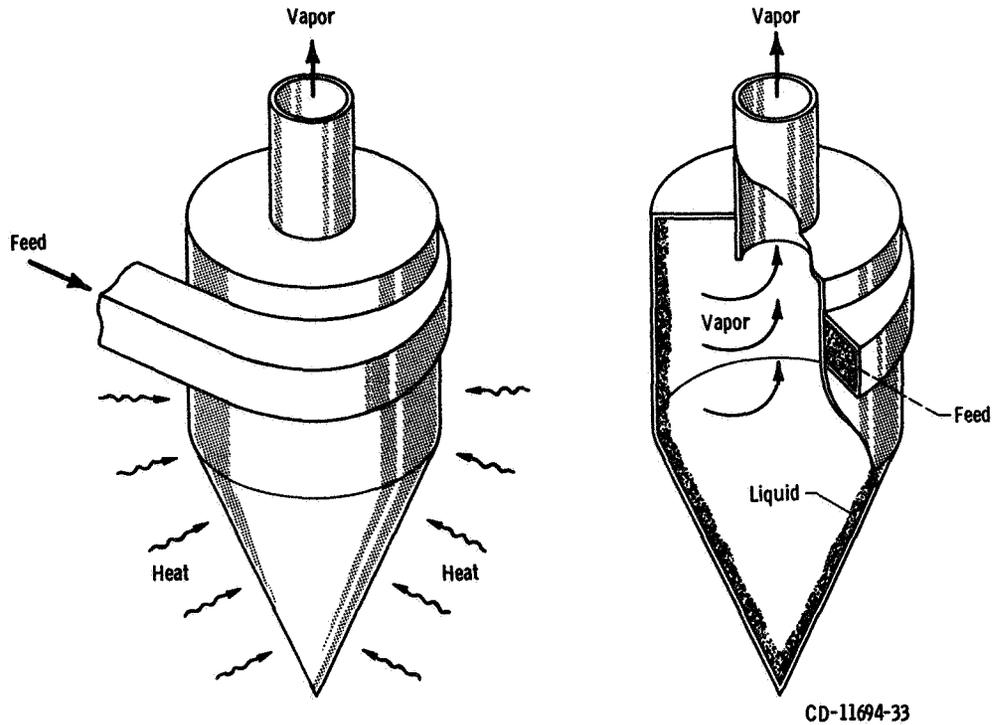
8

Figure 9. - Cyclone boiler concept.

secondary flow effects (ref. 81) augmented by surface tension and, for some cases, gravity, while the vapor exits from the top.

Still another method of drying is the crossflow heat exchanger, wherein the two-phase flow passes through a bank of heated tubes on which the liquid impinges and is vaporized (ref. 82).

9

Part I

BOILER CONFIGURATIONS

One of the major problem areas in the technology of Rankine-cycle power systems has been the design of high-performance, dependable, compact boilers. The boilers must operate stably with a minimum of entrained liquid in the exit vapor stream. Numerous boiler configurations have been tested in attempts to obtain the desired performance. A summary and review of these configurations is presented in part I. Part II presents data and correlations for the various boiling characteristics of interest, that is, stability, initiation of two-phase flow, pressure drop, and heat transfer

PLAIN, STRAIGHT TUBES WITH NO INSERTS

The simplest forced-flow, once-through boiler design is the plain, straight tube with no inserts. Table I summarizes the experiments on this type of geometry for heat-exchanger boilers. There have also been numerous direct-heated experiments (see the bibliography), but these have generally been limited to the low-quality and subcooled boiling ranges.

SODIUM BOILING

Because alkali metal working fluids are desirable for space power systems from a thermodynamic viewpoint, experiments were conducted at the Lewis Research Center on sodium boiling in a refractory-metal, heat-exchanger boiler (ref. 83).

TABLE I - SUMMARY OF EXPERIMENTS ON PLAIN-TUBE HEAT-EXCHANGER BOILERS

Boiling fluid	Heating fluid	Boiler tube[a]				Ranges of test variables					Reference
		Heated length, L_H		Inside diameter, D		Boiler-exit saturation temperature, $T_{be,s}$		Boiling-fluid flow rate, W_b		Exit quality, x_e	
		cm	in.	cm	in.	K	°F	g/sec	lbm/hr		
Sodium	Sodium	124	49	1 27	0 50	1211 - 1355	1720 - 1980	9.5 - 48	75 - 380	0.08 - 0.93	[b]83
Water	Water	113	44.5	1 09	430	~377	~219	5.7 - 65	45 - 518	0 - 1.0	85
		154	60.5	1.11	436	337 - 388	147 - 238	6.2 - 109	49 - 864	0.002 - 1 0+	
Freon-113	Water	91.5	36	80	315	321 - 333	117 - 139	22.1 - 82.6	175 - 656	0.12 - 0.63	10
Potassium	Sodium	232	91.5	1.70	67	1089 - 1229	1500 - 1750	17.7 - 366	140 - 2900	0.06 - 0.93	94
Water	Steam (condensing)	609	240		1.00	355 - 404	180 - 267	30.2 - 693	240 - 5500	0 - 1 0	66

[a]Vertical upflow, single tube, unless otherwise noted.

[b]2.08-mm (0.082-in.) orifice upstream of inlet; not considered an inlet device.

Test Facility

Figure 10 is a simplified diagram of the two main flow loops of the sodium-boiling heat-transfer facility, described in more detail in reference 83 Both main loops contained sodium and were joined thermally by the single-tube-in-shell heat-exchanger boiler All components designed to operate at temperatures above 1090 K were fabricated of niobium—1-percent-zirconium alloy and were contained in a high-vacuum vessel Complete details of this vessel and its pumping and monitoring systems were reported by Groesbeck (ref 84). The lower temperature components of the system were constructed of 316 stainless steel The heat was generated by electric resistance heaters, and the heat rejection was by sodium-to-air heat exchangers.

Two-phase loop. - The alternating-current (ac) conduction pump (pump 1 in fig. 10) pumped the test fluid through a throttle valve and an electromagnetic flowmeter to the preheater Power was supplied by a 125-kilowatt saturable-core reactor Heat was generated in both the preheater tubing wall and the flowing sodium. In preliminary tests the sodium flowed directly from the preheater to the boiler inlet. Extreme flow and pressure instabilities often occurred, including reverse flow, when the preheater often filled with vapor So, prior to the final tests, pressure-drop devices were installed between the preheater and boiler These were a 0.208-cm-diameter orifice (fig. 11) and a reversible helical-induction electromagnetic pump (pump 3 in fig. 10). When operated in the reverse mode, this pump opposed pump 1 and provided a pressure drop analogous to the
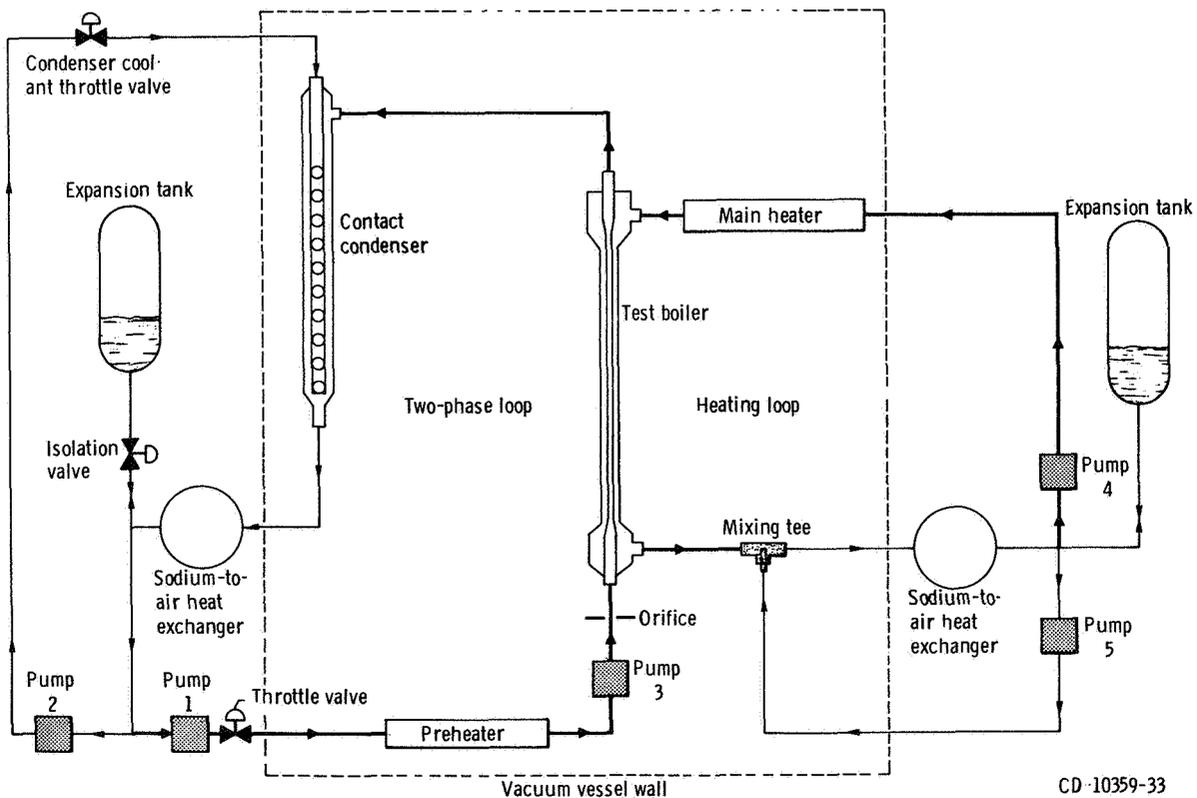

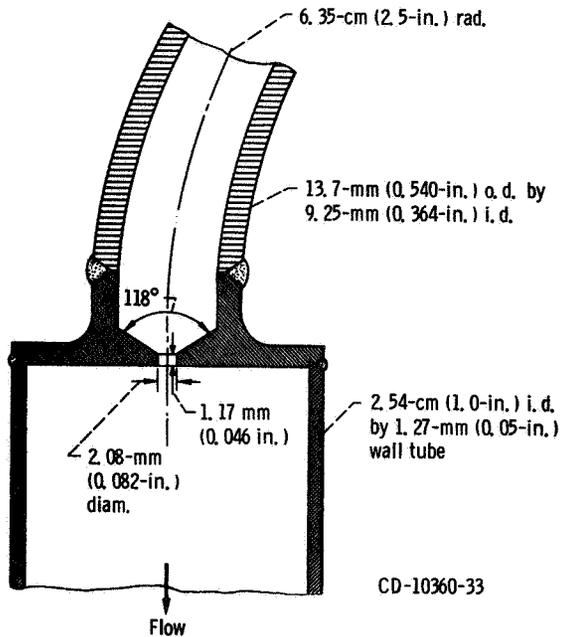Figure 10. Simplified schematic of sodium-boiling test facility.

dynamic braking of an induction motor. On leaving the boiler the test fluid entered the shell side of the contact condenser, where it was condensed and cooled by mixing with bypass coolant flow The condenser consisted of a vertical shell containing a coolant distributor tube. The flow then passed to the air-cooled finned heat exchanger.

Heating-fluid loop. – The heating loop was very similar to the two-phase loop. The main heater was similar to the preheater but was larger (600 kW). In place of a condenser the heating loop used a mixing tee to cool the heating fluid for recirculation to the lower temperature stainless-steel piping.

Test section. – A single-tube-in-shell heat exchanger with no inserts, described in the preceding section and in more detail in references 83 and 84, was tested in the sodium-boiling heat-transfer facility (fig. 10). The experimental boiler is shown in figure 12. The boiling fluid flowed vertically upward, and the heating fluid flowed downward. The test section is described and the ranges of test variables given in table I.
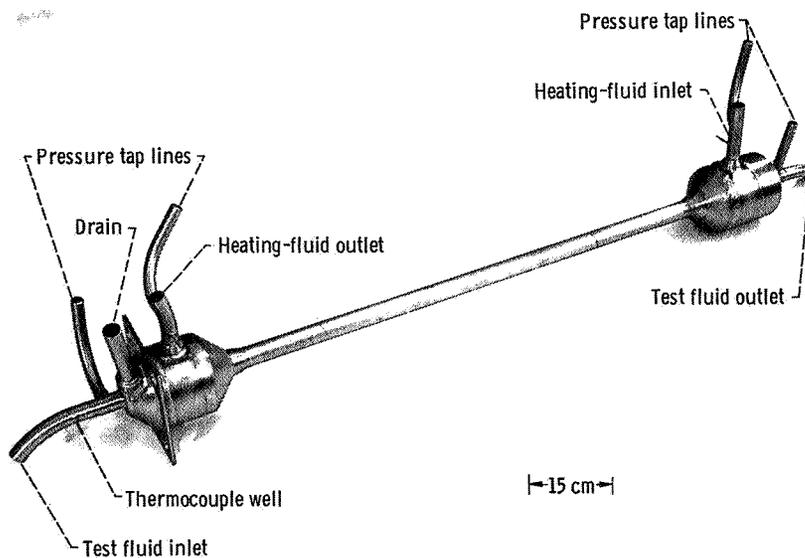
Figure 11 Orifice upstream of test boiler
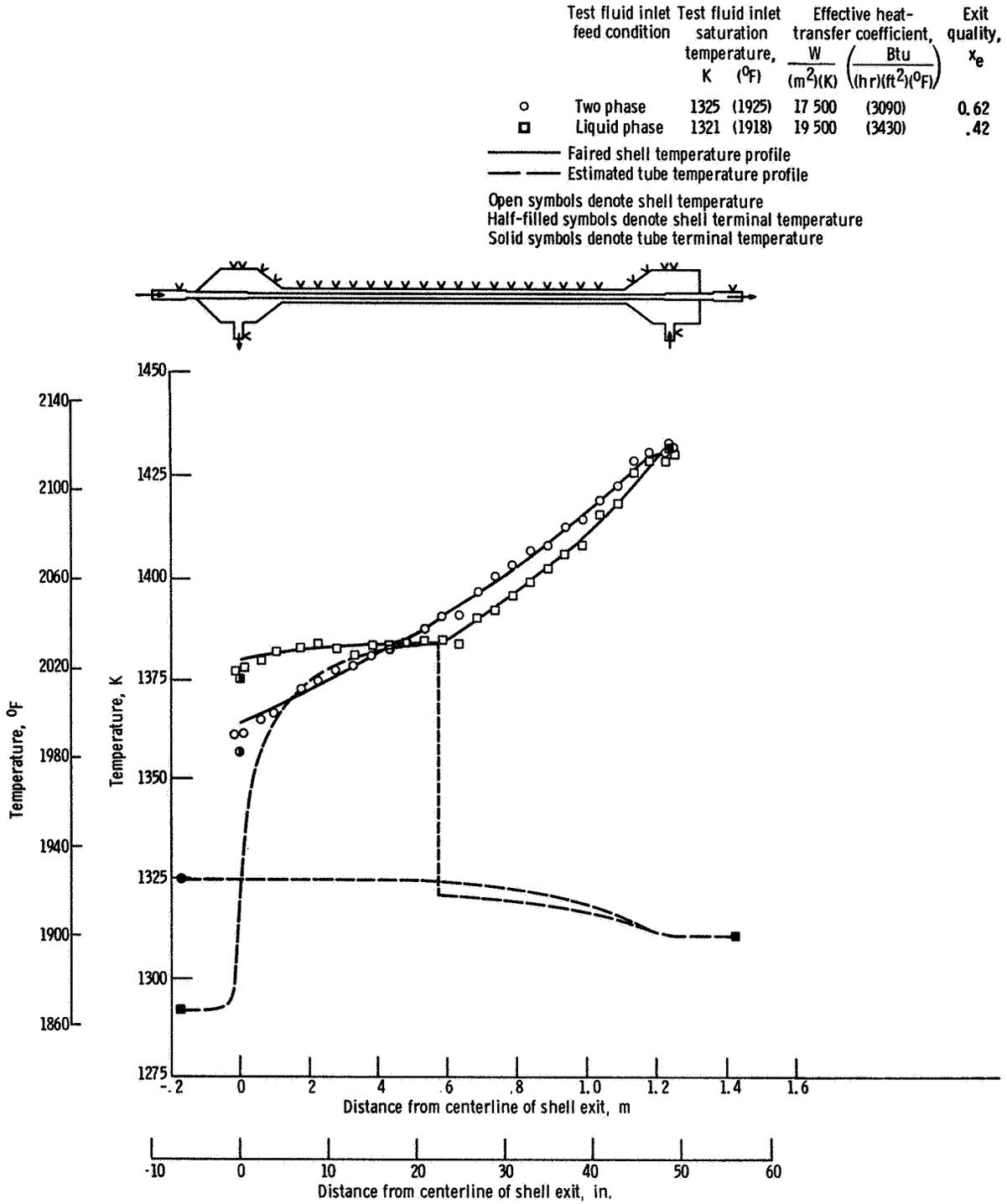

Figure 12. Sodium boiler

Figure 13. - Comparison of sodium boiler temperature profiles for two-phase and liquid-phase boiling-fluid inlet conditions. Nominal boiling-fluid flow rate, 27 g/sec (215 lbm/hr); nominal heating-fluid flow rate, 630 g/sec (5000 lbm/hr).

General Results

Average overall heat-transfer coefficients, two-phase pressure drops, and boiling crisis conditions were obtained. Both steady and unsteady boiling performances were evaluated. The boiler heat-transfer performance depended greatly on the boiler-inlet flow condition, whether liquid or two phase. Critical (boiling crisis) qualities in excess of 0.90 were sometimes obtained under steady conditions. But also, liquid bulk superheat temperatures as high as 140 K were obtained in the test section before the initiation of boiling.

The initiation of boiling was one of the major problems encountered because the alkali metals have the ability to remain in the liquid state at bulk temperatures well above saturation. However, with two-phase flow at the boiler inlet the problem of liquid superheat within the boiler was eliminated.

The effect on boiler performance of flashing at the upstream orifice was quite complicated since a liquid boiler-inlet condition gave both the most steady and the most unsteady results of the entire investigation. Figure 13 illustrates the differences between two-phase and liquid inlet conditions. Shell and boiling-fluid temperatures are plotted against axial distance. Both sets of conditions were essentially the same except that, in one case, the sodium entering the boiler tube was in a two-phase state (flashing at the orifice) and, in the other case, the inlet feed was a subcooled liquid. For the two-phase feed the shell temperature increased along the boiler, following a generally smooth curve, which indicates a continuous increase in vapor quality and the same general regime of heat transfer. (The boiling-fluid temperature was estimated from considerations of two-phase pressure drop, as no local fluid measurements were made.)

In contrast, the shell temperatures for the liquid inlet case showed a slight initial increase and then were almost uniform to about halfway along the boiler. At this point there was a sudden transition and the shell temperatures increased rapidly and followed a curve very similar to that for the two-phase inlet condition. The isothermal zone represented a region of liquid sodium superheated by about 60 K. Sudden flashing from this superheat would yield a heat-balance vapor quality of about 0.02. Beyond this point, the overall heat-transfer coefficient was even greater than that for the two-phase inlet case. The reduced exit quality, in this case for the liquid inlet condition, reflected the sizable length of the boiler over which little or no heat transfer took place. Obviously, these flow regimes were not optimum, and they could not be conveniently studied or visualized in such a complex, high-temperature facility.

WATER BOILING

Because experiments on the boiling of alkali metals are difficult and expensive to perform, and since water may be of interest in some cases and has many boiling properties similar to those of the alkali metals, a series of experiments on water-boiling heat exchangers were conducted at the Lewis Research Center. Most of the results are presented in references 85 to 87

Test Facility

In order to understand the effects of inserts and inlet restrictors on boiler performance, it is necessary to know how a boiler performs without such devices. For this reason and generally to support the alkali
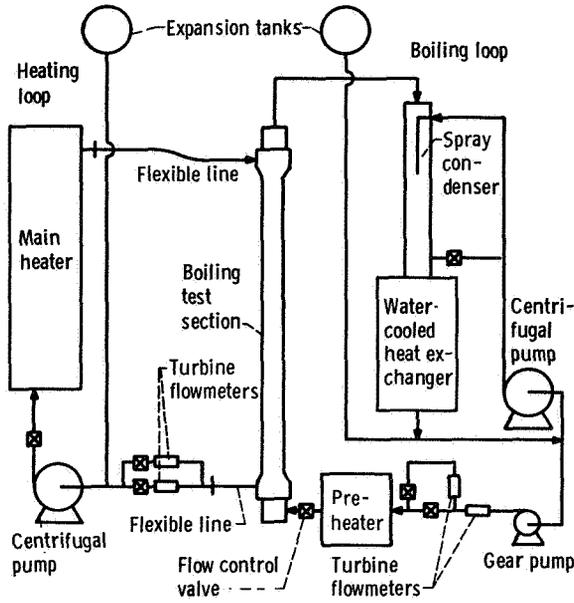
Figure 14.   Schematic of water-boiling facility.

metal boiling research, the experimental studies of reference 85 on pressure drop and heat transfer for water boiling in vertical-upflow single-tube boilers were undertaken on the test facility shown in figure 14. This facility with some modifications, including the use of electrically heated test sections, was also used for the experiments of references 4, 9, and 86 to 92.

Two-phase loop. – The boiling-fluid flow was supplied by a gear pump at pressures to about 1000 kN/m² absolute and was measured by a turbine flowmeter. The flow then passed through a coiled stainless-steel electric preheater having a maximum power of 70 kilowatts and then through a control valve into the test section. From the test section exit the fluid was piped to a spray condenser The condenser coolant (recirculated water) was supplied by a centrifugal pump. From the condenser the fluid passed to a multiple-tube heat exchanger cooled by cooling-tower water In most cases the condensate recirculating pump was shut

off, and the condensing was done in the heat exchanger.

Heating-fluid loop. – The heating-fluid loop was designed for operation at pressures to 1400 kN/m² absolute and temperatures to 450 K. The heating water was pumped into a tank equipped with immersion heaters of 220-kilowatt maximum output. The flow of heating water through the test section could be changed from the usual direction counter to the boiling-fluid current to a parallel flow direction by reversing the two connecting flexible lines. The heating-fluid flow rate was measured by a turbine flowmeter.

Test sections. – A heat-exchanger test section is shown schematically in figure 15. There were two such test sections, both consisting of two concentric stainless-steel tubes. The test section dimensions are given in table I and figure 15. Thermocouples were inserted in both inlet and exit plenum chambers and in the heating-fluid inlet and exit lines. Also, thermocouples were installed on the outer walls of both the shell and boiler tubes. The ranges of test variables for both test sections of reference 85 are given in table I.

General Results

Correlations of overall pressure drop and mean boiling-side heat-transfer coefficient were obtained. These correlations are presented in chapters 6 and 7, respectively. The correlations are also used in chapter 2 for baseline comparisons in determining the effects of boiler tube inserts on heat transfer and pressure drop. The pressure-drop correlation used herein is shown in reference 93 to agree fairly well with the data of reference 83 for sodium, reference 94 for potassium, and reference 66 for water. These comparisons are all for boiling in heat exchangers with no inserts.

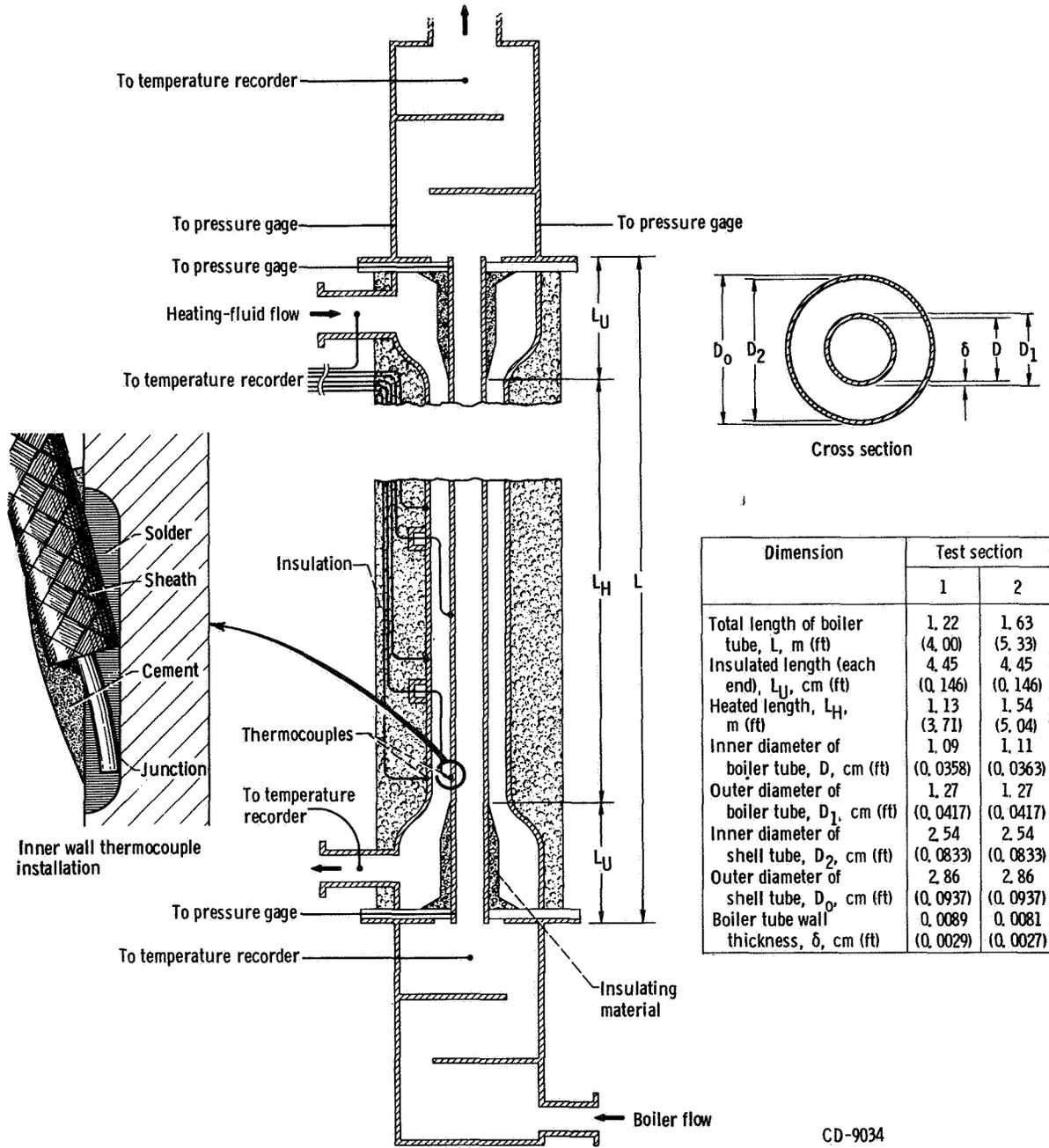| Dimension	Test section	
	1	2
Total length of boiler tube, L, m (ft)	1.22 (4.00)	1.63 (5.33)
Insulated length (each end), L_U, cm (ft)	4.45 (0.146)	4.45 (0.146)
Heated length, L_H, m (ft)	1.13 (3.71)	1.54 (5.04)
Inner diameter of boiler tube, D, cm (ft)	1.09 (0.0358)	1.11 (0.0363)
Outer diameter of boiler tube, D_1, cm (ft)	1.27 (0.0417)	1.27 (0.0417)
Inner diameter of shell tube, D_2, cm (ft)	2.54 (0.0833)	2.54 (0.0833)
Outer diameter of shell tube, D_0, cm (ft)	2.86 (0.0937)	2.86 (0.0937)
Boiler tube wall thickness, δ, cm (ft)	0.0089 (0.0029)	0.0081 (0.0027)

CD-9034

Figure 15. Diagram and dimensions of plain-tube water-boiling heat exchanger

19

DISCUSSION OF PLAIN, STRAIGHT TUBES

Since complete vaporization to a vapor quality of 1.0 was not obtained for any case tested with straight hollow tubes, these results were primarily useful in establishing criteria for the selection of necessary inserts and inlet devices. It was found that an inlet device must provide enough pressure drop to stabilize the flow and, in addition, that it may be advantageous to cause the fluid to flash across the inlet device in order to fix the point of boiling initiation. Inlet-region plugs also help to prevent the formation of the generally unstable slug-flow regime. Several types of helical flow inserts have been tested in alkali metal boilers (refs. 94 and 95). The purpose of such inserts is to maintain liquid on the boiler tube wall at high vapor qualities. For many of the experiments to be described in subsequent chapters a full-length helical wire insert was used for this purpose.

Chapter 2

BOILER TUBE INSERTS AND INLET RESTRICTORS

Swirl-generating inserts have commonly been used to improve boiler tube performance. By swirling the two-phase mixture the heavier liquid is centrifuged to the wall and liquid entrainment in the vapor is reduced. This swirl has been obtained by inserting twisted tape (fig. 7(a)), helical vanes (fig. 7(b)), or helical wires (fig. 7(c)) into the boiler tube; by coiling the tube, or by a combination of inserts and tube coiling. Experiments on heat-exchanger boilers with inserts or tube coiling are summarized in table II. Flow-stabilizing inlet restrictors, such as orifices and venturis, were also investigated in heat-exchanger boiler tubes and are discussed later in this chapter, along with a novel blade-type insert.

WATER BOILER WITH HELICAL WIRE INSERTS

A water-boiling heat exchanger with a full-length helical wire insert, shown in figure 16, was employed for a variety of tests. The dimensions and the ranges of test variables for each configuration are given in table II. The test section dimensions are the same as those of test section 2 of reference 85. The wire was 0.16 cm in diameter and had a pitch-to-tube-diameter ratio of 1.9. This test section was first tested with no inlet restrictor and with and without inlet-region central plugs, as reported in reference 86 and

dimensioned in table II. The test section flows were countercurrent.

No Inlet-Region Plug

Typical results for the boiler with the helical wire insert but with no inlet-region plug or inlet restrictor are shown in figure 17.
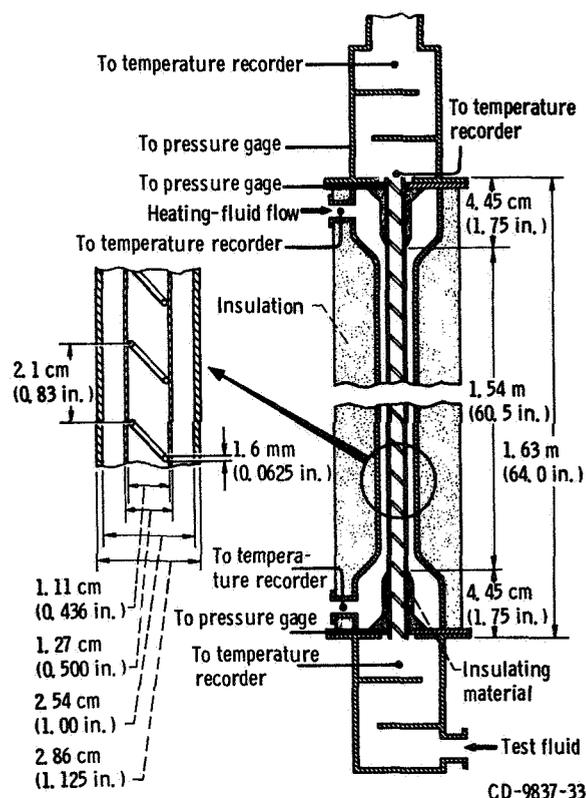

Figure 16. Diagram and dimensions of water-boiling heat exchanger with full-length helical wire insert.

TABLE II. SUMMARY OF EXPERIMENTS ON HEAT-EXCHANGER BOILERS WITH HELICAL FLOW PROMOTERS BUT NO INLET PRESSURE-DROP DEVICE

Boiling fluid	Heating fluid	Boiler tube[a] Heated length, L_H		Inside diameter, D		Helical flow promoter	Inlet-region plug length		Boiler-exit saturation temperature, $T_{be,s}$		Boiling-fluid flow rate, W_b		Exit quality, x_e	Reference
		cm	in.	cm	in.		cm	in.	K	°F	g/sec	lbm/hr		
Water	Water	154	60.5	1.11	0.436	Full-length, 2.10-cm- (0.83-in.-) pitch, 1.6-mm- (0.0625-in.-) diameter helical wire	----	----	~378	~219	7.4 - 13	59 - 102	0.08 - 1.0⁺	86
							12.7	5.0	~380	~222	7.4 - 13	58 - 101	11 - 1.0⁺	
							25.4	10.0	~377	~219	~7.4	~59	.05 - 1.0⁺	
Freon-113		81.3	32	1.09	430	Full-length, 3.17-cm- (1.25-in.-) pitch, 1.6-mm- (0.0625-in.-) diameter helical wire	12.7	5.0	~322	~120	23.0 - 99.8	182 - 793	20 - 1.0⁺	11
Freon-113		81.3	32	1.09	430	Full-length, 3.17-cm- (1.25-in.-) pitch, 1.6-mm- (0.0625-in.-) diameter helical wire	12.7	5.0	326 - 340	27 - 153	16.2 - 65.4	129 - 520	12 - 1.0⁺	12
Freon-113		81.3	32	1.09	430	Full-length, 3.17-cm- (1.25-in.-) pitch, 1.6-mm- (0.0625-in.-) diameter helical wire	12.7	5.0	326 - 340	27 - 153	14.5	115	1.0⁺	13
Potassium	Sodium	232	91.5	1.70	.67	Helical vane with 0.64-cm- (0.25-in.-) diameter centerbody { p/D = 6.0	----	----	1047 - 1211	1425 - 1720	31.5 - 290	250 - 2300	0.09 - 1.0⁺	94
				2.34	.92	p/D = 6.0	----	----	1089 - 1228	1500 - 1750	27.7 - 75.7	220 - 600	09 - 1.0⁺	
				2.34	.92	p/D = 2.2	----	----	1061 - 1246	1450 - 1765	27.7 - 302	220 - 2400	02 - 1.0⁺	
Potassium (boiler 1)	Lithium	[b]229	[b]90	1.70	67	Helical vane for two-thirds of boiler length, followed by 0.32-cm- (0.125-in.-) diameter helical wire to exit; p/D ~ 3	[c]9.4	[c]3.7	[d]1255 - 1420	[d]1800 - 2100	[d]30 - 80	[d]240 - 630	[d]0.5 - 1.0⁺	96, 97, 98

[a]Vertical upflow, single tube, unless otherwise noted.
[b]Horizontal, curved tube.
[c]Tapered down to 0.64-cm- (0.25-in.) diameter centerbody in length of 8.4 cm (3.3 in.); extended two-thirds of boiler length
[d]Approximate; detailed data not published.

Exit quality x_e and boiler pressure drop ΔP_B are plotted as a function of the boiler-exit temperature difference $\theta_{se} = T_{hl} - T_{be,s}$ in figures 17(a) and (b), respectively, for nominally constant flow rates, boiling-fluid inlet temperature, and exit pressure. For exit qualities less than that at which the boiling crisis (dry-wall boiling) occurs in the plain tube ($x_e \approx 0.82$), there is little effect of the helical wire on x_e for a given θ_{se}. Actually, the exit quality for a given θ_{se} appears to be slightly less with the helical wire than with the plain tube. However, the rate of increase of x_e with θ_{se} remains unchanged to $x_e \approx 1.0$ with the helical wire, indicating that there is no significant change in the overall heat-transfer coefficient, which would be the result of delaying the boiling crisis to very high quality. For the plain tube (ref. 85), the performance beyond the onset of dry-wall boiling was very erratic and unpredictable. Even with the helical wire, however, an exit quality of 1.0 was not reached without flow oscillations of at least ±5 percent. These flow oscillations were usually accompanied by pulsating high-temperature readings at the boiling-fluid inlet. These temperature rises were, at times, as much as 35 K. Since the boiling-fluid inlet thermocouple was located just upstream of the boiler tube inlet end, these erratic high-temperature readings may have been caused by back slugging of vapor or hot liquid.

The pressure drop shown in figure 17(b) is considerably greater than that for the plain tube. It was generally found necessary to adjust the throttle valve to cause a fairly large total-system pressure difference in order to maintain a reasonably steady boiling-fluid flow rate. At high exit qualities the pressure

drop across the throttle valve was about 90 kN/m^2. Comparable throttle-valve pressure drops with the plain tube did not yield such high qualities with stable flow.

(a) Exit quality.
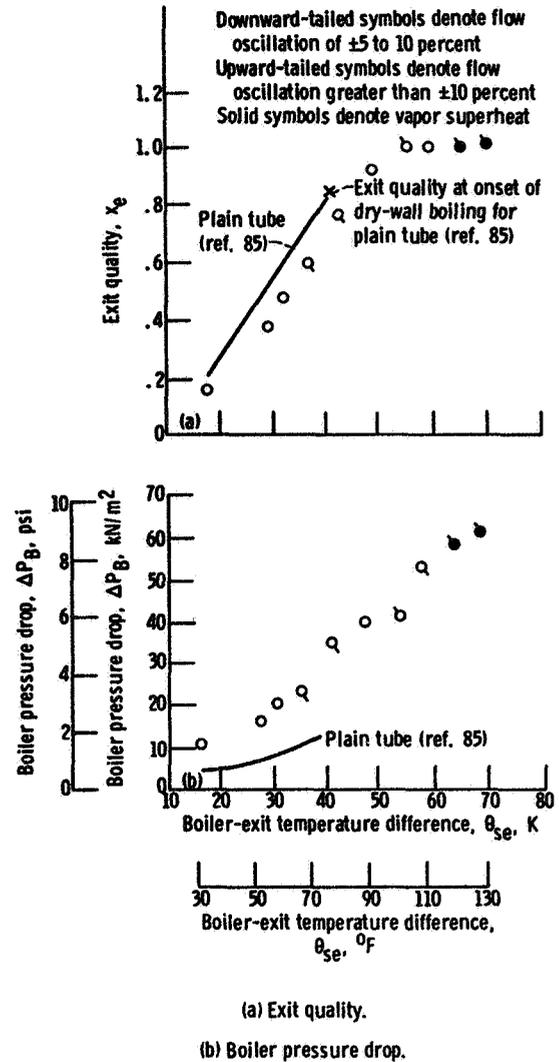
(b) Boiler pressure drop.

Figure 17. - Boiler performance as function of boiler-exit temperature difference with helical wire insert and no inlet-region plug or inlet restrictor. Heating-fluid flow rate, ~1.0 kg/sec (~8000 lbm/hr); boiling-fluid flow rate, ~7.5 g/sec (~60 lbm/hr); boiling-fluid inlet temperature, ~300 K (~80° F); exit pressure, ~117 kN/m^2 abs (~17 psia).

23

With Inlet-Region Plug

Two different inlet-region center plugs were tested with this boiler with no inlet restrictor. It was intended that a plug, by preventing slug flow, might allow the throttle valve to supply sufficient pressure drop for stability. The shorter of these plugs is shown in figure 18. The other plug was twice as long, with the same diameter. Typical data are shown in figure 19; the nominal conditions are the same as those for figure 17, which had no inlet-region plug. The variations of x_e and ΔP_B with θ_{se} are essentially the same as those for no plug or inlet device (fig. 17). But with the plugs an exit quality of 1.0 could be reached with flow oscillations less than ±5 percent. However, the flow stability was not always repeatable; and when flow oscillations did occur, they were generally accompanied by high and erratic boiling fluid inlet temperature readings, as was the case with no plug. The throttle-valve pressure drops were about the same as for no plugs. However, these are not necessarily the minimum values required for stability.
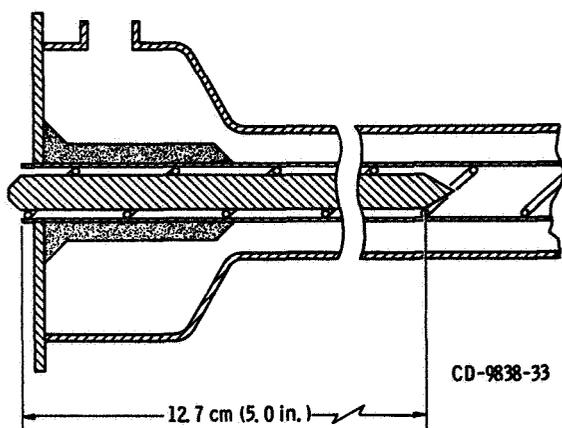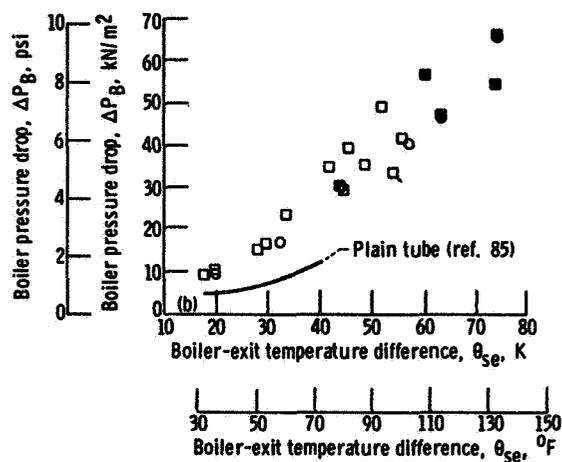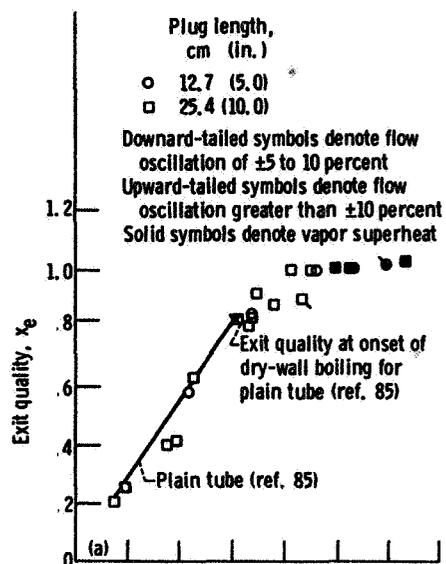
Plug length,
cm (in.)

o 12.7 (5.0)
□ 25.4 (10.0)

Downard-tailed symbols denote flow
oscillation of ±5 to 10 percent
Upward-tailed symbols denote flow
oscillation greater than ±10 percent
Solid symbols denote vapor superheat

(a) Exit quality.

(b) Boiler pressure drop.

Figure 19. - Boiler performance as function of boiler-exit temperature difference with helical wire insert and inlet-region central plug. Heating-fluid flow rate, ~1.0 kg/sec (~8000 lbm/hr); boiling-fluid flow rate, ~7.5 g/sec (~60 lbm/hr); inlet temperature, ~300 K (~80° F); exit pressure, ~117 kN/m² abs (~17 psia).

CD-9838-33

Figure 18. - Inlet end of water-boiling heat exchanger with helical wire insert and 12.7-cm- (5.0-in. -) long, 0.79-cm- (0.311-in. -) diameter inlet-region central plug.

Discussion of Inserts

From the results presented, it is apparent that inserts can improve boiler performance. Swirl flow devices delay the boiling crisis to higher qualities at the expense of increased pressure drop. Inlet-region plugs contribute to

flow stability by reducing the tendency for reverse flow and slug flow, with minimal increase in pressure drop. However, stable and complete vaporization was not consistently obtained with these devices alone.

Some of the boiling flow instabilities described in chapter 1 were attributed to insufficient boiler-inlet pressure drop. As a consequence, various inlet flow restrictors were studied. The following sections describe tests with water and potassium performed on boilers with inserts and inlet restrictors over the ranges of test variables listed in table III. The water boiler with full-length helical wire

TABLE III.   SUMMARY OF EXPERIMENTS ON BOILERS WITH INSERTS AND INLET RESTRICTORS

Boiling fluid	Heating fluid	Boiler tube[a]				Helical flow promoter	Inlet-region plug length		Inlet restrictor	Ranges of test variables					Reference
		Heated length, L_H		Inside diameter, D			cm	in.		Boiler-exit saturation temperature, $T_{be,s}$		Boiling-fluid flow rate, W_b		Exit quality, x_e	
		cm	in.	cm	in.					K	°F	g/sec	lbm/hr		
Water	Water	154	60.5	1.11	0.436	Full-length, 2.10-cm-(0.83-in.-)pitch, 1.6-mm-(0.0625-in.-)diameter helical wire	-----	-----	0.64-mm (0.025-in.) orifice	~377	~219	6.5-9.2	52-73	0.14-0.96	86
							-----	-----	0.78-mm (0.0305-in.) orifice			7.4	59	0.59-0.79	
							-----	-----	Two 0.64-mm (0.025-in.) wall orifices			7.4-13.4	59-107	0.06-0.97	
							-----	-----	Four 0.34-mm (0.0135-in.) angled wall orifices			~7.4	~59	0.09-0.93	
							25.4	10.0	0.71-mm (0.028-in.) orifice			4.8-8.5	38-68	0.02-0.91	
							25.4	10.0	0.78-mm (0,0305-in.) venturi			~10	~80	0.06-1.0+	
Water	Water	154	60.5	1.11	436	Full-length, 2.10-cm-(0.83-in.-)pitch, 1.6-mm-(0.0625-in.-)diameter helical wire	25.4	10.0	0.72-mm (0.0285-in.) venturi			5.5-15.5	44-123	0.02-0.98	87
							4.52	1.78	0.72-mm (0.0285-in.) venturi	334-430	142-314	~10	~80	0.01-0.96	
Potassium	Sodium	[b]~102	[b]40	78	307	Twisted tapes; p/D ≈ 6	-----	-----	1.02-mm (0.040-in.) orifice (each tube)	978-1144	1300-1600	38-151	300-1200	0.40-1.0+	95
		[c]~102	[c]40	622	.245	Twisted tapes; p/D ≈ 6	-----	-----	0.89-mm (0.035-in.) orifice (each tube)	1061-1172	1450-1650	38-113	300-900	0.40-1.0+	
Potassium (boiler 2)	Lithium	[e]229	[e]90	1.70	.67	Full-length, 0.24-cm-(0.94-in.-)diameter helical wire; p/D ≈ 3	20.8	8.2	1.93-mm (0.76-in.) throat-diameter conical converging-diverging nozzle	[f]1057-1395	[f]1440-2050	[f]23-59	[f]180-470	[f]0.5-1.0+	(d)

[a]Single, straight, vertical tube, unless otherwise noted.
[b]Twelve curved, horizontal tubes of slightly different lengths.
[c]Nineteen curved, horizontal tubes of slightly different lengths.
[d]See p. 32.
[e]Horizontal, curved single tube.
[f]Approximate; data not published.

insert, described in figure 16, was tested with the addition of a series of inlet restrictors (refs. 86 and 87). Orifices were tested first (rather unsuccessfully) without and then with inlet-region plugs, then a converging-diverging inlet nozzle followed by a center plug was tested. This latter configuration was then tested (and compared with a similar one without the nozzle) in potassium in a General Electric refractory-metal facility under NASA Lewis Contract NAS3-9426. In all these cases the heating-fluid flow was countercurrent to the boiling-fluid flow Flashing at the boiler inlet obtained by preheating the boiling fluid was also studied as a means of improving inlet performance.

Upstream (inlet-plenum) side

(a)   CD-9839-33

WATER BOILER WITH INLET ORIFICE(S) AND INSERTS

No Inlet-Region Plug

Two different-size center orifices, as well as the two multiple-hole orifices shown in figure 20, were tested with no inlet-region plug. The orifice dimensions and the ranges of test variables are given in table III. Figure 21 shows typical data for these configurations at the same nominal conditions as figures 17 and 19. For exit qualities to about 0.7 the quality for a given θ_{se} is about the same as for the plain tube. However, increases in θ_{se} do not yield much increase in x_e, compared to the configurations with no inlet device. In addition, vapor superheat was indicated at exit qualities ranging from 0.73 to 0.93 This problem was attributed to the existence of a metastable jet issuing from the orifice, a condition which was observed in tests of similar inlets in a transparent tube. Note, however, that no erratic high-temperature readings were observed at the boiler inlet, indicating that the orifices eliminated the backslugging problem.

Upstream (inlet-plenum) side   Downstream (test section) side

(b)   CD-9840-33
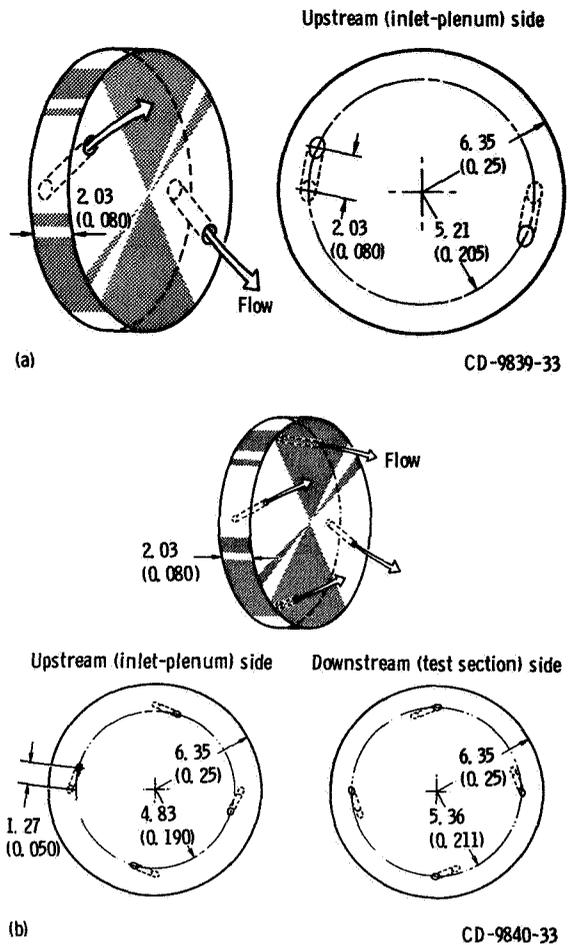
(a) Two-orifice inlet. Hole diameter 0.64 mm (0.025 in.).

(b) Four-orifice inlet. Hole diameter 0.34 mm (0.0135 in.).

Figure 20. Various orifice configurations tested without inlet-region plug on water-boiling heat exchanger with full-length helical wire insert. (Dimensions are in mm (in.).)

With Inlet-Region Plug

In an attempt to eliminate the problem of relatively low-quality vapor superheat, an inlet orifice was tested with a plug. This configuration is shown in figure 22. The plug was bonded to the orifice plate, which was soldered to the inlet end of the boiler tube. A slot passage was cut at the inlet end of the plug to provide a flow passage from the orifice into the boiler tube. Figure 23 shows typical data for this configuration at the same

nominal conditions as figures 17, 19, and 21. The results are similar to those for the other orifice configurations (fig. 21), nonequilibrium vapor superheat is seen for exit qualities from 0.79 to 0.91. Thus, with orifices, it appears that a poor flow distribution is set up in the inlet region, and its effect persists throughout the tube, in spite of the plug and forced swirling. The orifice pressure drop at the nominal conditions was about 170 kN/m²

Figure 22. Inlet end of water-boiling heat exchanger with helical wire insert, 0.71-mm (0.028-in.) orifice, and 25.4-cm (10.0-in.) plug.
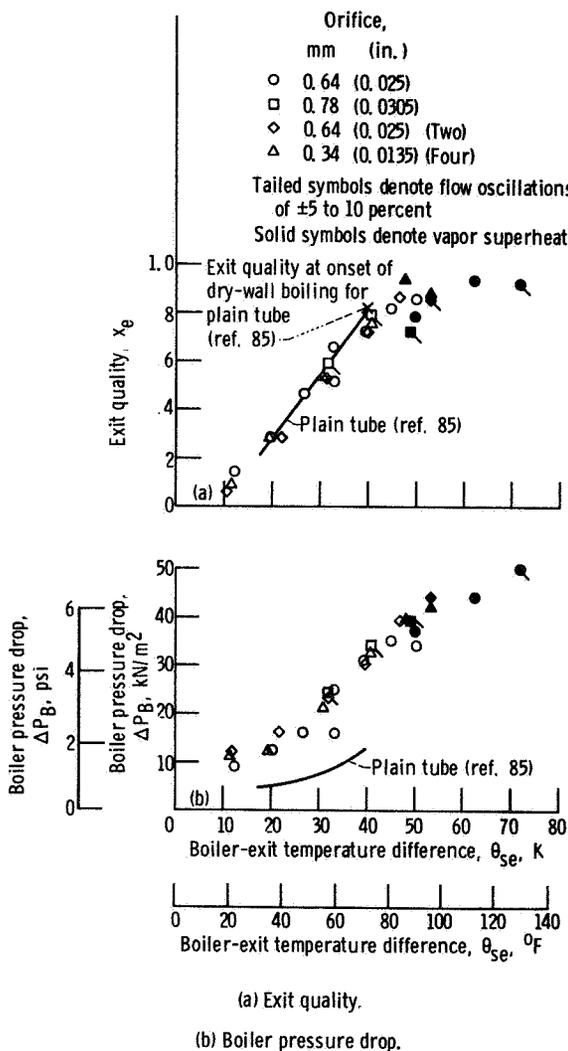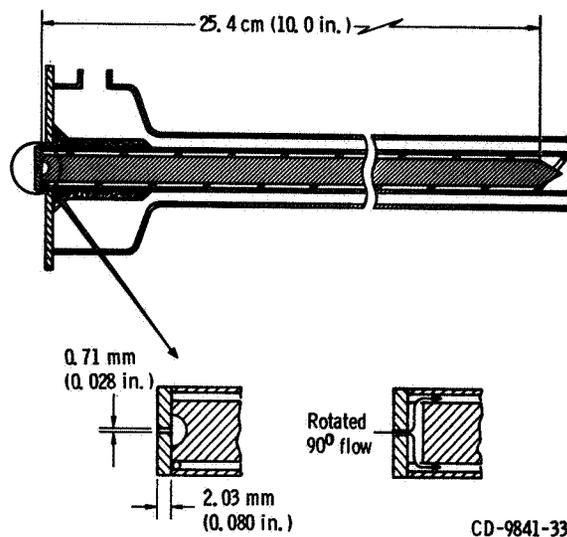

(a) Exit quality.

(b) Boiler pressure drop.

Figure 21. Boiler performance as function of boiler-exit temperature difference with helical wire insert, various inlet orifice configurations, and no inlet-region plug. Heating-fluid flow rate, ~1.0 kg/sec (~8000 lbm/hr); boiling-fluid flow rate, ~7.5 g/sec (~60 lbm/hr); inlet temperature, ~300 K (~80° F); exit pressure, ~117 kN/m² abs (~17 psia).

(a) Exit quality.
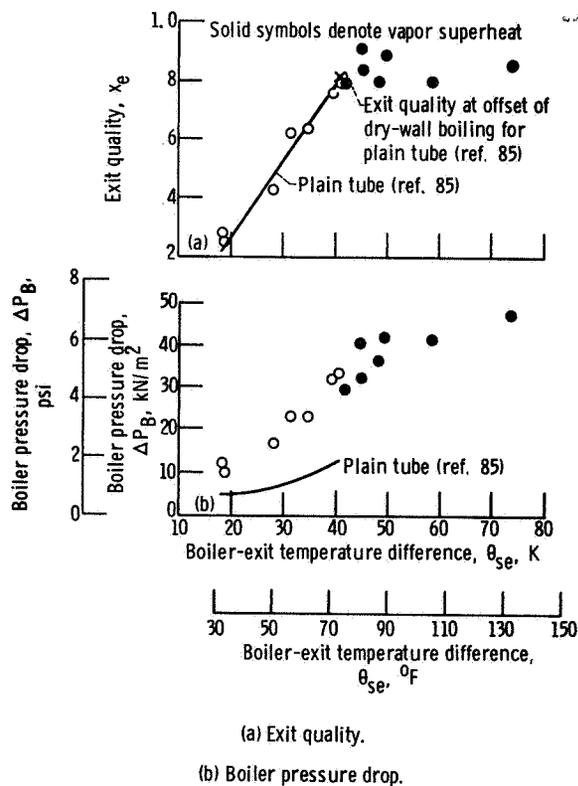
(b) Boiler pressure drop.

Figure 23. Boiler performance as function of boiler-exit temperature difference with helical wire insert, 0.71-mm (0.028-in.) orifice, and 25.4-cm (10.0-in.) plug. Heating-fluid flow rate, ~1.0 kg/sec (~8000 lbm/hr); boiling-fluid flow rate, ~7.5 g/sec (~60 lbm/hr); inlet temperature, ~300 K (~80° F); exit pressure, ~117 kN/m² abs (~17 psia).

27

WATER BOILER WITH CONVERGING-DIVERGING NOZZLE AND INLET-REGION PLUG

Since an exit quality of 1.0 could not be obtained with orifices at the boiler inlet, at least over the range of conditions listed in table III, orifices were replaced by nozzles in subsequent tests. Figure 24 shows the inlet region of the test section with a venturi-type inlet nozzle with a tapered central plug in the diffuser starting at a point just downstream of the nozzle throat. A short length of stainless-steel tubing was rolled down to form the venturi. The rolling process left a small notch in the diffuser, as shown in the figure. The extension of the diffuser and the plug was brass. A wire with the same pitch as in the boiler tube was bonded to the tapered section of the plug, and the upstream end of the wire was tapered down to a point. Plots of exit quality and boiler pressure drop against the boiler-exit temperature difference for the venturi and plug are shown in figures 25(a) and (b), respectively, for a boiling-fluid flow rate of about 10 g/sec at otherwise nominal
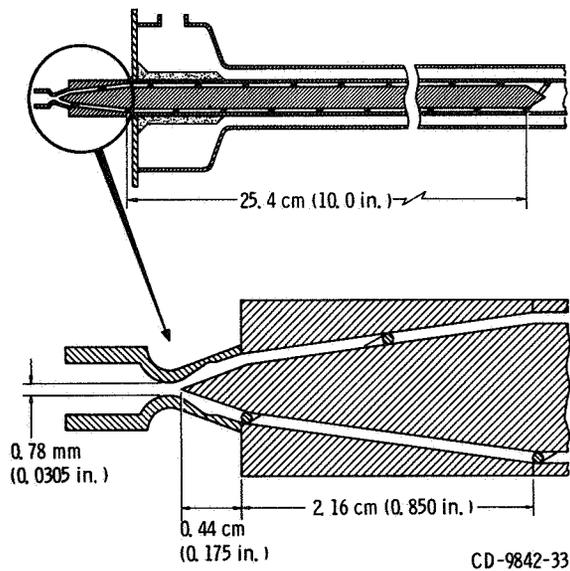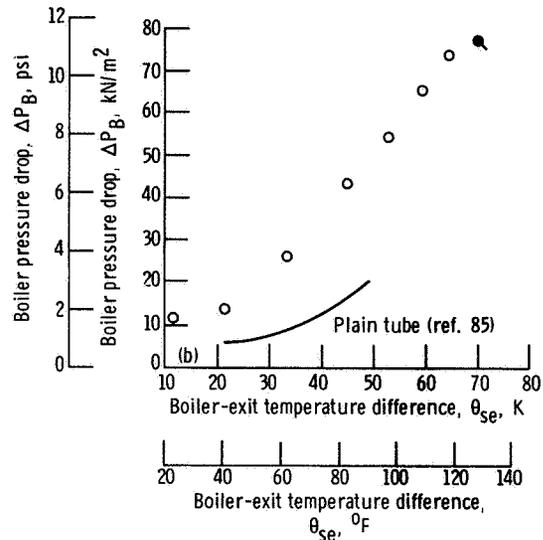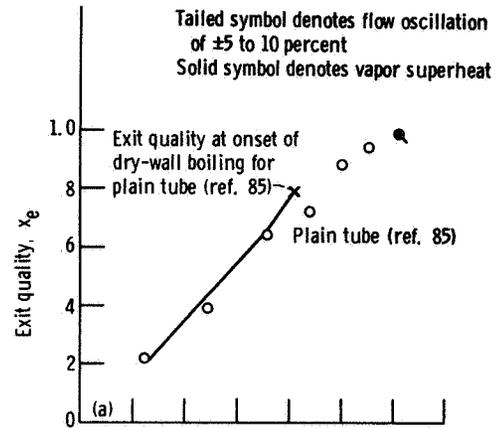

Figure 24. Inlet end of water-boiling heat exchanger with helical wire insert, 0.78-mm- (0.0305-in. -) throat-diameter venturi nozzle, and 25.4-cm (10.0-in.) plug.

(a) Exit quality.

(b) Boiler pressure drop.

Figure 25. Boiler performance as function of boiler-exit temperature difference with helical wire insert, 0.78-mm- (0.0305-in. -) throat-diameter venturi, and 25.4-cm (10.0-in.) plug. Heating-fluid flow rate, ~1.0 kg/sec (~8000 lbm/hr); boiling-fluid flow rate, ~10 g/sec (~80 lbm/hr); inlet temperature, ~300 K (~80° F); exit pressure, ~117 kN/m² abs (~17 psia).

conditions. (Stable operation was not obtained at a boiling-fluid flow rate of 7.5 g/sec, probably because of unsteady cavitation in the nozzle.) Vapor superheat was first indicated at $x_e = 0.98$, flow oscillations in the range of ±5 to ±10 percent were observed at that point. No erratic boiling-fluid inlet temperature behavior like that seen

28

without an inlet device was observed. The pressure drop across the venturi and diffuser was about 170 kN/m² with a flow rate of 10 g/sec and a temperature of 300 K.

Another series of runs were made with the same flow rates and boiler-exit pressure but with higher boiling-fluid inlet temperature (371 to 389 K). The exit quality and boiler pressure drop are plotted against θ_{se} for this series in figures 26(a) and (b), respectively. Vapor superheat was observed at exit qualities from 0.96 to 1.02. Boiling-fluid flow

oscillations were less than ±5 percent; however, additional pressure drop (as much as 70 kN/m²) was required at the throttle valve for flow stability at the high exit qualities. In these runs, conditions were established such that flashing (sudden initiation of vapor) probably occurred in the venturi, but persistence of the vapor into the heated region of the boiler tube was marginal. This vapor initiation problem is discussed in greater detail in appendix B, based on test results from water in transparent test sections and from potassium under adiabatic flow conditions.

POTASSIUM BOILER WITH CONVERGENT-DIVERGENT NOZZLE AND INLET-REGION PLUG

The General Electric advanced Rankine-cycle test facility used for these tests is described in references 96 to 98. A simplified schematic of the test facility is shown in figure 27, and the lithium-heated boiler tube arrangement is shown in figure 28. Two T-111 alloy boiler tubes were tested, differing principally in inlet restrictor geometry. The boiler dimensions are given in tables II and III. Boiler 1 (table II) had a composite insert consisting of a center plug wrapped with a single-pitch ribbon-type helical vane. Following this, the plug tapered down to a 0.64-cm-diameter centerbody (hollow for thermocouple installations) that extended for about two-thirds of the boiler length as did the helical vane. Then the helical vane joined (at the same pitch) a wire coil that extended to the boiler tube exit. The instrumented centerbody extended to the exit but had a 20-cm gap at the start of the wire coil (designed to prevent liquid flow along the upstream centerbody from being carried over onto the downstream centerbody).

Boiler 2 (table III) was similar to boiler 1, except that at the boiler tube inlet a

(a) Exit quality.

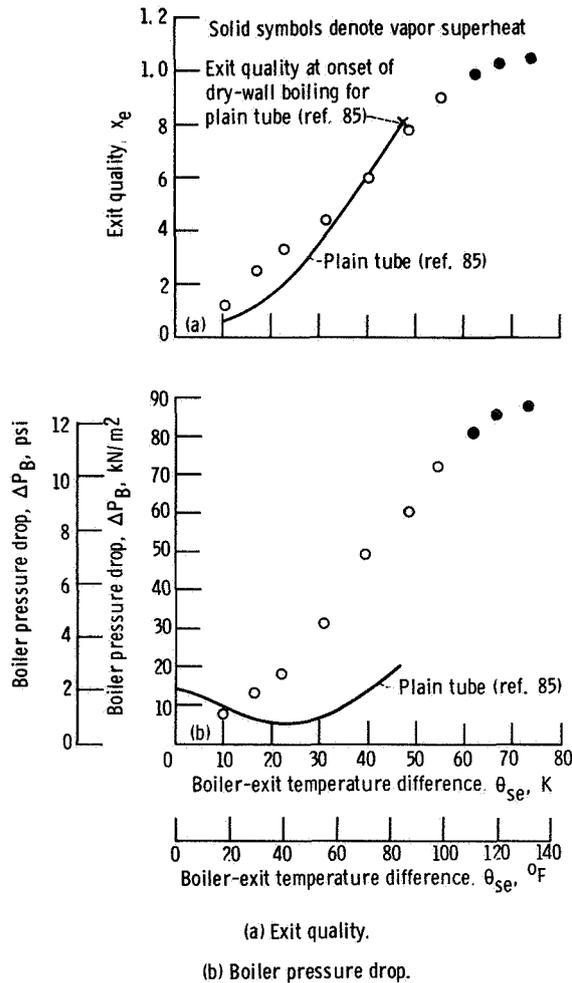(b) Boiler pressure drop.

Figure 26. Boiler performance as function of boiler-exit temperature difference with helical wire insert, 0.78-mm- (0.0305-in. ·) throat-diameter venturi, and 25.4-cm (10.0-in.) plug. Heating-fluid flow rate, ~1.0 kg/sec (~8000 lbm/hr); boiling-fluid flow rate, ~10 g/sec (~80 lbm/hr); inlet temperature, 372 to 389 K (210° to 241° F); exit pressure, ~117 kN/m² abs (~17 psia).
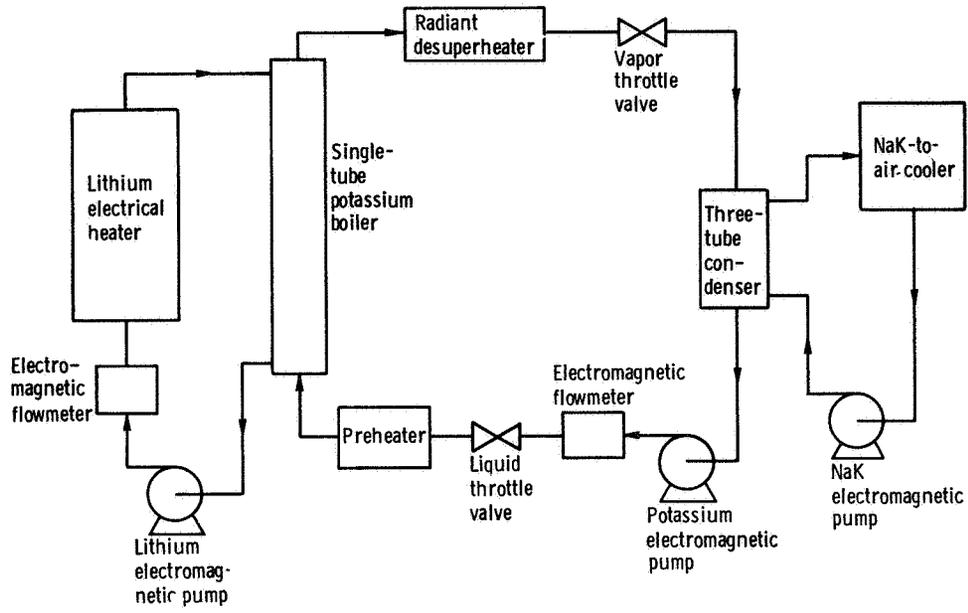
Figure 27. Simplified schematic of advanced Rankine cycle test facility.
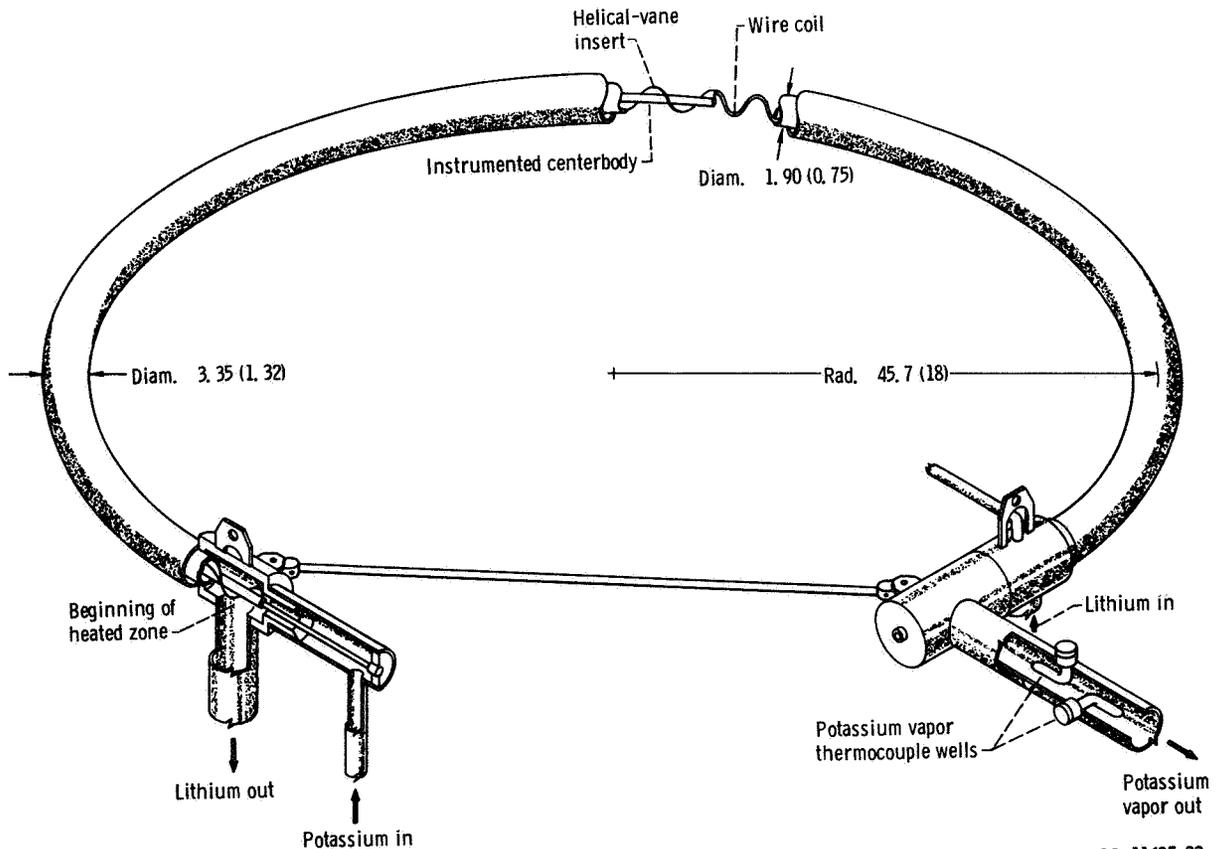

Figure 28. Schematic of single-tube potassium boiler. (Dimensions are in cm (in.).)

CD-11695-33

30

conically convergent-divergent venturi nozzle with a throat diameter of 0.193 cm was installed, with a central plug (similar to that shown in fig. 24) starting in the nozzle diffuser. Wrapped around the plug and extending the full length of the boiler tube was a helical wire coil. An instrumented centerbody was installed for only the last one-third of the boiler tube. The lithium outlet from the shell was approximately 7.6 cm downstream of the potassium flow exit from the inlet venturi nozzle.

The performance of these two boilers is shown in the next few figures, taken mainly from unpublished data from NASA contract NAS3-9426. Typical temperature patterns throughout the length of boiler 1 are shown in figure 29, taken from reference 97 Similar patterns for boiler 2 are shown in figure 30. Temperature distributions are shown in figure 31 for boiler 2 operating with flow in the flashing mode in the inlet venturi. Except for the initial few inches of potassium flow, these temperatures are comparable to those of figure 30 for a liquid-filled venturi. The average boiling heat-transfer coefficients for both boilers under comparable conditions are compared in figure 32. Very high average coefficients were obtained, some in excess of 6×10^4 W/(m²)(K). In one example with boiler 2 the average coefficient with 83 K of vapor superheat at the exit was as high as for a case with an exit quality of 0.55, demonstrating good heat transfer in the high-quality region of the boiler.

Typical boiler tube overall pressure losses are shown in figure 33 as a function of potassium flow rate for three heating rates and for both boilers. The predicted curves for exit qualities of 0.5 and 1.0 are shown, as well as for 56 K exit vapor superheat. Generally, the pressure losses are nearly constant over the range of exit qualities at constant power, but they increase rapidly as appreciable amounts of vapor superheat are formed (solid symbols). Boiler 2, exclusive of the inlet
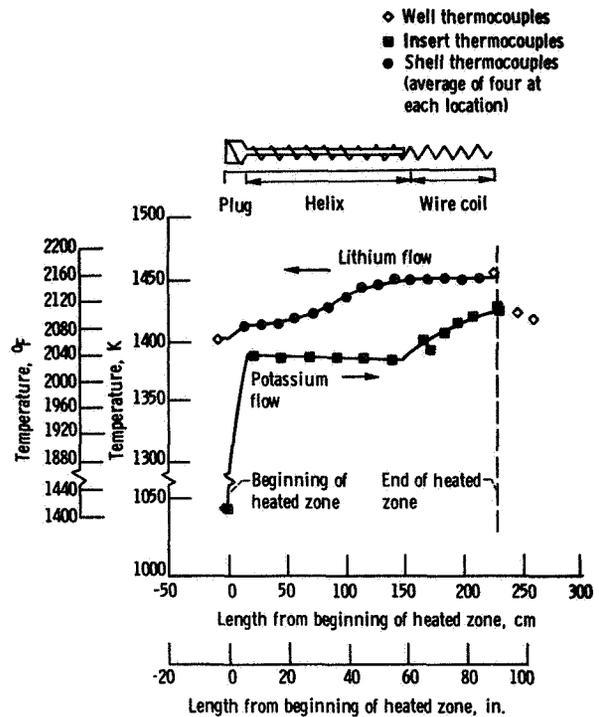

Figure 29. Temperature distribution for boiler 1 (ref. 97). Heating-fluid flow rate, 0.42 kg/sec (0.93 lbm/sec); boiling-fluid flow rate, 0.044 kg/sec (0.097 lbm/sec); heating rate, 99.8 kW (34 000 Btu/hr).

venturi, shows about the same amount of pressure drop as boiler 1 (untailed symbols).

The thermal performance of boiler 2 is shown in figure 34 in terms of measured boiler power as a function of exit saturation temperature and exit enthalpy. Predicted curves and limiting lines are also shown. Data and predictions agree fairly well with operation at positive exit qualities and moderate vapor superheats. However, at higher values of vapor superheat the predictions underestimate the boiler heat-transfer power (Data for one run yielded an exit vapor superheat of 250 K above the exit saturation temperature of 1090 K, believed to be the highest superheat achieved in any potassium boiler.) The maximum boiler thermal power attained was about 210 kW at a 1055 K saturation temperature and an exit quality less than 1.0. This power level is 242 percent of the design value of 87 kW.

31

Figure 30. Uncalibrated lithium and potassium temperature profiles through boiler 2 during design point demonstration runs. Heating-fluid flow rate, 0.409 kg/sec (0.901 lbm/sec); boiling-fluid flow rate, 0.0500 kg/sec (0.1102 lbm/sec); heating rate, 94.6 kW (32 300 Btu/hr); boiling-fluid pressure drop (venturi exit to boiler exit), 152 kN/m² (22 psi); boiler-exit pressure, 1103 kN/m² abs (160 psia); nozzle-inlet pressure, 1400 kN/m² abs (203 psia); nozzle-inlet temperature, 1135 K (1583° F); boiler-exit temperature minus boiler-exit saturation temperature, 44 K (80° F); nozzle-inlet temperature minus nozzle-exit temperature, 59 K (106° F); venturi liquid flooded.

Essentially, boiler 2 had a pressure drop larger than that of boiler 1 by the amount of drop caused by the inlet venturi, but boiler 2 was more stable in operation than boiler 1 and performed thermally as well as or better than boiler 1
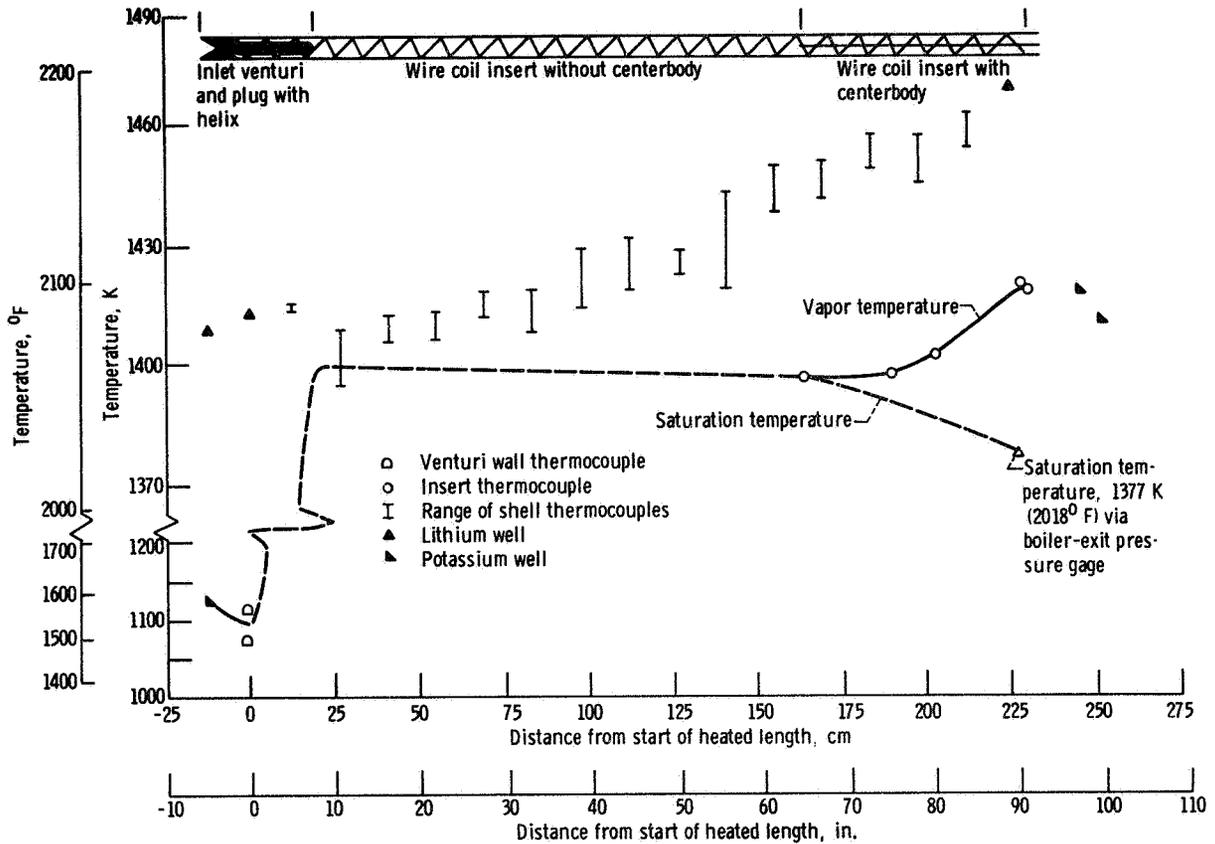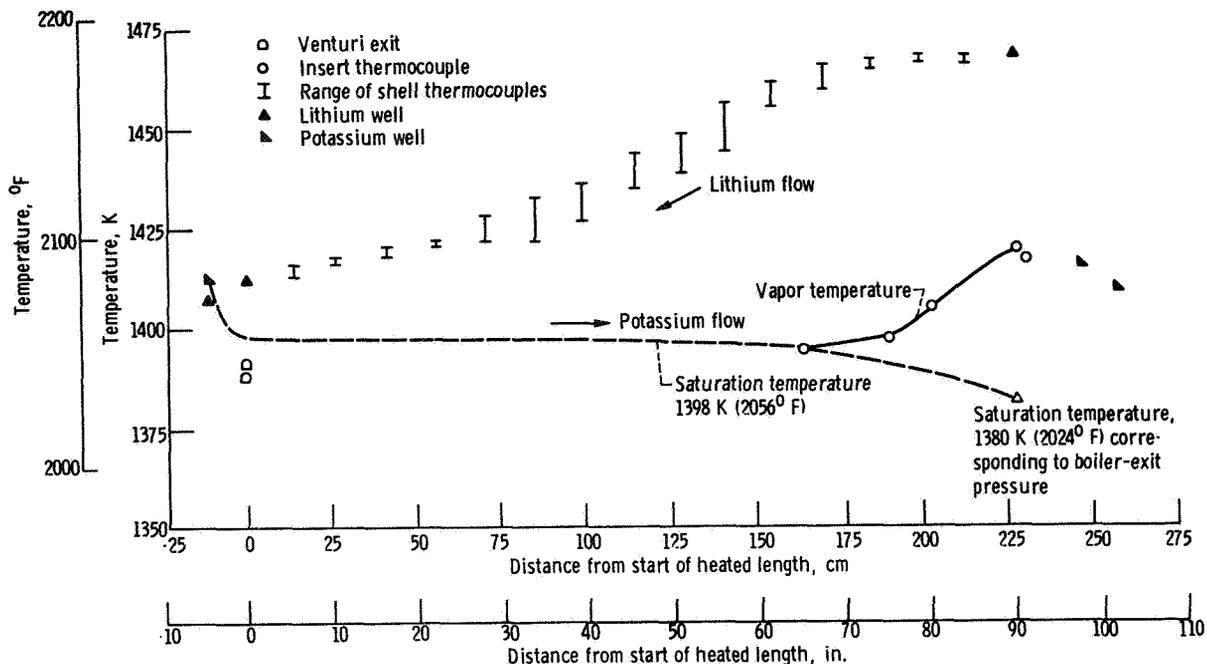
Figure 31. Calibrated lithium and potassium temperature profile through boiler 2 with flashing at inlet venturi. Heating-fluid flow rate, 0.399 kg/sec (0.878 lbm/sec); boiling-fluid flow rate, 0.0503 kg/sec (0.111 lbm/sec); heating rate, 87 5 kW (29,800 Btu/hr); boiler pressure drop, 99 kN/m^2 (14.4 psi); boiler-exit pressure, 1125 kN/m^2 abs (163 psia); nozzle-inlet pressure, 1557 kN/m^2 abs (225.8 psia); nozzle-inlet temperature, 1413 K (2083° F); boiler-exit temperature minus boiler-exit saturation temperature, 40 K (72° F); heating-fluid inlet temperature minus heating-fluid exit temperature, 57 K (102° F); flashing at venturi $(P_{ni} \quad P_{ne})/(W_b^2/2\rho_2 g_c A_{min}^2) = 1.24$.

(a) Heating-fluid inlet temperature minus boiler-exit temperature, 1382 K (2028° F).

(b) Heating-fluid inlet temperature minus boiler-exit temperature, 1256 K (1800° F).
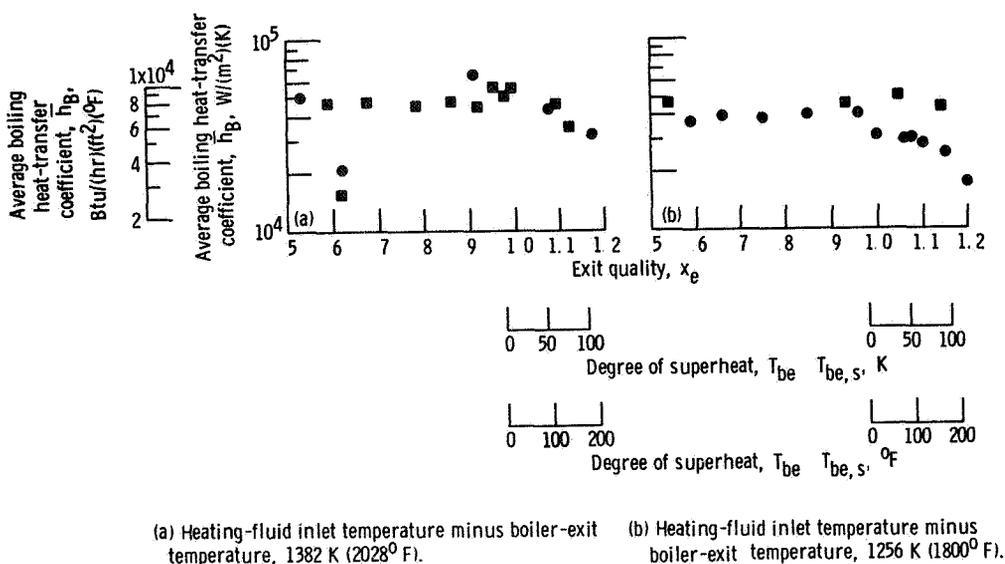
Figure 32. - Comparison of average boiling heat-transfer coefficient as function of exit enthalpy between boiler 1 and 2. Heating rate, 87 kW (29 600 Btu/hr); nominal heating-fluid temperature difference, 56 K (100° F); nozzle-inlet temperature, 928 K (1211° F).
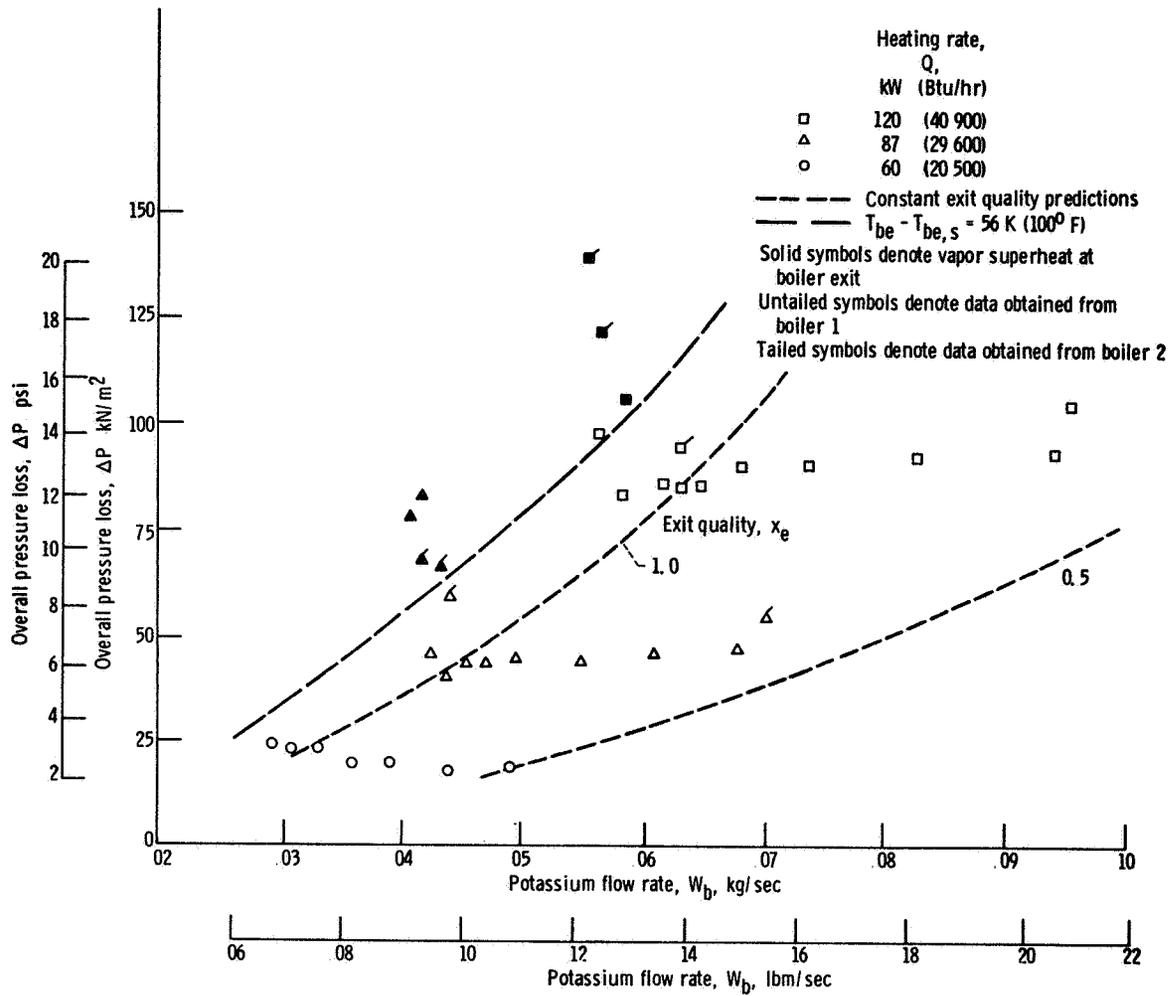
33

Figure 33. Experimental boiler overall pressure losses as function of potassium flow rates at constant thermal power levels; potassium exit saturation temperature, 1382 K (2028° F).
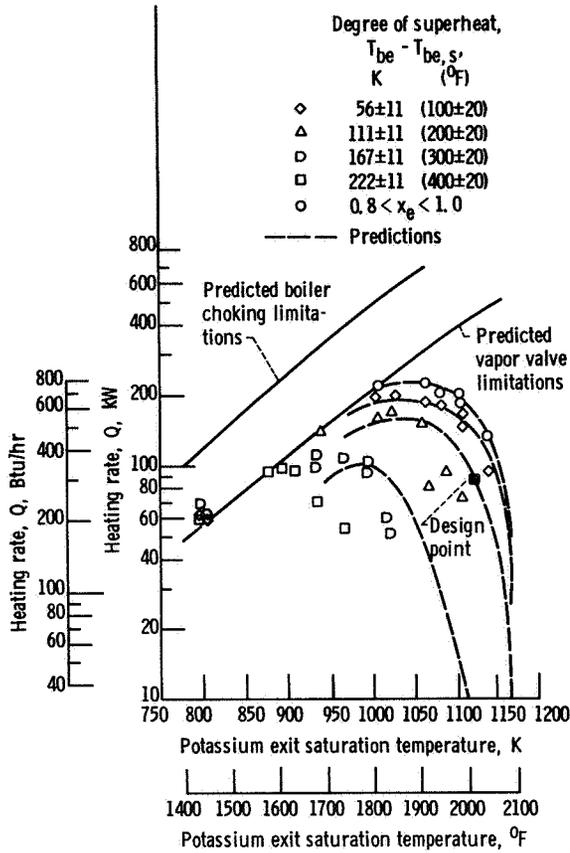
Figure 34. Maximum boiler power capability data obtained from from boiler 2. Nominal heating-fluid inlet temperature, 1367 K (2200° F); nominal heating-fluid temperature difference, 56 K (100° F); nominal nozzle-inlet temperature, 928 K (1211° F).

TABLE IV - SUMMARY OF EXPERIMENTS ON DIRECT-HEATED BOILERS WITH HELICAL FLOW PROMOTERS, BUT NO INLET PRESSURE DROP DEVICE[a]

Boiling fluid	Water
Heated length of boiler tube[b], L_H, cm (in.)	102 (40)
Inside diameter of boiler tube[b], D, cm (in.)	1.43 (0.563)
Helical-flow promoter	Blade-type swirlers[c]
Range of test variables:	
Boiler-exit saturation temperature, $T_{be, s}$, K (°F)	~377 (~219)
Boiling-fluid flow rate, W_b, g/sec (lbm/hr)	25 - 50 (200 - 400)
Exit quality, x_e	0.12 - 0.70

[a]From ref 88.
[b]Vertical upflow, single tube.
[c]See fig. 16.

ELECTRICALLY HEATED WATER BOILER WITH BLADE-TYPE HELICAL FLOW INDUCERS

An alternative to the helical wire for swirling and stabilizing flow within a boiler is to use individual swirlers spaced to give a maximum improvement in boiler performance and a minimum increase in pressure drop. The two-phase loop of the test facility shown in figure 14 was also used to evaluate the performance of blade-type helical flow inducers in an electrically heated water boiler, as described in reference 88. The test conditions and ranges of variables are summarized in table IV The test sections were fabricated from 1.43-cm-inside-diameter 304 stainless-steel tubing. Each test section was 101.6 cm long. A disassembled test

35

section is shown in figure 35 Stationary rotor elements obtained from turbine-type flowmeters were used to swirl the flow and centrifuge the liquid droplets to the tube wall. The blades were at a constant angle of 30° to the tube centerline. Various numbers of these nonrotating rotor elements were centrally installed within the test section by axially positioning them on a wire centered within the test section. The wires and rotor elements were electrically insulated from the tube. The number of swirlers and their respective locations within the tube are listed in the following table

Test section	Number of swirlers	Locations of swirlers: distance from outlet, cm (in.)
A	0	....
B	1	25. 4 (10)
C	1	12. 7 (5)
D	2	12. 7 (5) and 25. 4 (10)
E	2	10. 2 (4) and 20. 3 (8)
F	3	10. 2 (4), 20. 3 (8) and 30. 5 (12)
G	4	10. 2 (4), 20. 3 (8), 30. 5 (12), and 40. 7 (16)
H	5	10. 2 (4), 20. 3 (8), 30. 5 (12), 40. 7 (16), and 50. 8 (20)
I	6	10. 2 (4), 20. 3 (8), 30. 5 (12), 40. 7 (16), 48. 2 (19), and 55. 9 (22)
J	7	10. 2 (4). 20. 3 (8), 30. 5 (12), 40. 7 (16), 48. 2 (19), 55. 9 (22), and 63. 5 (25)

The testing sequence was as follows. After each configuration was tested and the boiling crisis location was determined, an additional swirler was added or the previous ones were relocated. This process was continued until no additional improvement in the maximum exit quality occurred. Because no boiler-inlet stabilizing devices were used, maximum exit quality was limited by system flow instabilities resulting from interaction of the feed system and boiler

The results of all configurations tested are summarized in figure 36. Maximum quality and heat flux are shown. The calculated (heat balance) start of the boiling region is indicated with respect to the test section length for all configurations tested. The calculated quality (in percent) at the point of boiling crisis (usually a tube burnout) is shown in parentheses under the burnout locations. Comparing test sections A and H shows that the maximum exit quality was doubled from 0.3 to 0.6, with a 58 percent increase in pressure drop measured at an exit quality of 0.3. With this relatively small increase in pressure drop, it appears that these blade-type swirlers might be better in a boiler tube than a helical wire for the middle range of quality

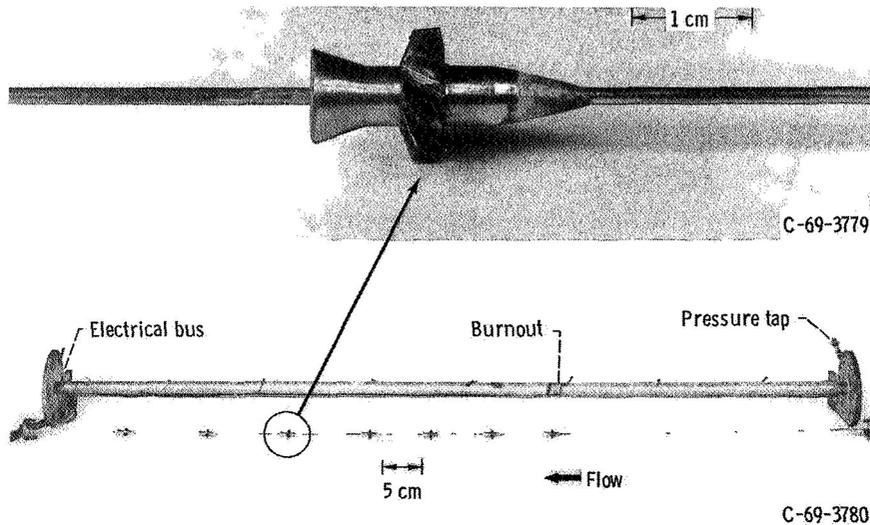

Figure 35. Disassembled test section with blade-type swirlers in electrically heated tubes.
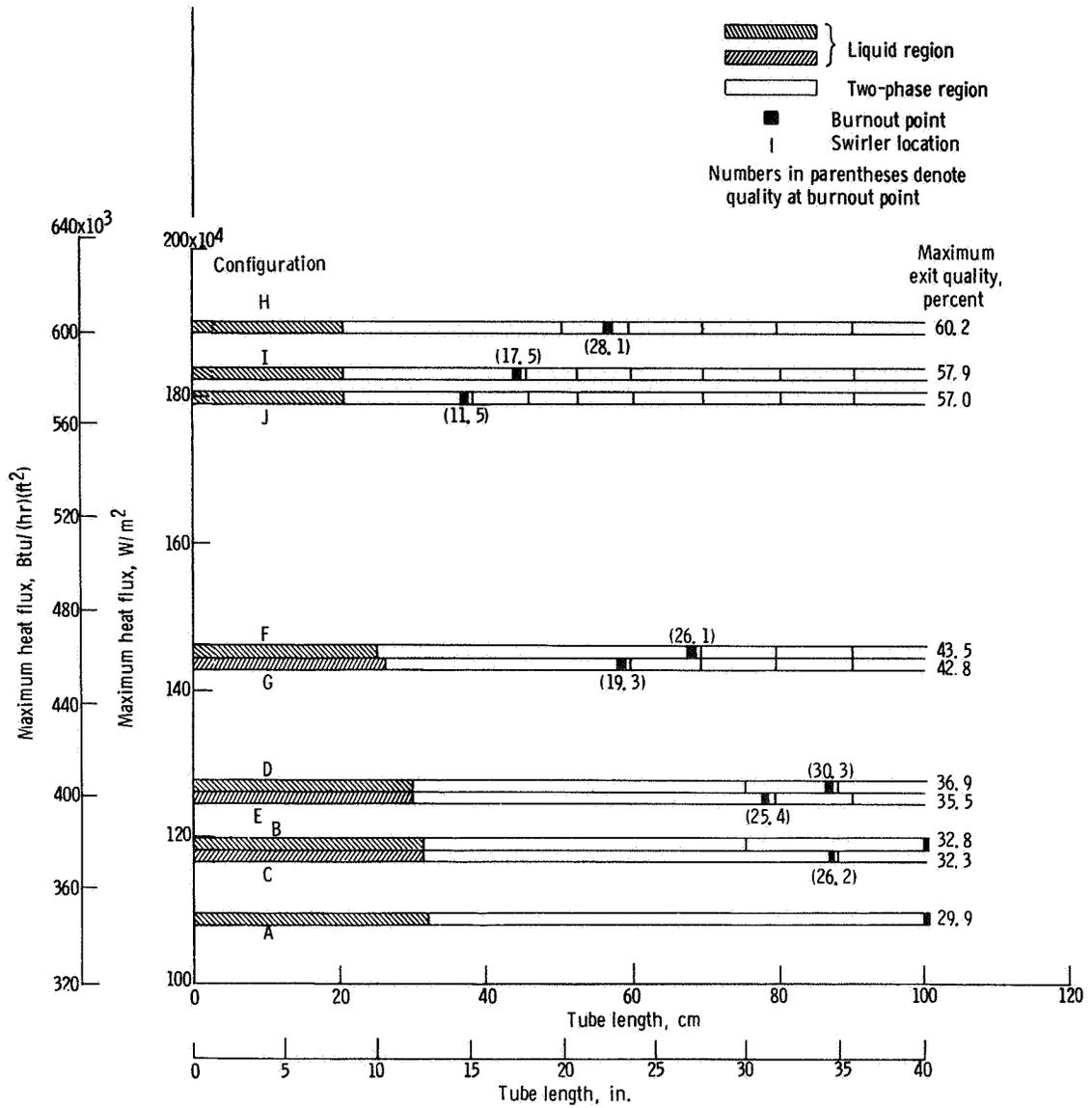
Figure 36. Summary of boiling crisis results for electrically heated tube with blade-type swirlers at flow rate of 50 g/sec (400 lbm/hr).

37

COMPARISON OF INSERTS AND
INLET RESTRICTORS

The best performance obtained from the various boiler combinations tested in water, and substantiated in potassium, was from a venturi-type converging-diverging nozzle followed by a tapered inlet-region plug extending into the nozzle diffuser and then a full-length helical wire insert. An attractive feature of such an inlet configuration is that by sufficiently preheating the liquid, flashing can be caused in the nozzle, giving a fixed location for the initiation of two-phase flow and a desirable flow regime entering the boiler proper. This procedure avoids instability problems associated with motion of the zero-heat-balance-quality interface and also the problem, often encountered with alkali metals, of nonequilibrium liquid superheat in the boiler tube. Preheating the liquid might increase the complexity of the system, but the benefits should be worth the cost.

It was found that the performance of inlet restrictors had strong effects on boiler performance. Further studies of various inlet devices are reported in appendix B, including some devices that were unsuccessful and one technique—the vortex flow inlet—that has considerable merit and potential but unfortunately was not thoroughly investigated.

Chapter 3

NONTUBULAR BOILERS

As is pointed out in the preceding chapters, swirl flow techniques generally improve boiler performance. But these swirlers also tend to promote rivulet flow with its associated problems and considerably increase the pressure drop. More novel approaches are to rotate the boiler or to construct the boiler as a cyclone. These nontubular boilers are the subject of this chapter.

ROTATING BOILER

Test Facility

Figure 37 is a sketch of the rotating-boiler test facility described more fully in references 79 and 80. Distilled water was pressure fed from the supply tank through a rotating face seal into the
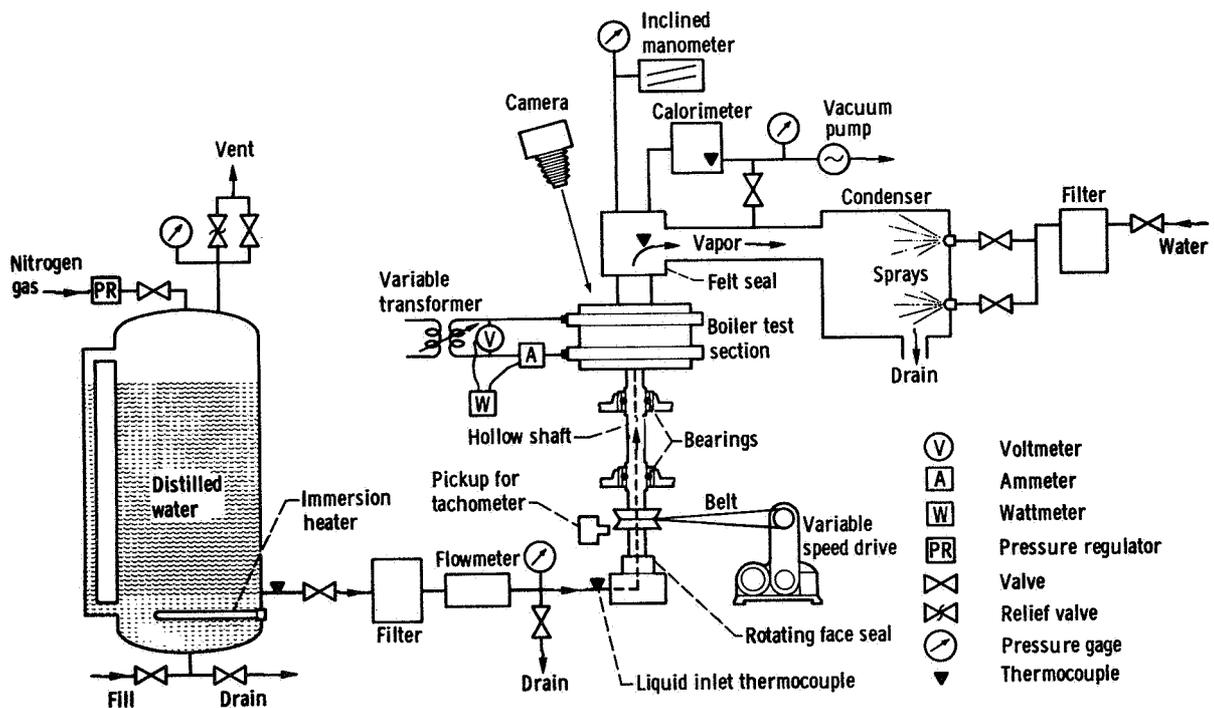

Figure 37   Schematic of test facility for rotating water boiler

CD-9170

39

10.2-cm-diameter by 5.1-cm-high test section of the boiler. The outlet vapor duct engaged a stationary felt-type seal in the pipe assembly leading to the atmospheric spray condenser.

As shown in figure 37, cameras were mounted above the boiler looking downward at the liquid-vapor interface. Throttling calorimeters were used to determine exit vapor quality. The photographic system and other instrumentation are described in more detail in reference 79.

General Results

Some general comments about the rotating-boiler operation are pertinent to an understanding of the data of references 79 and 80. The boiler had an approximately constant volume inventory of fluid but with a continuous throughflow, the rate of which was determined by the heating rate. At low heating rates (and therefore low flows), the boiler inventory was large relative to the throughflow, and pool boiling was approximated. Because of the annular symmetry of the boiler and the several small holes for the liquid inlet, the boiler inventory rotated with the heated wall, in wheel flow. This condition ideally simulated pool boiling at increased radial accelerations. At high heating rates, throughflow was larger and, at high accelerations, vigorous secondary-flow cells developed in the boiling annulus as a result of convection. This subject is discussed further in chapter 7 in the section Rotating Water Boiling.

The rotating boiler is a low-pressure-drop device. This is an important advantage in a Rankine–cycle system; however, it is partially offset by the power required to rotate the boiler. The liquid flow into the boiler and the vapor flow out were both steady. It was not necessary to add baffles or vanes in the boiler to correct for interface waviness or unbalance.

The rotative centrifugal accelerations, expressed herein as gravities (g's) are those acting normal to the heated cylindrical wall. At rotative accelerations below 25 g's, the parabolic shape of the interface became observable. Above 25 g's, the interface in the boiler was essentially a cylindrical, vertical surface concentric with the heated surface. Therefore, above 25 g's, the boiler is essentially insensitive to its orientation to earth gravity.

Below 14 g's, a constant fluid thickness could not be maintained during the boiling process, and no data were obtained. Part of this trouble was caused by corrosion, which permitted liquid to leak into the hollow rotating float. This leakage was discovered later and corrected. At all accelerations above 14 g's and at all flow rates, the float valve worked well.

In general, comments pertaining to the boiling action and the two-phase flow mechanisms are based on careful study of high-speed motion pictures, most of which were taken in color to provide good contrast and definition to the bubbles, interface, and droplets in the vapor space. The principal features to be seen in a typical frame from a high-speed motion picture taken through the top annular window are shown in figure 38. The outer circular arc is the edge (end view) of the cylinder The thin annulus of boiling fluid lies against this surface, which is the heated (outer) wall of the cylinder Vapor
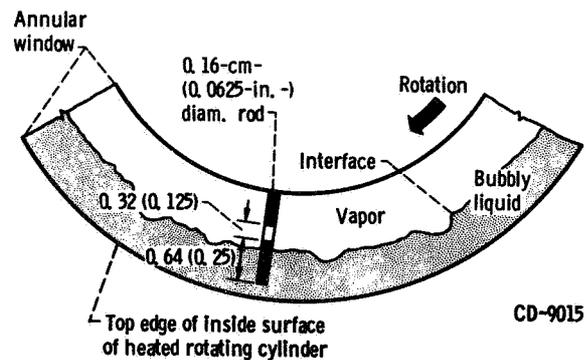

Figure 38. Typical view through top annular window of rotating boiler (Dimensions are in cm (in.).)

bubbles form at this surface and move radially inward to break at the interface. The 0.16-cm-diameter horizontal rod shown in most of the following photographs turns with the boiler and is used for visualization and scale purposes.

The boiling annulus at 25 g's is shown in figure 39 by three consecutive frames from a 16-mm motion picture taken at about 8000 frames per second. The heat flux was 280 kW/m^2 The interface is very irregular and turbulent at this gravity level. Many times, several vapor bubbles or clusters are pumped into a certain region and, upon reaching the

Figure 39. Sequence of three consecutive frames from high-speed motion picture of rotating boiler showing boiling and collapse of vapor dome at 25 g's and heat flux of 280 kW/m^2 (88 000 Btu/(hr)(ft^2)).

interface, balloon into large vapor "domes" before breaking. The dome to the left of the rod in figure 39 (top) is breaking open (from the left) to let out the vapor The liquid that forms the roof of the dome can be seen (center and bottom) pulling together into a ring of droplets that fall back into the interface. Occasionally, a drop or stream of liquid is propelled far into the vapor region beyond the interface. This liquid generally returns to the interface after completing an arcing trajectory. The interface activity at various accelerations is clearly shown in the motion picture supplement to reference 79 (film supplement C-253, available on loan).

Effects of acceleration and heat flux on nucleate boiling. — The effect of acceleration on boiling can be seen by comparing the sequence shown in figure 39 with figure 40. The photographs are all at the same heating rate of 280 kW/m^2 but at steadily increasing accelerations to 400 g's (fig. 40(d)). The bubble size and number markedly decrease, and the interface becomes more continuous and smooth at higher accelerations. At 400 g's the fluid in the annulus is mostly clear liquid, with only an occasional cluster of bubbles. The rod can be seen easily, as can the liquid feed holes (dark spots) in the bottom plate of the boiler Figures 40(c) and (d) show the typical bubble patterns at high accelerations, clusters of bubbles separated by relatively clear liquid. This pattern strongly suggests that secondary-flow convective cells exist, with the bubbles appearing in the warmer updrafts. So few bubbles exist at the highest g's, however, that transport of all the heat by vapor bubbles alone appears very doubtful. Direct evaporation at the interface must also occur This secondary-flow and evaporation process is illustrated and discussed in motion picture supplement C-253 to reference 79.

Boiling at low heat flux (55 kW/m^2) is illustrated in figures 41(a) and (b) at 25 and 100 g's, respectively Figure 41(a) shows two consecutive frames. At 100 g's (fig. 41(b)),
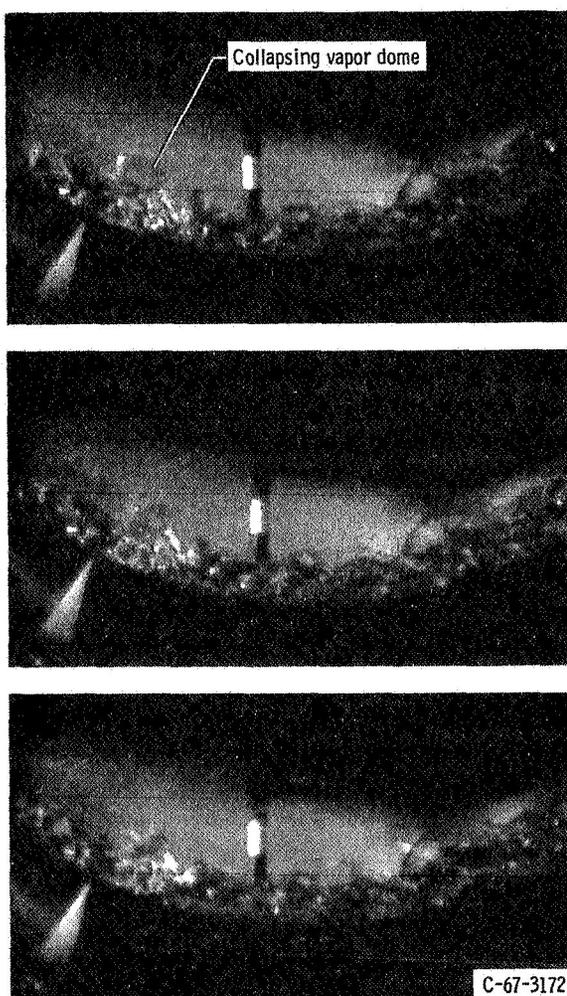
(a) Acceleration, 50 g's

(b) Acceleration, 100 g's.

(c) Acceleration, 200 g's.

(d) Acceleration, 400 g's.
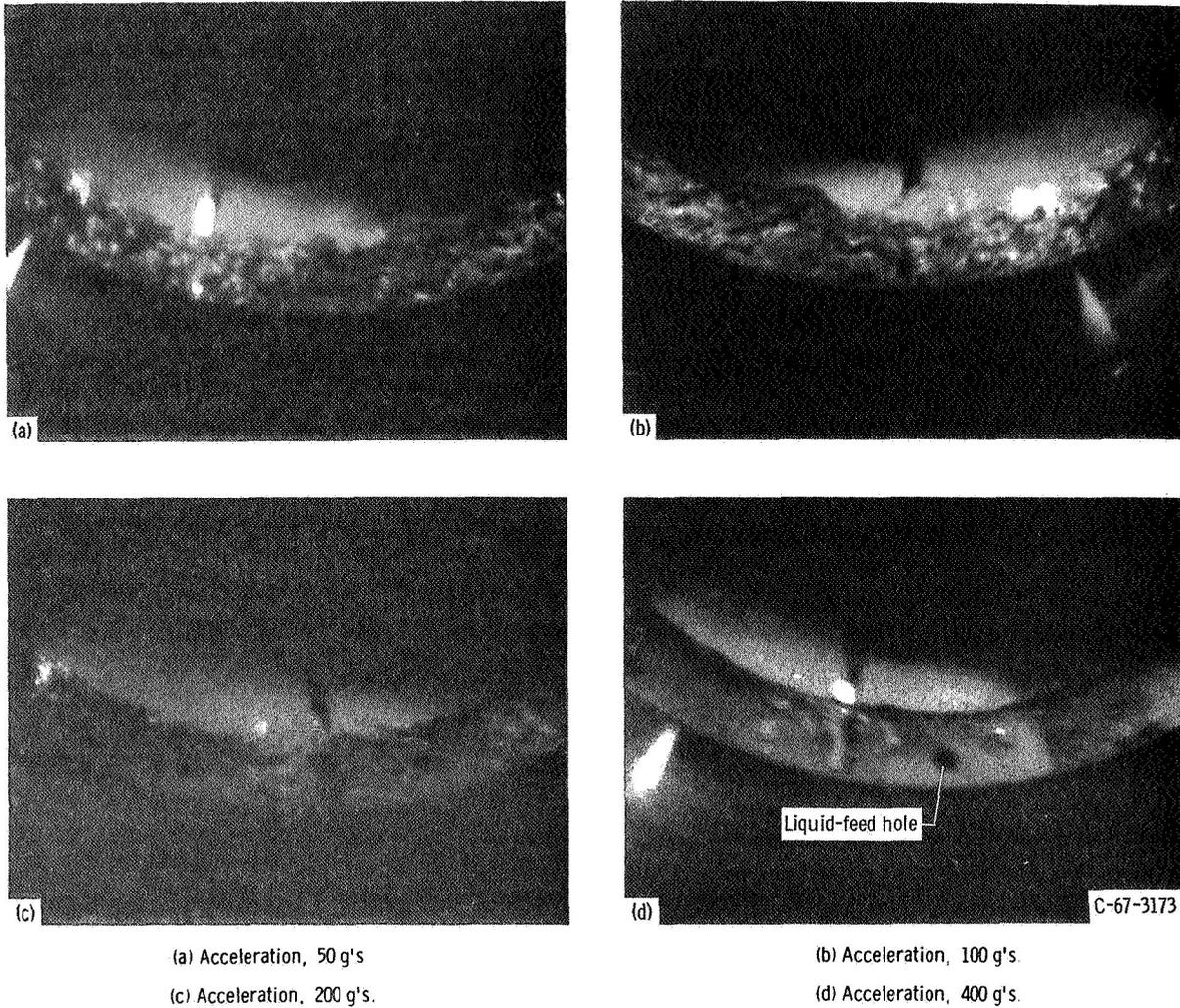
Figure 40.   Effect of increasing gravity on rotation boiling at constant heat flux of 280 kW/m^2 (88 000 Btu/(hr)(ft^2)).

individual bubbles and chains of bubbles can be seen easily It appears that the bubbles, upon nearing the interface, grow larger, agglomerate, and spread out laterally along the interface as they break

Boiling at high heat flux (1480 kW/m^2) is shown in figure 42. Figure 42(a), at 100 g's, appears almost foamy The rod cannot be seen through the 0.64 cm of boiling fluid At 400 g's (fig. 42(b)), the rod can be seen, as well as many areas of clear liquid This heat flux is comparable to or above a normal boiling crisis condition for pool boiling at 1 g

(ref 99) Previous experimenters (refs. 100 and 101) have established that the boiling crisis heat flux increases with acceleration to approximately the one-fourth power No boiling crisis experiments were attempted in reference 79 or 80, although in reference 80 about twice the normal boiling crisis heat flux for 1 g at atmospheric pressure was obtained at 400 g's with stable boiling.

The effect of heat flux on boiling at 100 g's can be seen by comparing figure 42(a) at q = 1480 kW/m^2, figure 40(b) at q = 280 kW/m^2, and figure 41(b) at q = 55 kW/m^2
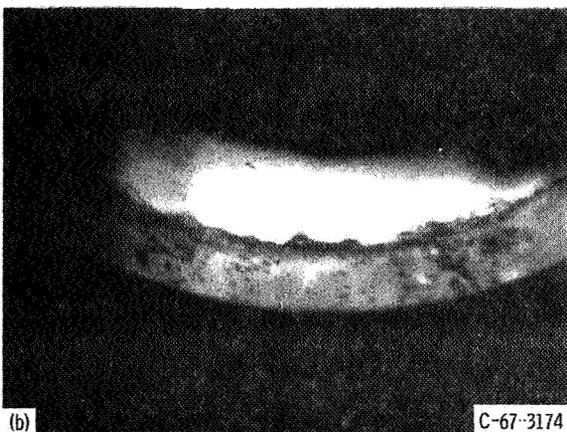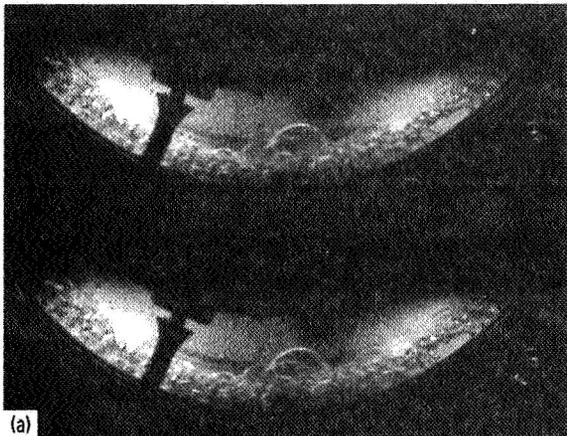
(a) Acceleration, 25 g's.

(b) Acceleration, 100 g's.

Figure 41. Rotating boiler at low heat flux of 55 kW/m^2 (17 400 Btu/(hr)(ft^2)).

Exit vapor quality. – The exit vapor quality in reference 79 was always above 0.99. The quality apparently increased with acceleration and inlet temperature and decreased with heating rate. Except for five observed cases of exit vapor superheat, the measured exit vapor temperatures agreed with the saturated vapor temperatures calculated from measured exit pressures within ±0.06 K.

Evidence of vapor superheat is remarkable. The vapor outflow could not come in contact with the heated surface, as it can in conventional boiler tubes near the exit,

Flash photographs with a 1-μsec duration are shown in figure 43 for a heat flux of 370 kW/m^2 At 73 g's a continuous cloud of bubbles is apparent along the interface (fig. 43(a)), whereas at 475 g's (fig. 43(b)), one isolated cluster of bubbles appears. Elsewhere, the interface is a thin gray line.

Unquestionably, interface disturbances were reduced and smoothed out by high accelerations. The bubbles and voids were much less numerous and appeared smaller at higher g's. Apparently, acceleration can be increased to overcome and suppress boiling at any conventional boiling heat flux level.

(a) Acceleration, 100 g's.

(b) Acceleration, 400 g's.

Figure 42   Rotating boiler at high heat flux of 1480 kW/m^2 (468 000 Btu/(hr)(ft^2)).
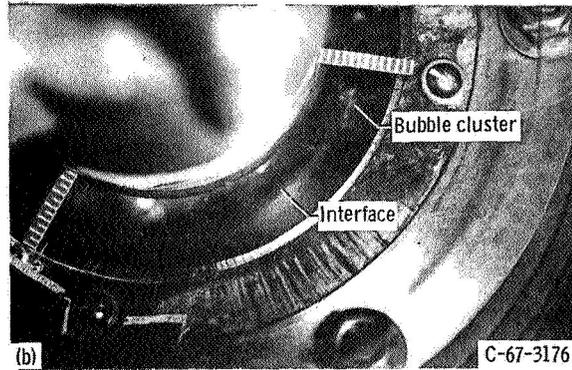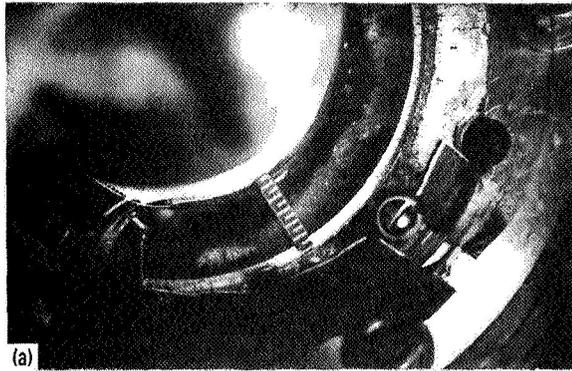
(a) Acceleration, 73 g's.

(b) Acceleration, 475 g's.

Figure 43. Short-duration flash photographs of rotating boiler in operation at heat flux of 370 kW/m^2 (117 000 Btu/(hr)(ft^2)).

where the liquid film does not completely cover the tube wall. At very high accelerations, vapor apparently left the interface at temperatures several degrees above the vapor saturation temperature, probably as a result of the pressure rise within the boiling annulus. For example, at 400 g's the liquid saturation temperature at the boiler wall was 5.8 K hotter for a 0.64-cm-thick annulus of water than at the interface (corresponding to a pressure rise of 23 kN/m^2). The hotter liquid and vapor created near the heated wall were probably centrifuged quickly to the interface, and evaporation occurred directly across the sharp interface. Ultimately, as the acceleration

increased and the heating rate was held constant, all the vapor was generated by evaporation at the interface and nucleate boiling was suppressed.

Average void fraction. – As described in reference 80, a nonboiling liquid annulus was located above and connected to the two-phase fluid in the boiling chamber. This yielded measurements that allowed the average void fraction in the two-phase annulus to be calculated. These data are shown in figure 44 for six levels of acceleration and three levels of heat flux.

Even though the uncertainty in these data is fairly large because of the difficulty in measuring the thickness of the two-phase fluid annulus, a definite trend can be observed. As the acceleration increases at a fixed heating rate, the average void fraction decreases. This shows there are fewer vapor voids in the boiling fluid, presumably because there are fewer active nucleation sites and also smaller size bubbles. This trend agrees with the results of Graham and Hendricks (ref 102), who showed that both the number of active sites and the maximum bubble departure diameter decrease with increasing
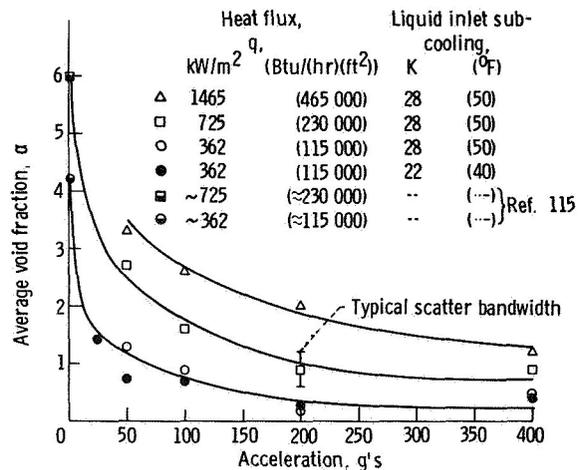

Figure 44. Average void fraction of two-phase boiling annulus.

acceleration. It is also apparent in figure 44 that, at any given rotative speed, the void fraction increases with heat flux, as expected.

CYCLONE BOILER

The cyclone boiler concept (fig. 9) represents an attempt to combine the benefits of the rotating boiler with the simplicity of having no moving parts. The feed is flashed into the boiler tangentially in such a manner that a vortex flow pattern is established. The liquid is centrifuged to the wall and then is driven toward the apex of the cone by secondary-flow effects (ref. 81) augmented by surface tension and, in some cases, gravity, while the vapor exits from the opposite end

Description

In order to study two-phase flow in a cyclone boiler, in particular the effect of inlet geometry, air-water flow tests were conducted with the transparent section shown in figure 45 Two cyclone boiler configurations were tested, as shown in figure 46, with the only difference being the inlet With inlet 1, which was quite similar to that of reference 81, it was found that a smaller inlet was required to get complete wetting of the walls. Thus, a metal insert was added as shown in figure 46(b). Also an additional 0.71-cm liquid drain had to be added.

Results

Figure 47 shows the operation of the cyclone boiler at typical conditions with inlet 2 (fig. 46(c)). The water flow rate was held at ~80 g/sec (figs. 47(a) and (b)), and the airflow rate was then increased until the liquid film covered the entire cyclone boiler wall. Figure 47(a) shows the cyclone boiler
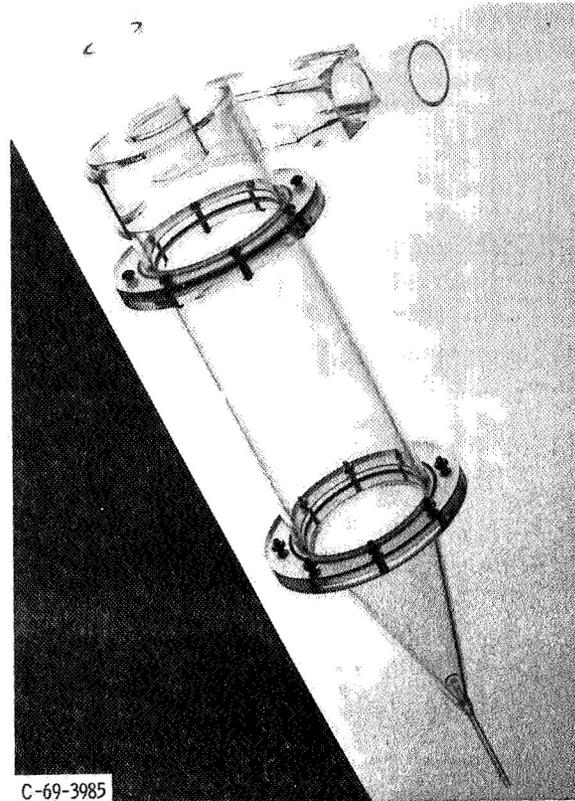
C-69-3985

Figure 45. Transparent test section for air-water tests of cyclone boiler

with an airflow rate of 3.5 g/sec, not quite sufficient to cause complete wetting. In figure 47(b) the airflow rate is 8.3 g/sec, and the cyclone is completely wetted The airflow rate was then further increased and the water flow rate decreased, simulating an increase in vapor quality Complete wetting and no liquid carryover in the airstream were obtained for an airflow rate of 11 1 g/sec with a water flow rate of 49.2 g/sec, as shown in figure 47(c). Finally, for an airflow rate of 17.8 g/sec and a water flow rate of 34.0 g/sec, a dry streak can be seen, as well as some liquid droplets being carried over in the air exit pipe Note that these air and water flow rates simulate inlet conditions to a cyclone boiler, and experiments have not been performed to verify the effects of heat addition and phase change within the cyclone

45

(a) Cross-sectional side view with inlet 1.

(b) Bottom view of inlet 1 for cyclone separator showing metal insert.

(c) Top view of inlet 2.
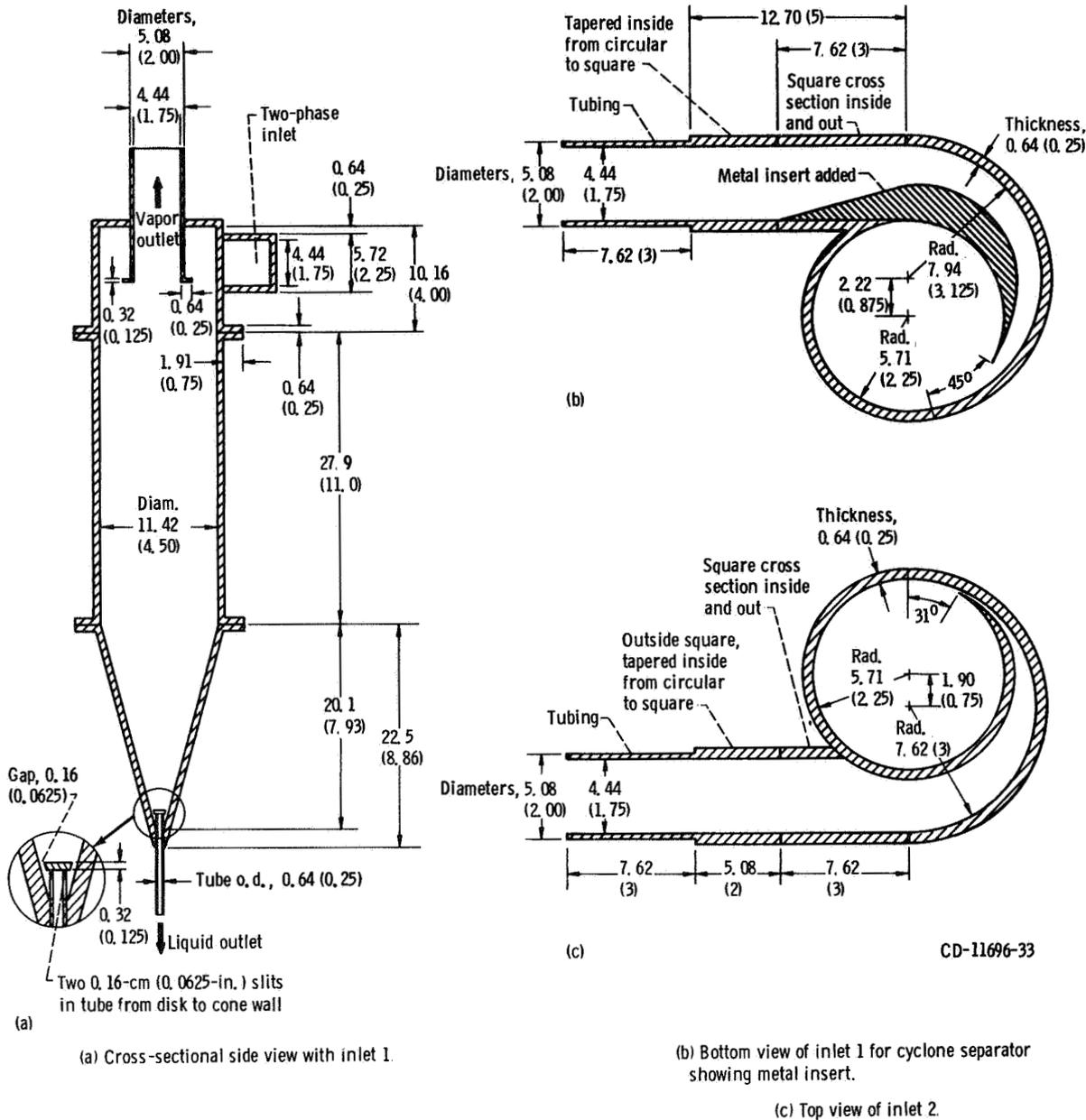
Figure 46.   Transparent, unheated cyclone boiler test section.   (Dimensions are in cm (in.) unless indicated otherwise.)

Discussion of Cyclone Boilers

The cyclone boiler appears to be capable of providing moisture-free vapor at a steady rate. Distinct separation of liquid and vapor can be achieved without the use of inserts, thus making the cyclone boiler a relatively low-pressure-drop device. The cyclone boiler should have many of the advantages of the rotating boiler without the moving parts.

46
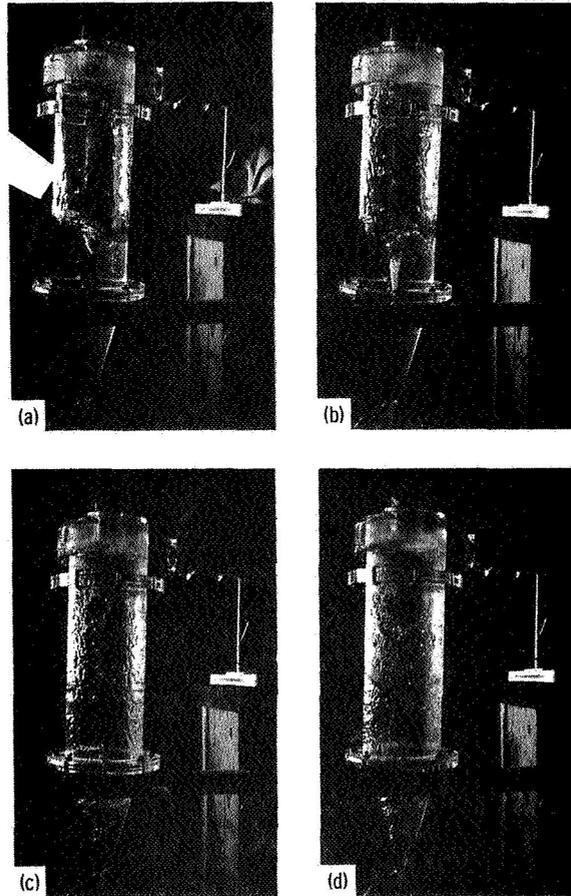
(a) Incomplete wetting; no liquid carryover Airflow rate, 3.5 g/sec (28 lbm/hr); water flow rate, 81.8 g/sec (649 lbm/hr).

(b) Complete wetting; no liquid carryover Airflow rate, 8.3 g/sec (66 lbm/hr); water flow rate, 80.5 g/sec (639 lbm/hr).

(c) Complete wetting; no liquid carryover Airflow rate, 11.1 g/sec (88 lbm/hr); water flow rate, 49.2 g/sec (390 lbm/hr).

(d) Incomplete wetting; some liquid carryover Airflow rate, 17.8 g/sec (141 lbm/hr); water flow rate, 34.0 g/sec (269 lbm/hr).

Figure 47   Typical operating conditions for unheated cyclone boiler

Part II

BOILING CHARACTERISTICS

Various new boiler configurations that have been tested with conventional and alkali metal fluids have been described in part I. In the general problem of designing once-through boilers, various thermal and hydraulic parameters must be estimated. In order to aid in this design problem, part II presents experimental data and empirical correlations for these boiling characteristics: specifically, stability, initiation of two-phase flow, pressure drop, and heat transfer.

Chapter 4

STABILITY AND DYNAMICS PROBLEMS

In this chapter some problems related to the stability and dynamics of boiling sodium and water are discussed. The results presented were obtained during studies related primarily to heat transfer.

SODIUM BOILER OSCILLATIONS

Oscillations of the boiling-fluid flow rate, pressure, and temperature were frequently encountered during the sodium-boiling investigation (ref 83). The variations in time of certain variables were recorded as a possible aid in characterizing and understanding the range of boiler performance obtained. For this purpose the output of the flowmeters, the boiling-fluid strain-gage pressure transducers, and two thermocouples located on the shell wall were recorded on a multichannel oscillograph. Typical traces are shown in figure 48. (Considerable noise is apparent in some of the signals, particularly flow rate, which was attributed to readout system deficiencies as well as to the large electric heaters.) For the two-phase inlet condition (flashing caused by the orifice pressure drop), the boiling-fluid flow rates and pressures exhibit a regular oscillation with a dominant frequency of 1 to 2 Hz (cycles/sec). For the two-phase inlet tests with no boiling crisis occurring, the amplitude of the flow and pressure oscillations varied from that barely detectable to approximately ±10 percent, and the shell

wall thermocouples were steady With boiling crisis occurring, somewhat larger amplitudes were obtained and the shell wall temperatures began to show some variation.

When the boiling-fluid inlet condition was alternately two phase and liquid, the oscillations became more complicated and irregular, the amplitude of the flow and pressure variations increased markedly, and the shell wall temperatures varied continuously

For the case of the boiling-fluid inlet condition being in the liquid phase, the flow, pressure, and temperature traces were either very steady or extremely unsteady In fact, the liquid inlet condition gave the most steady and the most unsteady results of the entire investigation. When unsteady, the oscillations grew and became increasingly complicated and irregular, and a lower frequency (1/4 to 1/3 Hz) appeared than was obtained with the two-phase inlet results. In some cases the oscillations became so severe that backflow occurred, which sometimes shut off the heaters by activating safety interlocks.

In all cases the inlet pressure and flow oscillations were out of phase by approximatley 180° For the liquid inlet case, the inlet and exit pressures were always in phase, while for the two-phase cases they were both in and out of phase. Generally, the pressures were in phase for the two-phase case only at conditions of low quality, high heat-transfer coefficients, and small
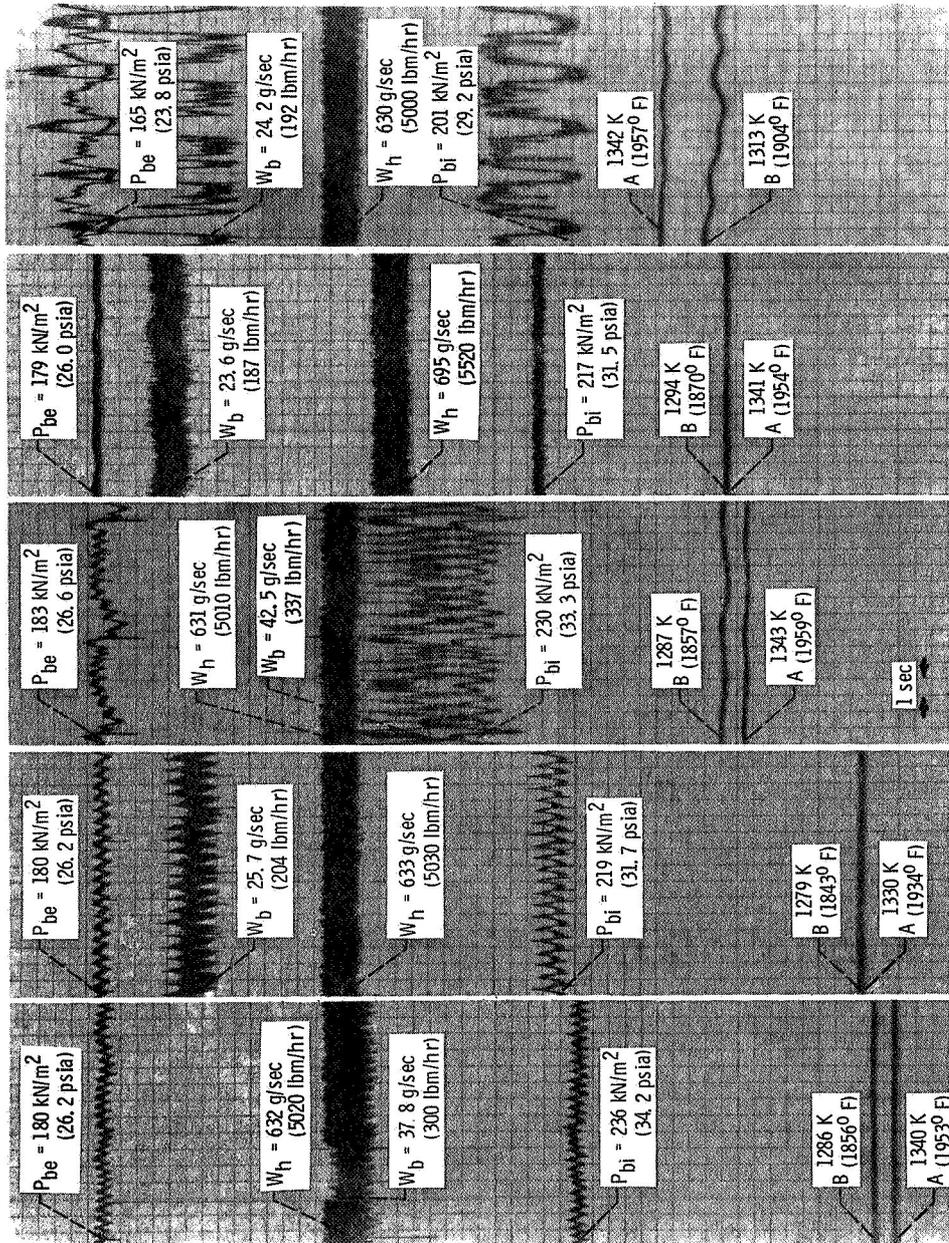
51

Figure 48. Typical oscillations of flow rates, pressures, and shell wall temperatures for sodium boiler with various boiling-fluid inlet conditions. Only mean values are listed; A and B denote shell wall temperatures at 114 cm (44.9 in.) and 10 cm (4.1 in.), respectively.

52

oscillations. As concluded in reference 83, any attempts to analyze these oscillations and boiler instabilities must take into account the particular conditions of the tests, including the large liquid inventory outside the boiler, the expansion tank, the condenser coolant bypass loop, and the compressibility of the feedline for the two-phase inlet tests.

SUBCOOLED-WATER-BOILING PRESSURE FLUCTUATIONS

Subcooled boiling generates vapor within a fluid whose bulk temperature is below its saturation temperature. Thus, when a cold liquid contacts a sufficiently hot surface, vapor forms at the hot wall and some of it condenses in the cold liquid stream. This vapor formation and collapse can produce high-frequency and high-amplitude pressure fluctuations, as reported in reference 89. In this study, the fluctuations repeated with enough regularity that their amplitudes could be determined. The effects of pressure, heat flux, and amount of subcooling on the amplitude of the inlet pressure fluctuations are shown in figures 49 and 50. At high heat fluxes, the amplitudes of pressure fluctuations can approach or even exceed the average pressure level. The amplitude of the fluctuations increases from the inception of boiling to some heat-balance liquid bulk temperature about 20 to 45 K below saturation, depending on the pressure and heat flux, and then decreases to approach zero as the liquid bulk temperature approaches saturation. It seems reasonable, therefore, that the fluctuations are caused by void collapse. A similar phenomenon was observed in cavitation studies, where cavitation damage (weight loss) was plotted against fluid temperature. Such graphs are given in reference 103, and the similarity between the curve shapes therein and those in figures 49 and 50 is very apparent.
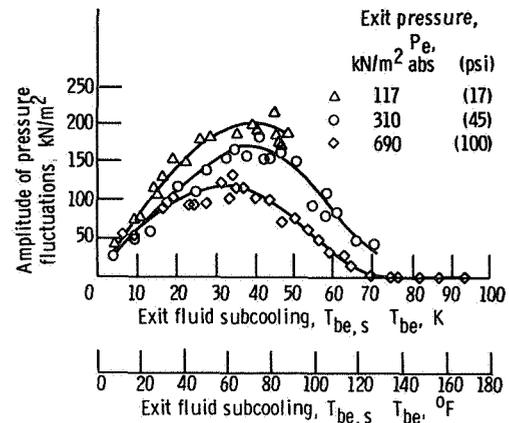
Figure 49. Inlet-plenum pressure fluctuations as function of boiler-exit subcooling at various pressures. Mass velocity, 2790 kg/(m²)(sec) (2.06x10⁶ lbm/(ft²)(hr)); heat flux, 3150 kW/m² (1.0x10⁶ Btu/(hr)(ft²)).
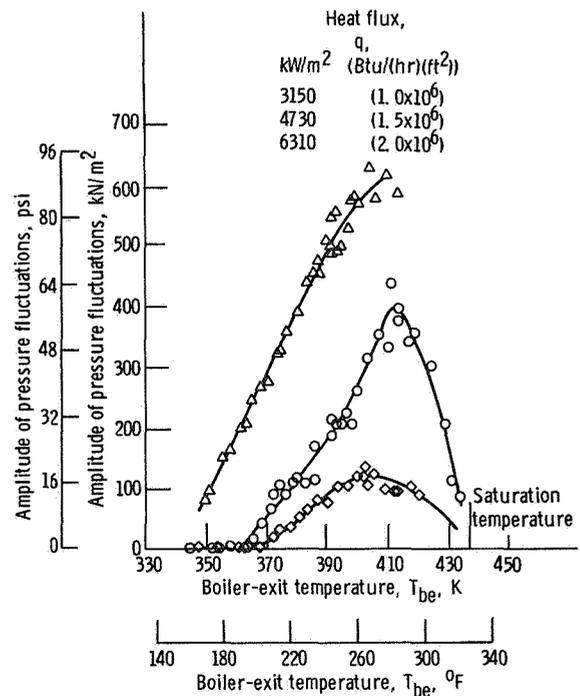
Figure 50. Inlet pressure fluctuations as function of boiler-exit temperature for various values of heat flux. Mass velocity, 2790 kg/(m²)(sec) (2.06x10⁶ lbm/(ft²)(hr)); exit pressure, 690 kN/m² abs (100 psia).

53

STABILITY CRITERIA

The main thrust of this publication has been to chronicle the various ways in which boiling stability has been improved by forcing the flow into desirable, stable regimes. General solutions to problems of boiler dynamics are beyond the scope of this report However, limited stability criteria have been presented in references 3 and 4 for subcooled boiling and in reference 9 for low-net-quality boiling. These experiments were performed on water boiling in an electrically heated tube. In addition, extensive and detailed boiler dynamics studies, dealing primarily with boiler and flow system transfer functions, are presented in references 10 to 14 These experiments were performed by using heat exchangers wherein Freon was boiled, with pressurized water as the heat source

Chapter 5

INITIATION OF VAPORIZATION

This chapter deals with the initiation of vaporization in liquid metals. The initiation of vaporization in conventional fluids is well documented in the literature (see the section BACKGROUND and also the bibliography).

BULK SUPERHEAT IN LIQUID SODIUM

The initiation of boiling was one of the major problems encountered in the sodium-boiling investigation (ref 83). This problem arises from the ability of sodium to maintain itself in a liquid state at temperatures considerably above saturation. This condition of liquid superheat was experienced by Bond and Converse (ref 19) and by Edwards and Hoffman (ref 20) for both potassium and sodium in natural-circulation and forced-flow loops with constant wall heat flux. A series of tests were made in reference 83 to determine the maximum bulk superheat attainable at boiling initiation. Runs were made wherein boiling was initiated at the boiler exit by raising the heating-fluid inlet temperature and also by lowering the boiling-fluid exit pressure with all other conditions held constant. The results of these tests are shown in figure 51 The bulk superheat is defined as the boiling-fluid bulk temperature minus the local saturation temperature at the point just before boiling was initiated. Included in the figure are the predicted bulk superheats obtained from

static force balances on a spherical bubble as given by the relation obtained by rewriting equation (1)

$$P_s - P_l = \frac{2\sigma}{r}$$

and using the vapor-pressure curve of reference 104. This computed bubble radius is a measure of the effective cavity size required for the initiation of nucleation.

Figure 51. Liquid bulk superheat required to initiate boiling at boiling exit for sodium (ref. 83). Nominal heating-fluid flow rate, 0.63 kg/sec (5000 lbm/hr).

The experimental results appear to follow a line of constant radius ($\sim 8.1 \times 10^{-5}$ cm). No significant differences in bulk superheat appear to be caused by either the method of boiling initiation or the boiling-fluid flow rate. Note that, because of the large heating-flu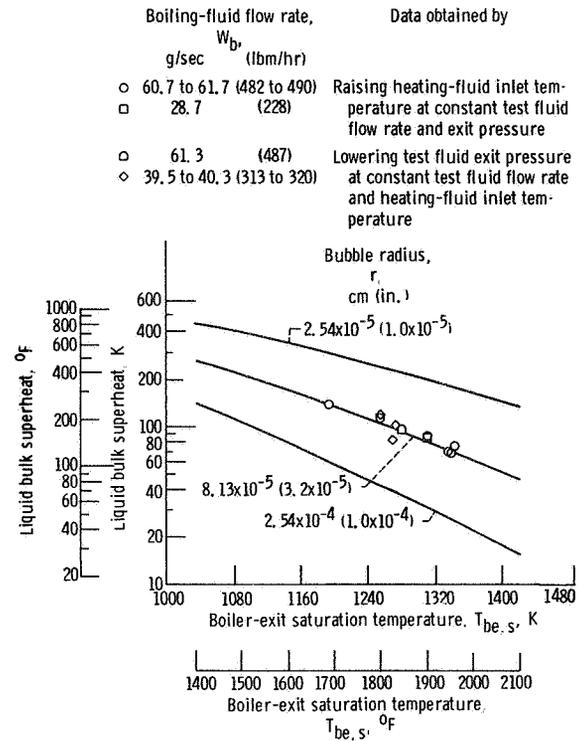id flow rate relative to the boiling-fluid flow rate, the exit region of the boiler during all-liquid flow was essentially isothermal with zero heat flux. The effective radius indicated by the data of figure 51 is extremely small, but photomicrographs of the niobium–1-percent-zirconium tube wall given by Bond and Converse (ref. 19) indicate that the radii of their available effective cavities were in the range of 1.3×10^{-5} to 2.5×10^{-4} cm. Edwards and Hoffman (ref. 20) also indicated effective cavity sizes of the same order of magnitude for the initiation of potassium boiling in a 316 stainless-steel "as received" tube.

Holtz (ref. 22) and Chen (ref. 23) have suggested that the incipient boiling condition is determined by the effective cavity size corresponding to the maximum cavity deactivation condition (maximum pressure and minimum temperature) encountered before nucleation. To apply Chen's prediction, however, requires knowledge of the cavity geometry, contact angle, and residual inert-gas pressure in the cavity as well as the prior pressure-temperature history. If a cylindrical cavity with a residual inert-gas partial pressure of 6.9 kN/m² absolute is assumed, Chen's analysis predicts that a cavity of 8.9×10^{-5} cm would give approximately the experimental values of bulk liquid superheat for boiling incipience obtained in reference 83.

phase. The maximum amount of liquid tension (or superheat) supported before the inception of vaporization is of prime importance in determining how far the venturi pressure must be lowered, or its flow rate increased, to initiate two-phase flow.

Two different types of incipiency points were detected during the experimental program of reference 105:

(1) Incipient cavitation (determined by the output of the accelerometer attached to the venturi body): The sudden increase in amplitude of the "noise" signal was taken as an indication of bubble collapse.

(2) Incipient flow-limited condition (determined by the sudden change in the pressure-drop characteristics of the venturi): The nearly constant mass-flow rate with progressively larger pressure drops across the venturi was taken as an indication of greatly increased volume generation of vapor downstream of the venturi throat. In some instances the cavitation and flow-limited incipiency points coincided; in other cases, cavitation was detected prior to flow-limited behavior.

The incipiency results obtained in reference 105 are presented in figures 52 to 54 in plots of pressure at the throat P_t as a function of nozzle inlet liquid temperature. This type of presentation permits direct comparison of incipient boiling data with the data of reference 105 for potassium flowing adiabatically through a variable pressure field. In addition, vapor initiation tests with potassium and water are described in detail in appendix B, including some important flow-system hysteresis effects.

Incipient Cavitation

The minimum values of throat pressure P_t obtained before cavitation noise was detected by the accelerometer are plotted in figure 52 as a function of nozzle inlet temperature T_{ni}. The throat pressures were

LIQUID TENSION FOR POTASSIUM AT INCIPIENT CAVITATION

An important aspect of a cavitating venturi as a potassium-boiler inlet device is its behavior at the initial appearance of the vapor
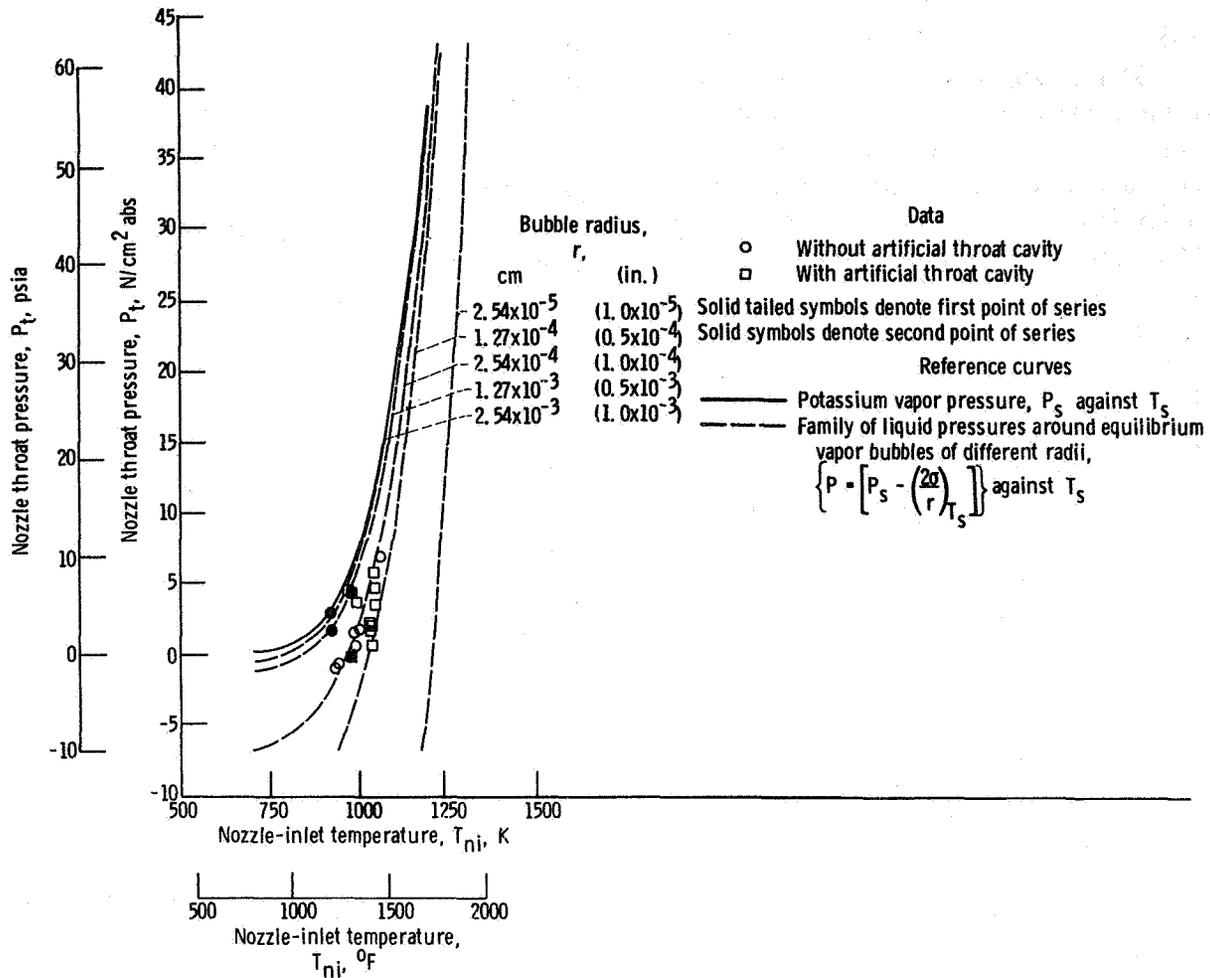
Figure 52. - Throat pressure as function of inlet temperature for incipient cavitation.

determined from the liquid characteristics of the venturi nozzle. The results cover two series of runs: with and without an artificial throat cavity (ref. 105). Also identified individually in this figure are the first and second (chronologically) incipient cavitation points for each series. Superimposed on the data are two types of reference curves:

(1) The potassium vapor-pressure curve (solid)

(2) A family of pressure-temperature curves (dashed) representing the liquid pressures necessary to maintain a force balance around vapor bubbles of different radii at thermal equilibrium with the liquid, calculated from equation (1)

The following conclusions can be drawn from figure 52:

(1) Fluid conditions for incipient cavitation at the throat of the venturi were not at equilibrium. This nonequilibrium, for most of the data, fell between the curves for bubble radii of 2.54×10^{-4} and 1.27×10^{-4} cm. The few points which deviated are discussed in items 2 and 3.

(2) The first incipient cavitation points in each series, with and without the artificial throat cavity, occurred very close to the vapor-pressure curve. This behavior could have been caused by residual argon trapped in surface cavities when the loop was filled with potassium. It could have resulted in larger effective nucleation sites at first, but these

57

sites must have subsequently become liquid filled.

(3) The artificial cavity at the throat did not have any effect on the mean value of the liquid tension obtained. This indicates that in the adiabatic case, neither the 0.02-cm-diameter reentrant hole nor the 0.0013-cm annular gap between the cavity insert and the drilled hole were generally active nucleation sites. However, a few of the incipiency points approached the $r = 1.27 \times 10^{-3}$-cm line, indicating the artificial cavity may have sometimes been active.

Onset of Flow-Limited Condition

The results obtained for the onset of flow-limited behavior are presented in figure 53. The reference curves are the same as those for figure 52. The data plotted are throat pressures, measured immediately before the sudden change in pressure-drop characteristics, as a function of nozzle inlet temperature. If the cavitating venturi is to be used as a boiler inlet, this transition point may be of greater practical importance than the inception of cavitation noise.

The following conclusions can be drawn about the onset of the flow-limited condition:

(1) Fluid conditions at the throat were not at equilibrium, throat pressures were as much as 110 kN/m^2 below vapor pressure.

(2) The throat pressures at the onset of flow-limited behavior followed the trend indicated by constant-radius lines. There was no appreciable difference in the mean value of
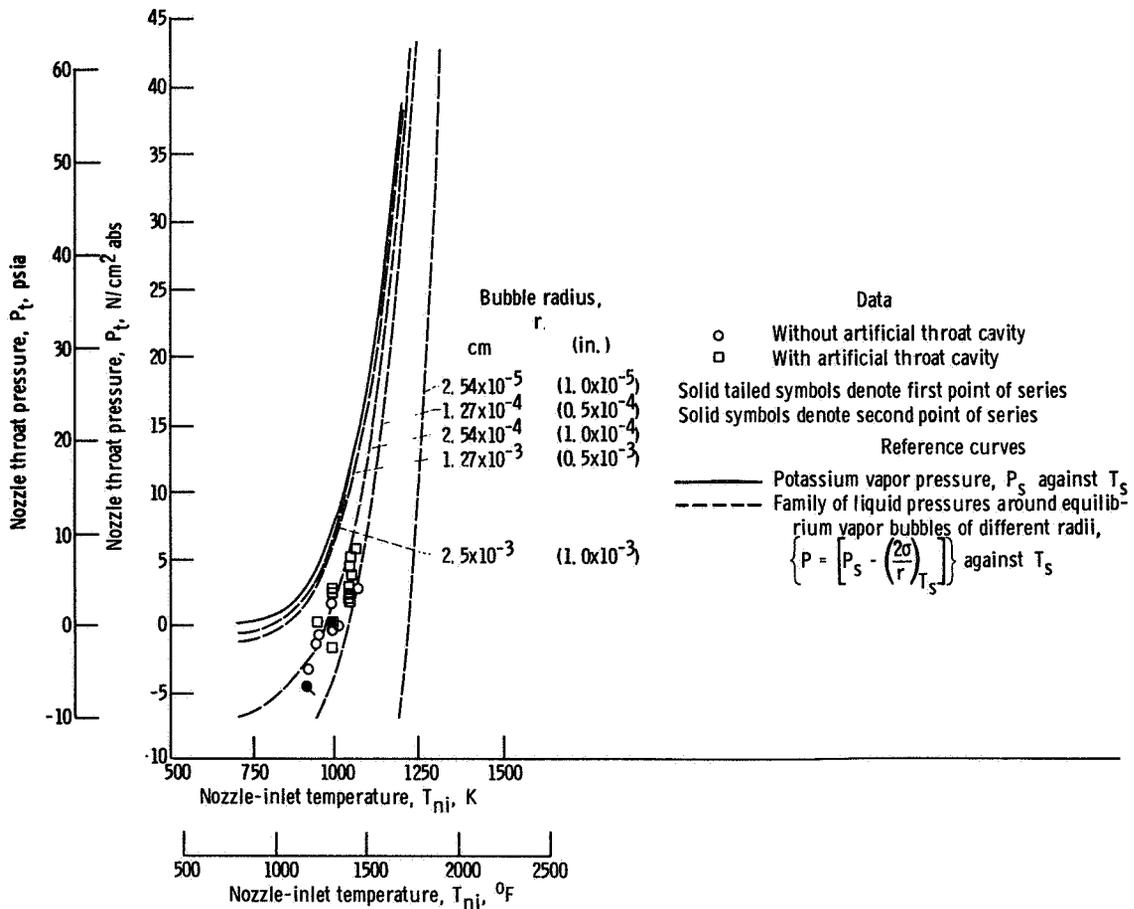
Figure 53. - Throat pressure as function of inlet temperature for onset of flow-limited conditions.

58
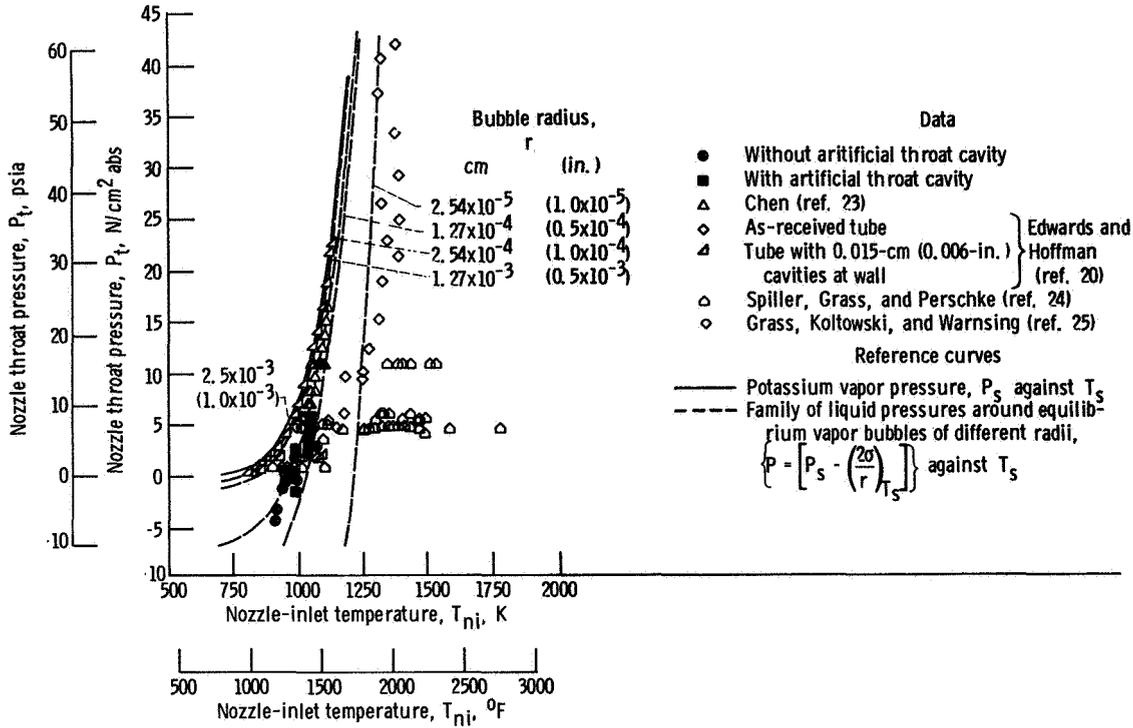
Figure 54. - Comparison of data for onset of flow limited condition with potassium boiling-initiation data.

critical radius required to fit these data from that for the inception of cavitation (fig. 52), but the incipient cavitation data show more randomness.

(3) The artificial cavity had no effect on the onset of flow-limited behavior

Comparison with Data on Boiling Initiation

The incipient flow-limited data of reference 105 are replotted in figure 54, along with data on incipient boiling of potassium obtained from the literature. The reference curves are the same as those in figures 52 and 53. No data on the onset of either cavitation or flow-limited behavior were found in the literature. A few investigators, however, have published data on the initiation of boiling in potassium. Shown in figure 54 are the data of Edwards and Hoffman (ref. 20), Chen (ref. 23); Spiller, Grass, and Perschke (ref. 24), and Grass, Kottowski and Warnsing (ref. 25). The

methods used by these investigators to promote boiling and to determine the points of incipiency were quite varied. Great variation also existed in the types of surfaces used, the range of heat fluxes, the potassium purity, the gas content, and the fluid velocity, among other factors, as pointed out by Fauske (ref. 106).

The data of reference 24 on stagnant potassium show a large scatter, and the results appear to have no relation to the surface tension curve. The other referenced data do appear to follow surface tension trends. However, the values of critical bubble radius vary greatly from one investigator to another. The adiabatic flow-limited data obtained in reference 105 seem to agree best with Chen's data (ref. 23). This should be expected, because in his tests the fill and testing procedure and the nature of the test surface most closely approximated the conditions of reference 105.

59

Comparison of the adiabatic results of reference 105 with those of Edwards and Hoffman (ref. 20) shows the difference in effect of relatively large cavities at the wall between the adiabatic and diabatic cases. With heat addition, the presence of eight 0.015-cm-diameter holes in the wall markedly decreased the liquid superheat for incipient boiling. The adiabatic data, as mentioned previously, showed no effect on the incipient flow-limited condition from the 0.02-cm-diameter reentrant cavity or the 0.0013-cm annular gap around the cavity insert. This indicates that potassium flooded these cavities; therefore, such cavities may become active nucleation sites if heated but do not under adiabatic conditions.

Chen's data (ref. 23) indicate a critical radius of 2.5×10^{-4} cm, similar to the data of reference 105. The Edwards and Hoffman data (ref. 20) suggest a critical radius smaller than 2.5×10^{-5} cm for the as-received surface, while the stagnant potassium data of Spiller (ref. 24) show no definite critical radius but indicate very large superheats.

Chapter 6

PRESSURE DROP

Knowledge of the pressure drop in boiling is important in both power systems and cooling applications. The pressure drop must be known to determine local saturation temperatures and pumping power requirements. In addition, the pressure drops of the boiler and any inlet device are important parameters in the stability of the system.

to the boiler-inlet pressure P_{bi} which continues to decline. This insensitivity of the nozzle inlet to boiler-inlet (nozzle exit) pressure variations tends to isolate the boiler from the feed system, when cavitation or flashing occurs at the inlet nozzle.

(2) The boiler-inlet pressure P_{bi} generally decreases with decreasing exit-plenum pressure. But at very low exit

TYPICAL DATA

The problems of pressure drop are illustrated by typical plots of data (ref. 87) for a water boiler with full-length helical wire insert, inlet nozzle, and inlet-region plug, as shown in figure 55. The data were taken with a boiling-fluid flow rate of approximately 10 g/sec and a heating-fluid flow rate of approximately 1 kg/sec. In figure 55, the nozzle-inlet pressure, boiler-inlet pressure, and boiler-exit pressure are plotted against exit-plenum pressure for constant nozzle-inlet and heating-fluid exit temperatures as well as for constant flow rates. These data are for a nozzle-inlet temperature of approximately 400 K.

Some observations which can be made from figure 55 are the following:

(1) The nozzle-inlet pressure P_{ni} decreases linearly, goes through a transition region, and then becomes essentially constant as exit-plenum pressure decreases, in contrast

Figure 55. Typical pressure data for boiler with full-length helical wire insert, inlet nozzle, and inlet-region plug (ref. 87). Boiling-fluid flow rate, ~10 g/sec (~80 lbm/hr); heating-fluid flow rate, ~1 kg/sec (~8000 lbm/hr); nozzle-inlet temperature, ~400 K (~260° F); heating-fluid exit temperature, ~433 K (~320° F).

61

pressures, the boiler-inlet pressure becomes essentially constant over a range of exit pressures. This might tend to dynamically isolate the boiler inlet from pressure changes occurring near the exit.

(3) The boiler-exit pressure P_{be} decreases with decreasing exit-plenum pressure, until the exit-plenum pressure reaches values below approximately 24 kN/m² absolute. At these low pressures, there is a fairly large pressure drop between the boiler exit and the exit plenum, this effect is most pronounced at high exit qualities. The differences are too great to be due entirely to instrument error. This pressure drop could well be caused by two-phase choking at the tube exit. With no exit vapor superheat the data are in the range predicted from Fauske's slip-equilibrium model for two-phase critical flow (ref. 107).

ANALYSIS

Application of the laws of conservation of energy, mass, and momentum yields the pressure drop as the sum of three terms: inertial, gravitational, and frictional. From mass-balance considerations,

$$u_l = \frac{G}{\rho_l g_c} \left(\frac{1 - x}{1 - \alpha} \right) \qquad (3)$$

and

$$u_g = \frac{G}{\rho_g g_c} \left(\frac{x}{\alpha} \right) \qquad (4)$$

Dividing equation (4) by equation (3) and solving for the void fraction α yields

$$\alpha = \frac{x \left(\dfrac{u_l}{u_g} \right) \left(\dfrac{\rho_l}{\rho_g} \right)}{1 + x \left[\left(\dfrac{u_l}{u_g} \right) \left(\dfrac{\rho_l}{\rho_g} \right) - 1 \right]} \qquad (5)$$

(This equation is the same as eq. (2) and is repeated for convenience.) Thom (ref. 61) fit void-fraction data for water boiling at pressures from 10^5 to 2×10^7 N/m² absolute and vapor qualities greater than or equal to 0.03 by assuming that the slip ratio u_g/u_l is a function of pressure only. The boiling pressure-drop correlation of reference 85 used the approximation $u_g/u_l = \sqrt{\rho_l / \rho_g}$ The assumption that the slip ratio is equal to the square root of the density ratio has often been utilized previously Although this differs from the relation used by Thom (ref. 61), it should be noted that Thom presents pressure-drop results only for water at pressures of 1.7×10^6 N/m² absolute or greater ($\rho_l / \rho_g < 100$), whereas the present discussion deals mainly with data for $\rho_l / \rho_g >$ 300. The following analysis is otherwise similar to that of Thom (ref 61), except for the treatment of the two-phase friction factor

Inertial Pressure Drop

The inertial pressure drop for all-liquid flow at the inlet is obtained as follows:

$$\Delta P_I = \frac{G}{g_c} (1 - x_e) u_{l,e} + \frac{G x_e u_{g,e}}{g_c} - \frac{G^2}{\rho_l g_c} \qquad (6)$$

Substituting from equations (3) to (5) and assuming constant flow area and constant

physical properties yields

$$\Delta P_I = \frac{R_1 G^2}{\rho_l g_c} \qquad (7)$$

where R_1 is a function of density ratio and quality as follows:

$$R_1 = \left[1 + \left(\sqrt{\frac{\rho_l}{\rho_g}} - 1 \right) x_e \right]^2 - 1 \qquad (8)$$
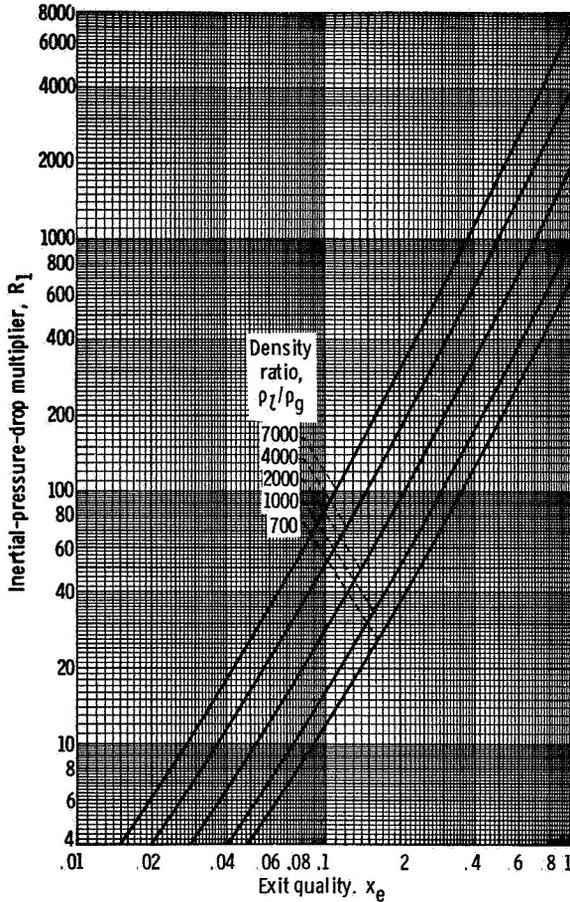
Figure 56. Inertial-pressure-drop multiplier as function of exit quality for various values of density ratio.

The quantity R_1 is plotted as a function of exit quality for various values of density ratio in figure 56.

Gravitational Pressure Drop

The gravitational pressure drop for vertical upward flow is given by

$$\Delta P_G = \frac{g}{g_c} \int_0^{L_H} \rho_m \, dz \qquad (9)$$

For constant heat flux and constant physical properties, Thom (ref. 61) obtained

$$\Delta P_G = \left(\frac{g}{g_c} \right) \rho_l L_H R_2 \qquad (10)$$

where R_2 is a function of density ratio and quality and, for the slip ratio assumption of reference 85, is given by

$$R_2 = \frac{\sqrt{\dfrac{\rho_g}{\rho_l}} - 1}{\sqrt{\dfrac{\rho_l}{\rho_g}} - 1} + \frac{\sqrt{\dfrac{\rho_l}{\rho_g}} - \sqrt{\dfrac{\rho_g}{\rho_l}}}{x_e \left(\sqrt{\dfrac{\rho_l}{\rho_g}} - 1 \right)^2}$$

$$\times \ln \left[1 + x_e \left(\sqrt{\frac{\rho_l}{\rho_g}} - 1 \right) \right] \qquad (11)$$

The quality R_2 is plotted against x_e for various ρ_l / ρ_g in figure 57

63
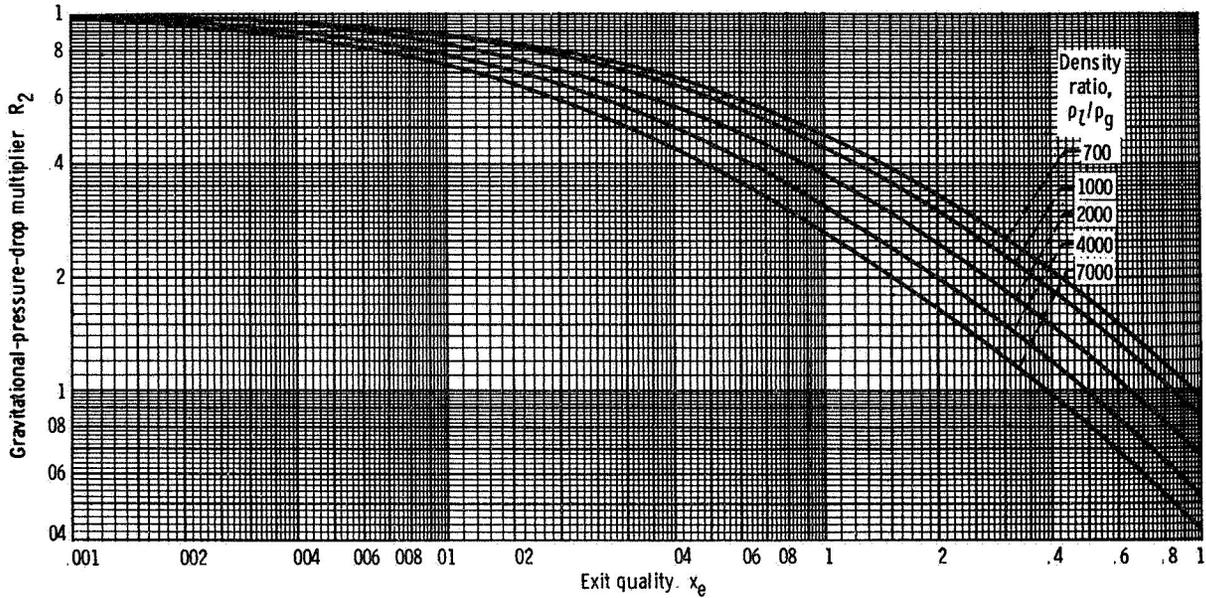
Figure 57. Gravitational-pressure-drop multiplier as function of exit quality for various values of density ratio.

Frictional Pressure Drop

By analogy to single-phase flow, the frictional pressure drop may be written

$$\Delta P_F = 4f\left(\frac{L_H}{D}\right)\left(\frac{G^2}{2g_c}\right)v_m \qquad (12)$$

Thom (ref. 61) arbitrarily assumed the effective mean specific volume is given by the arithmetic average of inlet and exit specific volumes, thus,

$$\Delta P_F = 4f\left(\frac{L_H}{D}\right)\left(\frac{G^2}{2\rho_l g_c}\right)(R_1 + 2) \qquad (13)$$

In reference 85, the constants 2 and 4 were lumped with f so that

$$\Delta P_F = f_{TP}\left(\frac{L_H}{D}\right)\left(\frac{G^2}{\rho_l g_c}\right)(R_1 + 2) \qquad (14)$$

PLAIN-TUBE NET-QUALITY BOILING

A semiempirical, slip-flow model was used to evaluate the two-phase friction factors from experimental pressure-drop data, using equation (15):

$$f_{TP} = \frac{\Delta P - \Delta P_I - \Delta P_G}{\left(\frac{G^2}{\rho_l g_c}\right)\left(\frac{L_H}{D}\right)(R_1 + 2)} \qquad (15)$$

In reference 85, the water-boiling data presented therein and those of Dengler and Addoms (ref. 66) were correlated as a function of the mean liquid and gas Reynolds numbers, defined as follows:

$$\left. \begin{array}{l} Re_l = \dfrac{DG}{\mu_l}\left(1 - \dfrac{x_e}{2}\right) \\[2em] Re_g = \dfrac{DG}{\mu_g}\left(\dfrac{x_e}{2}\right) \end{array} \right\} \qquad (16)$$

64

It was assumed that the variation of f_{TP} with the gas Reynolds number is given by $f_{TP} \propto Re_g^{-0.2}$. Therefore, $f_{TP}Re_g^{0.2}$ was plotted against liquid Reynolds number as shown in figure 58(a). The data were correlated by the following equation:

$$f_{TP} = 0.020\,Re_g^{-0.2}\,(\,1 + 0.027\,Re_l^{0.5}\,) \quad (17)$$

In order to demonstrate that this correlation (ref. 85) is applicable to alkali metal boilers, the plain-tube data for sodium (ref 83) and potassium (ref 94) are shown in figure 58(b). The parameter $f_{TP}Re_g^{0.2}$ is plotted as a function of Re_l for exit qualities above 0.1 but less than 1.0 and for $\Delta P_B > 25$ kN/m². From reference 83, only data categorized as stable with no critical heat-transfer phenomena, are shown. The phase condition at the boiler inlet is indicated as either liquid

or flashing. The data agree reasonably well with the correlation of reference 85 (eq. (17)) but on the average do fall somewhat lower. A better idea of the actual data scatter is given in figure 59, where experimental and calculated pressure drops are compared. For $\Delta P_{B,exp} > 50$ kN/m², 96 percent of the experimental data fall within the band 6 to -20 percent of calculated values. The percentage of scatter increases for lower $\Delta P_{B,exp}$, as might be expected, since in both references 83 and 94, ΔP_B is obtained from the difference between two numbers generally much larger than ΔP_B Thus, it is concluded that the correlation of reference 85 provides a valid limiting condition for no swirl ($p/D \to \infty$), over an exit vapor quality range of 0.1 to 1.0 for density ratios ρ_l/ρ_g from 330 to 6000, liquid Reynolds numbers from 1.6×10^3 to 10^5, and pressure drops no greater than boiler-exit pressure.

(a) Water data.
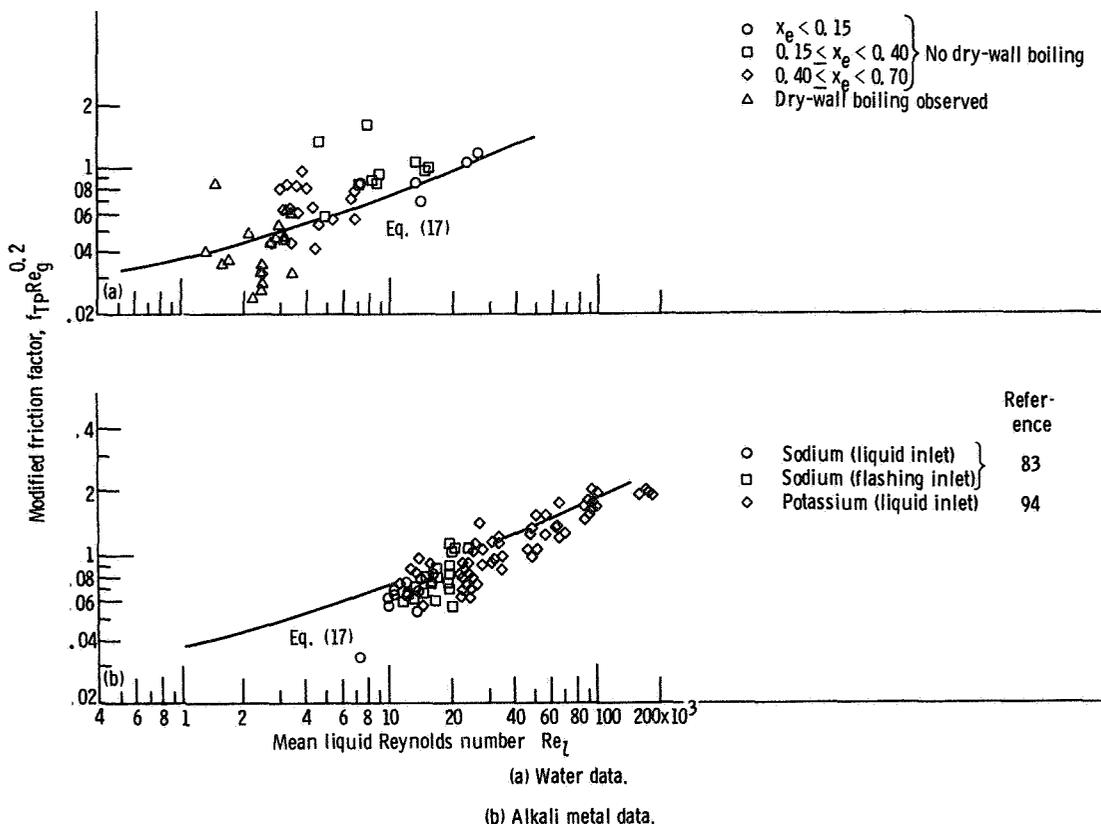
(b) Alkali metal data.

Figure 58.   Correlation of two-phase friction factor as function of mean Reynolds numbers of liquid and vapor.
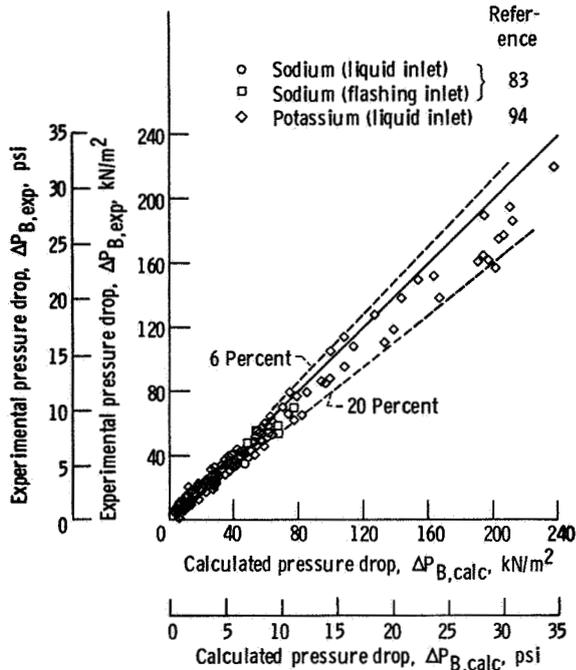
Figure 59. Experimental boiler pressure drop as function of calculated boiler pressure drop for alkali metal boiling with no inserts.

NET-QUALITY BOILING WITH INSERTS

In determining the frictional pressure drop from the experimental data, it is assumed that the insert affects only the frictional pressure drop. Any rotational effects, as well as any changes in ΔP_I and ΔP_G, are lumped with the actual frictional pressure drop. Two types of inserts are considered a helical wire touching the tube wall (refs. 86 and 87) and a helical vane attached to a center rod (ref 94). The effect of inlet-region plugs is considered negligible for the data correlated herein. The data of reference 95 are not used since the boiler pressure drop listed therein includes the pressure drop across the inlet orifices and unheated buffer zones.

It is assumed that the variation of f_{TP} with Re_g is similar to the relation with no inserts (i.e., $f_{TP} \propto Re_g^{0.2}$) Therefore, $f_{TP}Re_g^{0.2}$ is plotted as a function of Re_l in figure 60 and compared with the plain-tube correlation of reference 85. The data of reference 94 for potassium boiling in a tube with helical vane inserts and the data of references 86 and 87 for water boiling in a tube with a helical wire insert are shown in figure 60 for $0.1 \leqslant x_e < 1.0$ and $\Delta P_B > 25$ kN/m² Only those data from references 86 and 87 categorized as stable, with no exit vapor superheat, are shown. The data with inserts fall well above the plain-tube correlation, as expected, $f_{TP}Re_g^{0.2}$ increases with decreasing pitch-to-tube-diameter ratio p/D for a given Re_l It also appears that the dependence of $f_{TP}Re_g^{0.2}$ on Re_l is weaker than in the plain-tube case. The following equation, shown by the dashed curves in
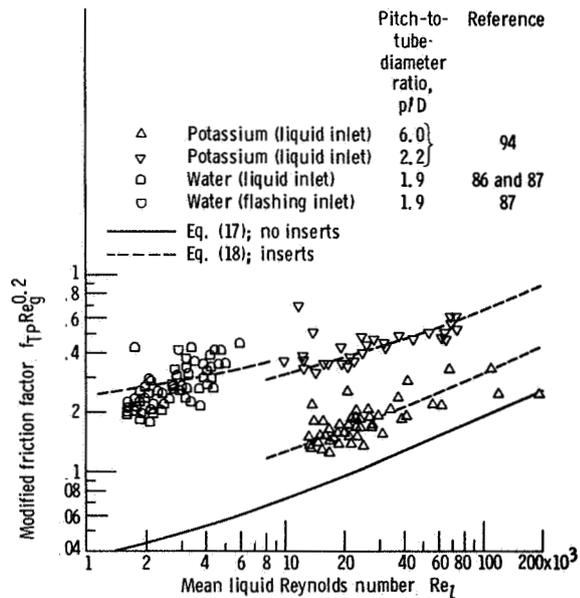
Figure 60. Correlation of two-phase friction factor as function of mean Reynolds numbers of liquid and vapor and pitch-to-tube-diameter ratio for net-quality boiling with helical flow inserts.

66

figure 60, is found to fit the data reasonably well for $Re_l \leqslant 10^5$

$$f_{TP} Re_g^{0.2} = 0.020 + 0.42 \left(\frac{D}{p}\right)^2$$

$$+ 0.00054 \left(1 + \frac{D}{p}\right)^3 Re_l^{0.5} \quad (18)$$

This equation reduces to the plain-tube correlation (eq. (17)) in the limit as $D/p \to 0$. There are insufficient data to extend the correlation beyond $Re_l = 10^5$ A better idea

Figure 61. - Experimental boiler pressure drop as function of calculated boiler pressure drop with helical flow inserts. Mean liquid Reynolds number $Re_l \leq 10^5$

of the actual data scatter is given in figure 61, where experimental and calculated pressure drops are compared. For $\Delta P_{B,exp} > 50$ kN/m^2, 95 percent of the experimental data fall within ±20 percent of the calculated values, with the scatter percentage increasing for lower $\Delta P_{B,exp}$, as expected.

NET-QUALITY BOILING PRESSURE DROP

The foregoing empirical correlation of boiling pressure drop, accounting for the effect of helical-flow-promoting inserts, is excerpted from reference 108. A constant-slip model based on a modification of Thom's analysis (ref. 61) is used, with the assumption that the inserts affect pressure drop through an increase in the friction factor and a reduction of the flow area. The correlation is based on data for water, sodium, and potassium, covering a range of liquid-gas density ratios of about 330 to 6000, at superficial liquid Reynolds numbers from 1.6×10^3 to 10^5 The range of boiler geometries includes p/D as low as 1.9 in tubes of 1.1 to 2.3 cm diameter and with length-diameter ratios from 73 to 140. The use of this correlation does not require a detailed knowledge of the heat-flux and void-fraction distributions within the boiler, nor does it require trial-and-error iterations. Thus, simple straightforward pressure-drop calculations are made possible.

SUBCOOLED BOILING

Subcooled boiling generates vapor within a fluid whose bulk temperature is below its saturation temperature. Thus, when a cold

67

liquid contacts a sufficiently hot surface, vapor forms at the hot wall, and some of it condenses in the cold liquid stream. The resulting increased volume and velocity of the stream produces both a higher heat-transfer coefficient and a pressure drop often several times greater than that for all-liquid flow

The problem of subcooled boiling pressure drop is a particular area of the more general problem of pressure drop in two-phase flow, which has been the subject of numerous experiments and correlations A comprehensive review of these studies is presented by Tong (ref 99) In order to apply such two-phase pressure-drop correlations to subcooled boiling, it has been necessary that the vapor fraction be known. Since this is not generally known, especially at low pressures, most correlations of subcooled boiling pressure-drop data have been made on a purely empirical basis, and the extent of their validity is unknown. The differences in form of the various correlations, and the fact that some data, such as those of reference 89, did not agree well with any of these correlations indicated that there was some uncertainty about the proper method of analyzing the data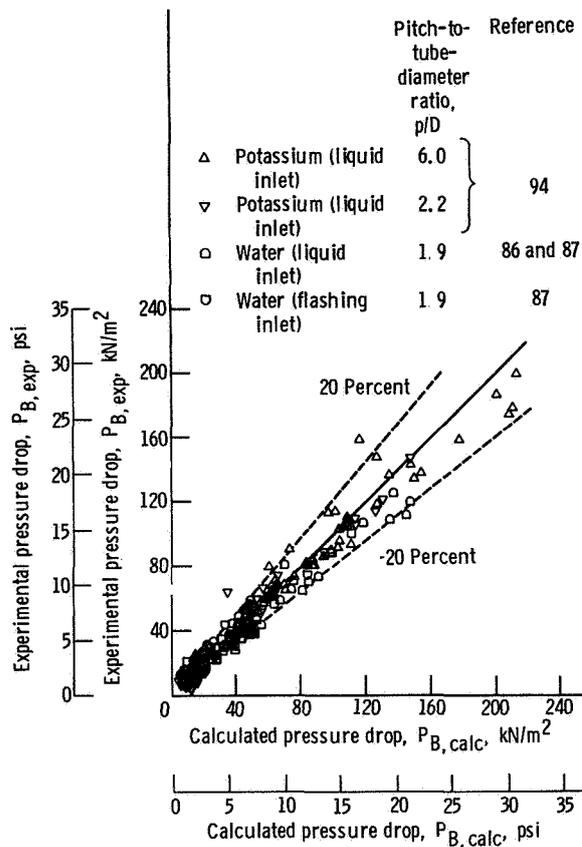. Therefore, a broadly applicable, but minimally complicated, correlation of subcooled boiling pressure drop for low-pressure water flowing in tubes with constant heat flux was developed (ref 109). Use of one of the available void-fraction predictions (e.g., refs 48 to 50) would have greatly increased the complexity of the formulation in reference 109 It was therefore necessary to approximate the effects of void fraction on pressure drop.

A one-dimensional flow model was developed which related the pressure drop for subcooled boiling inside straight, circular tubes with constant heat flux to parameters generally known (physical properties, heat flux, mass velocity, and geometry) and to one unknown variable, the net fraction of heat added to the fluid which goes into
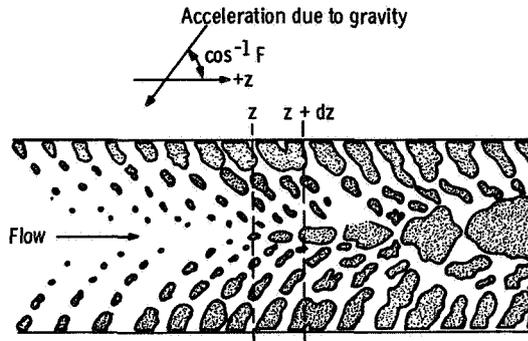
Figure 62. Differential control volume for subcooled boiling flow.

vaporization. The basic equations of change were applied to the differential control volume shown in figure 62. It was assumed that a modified single-phase friction factor could be used. Thus, an equation for the local pressure gradient was obtained, dependent only on known quantities and the vaporization rate parameter γ This equation was then integrated for constant heat flux, physical properties, and vaporization rate parameter The overall pressure drop was thus obtained as a function of known quantities and the effective mean value of the vaporization rate parameter The method of correlation was to determi nean values of this vaporization rate parameter from experimental pressure-drop data and then correlate this parameter as a function of test variables. This analysis is given in reference 109

The subcooled boiling pressure-drop data of references 89 and 110 were examined. The experimental pressure-drop data yielded mean values of the vaporization rate parameter $\bar{\gamma}$ As noted by Kroeger and Zuber (ref 39), the point of boiling initiation z_0 is quite important, and no widely applicable means is available to determine it. Therefore, reference 109 used only data for which were given either z_0 (ref 110) or the wall temperature distribution, from which z_0 may be estimated (ref 89). Whether this z_0 indicates the first surface bubble nucleation or the point of the

first bubble departure is uncertain. The mean vaporization rate parameter was correlated as a function of known variables. Finally, as a check, the correlation obtained was used to predict the pressure drop, and this calculated pressure drop was then compared with experimental data. This was done for the data (refs. 89 and 110) used in obtaining this correlation and also for the data of Owens and Schrock (ref. 111).

Figure 63 shows the mean vaporization rate parameter $\bar{\gamma}$ plotted against subcooling number N_{sc} for various values of boiling number N_b over a wide range of test variables at an exit pressure of 690 kN/m² absolute. It can be seen that $\bar{\gamma}$ decreases with increasing N_{sc} for constant N_b Also, $\bar{\gamma}$ increases with increasing N_b at constant N_{sc} No effects of heat flux or mass velocity, except as accounted for in N_b, are seen, nor are there any effects of geometry not accounted for in the equations. The data for a given pressure may be reduced to a single curve by plotting $\bar{\gamma}$ against $N_{sc}N_b^{0.7}$, as shown in figure 64. In order to account for the effect of pressure, $\bar{\gamma}$
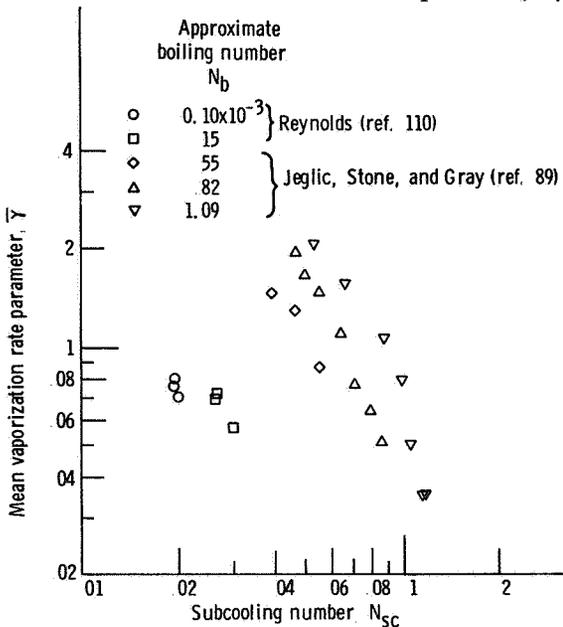
Figure 63. Mean vaporization rate parameter as function of subcooling number for various boiling numbers. Exit pressure, ~690 kN/m² abs (~100 psia).
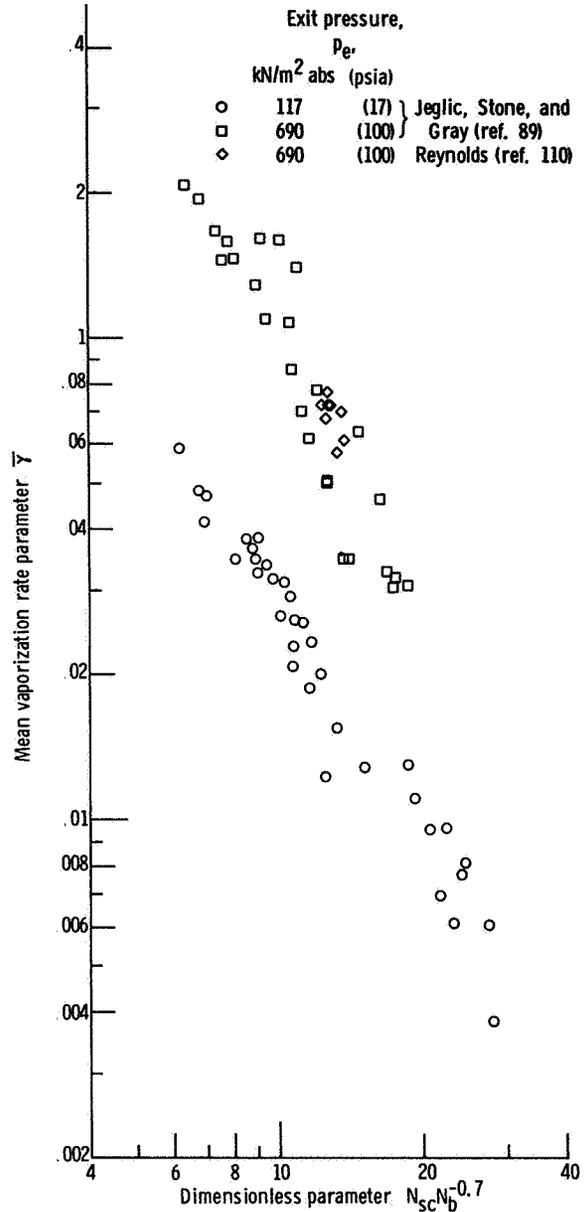
Figure 64. Mean vaporization rate parameter as function of dimensionless parameter $N_{sc}N_b^{-0.7}$ for exit pressures of 117 and 690 kN/m² abs (17 and 100 psia).

is plotted against $N_{sc}N_b^{0.7}(\rho_l/\rho_g)^{0.5}$ in figure 65. Data for very low pressure drops are not shown on this figure since there is considerable scatter in such data. It should be noted that N_{sc} is based on heat-balance enthalpies. As has been previously observed (refs. 39, 40, and 112), liquid temperatures in the subcooled boiling regime are less than a

69

heat balance would indicate, thus, establishment of limiting behavior can only be approximate. In the limit as $N_{sc} \to 0$, $\bar{\gamma}$ is assumed to approach 1.0, so the following simple equation yielding this limit is used:

$$\frac{\Delta P_B}{\left(\dfrac{G^2}{\rho_g g_c}\right)} = \left[4\bar{\gamma}N_b + 2\bar{f}_{TP}\left(\frac{\rho_g}{\rho_l}\right)\right]\left(\frac{L_b}{D}\right)$$

$$+ 4\bar{\gamma}\bar{f}_{TP}N_b\left(\frac{L_b}{D}\right)^2 + F\left[\frac{\rho_l L_b\left(\dfrac{g}{g_c}\right)}{\dfrac{G^2}{\rho_g g_c}}\right]$$

$$X\left\{\frac{\ln\left[1 + 4\bar{\gamma}N_b\left(\dfrac{\rho_l}{\rho_g}\right)\left(\dfrac{L_b}{D}\right)\right]}{4\bar{\gamma}N_b\left(\dfrac{\rho_l}{\rho_g}\right)\left(\dfrac{L_b}{D}\right)}\right\} \quad (19)$$

$$\bar{\gamma} = \left[\frac{1}{1 + 0.0145\,N_{sc}N_b^{-0.7}\left(\dfrac{\rho_l}{\rho_g}\right)^{0.5}}\right]^2 \quad (20)$$

where

No attempt is made to establish limiting behavior at low $\bar{\gamma}$. This would require prediction of the inception of boiling and is beyond the scope of this publication.

The data correlated are for water at pressures from 115 to 2860 kN/m² absolute, for mass velocities from 8.3 to 141 kg/(m²)(sec), and for heat fluxes from 410 to
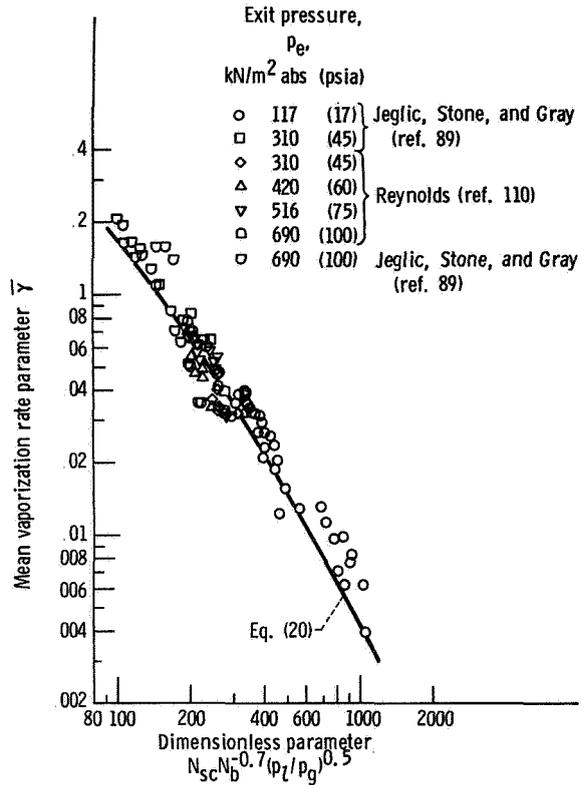
Figure 65. Mean vaporization rate parameter as function of dimensionless parameter $N_{sc}N_b^{-0.7}\,(\rho_l/\rho_g)^{0.5}$

11 000 kW/m². The boiling number, defined as heat flux divided by the quantity mass velocity times latent heat of vaporization, ranges from 0.06×10^{-3} to 1.56×10^{-3}. The effects of void fraction are lumped in the vaporization rate parameter. Therefore, this model should not be used to predict void fraction explicitly. Calculations based on this correlation are simplified since no independent prediction of void fraction nor experimental void fraction data are required in order to predict the pressure drop.

INLET NOZZLE

Since converging-diverging nozzles appeared attractive as boiler inlets, adiabatic flow tests were conducted with both metal and transparent venturis and double-cone

70

nozzles, as described in appendix B. Although not fully understood, in order to facilitate design calculations, the pressure-drop data obtained in those tests are presented here in the form of flow coefficients for both the two-phase and all-liquid flow cases.

Two-Phase Flow

Although no simple equation precisely describes all the flow regimes observed, the data generally fall with small scatter on plots of saturation two-phase flow coefficient C_s against heat-balance quality. This flow coefficient is given by

$$C_s = \frac{W_b}{A_{min}\sqrt{\dfrac{2\rho_l g_c(P_{ni} - P_{ni,s})}{K}}} \qquad (21)$$

Negative heat-balance qualities are the measure of nozzle-exit subcooling. Such plots are shown in figure 66 for each set of data. The potassium data (ref. 105) are shown in figure 66(a). The effect of quality on subcooling is so weak as to be probably insignificant, although C_s does increase slightly with increasing x_{ne}. The flow coefficients are lower by about 15 percent with the artificial throat cavity than without, indicating that some vaporization probably occurs in the throat region with the insert but not without it. The data for water flowing through this same size large venturi are shown in figure 66(b). These are the only data which do not all correlate well as C_s against x_{ne}, the nonequilibrium, hysteresis, separated flow data show quite low values for relatively large negative x_{ne} (therefore large nonequilibrium effects). Otherwise, the data agree fairly well with the potassium data, but they do show an increase with increasing x_{ne}. The data for the double-cone nozzle are shown in figure 66(c). On the average, coefficients may be somewhat lower with the insert than without, but the
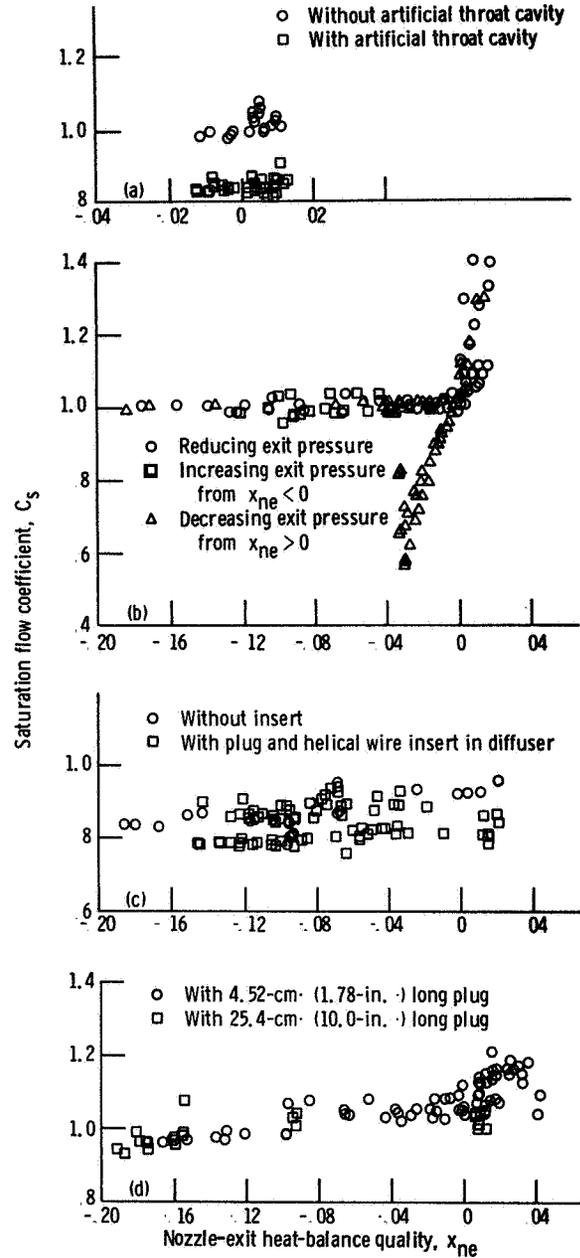
(a) Potassium flow through 2.58-mm- (0.1015-in. -) throat-diameter venturi (ref. 105).

(b) Water flow through 2.56-mm- (0.1008-in. -) throat-diameter venutri.

(c) Water flow through 0.635-mm- (0.025-in. -) throat-diameter converging-diverging nozzle (ref. 113).

(d) Water flow through 0.72-mm- (0.0285-in. -) throat-diameter venturi (ref. 87).

Figure 66. Saturation flow coefficient as function of nozzle-exit heat-balance quality for various fluids and geometries tested.

71

difference is small. There is no significant trend with x_{ne}. The coefficients are lower than for any other configuration, probably because of losses at the transition from the inlet cone to the throat section. The data for water flowing through the small venturi are shown in figure 66(d). These data agree fairly well with the large-venturi potassium data (fig. 66(a)) and the water data (fig. 66(b)) not affected by hysteresis. With this set of data, there does appear to be a consistent, though slight, trend for C_s to increase with increasing x_{ne}

All-Liquid Flow

For each combination of fluid and geometry tested, the all-liquid data normalize well as plots of flow coefficient against throat liquid Reynolds number, where the flow coefficient is given by

$$C = \frac{W_b}{A_{min}\sqrt{\dfrac{2\rho_l g_c(P_{ni} - P_{ne})}{K}}} \qquad (22)$$

Figure 67 shows plots of the all-liquid flow coefficient against throat liquid Reynolds number The data for potassium flowing through a 0.258-cm-throat-diameter venturi are shown in figure 67(a) for the venturi with and without the artificial throat cavity (ref. 105). In general, the flow coefficients without the cavity are higher, as expected. There does not appear to be any significant effect of Reynolds number. The data for water flowing through the same size venturi (0.258 cm) are shown in figure 67(b), no throat cavity was used. The coefficient increases with Re_t over almost the full range, and the coefficients at high Reynolds numbers are considerably larger than for potassium. The cause of this

has not been fully resolved but appears to be related to surface roughness. The data of reference 113 for water flowing through a 0.064-cm-throat-diameter, double-cone, converging-diverging plastic nozzle are plotted in figure 67(c), both with and without the tapered plug and helical wire insert in the diffuser. As might be expected, because of the smaller size and the sharp corners, these flow coefficients are less than those for the large, smooth venturi. The flow coefficients increase with increasing Reynolds number at low Reynolds numbers and then begin to flatten out at higher Re_t. At high Reynolds numbers, the flow coefficient is greater with the insert than without, indicating that the tapered cone in the diffuser decreased the effective diffuser angle. Finally, the data for water flowing through the 0.072-cm-throat-diameter venturi (ref 87) are shown in figure 67(d). Although two inlet-region plugs were used, they were identical between the venturi inlet and exit pressure taps. These data show flow coefficients increasing with increasing Reynolds number at low Re_t and then approaching a constant value. This small venturi appears to be intermediate in flow coefficient between the larger, smooth venturi and the small, sharp-cornered, double-cone nozzle, as might be expected.

Discussion of Inlet Nozzles

Although a complete understanding of nonequilibrium flow processes in nozzles is not contained herein, the data can serve as a guide to inlet design. From figures 66 and 67 the designer can readily size inlet nozzles. For example, for a fairly smooth venturi, $C_s \approx 1.0$, so if the flow rate, inlet temperature, and available pressure are specified, the throat area and hence diameter can be calculated from equation (21).
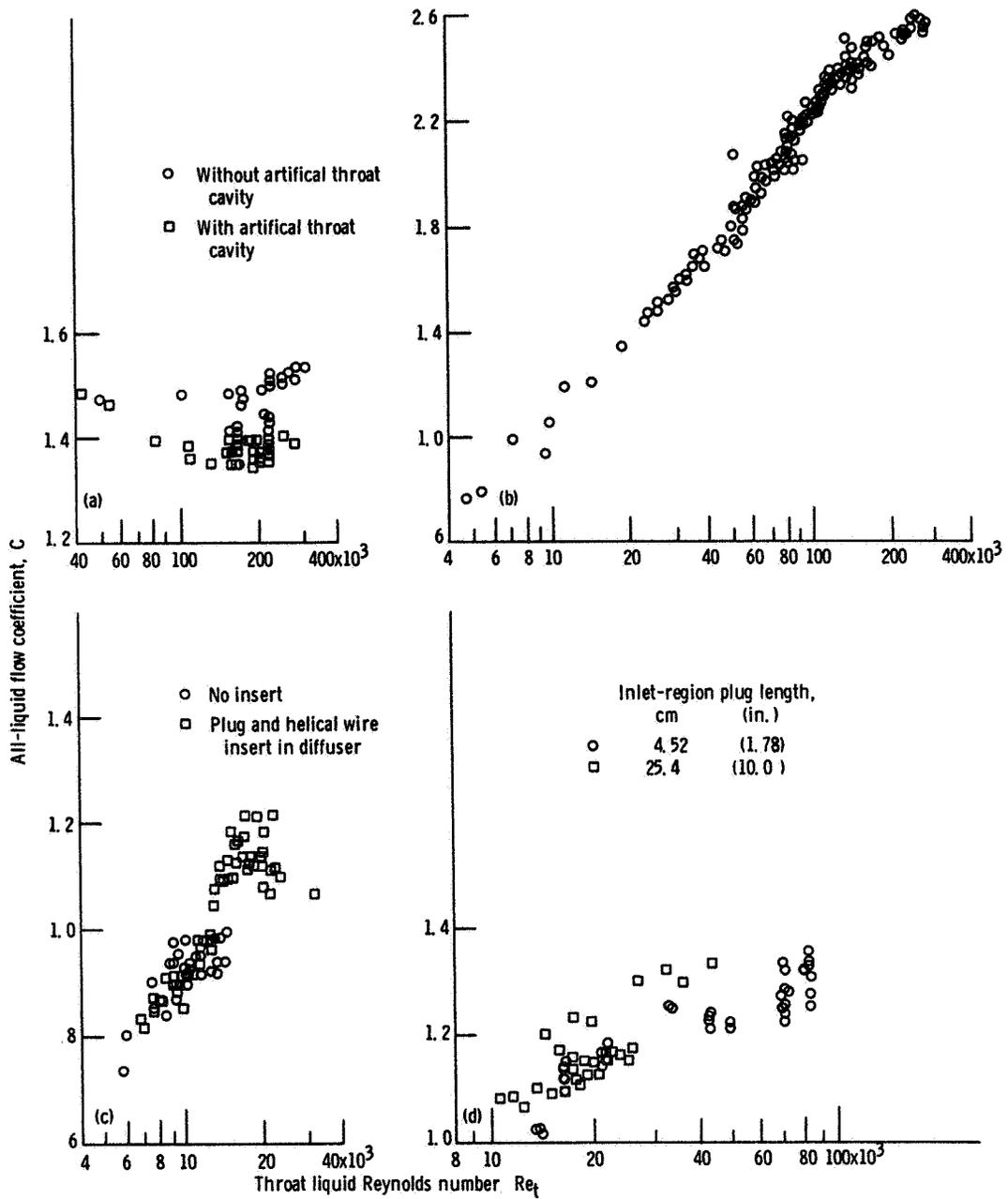
(a) Potassium flow through 2.58-mm- (0.1015-in. -) throat-diameter venturi (ref. 105).

(b) Water flow through 2.56-mm- (0.1008-in. -) throat-diameter venturi.

(c) Water flow through 0.635-mm- (0.025-in. -) throat-diameter, double-cone, converging-diverging nozzle (ref. 113).

(d) Water flow through 0.72-mm- (0.0285-in. -) throat-diameter venturi (ref. 87).

Figure 67. All-liquid flow coefficient as function of throat liquid Reynolds number for various fluids and geometries tested.

Chapter 7

HEAT TRANSFER

There have been numerous studies of boiling heat transfer, as can be seen in the bibliography But there is still no generally applicable means available to predict boiling heat transfer, especially for high-density-ratio fluids such as alkali metals and low-pressure water. Average boiling-side heat-transfer coefficients are required in order to size the boiler, and local heat-transfer coefficients are needed in order to determine the internal performance of the boiler Local heat-transfer coefficients are discussed first, followed by average coefficients.

LOCAL HEAT-TRANSFER COEFFICIENTS

Figure 68 shows typical temperature and voidage profiles for a boiler with uniform heat flux, subcooling at the inlet, and net quality at the exit. This figure also illustrates some of the terminology used in this chapter The point of boiling initiation, as determined from the wall temperature profile, is at z_0, other parameters evaluated at this position are denoted by the subscript 0 The subscript d denotes the point at which bubbles first detach from the tube wall. The point where the heat-balance quality is zero is indicated by the subscript 1 Any quantity which is corrected for nonequilibrium is indicated by a superscript prime. The data presented in this section are limited to the electrically heated water-boiling data of references 79, 80, and 89 to 91, since it is difficult to determine
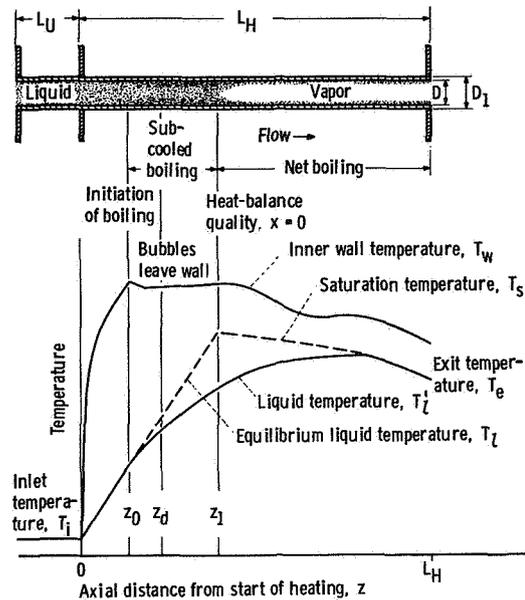
Figure 68. Typical boiler temperature and voidage profiles with definition of terminology.

local coefficients from heat-exchanger boiling data.

Typical Data for Water Boiling in Tube with Uniform Heat Flux

Large subcooling at inlet. - Typical heat-transfer data with large subcooling (~83 K) at the inlet are shown in figure 69. Local inner-wall and bulk temperatures are plotted against axial distance from the start of heating in figure 69(a). The bulk temperatures are based on an equilibrium heat balance. The resulting local heat-transfer coefficients, based

75
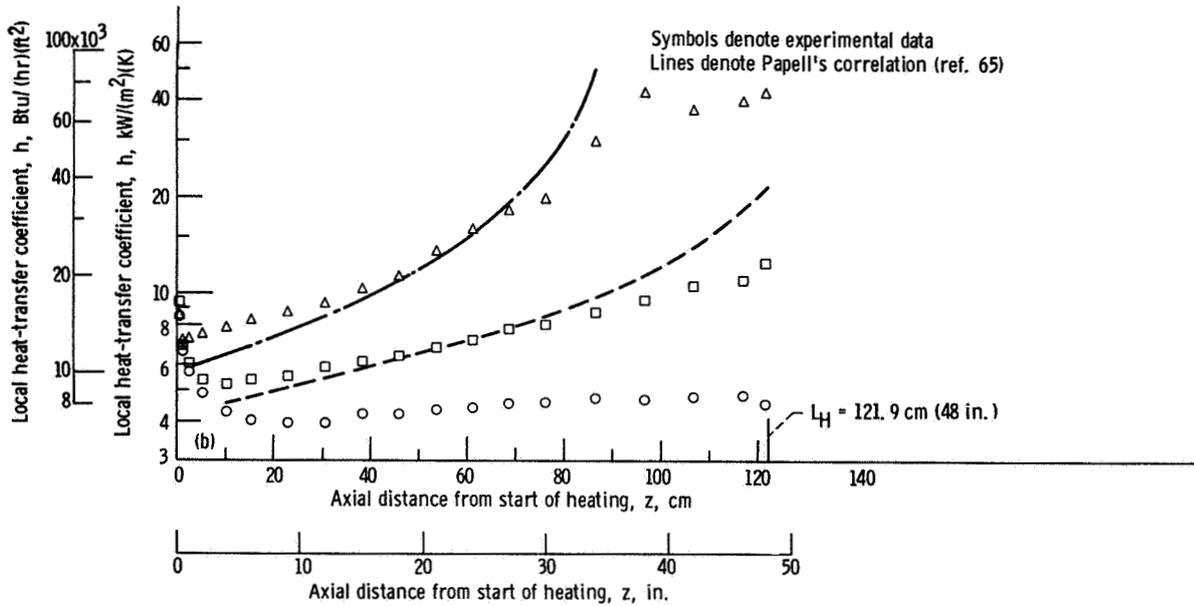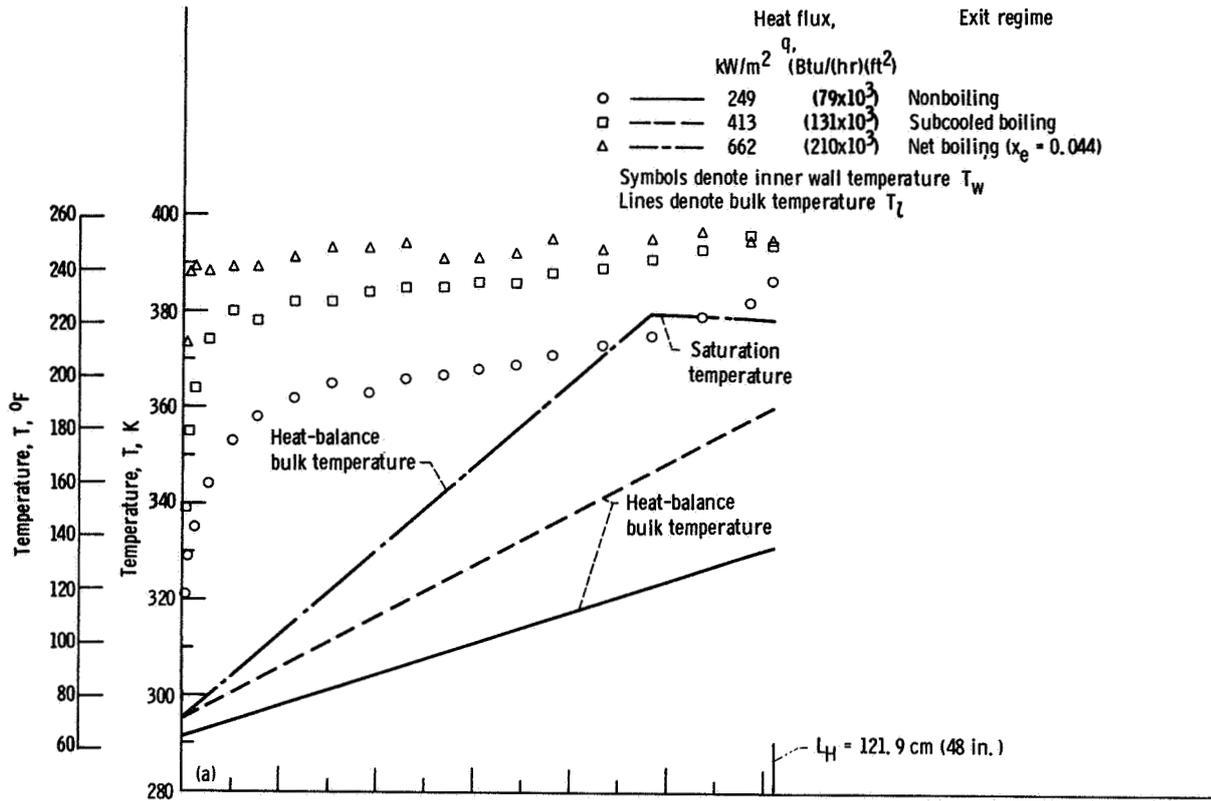
(a) Local bulk and inner wall temperatures plotted against distance.

(b) Local heat-transfer coefficient plotted against distance.

Figure 69. - Typical heat-transfer data for large subcooling at inlet (~83 K or ~310° F). Tube inside diameter, 1.219 cm (48 in.); mass velocity, ~590 kg/(m²)(sec) (~437x10³ lbm/(ft²)(hr)); exit pressure, ~117 kN/m² abs (~17 psia). (Data from ref. 90.)

on bulk temperature, are plotted against distance in figure 69(b). (The mass velocities reported in reference 90 are low by a factor of 100 but have been corrected herein.) Papell's correlation of subcooled boiling heat transfer (ref. 65) is shown for comparison. Three runs are shown with constant mass velocity, exit pressure, and inlet temperature and for various heat fluxes.

At the lowest heat flux, the inner-wall temperature does not rise above saturation temperature until near the exit, and no boiling occurs. The local heat-transfer coefficient decreases with distance in the thermal entrance region (ref. 91) and then increases slightly due to the effect of the increasing temperature on physical properties. For the intermediate heat flux, the inner-wall temperature rises with distance rapidly enough that subcooled boiling is initiated in the thermal entrance region. The heat-transfer coefficient then increases with distance throughout the rest of the tube, all in the subcooled boiling regime. Qualitatively similar results are seen for the highest heat flux although boiling is initiated nearer the inlet, net vapor is produced (x_e = 0.044), and the boiling heat-transfer coefficients are higher. Note that, for both runs with boiling in figure 69(a), the inner-wall temperature increases with distance in the subcooled boiling regime. This effect is not predicted by most subcooled boiling heat-transfer correlations (e.g., refs. 62 to 64) but is of small magnitude. Throughout most of the subcooled boiling regime the experimental heat-transfer coefficients do not deviate greatly from Papell's correlation (ref. 65). But the experimental data show less effect of distance (or subcooling) than predicted, and the deviation becomes large as the heat-balance (negative) quality approaches zero.

Small subcooling at inlet. – Typical heat-transfer data with small subcooling (~22 K) at the inlet are shown in figure 70. Local inner-wall and bulk temperatures are plotted against axial distance from the start of heating in figure 70(a). And the resulting local heat-transfer coefficients, based on bulk temperature, are plotted against distance in figure 70(b). Papell's correlation of subcooled boiling heat transfer (ref. 65) is again shown in figure 70(b) for comparison. Four runs are shown with different heat fluxes and the same mass velocity and inlet temperature, the resulting exit quality ranges to 0.247 The exit pressure is 119 kN/m² absolute at the lowest heat flux and increases by approximately 7 kN/m² for each successive increase in heat flux. This increase in exit pressure is caused by the increasing pressure drop between the boiler and condenser with increasing quality.

At the lowest heat flux, subcooled boiling is initiated somewhere near the middle of the tube, but the exact point is difficult to determine. The bulk condition at the exit is slightly subcooled. For the higher heat fluxes, subcooled boiling is initiated in the thermal entrance region, and net exit quality is produced. For all four runs, except very near the inlet, there is a general trend for inner-wall temperature to increase slightly with distance in the subcooled boiling regime. For the three higher heat fluxes, at a given position, the heat-transfer coefficient h increases as the heat flux q increases in the subcooling boiling regime (fig. 70(b)). But then at a fairly low net quality, h takes on values of ~60 kW/(m²)(K) and does not vary greatly thereafter with heat flux, distance, or quality. The agreement with Papell's correlation (ref. 65) is poorer here than for figure 69, especially for the lowest heat flux.

Subcooled Boiling of Water in Tubes

A common way of presenting boiling heat-transfer data is to plot heat flux q against wall superheat $T_w - T_s$. Figure 71 gives such
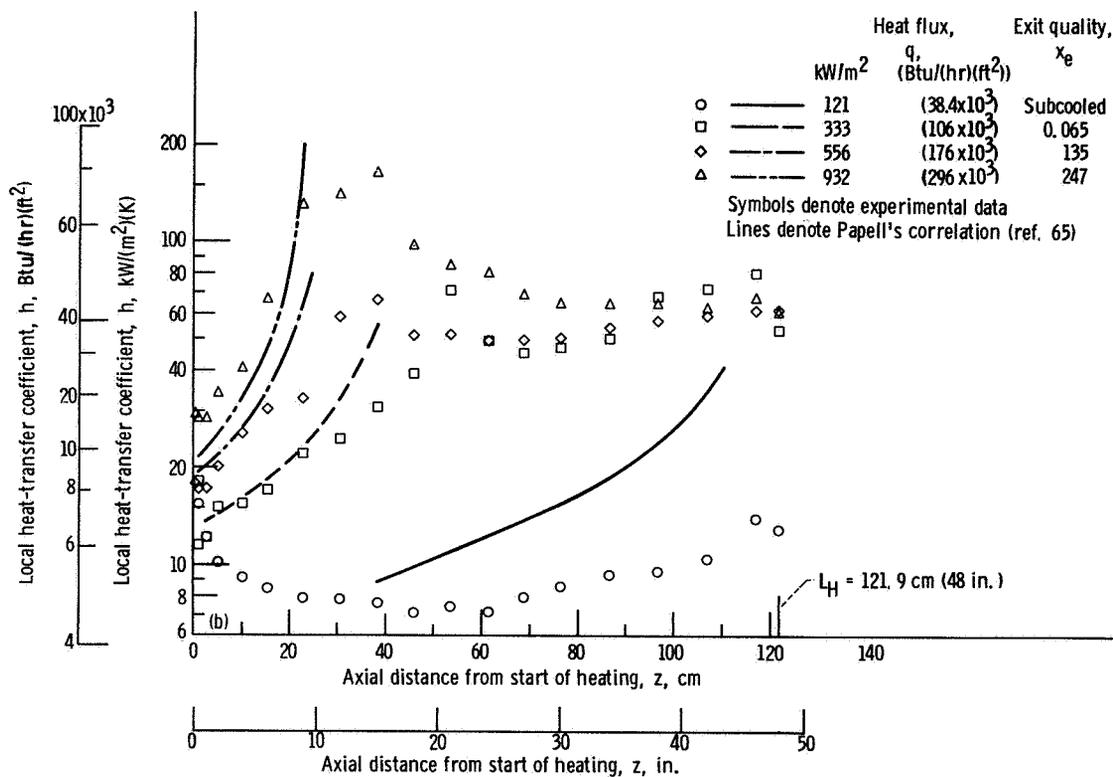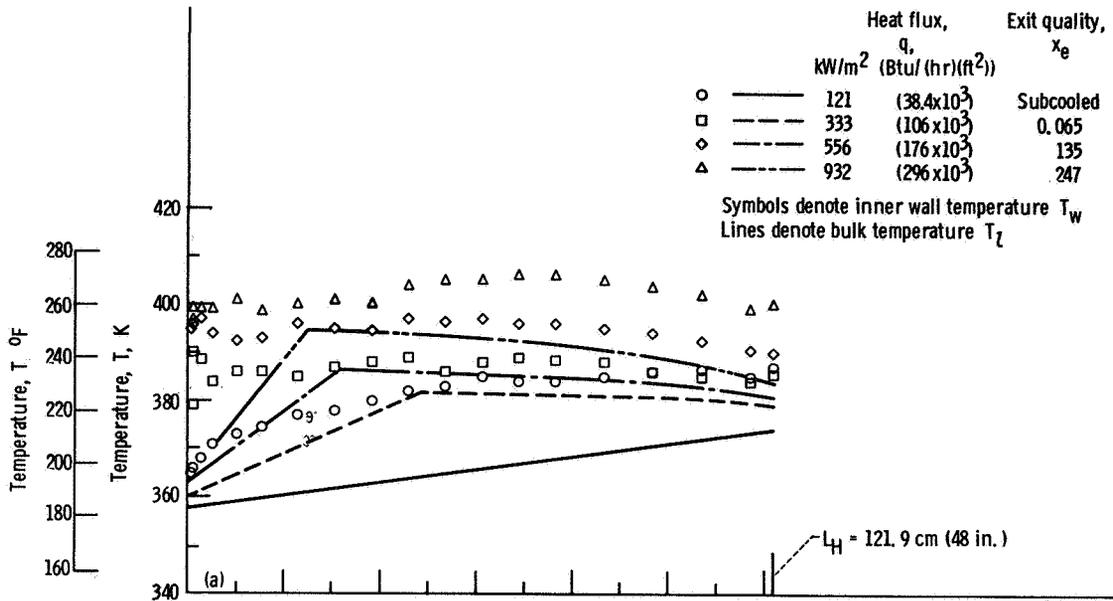
		Heat flux, q,		Exit quality, x_e
		kW/m^2	(Btu/(hr)(ft^2))	
o	————	121	(38.4x10^3)	Subcooled
□	– – – –	333	(106x10^3)	0.065
◇	—— ——	556	(176x10^3)	135
△	—··—··—	932	(296x10^3)	247

Symbols denote inner wall temperature T_w
Lines denote bulk temperature T_l

L_H = 121.9 cm (48 in.)

(a)

		Heat flux, q,		Exit quality, x_e
		kW/m^2	(Btu/(hr)(ft^2))	
o	————	121	(38.4x10^3)	Subcooled
□	– – – –	333	(106x10^3)	0.065
◇	—— ——	556	(176x10^3)	135
△	—··—··—	932	(296x10^3)	247

Symbols denote experimental data
Lines denote Papell's correlation (ref. 65)

L_H = 121.9 cm (48 in.)

(b)

Axial distance from start of heating, z, cm

Axial distance from start of heating, z, in.

(a) Local bulk and inner wall temperatures plotted against distance.

(b) Local heat-transfer coefficients plotted against distance.

Figure 70. Typical heat-transfer data for small subcooling at inlet (~22 K or ~420° F). Tube inside diameter, 1.219 cm (48 in.); mass velocity, ~590 kg/(m^2)(sec) (~437x10^3 lbm/(ft2)(hr)); exit pressure, 119 to 146 kN/m^2 abs (16.9 to 21.2 psia). (Data from ref. 90.)

78

	Mass velocity, G,		Tube inside diameter D,	
	kg/(m²)(sec)	(lbm/(ft²)(hr))	cm	(in.)
O	68 to 134	(50x10³ to 99x10³)		
□	236 to 463	(174x10³ to 340x10³)	1.219	(0.48)
◇	~600	(~440x10³)		
△	~1150	(~850x10³)		
□	970 to 2000	(710x10³ to 1470x10³)		
◻	2760 to 3880	(2030x10³ to 2860x10³)	584	(23)
◻	4020 to 7090	(2960x10³ to 5200x10³)		
◻	10 400 to 14 100	(7650x10³ to 10 400x10³)		

————— Correlation of Engelberg-Forster and Grief (ref. 63)
— — · — Correlation of Rohsenow (ref. 62)
— — — — Correlation of Forster and Zuber (ref. 64)

Open symbols denote data from ref. 90
Half-filled symbols denote data from ref. 91
Solid symbols denote data from ref. 89

Upper-left-tailed symbols denote L_H/D = 12.5
Untailed symbols denote L_H/D = 25
Lower-right-tailed symbols denote L_H/D = 50
Lower-left-tailed symbols denote L_H/D = 100

Figure 71. - Heat flux as function of wall superheat during subcooled boiling for various mass velocities and subcoolings. Exit pressure, ~114 kN/m² abs (~16.5 psia).

a plot for an exit pressure of ~114 kN/m² absolute; the data of references 89 and 90, as well as some limited data from reference 91, are shown. Two tube diameters and four length/diameter ratios are included. The wall temperature measuring station 0.64 cm upstream of the test section exit is used,

except for the 1.22-cm-inside-diameter-tube data of reference 91, where the station 1.90 cm upstream of the exit is used. Local subcooling $T_s - T_l$ ranges from 3 to 66 K. The range of mass velocity is from 67 to 14 100 kg/(m²)(sec), while the heat-flux range is from 101 to 11 400 kW/m². The

correlations of Rohsenow (ref. 62), Engelberg-Forster and Greif (ref. 63), and Forster and Zuber (ref. 64) are shown for comparison. Although the data fall into a rather broad band,($\sim$22 K) and cannot be said to agree with any correlation, the figure is useful in summarizing the range of results obtained. It may be that the effect of other variables, such as mass velocity and subcooling, must be accounted for. The correlation of reference 64 gives approximately the lower limit of q for a given $T_w - T_s$. But it appears that the correlation of either reference 62 or 63 would give reasonable, approximate results for many applications wherein the boiling-side thermal resistance is a small fraction of the overall thermal resistance, as is often the case.

Net Boiling of Water in Tubes

Most correlations of net-boiling heat-transfer coefficients relate h/h_l to the Martinelli parameter

$$X_{tt} = \left(\frac{1-x}{x}\right)^{0.9} \left(\frac{\rho_g}{\rho_l}\right)^{0.5} \left(\frac{\mu_g}{\mu_l}\right)^{0.1} \quad (23)$$

where h_l is the heat-transfer coefficient for all-liquid flow at saturation temperature. Figure 72 gives plots of h/h_l against $x/(1-x)$ for mass velocities of $\sim$68 and $\sim$590 kg/(m^2)(sec) at an exit pressure of $\sim$117 kN/m^2 absolute, for L_H/D = 100. The term h_l is determined from reference 91 and is approximated over the current range of interest by

$$\frac{h_l D}{k} = 0.0232 \left(\frac{DG}{\mu_l}\right)^{0.8} \left(\frac{c_p \mu_l}{k}\right)^{0.47} \quad (24)$$

in consistent units. Although some orderliness with regard to heat flux can be seen in both parts of the figure, it is apparent that the

effect of mass velocity is not properly accounted for. The correlation of Dengler and Addoms (ref. 66) is shown for comparison. Although the data are not in agreement with the correlation, the slopes appear to agree at relatively high qualities (fig. 72(a)).

Similar plots are shown in figure 73 for a mass velocity of $\sim$68 kg/(m^2)(sec) and for exit pressures of $\sim$114 and $\sim$26 kN/m^2 absolute for L_H/D = 50. The data of figures 72(a) and 73(a) show good agreement between the two different L_H/D test sections. But the experimental data show that, for constant heat flux, mass velocity, and quality, h/h_l (and also h) increases as pressure increases. However, the correlation of reference 66 (and also those of refs. 67 to 70) predicts the opposite because of the physical properties in X_{tt}. Although the correlations of references 66 and 70 include a nucleate-boiling term which is not directly a function of X_{tt}, the contribution of the nucleate term is not of sufficient magnitude to reverse the pressure effect in either case. Thus, these correlations in terms of X_{tt} are considered inadequate.

Selection of Form of Heat-Transfer Coefficient to Represent Boiling

In net boiling (equilibrium heat-balance quality $x > 0$) the heat-transfer coefficient is usually defined as $q/(T_w - T_s)$, while in the subcooled boiling regime, either $q/(T_w - T_s)$ or $q/(T_w - T_l)$ is commonly used. For cases where radial acceleration (and therefore, pressure gradients) are involved, $q/(T_w - T_{s,w})$ is often used. In figures 69(b) and 70(b) the definition $h = q/(T_w - T_l)$ is used with $T_l = T_s$ for $x > 0$. These heat-transfer coefficients are plotted against local equilibrium heat-balance quality x in figure 74(a). It can be seen that h increases rapidly with x in the subcooled region ($x < 0$) and passes through a maximum in the low-quality range. In figure 74(b), $h_s = q/(T_w - T_s)$ is plotted against x for

	Heat flux, q,	
	kW/m²	(Btu/(hr)(ft²))
o	43.8	(13.9x10³)
□	63.0	(20.0x10³)
◇	79.1	(25.1x10³)
△	103	(32.7x10³)
▽	127	(40.4x10³)
◻	155	(49.2x10³)
◻	198	(62.9x10³)
◻	223	(74.1x10³)
◻	272	(85.5x10³)

——— Correlation of Dengler and Addoms (ref. 66)

	Heat flux, q,	
	kW/m²	(Btu/(hr)(ft²))
o	163	(51.8x10³)
□	354	(112x10³)
◇	~550	(~175x10³)
△	580	(184x10³)
▽	662	(210x10³)
◻	932	(296x10³)

——— Correlation of Dengler and Addoms (ref. 66)

Untailed symbols denote $T_i \approx 361$ K (~190° F)
Tailed symbols denote $T_i \approx 294$ K (~70° F)

(a) Mass velocity, ~68 kg/(m²)(sec) (~50x10³ lbm/(ft²)(hr)); inlet temperature, ~355 K (~180° F).

(b) Mass velocity, ~590 kg/(m²)(sec) (~437x10³ lbm/(ft²)(hr)).

Figure 72. Ratio of boiling to liquid heat-transfer coefficients as function of equilibrium heat-balance flow ratio. Exit pressure, ~117 kN/m² abs (~17 psia); heated length-diameter ratio, 100.

these same conditions. Here, it is difficult to find any consistent trends. However, these definitions of the heat-transfer coefficient are not the only ones possible. Since some of the heat added to a fluid in subcooled boiling goes into the production of vapor, the remaining liquid has a lower average temperature T_l' than that calculated from an equilibrium heat balance. Performing a heat balance from the point of boiling initiation (subscript 0) to any downstream point,

$$T_l' = T_{l,0} + \frac{4q(z - z_0)}{DGc_p}\left(\frac{1 - \bar{\gamma}}{1 - x'}\right) \quad (25)$$

where x' is the actual quality and $\bar{\gamma}$ is the net fraction of the heat added from z_0 to z going into vaporization, $x'/(x - x_0)$. There are several means available for predicting x' and $\bar{\gamma}$; for the present discussion the following simple relation suggested by Levy (ref. 41) is used:

$$x' = x - x_d e^{(x/x_d) - 1} \quad (26)$$

where x_d is the equilibrium heat-balance quality at the point where bubbles first depart from the surface; hereinafter, x_d is taken to be x_0. The heat-transfer coefficient corrected

81

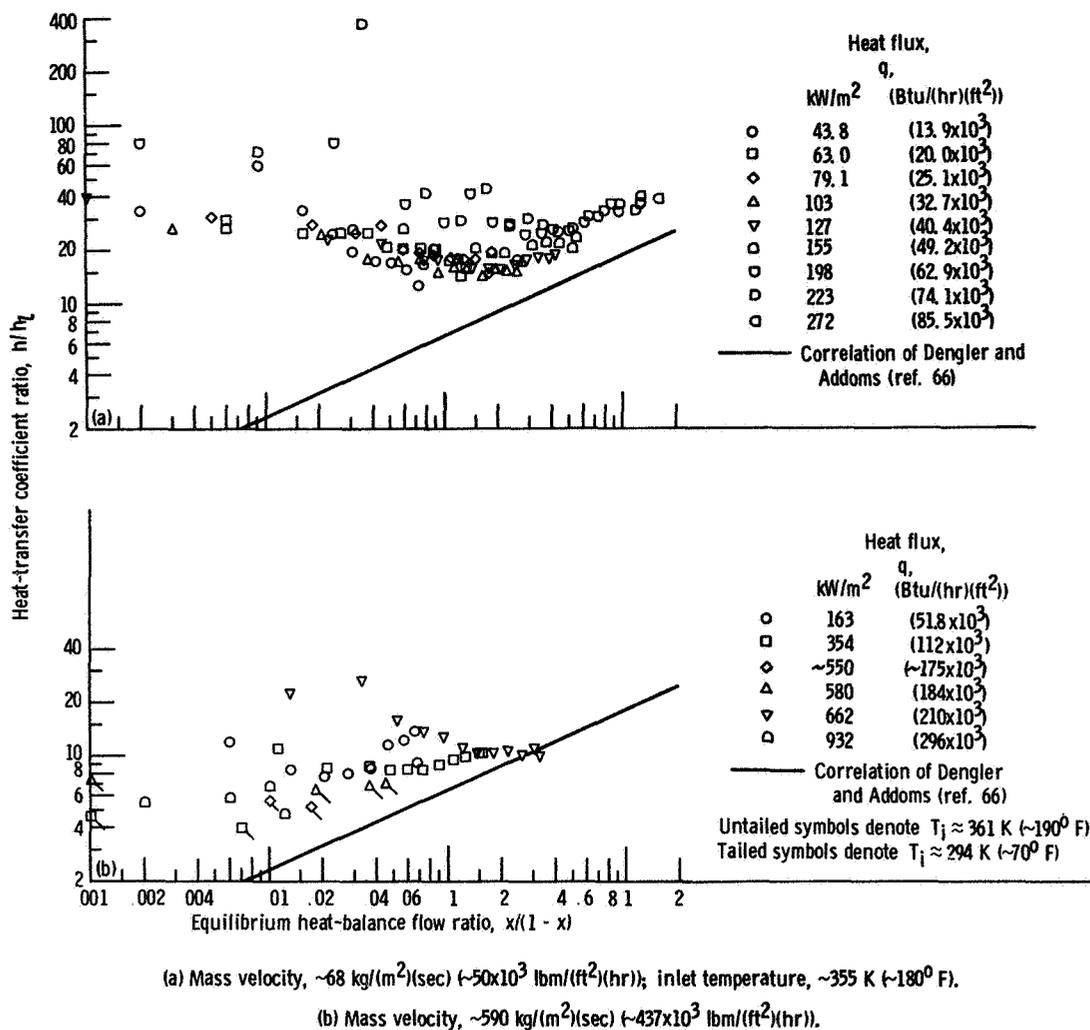(a) Exit pressure, ~114 kN/m² abs (~16.5 psia).

(b) Exit pressure, ~26 kN/m² abs (~3.8 psia).
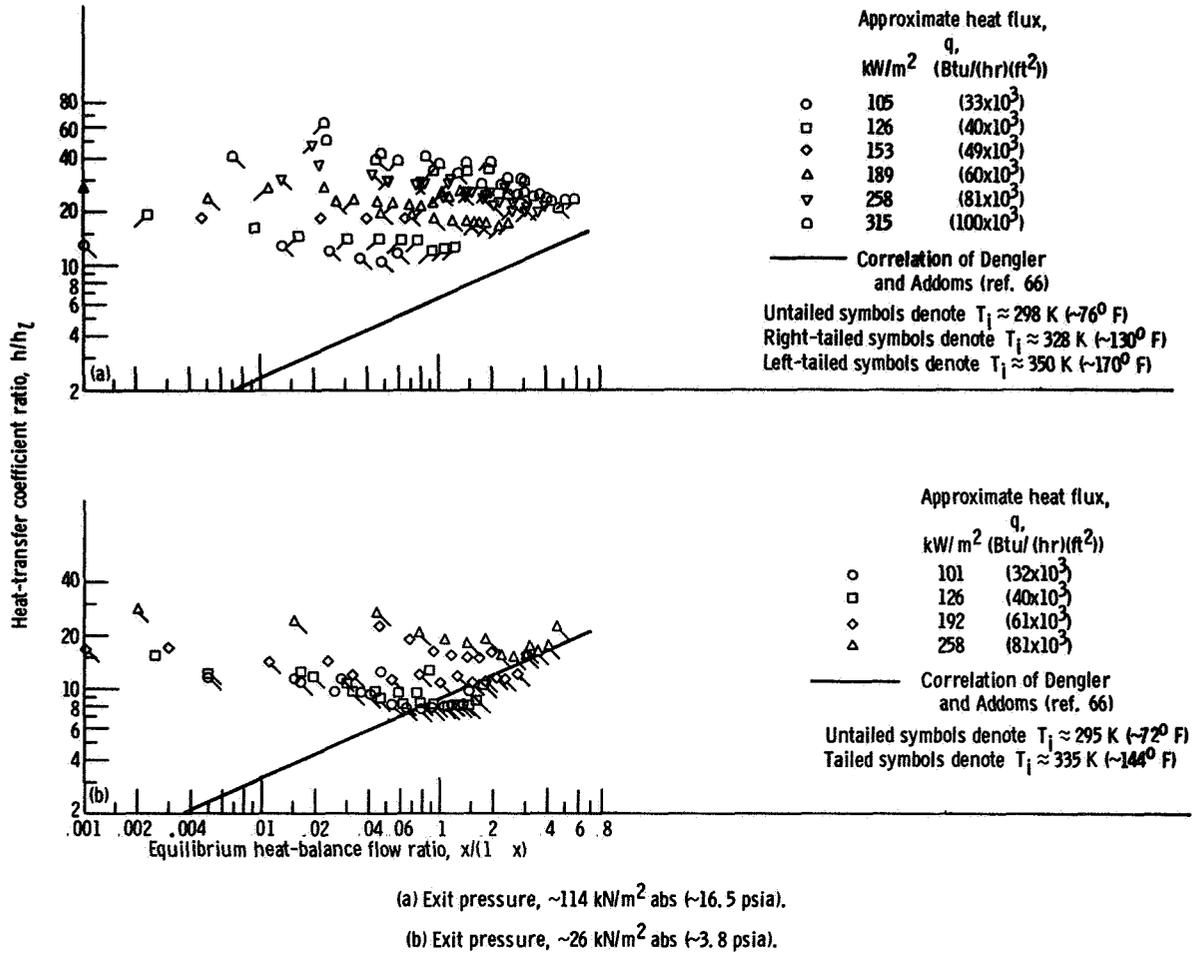
Figure 73. - Ratio of boiling to liquid heat-transfer coefficients as function of equilibrium heat-balance flow ratio. Mass velocity, ~68 kg/(m²)(sec) (~50x10³ lbm/(ft²)(sec)); heated length-diameter ratio, 50.

for nonequilibrium $h' = q/(T_w - T'_i)$ is plotted against the equilibrium heat-balance quality x in figure 74(c). It can be seen that the range of h' values is much less than that of h or h_s, and the variation of h' with x is less than that of h or h_s.

Another reasonable plot to make is h' against x'; this is shown in figure 75. In both figures 74(c) and 75 there is an apparent effect of inlet temperature, other relations, suggested by Kroeger and Zuber (ref. 39), give similar results. This may be due in part to the contribution of nucleate boiling; but neither of the correlations attempting to account for nucleate boiling (refs. 66 and 70), using nonequilibrium quality, agrees well with the

data. However, note that equation (26) is an assumed equation, used previously only for smaller subcoolings, and also that the assumption that $x_0 = x_d$ may contribure to the apparent subcooling effect. It appears that x' is calculated to be too large; pressure-drop calculations also indicate that x' is too large. Therefore, although it might be possible to obtain h' as a function of x or x', as well as q, G, and physical property values for a given initial subcooling, it appears that a nonequilibrium model valid over a wide range of subcooling and pressure is still required before a general correlation of the data will be successful.

Heat flux, q, kW/m^2 (Btu/ (hr)(ft^2))		Inlet temperature, T_i, K ($^\circ$F)
■	413 (131x10^3)	~294 (~70)
▲	662 (210x10^3)	
○	121 (38.4x10^3)	
□	334 (106x10^3)	~361 (~90)
◇	554 (176x10^3)	
△	932 (296x10^3)	
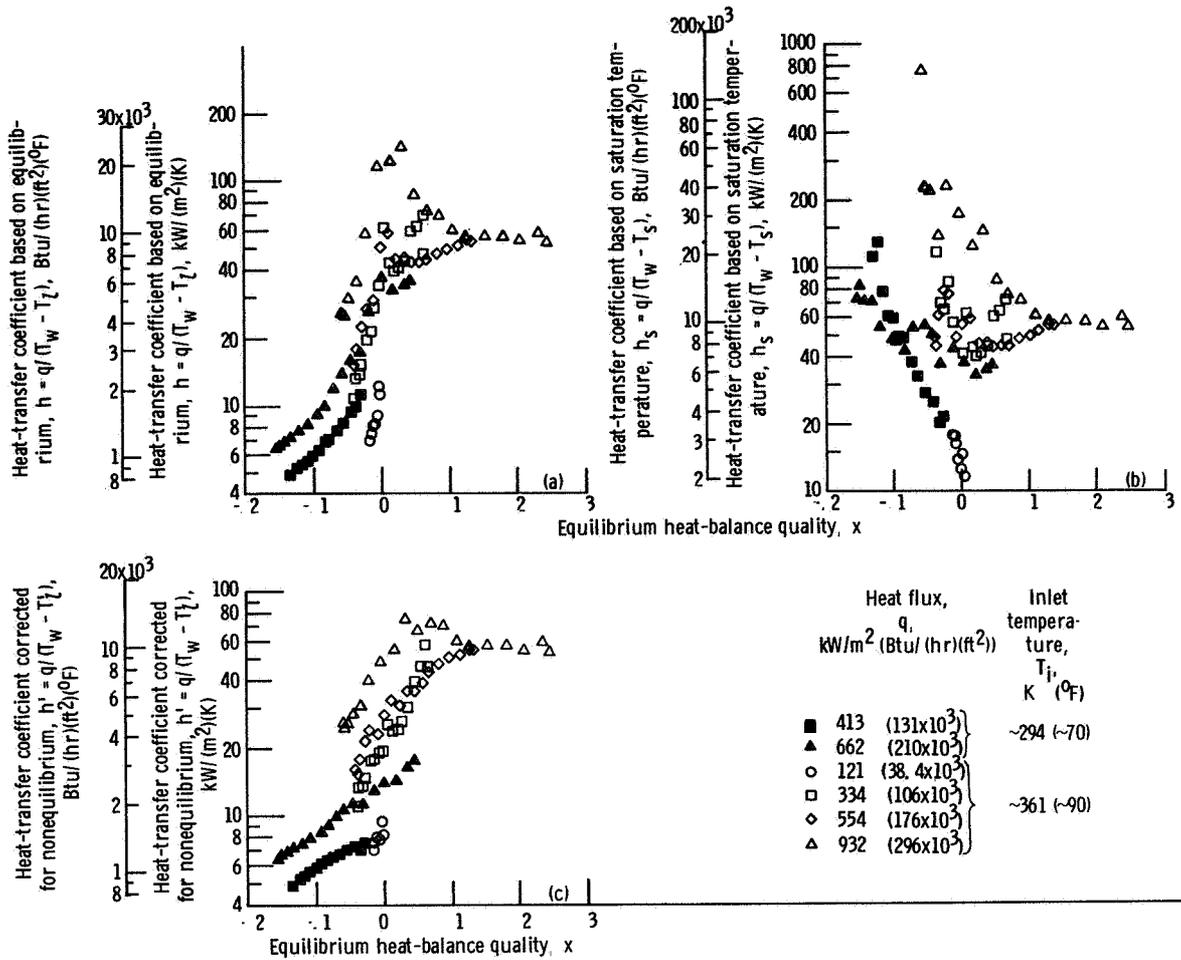
(a) Heat-transfer coefficient based on equilibrium heat balance or saturation temperature.

(b) Heat-transfer coefficient based on saturation temperature.

(c) Heat-transfer coefficient corrected for nonequilibrium.

Figure 74. - Heat-transfer coefficient corrected for nonequilibrium as function of nonequilibrium quality. Mass velocity, ~590 kg/(m^2)(sec) (~437x10^3 Btu/(ft^2)(hr)); exit pressure, 119 to 146 kN/m^2 abs (16.9 to 21.2 psia); heated length-diameter ratio, 100.

Rotating Water Boiling

The effects of gravity or acceleration on nucleate boiling can be independently controlled and studied in a rotating boiler such as that reported in references 79 and 80. Aside from the various vapor-separation effects discussed in chapter 3, the effect of acceleration on boiling heat-transfer coefficients is of interest here, as well as acceleration effects on inlet subcooling, liquid level, fluid temperature distribution, and

boiling incipience. These effects are now summarized from the results of references 79 and 80.

In figure 76, heat flux is plotted against wall superheat $T_w - T_{s,w}$ for accelerations of 50, 100, 200, and 400 g's. In the low-heat-flux boiling region (where natural convection is important), the boiling coefficient (ratio of ordinate to abscissa) increases markedly as acceleration increases. This coefficient increases as much as 60 percent from 50 to 400 g's. At the higher heat fluxes the heat-transfer curves for the various

83
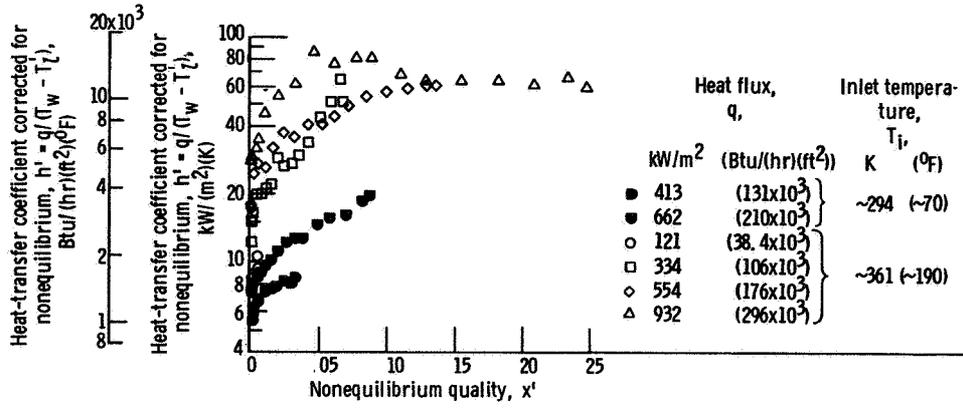
Figure 75. – Heat-transfer coefficient corrected for nonequilibrium as function of nonequilibrium quality. Mass velocity, ~590 kg/(m²)(sec) (~437x10³ Btu/(ft²)(hr)); exit pressure, 119 to 146 kN/m² abs (16.9 to 21.2 psia); heated length-diameter ratio, 100. (Data from ref. 90.)
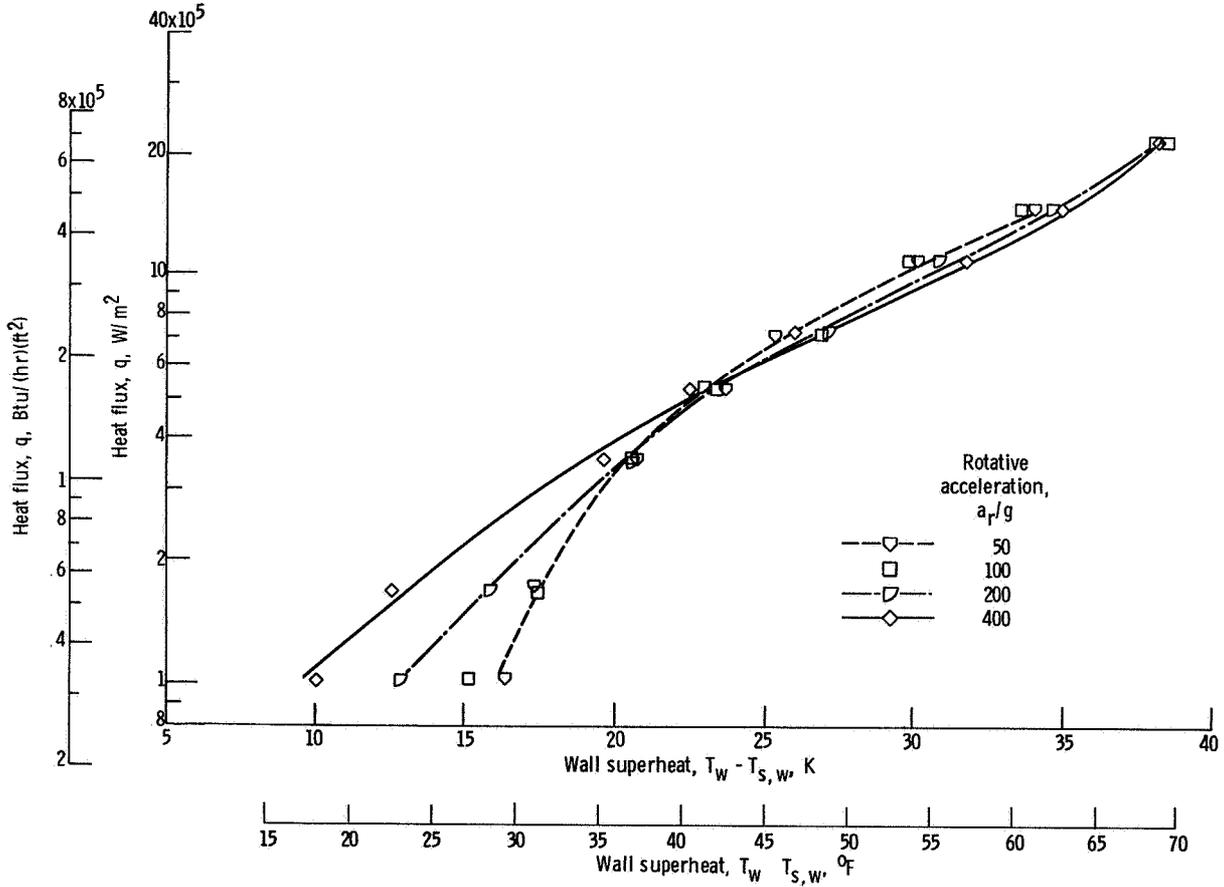
Figure 76. Effect of acceleration on nucleate boiling; two-phase fluid level constant at 0.95 cm (0.375 in.); liquid inlet subcooling, ~28 K (~50° F).

accelerations converge into a narrow band of wall superheat values (±1 K), with the higher accelerations converging at progressively higher heat fluxes. Within the narrow band of wall superheats at high heat fluxes, a slight trend is evident for a reversal of the effect of acceleration compared with that at low heat fluxes. However, any reversal at high heat fluxes is as small in magnitude as the usual scatter in such experimental data.

Inlet liquid subcooling to 36 K does not measurably affect nucleate-boiling coefficients over the range of 25 to 200 g's. This result is consistent with the subcooled, forced-flow, fully developed boiling data of reference 89, taken with water at 1 g and low pressures.

At increased accelerations, boiling heat-transfer coefficients increase consistently with increased depth of fluid. For example, at

200 g's and 179-kW/m² heat flux, the coefficient increased 24 percent for an increase in depth of 185 percent. At 25 g's, the changes in coefficient were much less. This trend is in agreement with that of increased pressure in normal pool boiling.

Temperature variations with depth of boiling fluid are accentuated with increased acceleration. Measurements of the radial temperature profile in the boiling annulus reveal a distinct inversion, which is undoubtedly linked to the secondary-flow cells and subcooled feed-water supply discussed in chapter 3. Two typical radial temperature profiles at 200 g's are shown in figure 77. They show the thin thermal layer near the heated surface covered by the bulk of the fluid, which is several degrees cooler than the vapor saturation temperature. At the liquid-vapor interface the fluid temperature
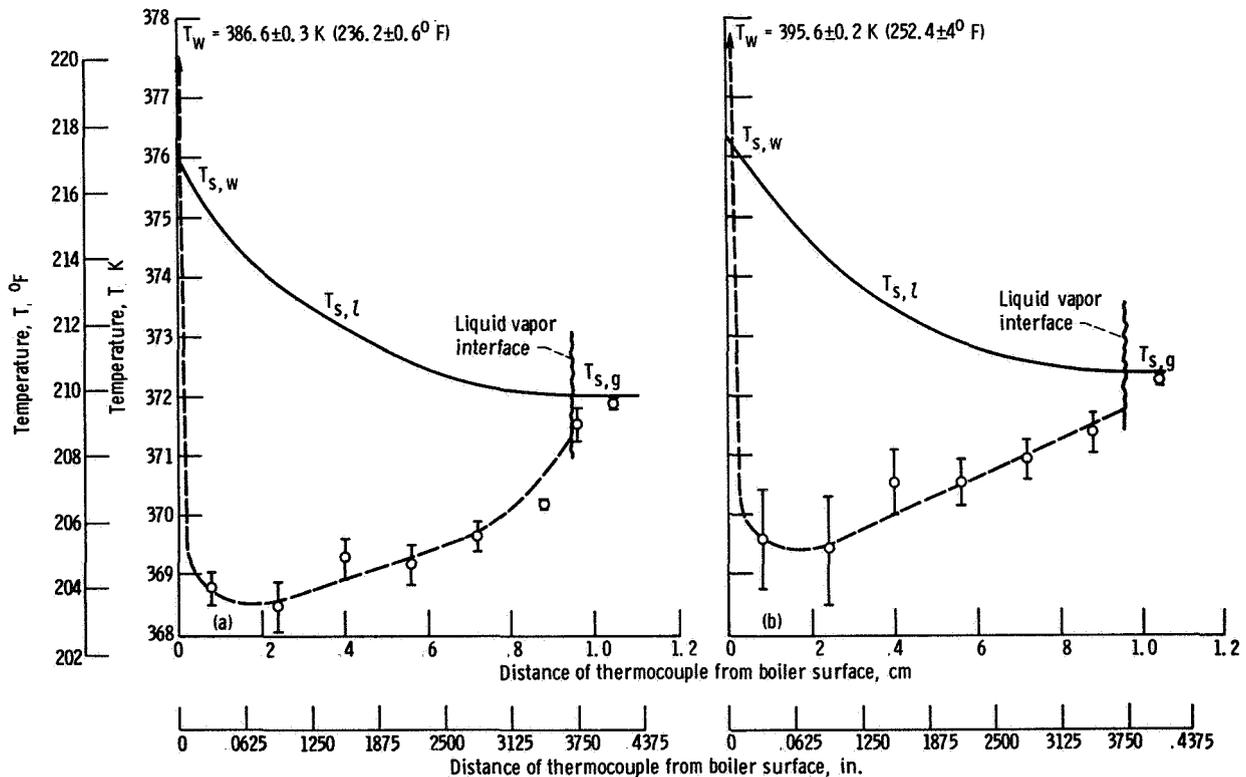
(a) Heat flux, 85 200 W/m² (27 100 Btu/(hr)(ft²)).

(b) Heat flux, 362 000 W/m² (115 000 Btu/(hr)(ft²)).

Figure 77. Radial temperature profiles in boiling annulus. Rotative acceleration, 200 g's.

closely approaches the vapor temperature. This complex, highly accelerated, once-through boiling process, although stable, is not in thermodynamic or phase equilibrium and is not characterized by saturated pool-boiling models.

Incipient boiling data, as expected, show that as acceleration increases, both heat flux and wall superheat increase at the points of incipient boiling. In common with more conventional boiling test results, the rotating-boiler data include minor complications attributable to hysteresis and surface aging effects.

SHELL TEMPERATURE PROFILES AND OVERALL HEAT-TRANSFER COEFFICIENTS

For boiling in heat exchangers, local parameters such as heat-transfer coefficients and quality are generally quite difficult to determine. The local heat flux must be obtained by differentiating the heating-fluid temperature profile, which is generally obtained from the shell outer-wall temperatures, this calculation is usually not very accurate. Furthermore, in many cases, boiling-fluid and tube inner-wall temperatures are not measured in order to avoid having thermocouples inside the experimental flow passages. Some insight into the nature of local overall coefficients, however, may be obtained by the use of measured shell outer-wall temperatures and boiling-fluid temperatures estimated from pressure-drop calculations.

Plain-Tube Sodium Boiling

Sodium-boiling shell temperature profiles were previously presented herein (fig. 13) in comparing all-liquid and two-phase inlet conditions. One way of utilizing the

measured shell temperatures is the method suggested by Stein (ref. 114), in which the natural logarithm of a dimensionless shell temperature $(T_{sh} - T_{bi})/(T_{hi} - T_{bi})$ is plotted against the dimensionless axial distance $4z/DPe$. A linear plot indicates a constant overall heat-transfer coefficient, with the value of the coefficient proportional to the slope of the curve. A few plots of this type were made by Lewis, Groesbeck, and Christenson (ref. 83), and they gave the following indications:

(1) For the liquid inlet tests, the local overall heat-transfer coefficient was constant in the boiling region, except for a short transition length following the point where the superheated liquid began to vaporize. The local coefficient upstream of the initiation of two-phase flow was also constant and agreed well with predictions based on liquid-phase convection.

(2) For the two-phase inlet tests, a constant local overall coefficient was obtained only in the downstream section of the boiler. Near the boiler inlet a lower value of the coefficient was obtained which gradually increased with length until it reached an asymptote whose maximum value corresponded with that of the boiling region of the liquid inlet tests. As the inlet quality was reduced and/or the initial temperature difference $T_{he} - T_{bi}$ increased, the value of this asymptote decreased.

The local heat-transfer coefficient may also be determined by assuming the heating-fluid coefficient and differentiating the shell temperature distribution to obtain an approximate heat flux. The actual local heating-fluid bulk temperature and heat flux can then be obtained by a trial process. A local boiling-fluid saturation temperature approximated from the pressure-drop data can be used to compute the local overall heat-transfer coefficient, quality, and tube wall temperatures. Results of such an approach are shown in figure 78. Details of
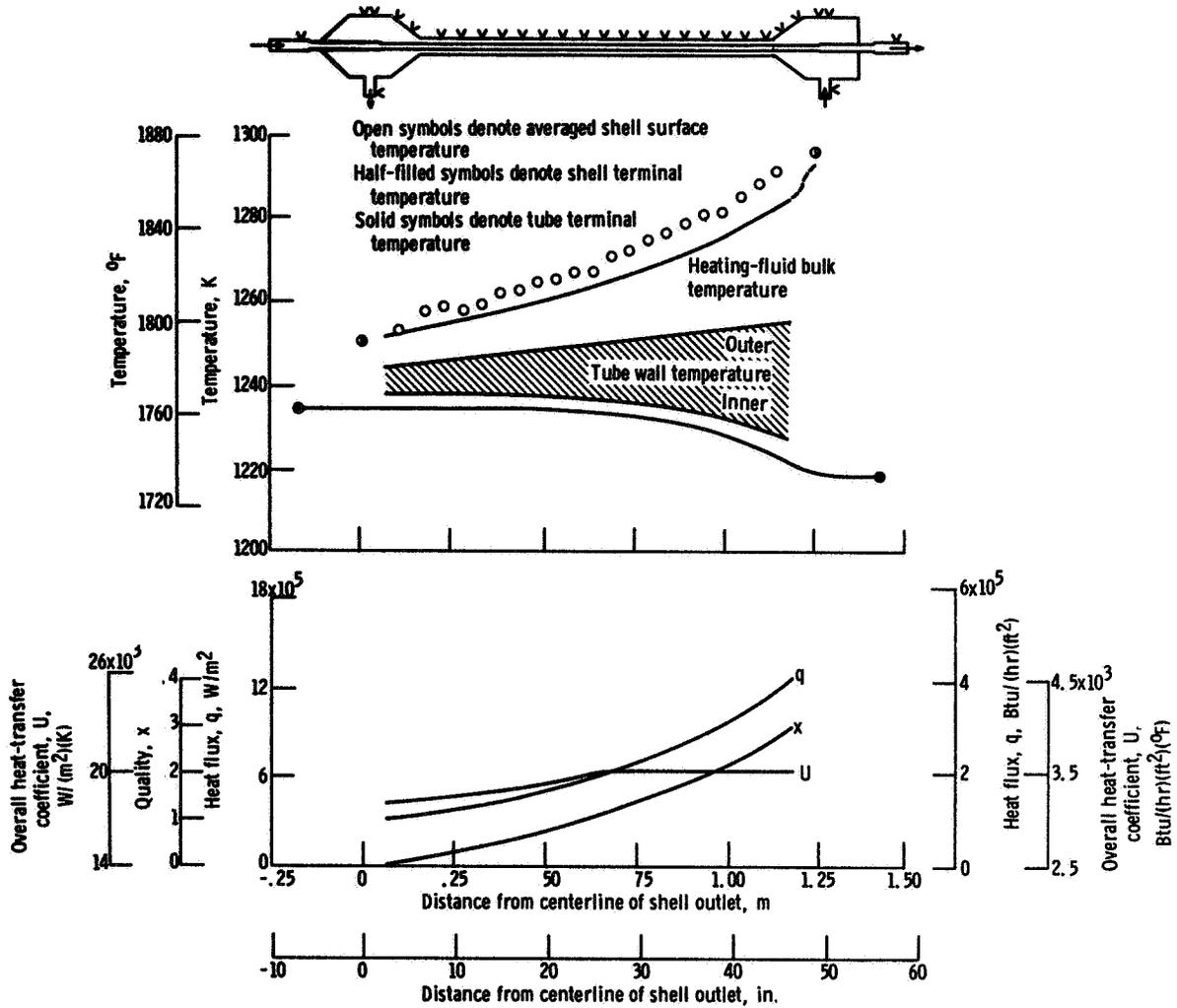
Figure 78. - Typical variations of local heat transfer and vapor quality along test boiler. Heating-fluid flow rate, 635 g/sec (5040 lbm/hr); test fluid flow rate, 24.8 g/sec (197 lbm/hr).

the computation are given in reference 83. This run had a two-phase inlet condition and was relatively steady. The local heat flux and quality varied almost exponentially with length, while the local overall heat-transfer coefficient increased in the upstream section of the boiler and was essentially constant thereafter. The computed results of figure 78 indicate that heating-fluid convection and tube wall conduction constitute the major parts of the thermal resistance. Hence, large variations in the local boiling coefficient would have only minor effects on local and average overall heat-transfer coefficients.

Water Boiling with Helical Wire Insert

Several runs were made in reference 87 with relatively low heating-fluid flow rates in order to get relatively large shell wall temperature gradients and thus better resolution of local heat-transfer data.

Figure 79 shows typical temperature profiles for exit quality low enough that no dry-wall boiling occurs and with the inlet nozzle flashing to ~0.03 vapor quality The shell wall temperatures shown are experimental data. For the boiling fluid, only
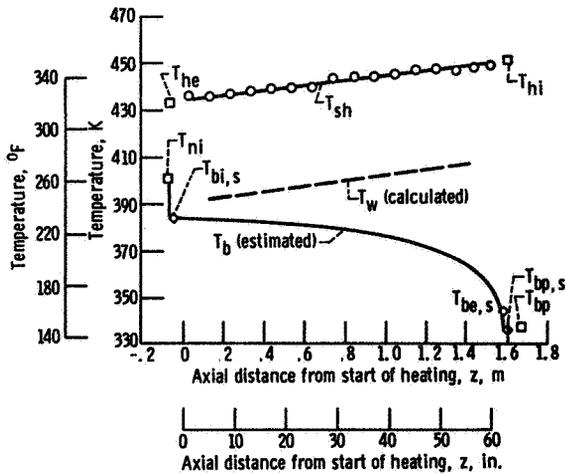
Figure 79. - Typical temperature profiles for water boiler with helical wire insert and flashing at venturi inlet at exit quality low enough that no dry-wall boiling occurs (x_e = 0.73).

This trend was consistently observed in references 85 and 86.

Figure 80 shows typical temperature profiles for high exit quality, again with the inlet nozzle flashing, this time to ~0.02 vapor quality. In this case the onset of dry-wall boiling was observed, at about 76 cm from the start of heating. The boiling-fluid

the inlet and exit temperature were obtained as experimental data. Therefore, the curve of T_b against distance was estimated by using the pressure-drop correlation presented in the preceding chapter. The inner-wall temperature was then calculated by using heating-fluid and wall resistances from reference 87 Note that the heat flux, which is proportional to dT_{sh}/dz, remains approximately constant, while the overall and boiling-side heat-transfer coefficients decrease with length, since $T_{sh} - T_b$ and $T_w - T_b$ increase.
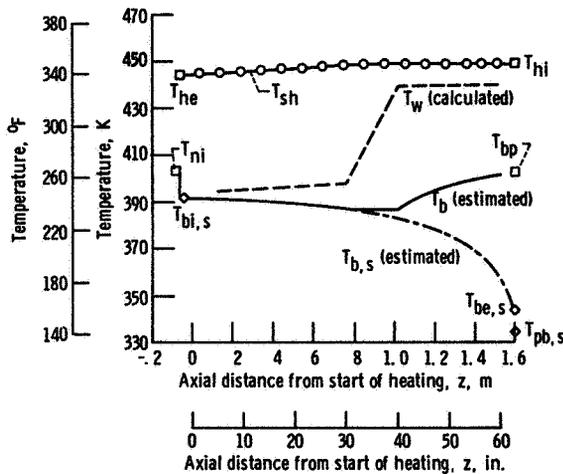
Figure 80. - Typical temperature profiles for water boiler with helical wire insert, flashing at venturi inlet, and vapor superheat at exit (x_e = 0.95).

Figure 81. - Local overall heat-transfer coefficient as function of axial distance from start of heating for various heating-fluid flow rates. Boiling-fluid flow rate, ~0.011 kg/sec (~85 lbm/hr).

exit-plenum temperature showed ~59 K vapor superheat, indicating that heat was being added to the vapor even though some liquid remained. Until the onset of dry-wall boiling, the trends are the same as those in figure 79.

The effect of the heating-fluid flow rate W_h on the variation of the local overall heat-transfer coefficient U with distance z is shown in figure 81. For relatively low qualities, U decreases with increasing z and, as expected, U increases with increasing W_h. At higher qualities, because of dry-wall boiling, the curves for various values of W_h cross. This is reasonable since the higher the heating-fluid flow rate, the higher the boiling-fluid quality at a given location, and in the region beyond the initiation of dry-wall boiling, the boiling-side heat-transfer coefficient generally decreases with increasing quality

Probably the most significant of these results is that, for these data, the local overall heat-transfer coefficient decreases with increasing distance, and therefore with quality, before the onset of dry-wall boiling. The opposite effect is often expected.

AVERAGE BOILING HEAT-TRANSFER COEFFICIENTS

Although there is considerable uncertainty in the prediction of local values of the boiling heat-transfer coefficient, the problem of determining the required heat-transfer area is not too severe. For the boiling of alkali metals, the boiling-side thermal resistance is nearly negligible prior to the boiling crisis. And a correlation of average boiling-side coefficients has been obtained for water.

Boiling-side heat-transfer coefficients were generally not computed for the sodium-boiling tests of reference 83 because of the limited prec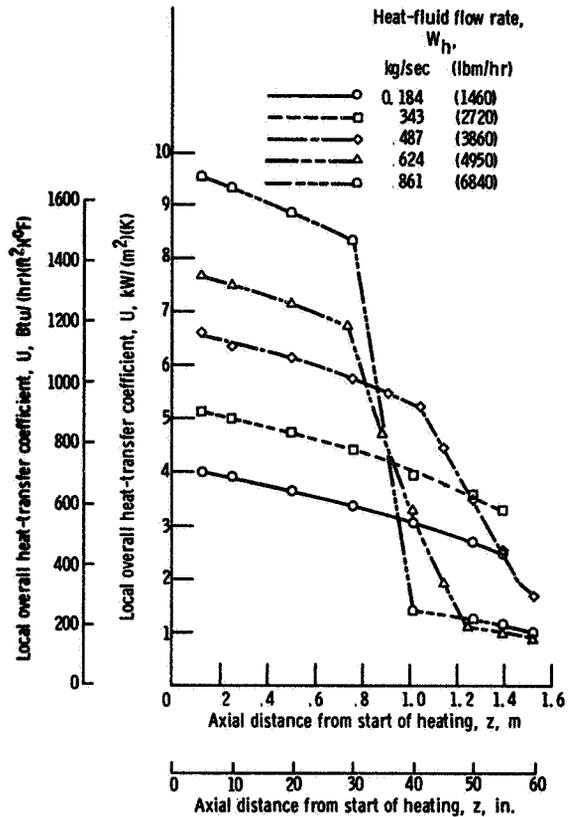ision of the data and uncertainty as to the correct value of the heating-fluid heat-transfer coefficient. Such problems are common for liquid-metal-boiling heat exchangers. The problem of accuracy is illustrated by figure 78. The estimated tube inner-wall temperature was less than 5.6 K above the estimated boiling-fluid temperature,

and this is close to the $\pm1/4$ percent limit of thermocouple error

Plain-Tube Water Boiling

Experimental values of the mean boiling-side heat-transfer coefficient h_b increase strongly with flow rate and exit quality (provided that the transition to dry-wall boiling does not occur). This increase of h_b with flow and exit quality indicates that the dominant mechanism may be of a convective nature. The effect of flow rate can be approached by assuming that h_b is proportional to h_l, the coefficient for all-liquid flow at the same total flow rate and temperature:

$$h_l = 0.023 \left(\frac{k_l}{D}\right)\left(\frac{DG}{\mu_l}\right)^{0.8}\left(\frac{c_p \mu_l}{k}\right)^{0.5}$$

$$W/(m^2)(K) \qquad (27)$$

This is shown in figure 82, where h_b/h_l is plotted against x_e for exit pressures of about 55 and 117 kN/m^2 absolute. The mean boiling-side heat-transfer coefficient increases with increasing pressure for a given flow rate and exit quality, even though the vapor velocity would tend to decrease because of the increasing vapor density. The effect of pressure may be correlated by plotting h_b/h_l against $x_e(P_{be}/P_c)^{0.5}$, where P_c is the thermodynamic critical pressure, as shown in figure 83. The data are those of references 57 and 85. The data may be correlated as follows, as long as dry-wall boiling does not occur, for exit qualities greater than $1.5 c_{p,l} (T_{be,s} - T_{bi})/\lambda$.

$$\frac{h_b}{h_l} = 1 + 200 x_e \sqrt{\frac{P_{be}}{P_c}} \qquad (28)$$

Boiling-fluid flow rate,
W_b,
kg/sec   (lbm/hr)

o	0.006 to 0.010	(50 to 80)
□	.010 to .019	(80 to 150)
◇	.019 to .038	(150 to 300)
△	.038 to 11	(300 to 870)

Open symbols denote exit pressure
of ~115 kN/m² abs (~17 psia)
Solid symbols denote exit pressure
of ~55 kN/m² abs (~8 psia)

Exit pressure,
kN/m² abs (psia)

~115 (~17)

~55 (~8)

Ratio of mean boiling-side heat-transfer coefficient to that for all-liquid turbulent flow, h_b/h_l
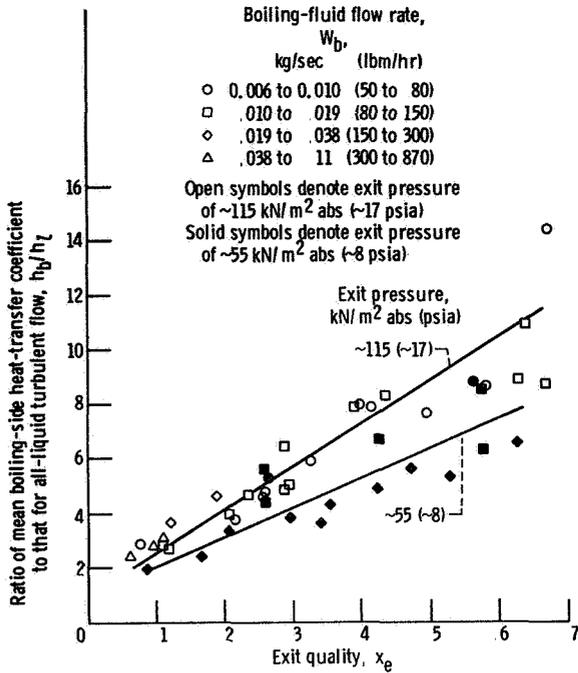
Exit quality, x_e

Figure 82. - Ratio of mean boiling-side heat-transfer coefficient to that for all-liquid turbulent flow as function of exit quality for exit pressures of ~55 and ~115 kN/m² abs (~8 and 17 psia), no dry-wall boiling, and $x_e > 1.5 c_{p,l} (T_{be,s} - T_{bi})/\lambda$.

	Test section	Flow	Boiler-exit pressure, P_{be}, kN/m² abs	(psia)
o	1	Countercurrent	~115	(~17)
□	1	Parallel	~115	(~17)
◇	2	Countercurrent	24 to 55	(3.5 to 8)
△	2	Countercurrent	55 to 83	(8 to 12)
▽	2	Countercurrent	110 to 166	(16 to 24)
▢	$x_e > 0.15$ (ref. 57)		55 to 207	(8 to 30)

Ratio of mean boiling-side heat-transfer coefficient to that for all-liquid turbulent flow, h_b/h_l

$h_b/h_l = 1 + 200 x_e (P_{be}/P_c)^{0.5}$

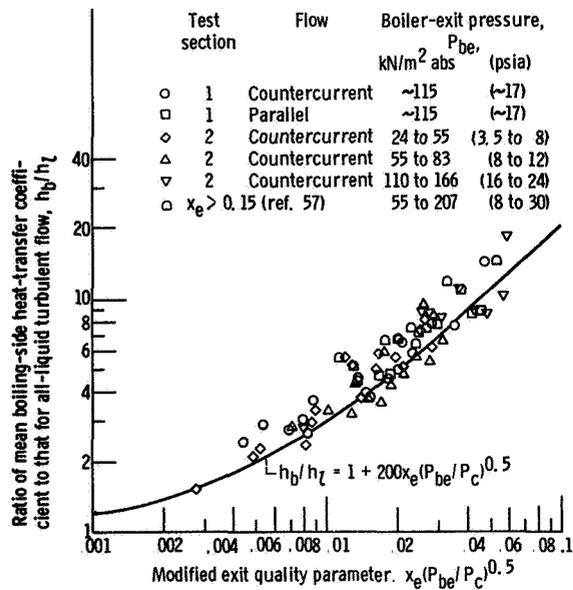Modified exit quality parameter. $x_e (P_{be}/P_c)^{0.5}$

Figure 83. - Ratio of mean boiling-side heat-transfer coefficient to that for all-liquid turbulent flow as function of exit quality and pressure for no dry-wall boiling and exit quality greater than $1.5 c_{p,l} (T_{be,s} - T_{bi})/\lambda$.

It is believed that subcooled boiling effects cause discrepancies at lower exit qualities, for the ranges of variables correlated. The data correlated are for P_{be}/P_c from approximately 10^{-3} to 10^{-2} Since the properties involved are uncertain, extrapolation is uncertain.

This correlation was based on an enthalpy-weighted mean temperature difference between heating and boiling fluids

$$\Delta T_m = \overline{\Delta T_{sc}} \left[\frac{W_b c_{p,l}}{Q} (T_{be,s} - T_{bi}) \right]$$

$$+ \overline{\Delta T_B} \left(\frac{x_e W_b \lambda}{Q} \right) \quad (29)$$

The arithmetic mean temperature difference in the subcooled region $\overline{\Delta T_{sc}}$ was averaged with the arithmetic mean temperature difference over the remainder of the boiler $\overline{\Delta T_B}$, with the heat loads in each region as weighting factors. Pressure drop was neglected. Note that for constant heat flux, $\overline{\Delta T_m}$ is the arithmetic mean temperature difference.

Water Boiling with Helical Wire Insert

Because of the larger pressure drops with the inserts, in applying this correlation to boilers with inserts (ref 87), pressure drop must be accounted for in ΔT_m Therefore,
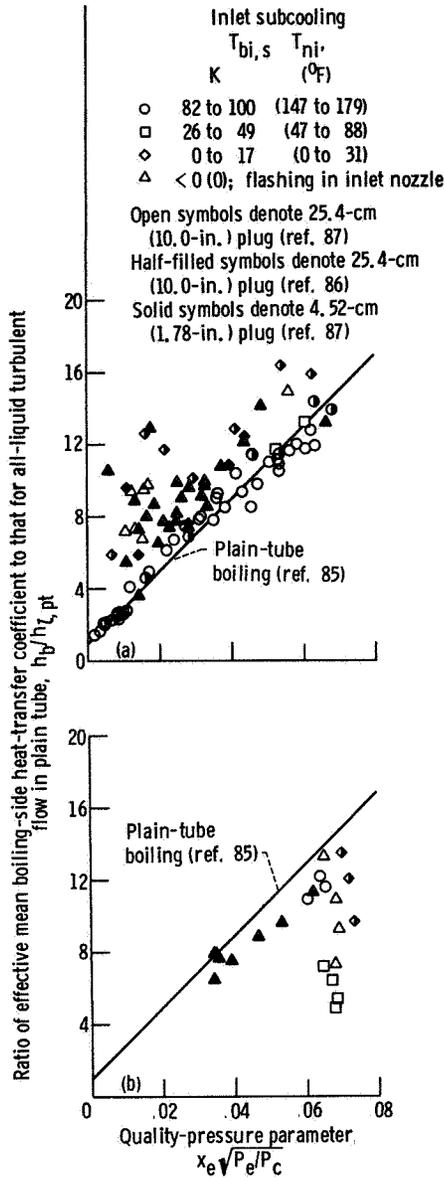
$$\Delta T_m = \overline{\Delta T_{sc}} \left[\frac{W_b c_{p,l}}{Q} (T_{bi,s} - T_{ni}) \right]$$

$$+ \overline{\Delta T_B} \left[1 - \frac{W_b c_{p,l}}{Q} (T_{bi,s} - T_{ni}) \right]$$

(30)

90

Inlet subcooling

	$T_{bi,s}$	T_{ni},
	K	(°F)
o	82 to 100	(147 to 179)
□	26 to 49	(47 to 88)
◇	0 to 17	(0 to 31)
△	< 0 (0); flashing in inlet nozzle

Open symbols denote 25.4-cm
(10.0-in.) plug (ref. 87)
Half-filled symbols denote 25.4-cm
(10.0-in.) plug (ref. 86)
Solid symbols denote 4.52-cm
(1.78-in.) plug (ref. 87)

Plain-tube boiling (ref. 85)

(a)

Plain-tube boiling (ref. 85)

(b)

Quality-pressure parameter,
$x_e\sqrt{P_e/P_c}$

(a) No exit vapor superheat indicated.

(b) Exit vapor superheat indicated.

Figure 84. Ratio of effective mean boiling-side heat-transfer coefficient to that for all-liquid turbulent flow in plain tube as function of quality-pressure parameter; comparison with plain-tube boiling (ref. 85).

and for flashing at the inlet nozzle, $\Delta T_m = \overline{\Delta T_B}$ Experimental values of the coefficient ratio $h_b/h_{l,pt}$, for runs showing no indications of vapor superheat or flow oscillations as great as ±5 percent, are plotted against the parameter $x_e\sqrt{P_{be}/P_c}$ in figure 84(a). The data of reference 86 for the same boiler and plug, but for a larger inlet nozzle, are also shown. For inlet subcoolings of 26 K or greater, the experimental data agree with the plain-tube correlation. But for inlet subcoolings of 17 K or less and for flashing at the inlet nozzle, coefficient ratios range from plain-tube values to about four times as great. No appreciable difference could be noted between the heat-transfer results from the short plug, which only reached to the beginning of the heated zone, and those from the long plug, which extended more than 20 cm into the heated zone. Experimental data with exit vapor superheat are shown in figure 84(b). As might be expected the coefficient ratios are generally less than with no indication of vapor superheat, and no general trend can be cited.

Chapter 8

CONCLUSIONS

The performance of boiling heat exchangers has been progressively improved by a systematic series of modifications and tests. The best tubular-boiler combination tested was a venturi-type converging-diverging nozzle followed by a tapered inlet-region plug extending into the nozzle diffuser and a full-length helical wire insert. An attractive feature of such an inlet configuration is that by sufficiently preheating the liquid, flashing can be caused in the nozzle, giving a fixed location for the initiation of two-phase flow and a desirable flow regime entering the boiler proper Thus, instability problems associated with motion of the zero-heat-balance-quality interface are avoided, as well as a problem often encountered with alkali metals, that is, nonequilibrium liquid superheat in the boiler tube.

Tests on novel nontubular and vortex-inlet boilers showed good potential, and more research on these configurations should be pursued.

The results of this experimental and analytical program directed toward the stabilization of once-through boilers may be summarized as follows:

1 The sodium-boiling investigation showed that metastable liquid superheat is a serious problem with alkali metals. It was also shown that a pressure-drop device is needed for flow stability In this case an orifice, well upstream of the inlet, was used Flashing across the orifice was found to be a useful means of eliminating the liquid-superheat problem. However, even with the orifice, complete vaporization to an exit quality of 1.0 could not be achieved.

2. A boiler tube with a helical wire insert yielded more stable performance than did plain hollow tubes of the same size, by postponing the boiling crisis transition to higher qualities. However, the pressure drop for comparable conditions was two to three times that for the plain tube. Inlet-region central plugs increased the range of stable performance for the boiler with the helical wire insert As a possible alternative, blade-type flow swirlers were found to markedly increase the heat flux at boiling crisis with considerably less pressure drop than with the helical wire insert. For example, the exit quality was doubled from 0.3 to 0.6 with a 58 percent increase in pressure drop for comparable conditions. However, with all these inserts, a pressure drop comparable to that across the boiler was required at the inlet throttle valve for flow stability

3 Orifice-type boiler inlets were found to be unsatisfactory, even though they did eliminate backflowing instability With them, the boiling-fluid exit temperatures rose well above saturation temperatures even though the exit vapor quality was considerably less than 1.0, generally about 0.8.

4 Venturi-type converging-diverging nozzle inlets were found to perform well, although the flow range for a given venturi size was limited. With boiling-fluid inlet temperatures only slightly below saturation,

flow was steady, no backslugging occurred, and the heat-balance exit quality achieved was greater than 1.0. Nozzle and boiler tests with potassium corroborated and extended the results obtained with low-pressure water

5. Design correlations are given for pressure drop and heat transfer, so that designers may properly size boilers and inlet nozzles for water and alkali metals in the same general ranges of size and properties as reported herein.

6. The rotating boiler was found to stably and reliably generate high-quality vapor. The vortex inlet and cyclone boiler concepts have also shown promise in preliminary tests.

Appendix A

SYMBOLS

A cross-sectional flow area, m^2; ft^2

a_r rotative acceleration, m/sec^2; ft/hr^2

C flow coefficient (eq. (22)), dimensionless

C_s saturation two-phase flow coefficient (eq. (21)), dimensionless

c_p heat capacity at constant pressure, $J/(kg)(K)$; $Btu/(lbm)(°F)$

D inside diameter of boiler tube, m; in.

D_{cb} diameter of centerbody, m; in.

D_o outside diameter of shell tube, m; in.

D_t diameter of nozzle throat, m; in.

D_1 outside diameter of boiler tube, m; in.

D_2 inside diameter of shell tube, m; in.

F orientation factor (eq. (19)), dimensionless

f friction factor, dimensionless

f_{TP} effective average two-phase friction factor, dimensionless

G mass velocity, $kg/(m^2)(sec)$; $lbm/(ft^2)(hr)$

g acceleration due to gravity, m/sec^2; ft/hr^2

g_c conversion factor, 1.00 $(kg)(m)/(N)(sec^2)$; 4.17×10^8 $(lbm)(ft)/(lbf)(hr^2)$

h heat-transfer coefficient, $W/(m^2)(K)$; $Btu/(hr)(ft^2)(°F)$

$\overline{h_B}$ average boiling heat-transfer coefficient, $W/(m^2)(K)$; $Btu/(hr)(ft^2)(°F)$

h_l heat-transfer coefficient for all-liquid, turbulent flow in tube with no inserts, $W/(m^2)(K)$; $Btu/(hr)(ft^2)(°F)$

h_s heat-transfer coefficient based on saturation temperature, $q/(T_w - T_s)$, $W/(m^2)(K)$;

95

Btu/(hr)(ft²)(°F)

K conversion factor, 1.00 m²/m²; 1/144 ft²/in.²

k thermal conductivity, W/(m)(K), Btu/(hr)(ft)(°F)

L total length of boiling tube, m; in.

L_b length of boiling region, $L_H - z_0$, m; in.

L_{cor} length of gas-vapor core, m; in.

L_H length of active heat-transfer surface, m; in.

L_U unheated (insulated) length, m; in.

N_b boiling number, $q/G\lambda$, dimensionless

N_{sc} subcooling number, $(c_{p,l}/\lambda)\left[T_s - (T_{l,0} + T_{l,e})/2\right]$, dimensionless

P pressure, N/m² abs, psia

P_c thermodynamic critical pressure, N/m² abs, psia

ΔP pressure drop, N/m²; psi

ΔP_B boiler pressure drop, N/m²; psi

ΔP_F frictional pressure drop, N/m²; psi

ΔP_G gravitational pressure drop, N/m²; psi

ΔP_I inertial pressure drop, N/m²; psi

Pe Peclet number, DGc_p/k, dimensionless

p insert pitch, m; in.

Q heating rate, W; Btu/hr

q heat flux, W/m²; Btu/(hr)(ft²)

R_1 inertial-pressure-drop multiplier (eq. (8)), dimensionless

R_2 gravitational-pressure-drop multiplier (eq. (11)), dimensionless

Re_g mean gas Reynolds number (eq. (16), dimensionless

Re_l mean liquid Reynolds number (eq. (16), dimensionless

Re_t throat liquid Reynolds number, dimensionless

r bubble radius, m; in.

T temperature, K, °F

T_l liquid bulk temperature, K; °F

T_{sh} temperature of shell wall outer surface, K; °F

$T_{2\varphi}$ temperature in two-phase rotating annulus, K; °F

ΔT temperature difference, K; °F

ΔT_B arithmetic average temperature difference over net boiling region, K; °F

ΔT_m mean temperature difference (eq. (29)), K, °F

96

SYMBOLS

ΔT_{sc} arithmetic average temperature difference over subcooled region, K; °F

t vane thickness, m; in.

U local overall heat-transfer coefficient, $W/(m^2)(K)$; $Btu/(hr)(ft^2)(°F)$

u velocity, m/sec, ft/hr

v_m mean two-phase specific volume, m^3/kg; ft^3/lbm

W flow rate, kg/sec; lbm/hr

X_{tt} Martinelli parameter (eq. (23)), dimensionless

x vapor quality (calculated from heat balance), dimensionless

z axial distance from start of heated section, m, in.

z_1 axial distance from start of heated section to point where heat-balance quality $x = 0$, m; in.

α void fraction, dimensionless

β_B physical property parameter,

$$\left(\frac{\rho_g}{\rho_{g,ref}}\right)^{0.5}\left(\frac{\rho_l}{\rho_{l,ref}}\right)^{0.5},$$

dimensionless

γ local vaporization rate parameter, dimensionless

$\overline{\gamma}$ mean vaporization rate parameter, dimensionless

γ_B physical property parameter,

$$\frac{\sigma}{\sigma_{ref}}\left[\frac{\mu_l}{\mu_{l,ref}}\left(\frac{\rho_{l,ref}}{\rho_l}\right)^2\right]^{1/3}$$

dimensionless

δ thickness of boiler tube wall, m; in.

θ_{se} boiler exit temperature difference, $T_{hi} - T_{be,s}$, K; °F

λ enthalpy of vaporization, J/kg, Btu/hr

μ viscosity, $kg/(m)(sec)$; $lbm/(ft)(hr)$

$\mu_{l,ref}$ reference liquid viscosity, $kg/(m)(sec)$; $lbm/(ft)(hr)$

ρ density, kg/m^3, lbm/ft^3

$\rho_{g,ref}$ reference gas density, kg/m^3; lbm/ft^3

$\rho_{l,ref}$ reference liquid density, kg/m^3, lbm/ft^3

ρ_m mean two-phase density, kg/m^3, lbm/ft^3

σ surface tension, N/m, lbf/ft

σ_{ref} reference surface tension, N/m, lbf/ft

Subscripts:

b boiling fluid

be boiler exit

bi boiler inlet

97

bp	boiling fluid exit plenum	*ne*	nozzle exit
calc	calculated value	*ni*	nozzle inlet
d	point of bubble departure from wall	*pt*	plain tube
		s	saturation
e	exit		
exp	experimental value	*se*	difference between heating-fluid inlet and boiler exit
g	gas phase		
h	heating fluid	*t*	nozzle throat
he	heating-fluid exit	*w*	boiler-tube inner wall
hi	heating-fluid inlet	0	point of boiling initiation

Superscript:

(')	corrected for nonequilibrium

i	inlet
l	liquid phase
min	minimum

PERFORMANCE AND EVALUATION OF

VARIOUS INLET RESTRICTORS

Since it was found that the performance of inlet restrictors had a strong effect on boiler performance, further studies of inlet devices were performed, including experiments with transparent test sections. These experiments and the ranges of test variables are tabulated in table V

INLET NOZZLES

Potassium

Test facility. – Figure 85 is a diagram of the test facility for the potassium-boiler inlet studies of reference 105, wherein a more detailed description of the apparatus is given.

TABLE V - SUMMARY OF EXPERIMENTS ON INLET RESTRICTOR CHARACTERISTICS

| Fluid	Restrictor description	Modifications	Minimum diameter		Area ratios		Ranges of test variables				Reference
			mm	in.	Inlet to throat	Exit to throat	Inlet temperature, T_{ni}		Flow rate, W_b		
							K	°F	g/sec	lbm/hr	
Potassium	Venturi	-------------	2 58	0.1015	67	14	882 - 1068	1128 - 1462	16 - 88	125 - 700	105
		Artificial throat cavity	2 58	1015			711 - 1058	820 - 1445	15 - 83	119 - 660	
Water	Stainless-steel venturi	-------------	2 56	1008			~300	~80	8 - 150	63 - 1200	---
	Lucite venturi	-------------	2. 62	103			~300	~80	8 - 150	63 - 1200	
Water	Double cone	-------------	635	025	400	310	287 - 346	56 - 164	3 5 - 9. 2	28 - 73	113
		Plug and helical wire	635	025	400	150	287 - 348	57 - 167	3 5 - 8. 8	28 - 70	
Water	Venturi	Plug and helical wire	72	0285	19	100	291 - 405	64 - 270	5. 6 - 15. 5	44 - 123	87
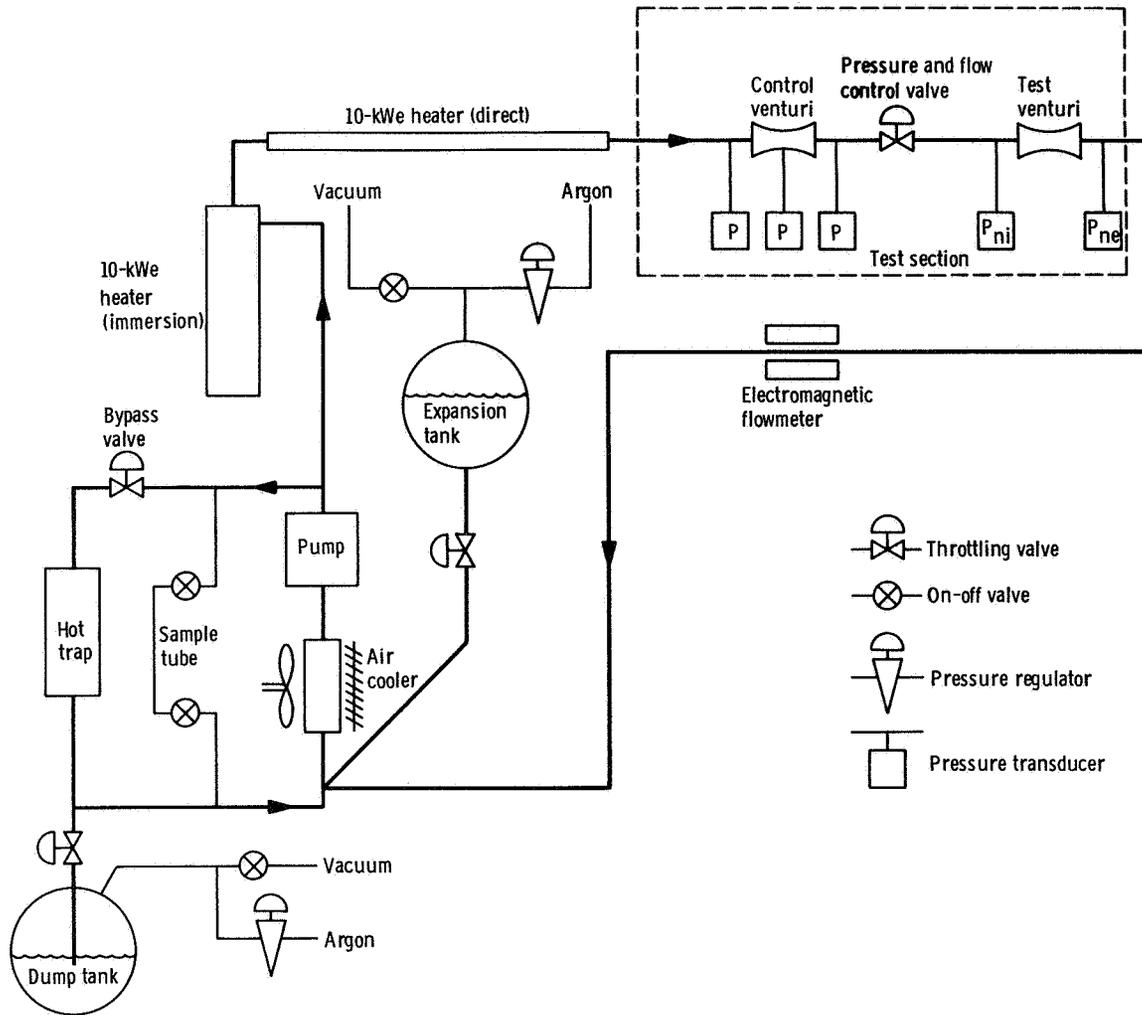
Figure 85. Schematic of adiabatic potassium two-phase flow facility.

The closed loop had an electromagnetic pump which circulated the liquid potassium through two electric heaters to the horizontal test section. The fluid then flowed through an air-cooled pipe (to prevent pump cavitation) back to the pump.

Test section. - The potassium test section, shown schematically in figure 86, consisted of two venturis of equal dimensions, mounted in series and separated by a valve. This valve created enough pressure drop to allow the upstream (control) venturi to operate always above the saturation vapor pressure, even when the test venturi

downstream of the valve experienced two-phase flow. The test venturi is shown in figure 87(a), it was also tested with an artificial throat cavity (fig. 87(b)).

Typical results. - Figure 88 shows typical potassium data from reference 105, throat pressure (calculated) is plotted against nozzle exit pressure for nominally constant flow rate and inlet temperature. The exit pressure started at a high level, was decreased to a minimum in a series of steady-state steps, and then increased again. The circles represent points taken during the pressure decreases; the squares were taken during pressure
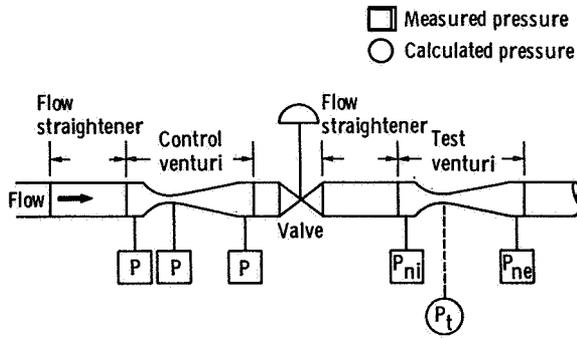
100

☐ Measured pressure
◯ Calculated pressure

Figure 86. Schematic of potassium venturi test section.

o Outlet pressure decrease
□ Outlet pressure increase
Open symbols denote cavitated and/or
   flashed conditions
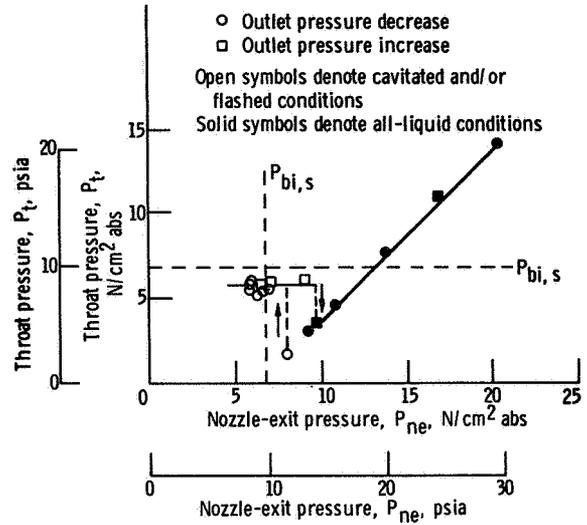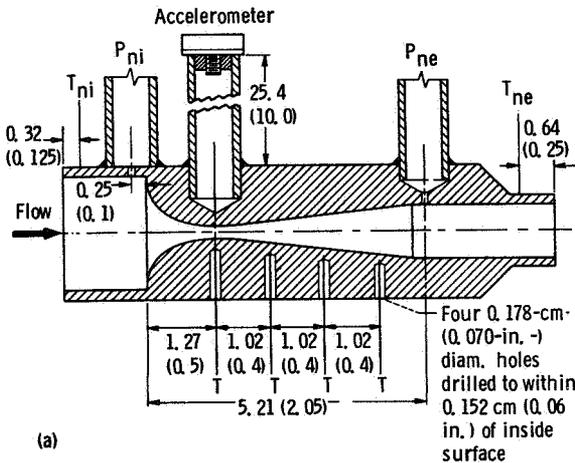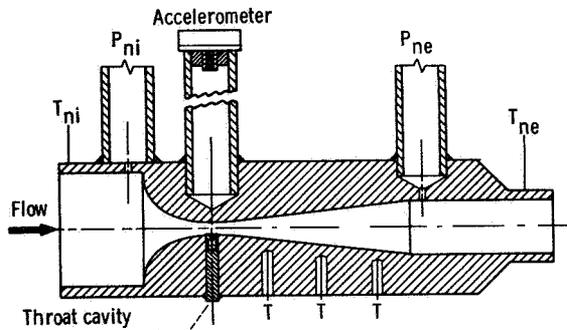Solid symbols denote all-liquid conditions

Figure 88. Typical venturi flow data for potassium: calculated throat pressure as function of exit pressure. No artificial throat cavity; flow rate, ~62.4 g/sec (~495 lbm/hr); inlet temperature, ~986 K (~1315° F).

(a) Test venturi without artificial throat cavity.

(b) Test venturi with artificial throat cavity.

Figure 87   Potassium venturi. (Dimensions are in cm (in.).)

increases. At first, the throat pressure decreased equally with the exit pressure. This relation remained unchanged even after the appearance of noise attributed to cavitation bubble collapse. Cavitation did not occur until the throat pressure was well below the vapor pressure, indicating liquid tension. Continued decrease in exit pressure resulted in a sudden and appreciable rise in throat pressure. Further exit-pressure decreases did not significantly affect the throat pressure.

There was appreciable hysteresis when the exit pressure was again increased. No effect on the throat pressure resulted until the exit pressure reached a considerably higher value than that at which the throat pressure rose suddenly for decreasing exit pressure. At this higher exit pressure, the throat pressure dropped back to the all-liquid characteristic.

Water

Test facility. - A schematic diagram of the test facility used in the double-cone, converging-diverging nozzle tests of reference 113, including its instrumentation, is shown

101

in figure 89(a). The flow passed through a filter to the heat exchanger, wherein the test fluid was either heated or cooled to provide the desired inlet temperature to the test nozzle. The flow then passed through the turbine flowmeter, the inlet flow-control valve, and the inlet plenum into the

transparent, vertically mounted test nozzle. The test nozzle discharged into a transparent tube, the upper end of which was connected to the exit-plenum chamber. The test fluid then discharged through the exit flow-control valve into a large vacuum exhaust system.
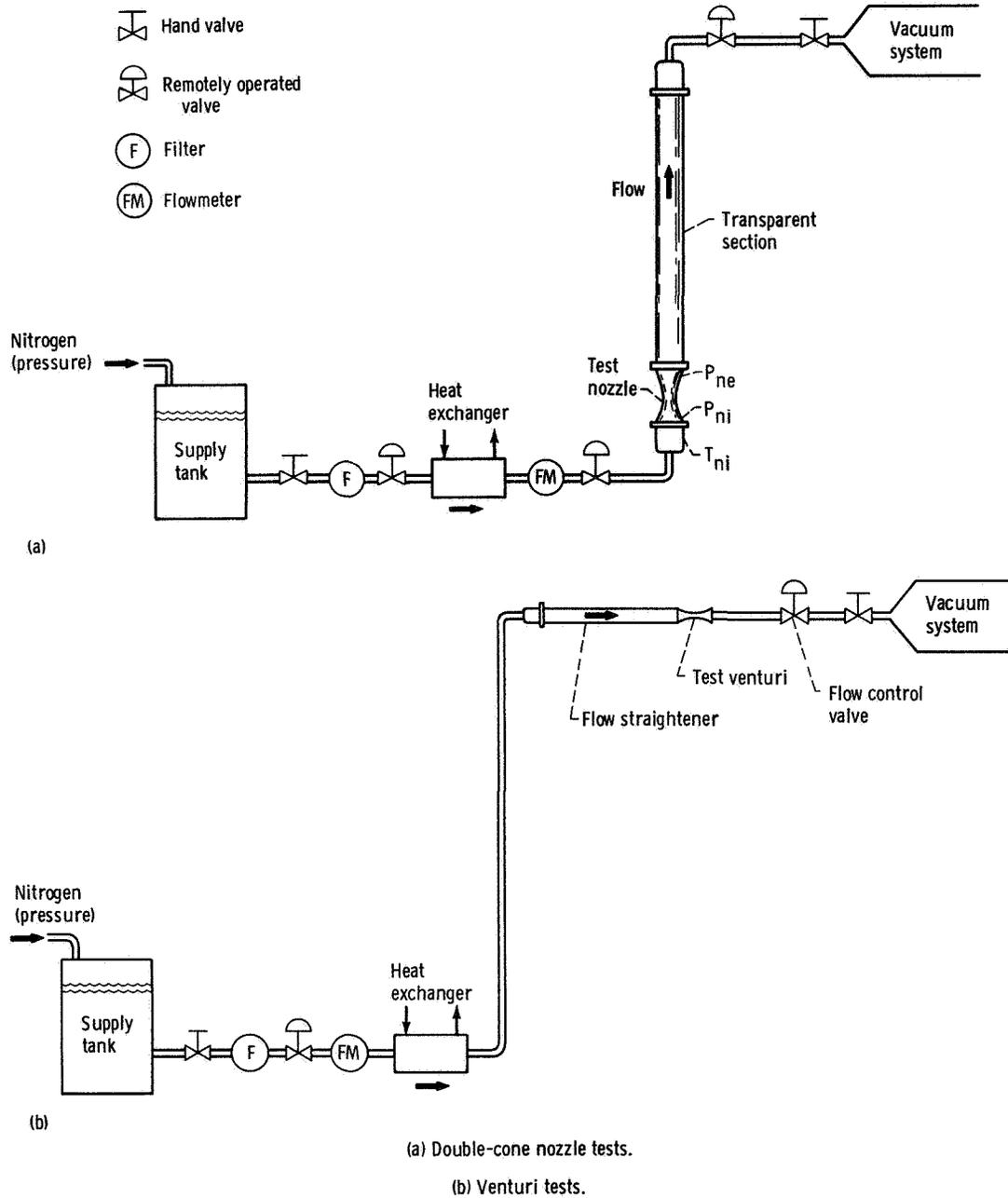

(a) Double-cone nozzle tests.

(b) Venturi tests.

Figure 89.   Schematic of adiabatic water two-phase flow facility.

Subsequent to these tests, two venturis of the geometry tested in potassium were tested in this facility. For these experiments, the test facility was modified somewhat (fig. 89(b)). The test section was mounted horizontally and was preceded by a flow-straightening section. No transparent section was used downstream of the test venturi.
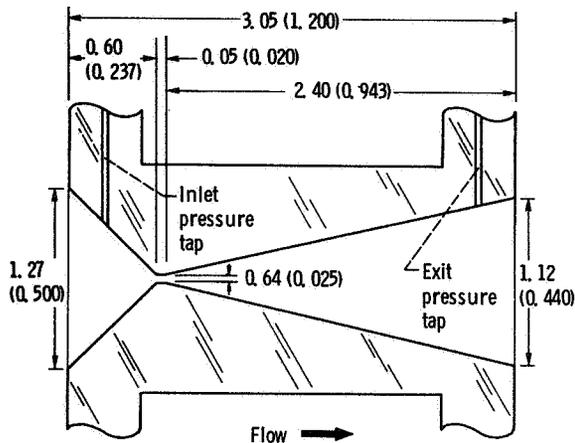

(a)

(a) Without inserts.

(b) With plug and helical wire insert.

Figure 90. - Double-cone converging-diverging nozzle. (Dimensions are in cm (in.).)

Test sections. – Two venturis of the same dimensions as the potassium test venturi (fig. 87(a)) were tested in the once-through water flow facility shown in figure 89(b). One of these venturis was made of stainless steel and the other of transparent plastic. The double-cone nozzle tests of reference 113 were made both without and with a tapered plug and helical wire insert, as shown in figures 90(a) and (b), respectively. The tests of a venturi nozzle with two different plugs at the inlet of a boiler (ref. 87) were done in the water-boiling facility (fig. 14).

Typical results. – Figure 91 shows typical data and photographs for the various regimes encountered in the flow of water through the transparent venturi, similar to the potassium test venturi shown in figure 87(a). Flow rate is plotted against pressure drop for essentially constant inlet temperature. The operating procedure for this series was to maintain the supply-tank pressure essentially constant and to lower the exit pressure, as much as possible, in steps. The exit pressure was then increased in steps until initial conditions were reestablished.

There are several interesting features of the flow regimes to be observed (the following paragraph numbers correspond to the data point and photograph numbers in fig. 91).

(1) Existence of nonequilibrium liquid superheat prior to initiation of cavitation is deduced from the large decrease in flow and simultaneous increase in pressure drop at the initiation of cavitation. The venturi minimum pressure had reached a value well below saturation before the first vapor appeared; after cavitation, the calculated throat pressure was only slightly less than P_s. Photograph 1 in figure 91(b) shows conditions just beyond the initiation point, with cavitation starting slightly downstream of the throat.

(2) Once cavitation is established, there is a flow-limited regime the pressure drop increases and the flow remains constant.
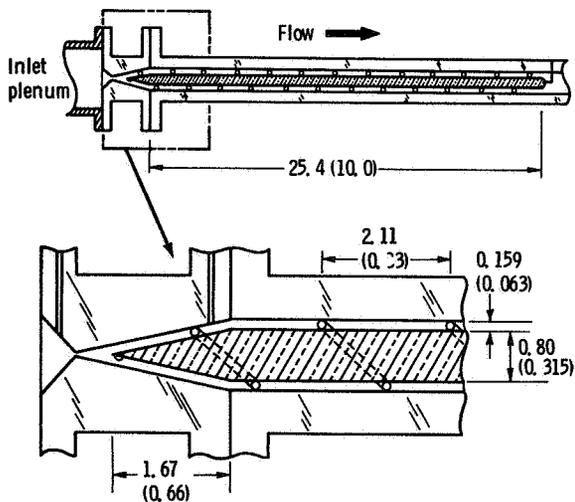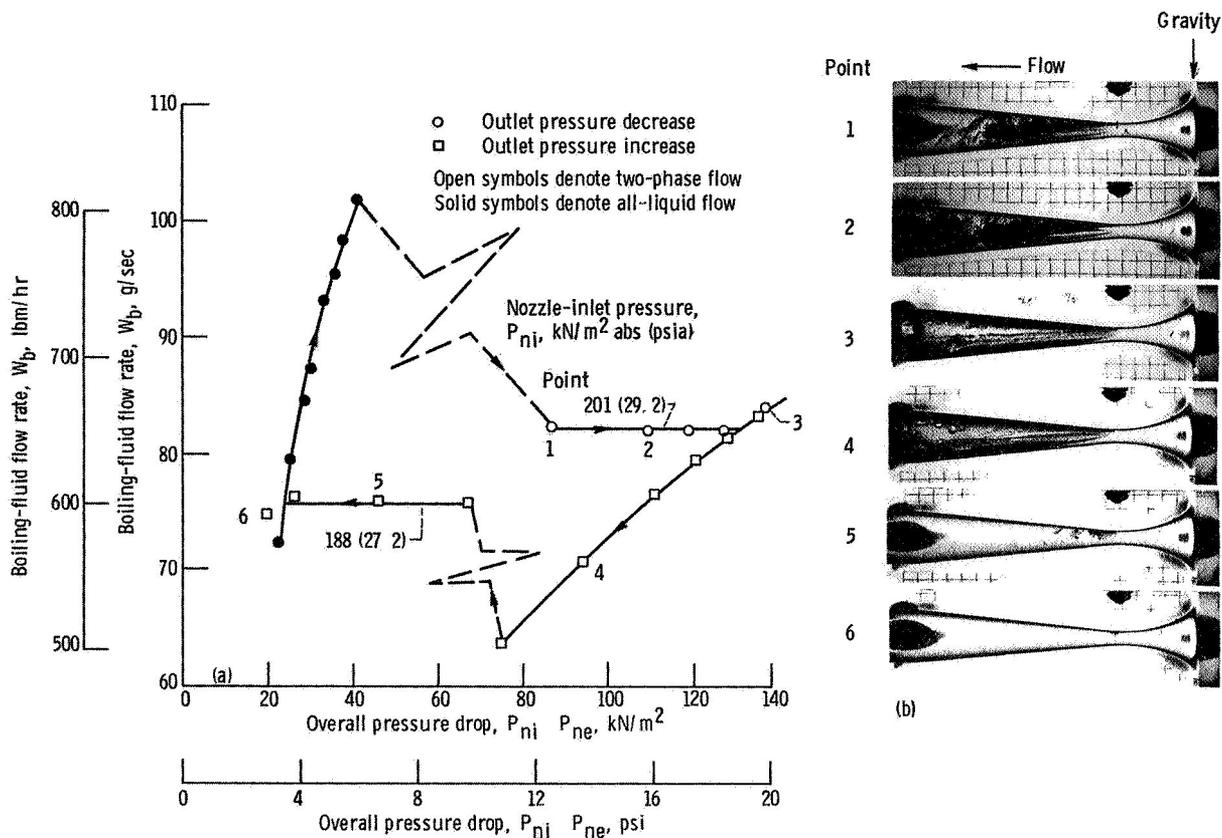
103

(a) Flow as function of pressure drop.

(b) Photographs taken at points indicated.

Figure 91. - Behavior of demineralized deaerated water flowing through 0.262-cm- (0.103-in.-) throat-diameter venturi. Nozzle-inlet temperature, ~92 K (~197° F); nozzle-inlet pressure, $186 < P_{ni} < 202$ kN/m² abs $(29.3 > P_{ni} > 27.1$ psia).

Photograph 2, in this regime, shows considerable vaporization in the diffuser, but the equilibrium heat-balance quality is negative (i.e., subcooled liquid).

(3) When the exit pressure is decreased still further, the flow rate starts to increase again with increasing pressure drop. When this occurs, the heat-balance quality is positive. Photograph 3 in figure 91(b) shows this regime. The phases appear to be separated, with a liquid film on the wall and a vapor core. The liquid exhibits a slight spiral motion, perhaps due to lack of symmetry in the vapor generation or to gravity. Some droplets of condensate appear to remain on the wall, indicating relatively low shear.

(4) On increasing the exit pressure, the flow pattern remains like that of photograph

3 to flows much less than that of the constant-flow region encountered when lowering the pressure. Photograph 4 is in this regime. The liquid velocity appears less than in photograph 3, and the heat-balance quality is negative, even though the appearance is still that of a separated flow.

(5) Eventually, when the back pressure becomes high enough, the flow-limited regime reinitiates with reattachment and a rise in flow. (The flow in this case is less than in the decreasing-pressure portion because the tank pressure has fallen.) The amount of cavitation is fairly small in photograph 5.

(6) Photograph 6 shows very slight cavitation when the flow-pressure relation is essentially that of all-liquid flow. An accelerometer was mounted on the venturi.

104

(The bottom of the mounting screw can be seen in the photographs.) Noise was indicated during the flow-limited cavitation regime, this was attributed to bubble collapse. In the separated-flow regime, no noise was observed.

These tests illustrate some of the complexities with two-phase flow in nozzles and venturis. More information on this subject is presented in chapter 5.
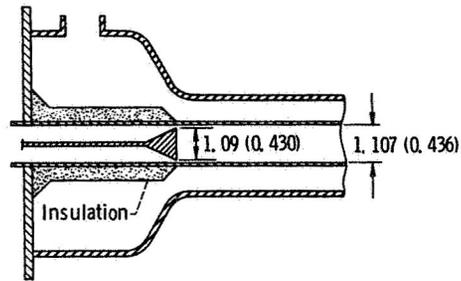

Figure 92.   Inlet end of water boiler with conical inlet centerbody. (Dimensions are in cm (in.).)

INLET RESTRICTORS WITH PLAIN-TUBE WATER BOILER

A few tests that resulted in poor boiler performance are described in this section. Test section 2 of reference 85 was used for tests of various inlet-restrictor designs with water Visual observations of flashing water flow through similar configurations were also made on a small, once-through facility that utilized a constant-pressure heated tank.

Conical Inlet

A conical centerbody, which produced a small annular gap near the tube wall was tested in the heat-exchanger boiler, as shown in figure 92. The gap height was 0.064 mm, and the open area was the same as for a 0.88-mm-diameter circular orifice. A similar model was tested in an adiabatic, transparent tube, this device operating in a flashing water flow is shown in figure 93. According to visual observations an annular flow pattern was established. However, no significant increase in the range of stable operation with the boiling heat exchanger was obtained, probably because this device did not give enough pressure drop at low flows (only 10 kN/m^2 at 12.6 g/sec). It was not considered feasible to try to operate with a smaller annular gap because of the difficulty in maintaining concentricity and clearances.
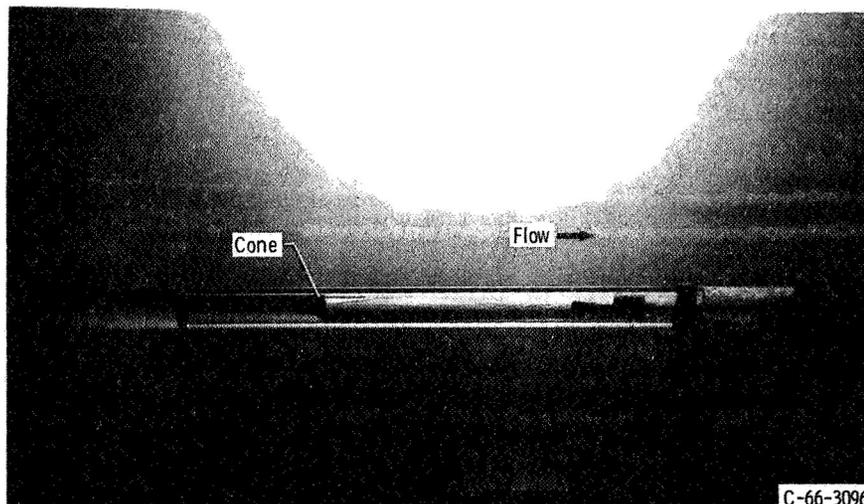

Figure 93.   Flashing water flow in tube with conical centerbody.
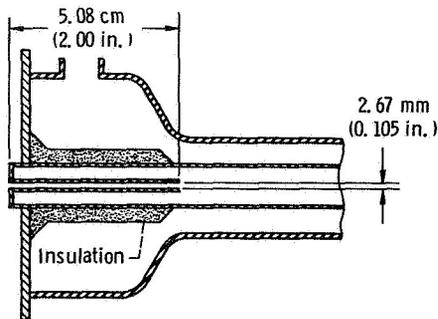
105

Figure 94. Water boiling heat exchanger with small-diameter-tube inlet.

Small-Diameter-Tube Inlet

A 2.67-mm-diameter-tube inlet, 5.08 cm long, was tested in the heat-exchanger boiler, as shown in figure 94, with the tube extending into the boiler A stable boiling-fluid flow rate could not be maintained with vaporization in the small tube. The flow rate tended to drift slowly, either upward (thus lowering the inlet temperature) until all-liquid flow was established or downward (raising the inlet temperature) until an overtemperature controller shut down the preheater Visual tests for tubes of 5 to 50 diameters in length, with the exit end of the small tubes at the start of the boiler tube, also gave negative results, including intermittent flashing and liquid jetting. Therefore, this configuration was not tested further

VORTEX INLET

An interesting possible technique for stabilizing boiler-inlet flow conditions is to generate a vortex flow upstream of a boiler-inlet nozzle. Such a vortex inlet has several potential advantages. First, it should give a fixed, stable liquid-vapor interface location and force the liquid to flow along the heated wall, starting at the nozzle inlet.

Second, the vortex flow through the nozzle should allow the throat diameter to be larger than for completely axial flow with the same pressure drop and flow rate. (Throat diameter is an important consideration for liquid metals, where plugging is a problem.) Third, by varying the proportions of axial and vortex flows through the nozzle, the effective nozzle pressure-loss coefficient may be varied over a wide range. This should permit better control of off-design flow conditions, similar to the use of a fluidic valve in single-phase flow

Description

Preliminary adiabatic vortex-flow tests were run with deaerated water in a small recirculating-flow facility at the Lewis Research Center. Transparent test sections were used, as shown in figures 95 and 96. Two spherical glass vortex chambers were used (fig. 95), one approximately 8.57 cm in diameter and one about 6.03 cm in diameter. Also a cylindrical plastic vortex chamber, measuring 6.35 cm in both diameter and axial length, was tested (fig. 96). The outlet tubes from all the vortex chambers contained convergent-divergent nozzles with throat diameters of 0.64 cm. The inlet tubes to the two spherical vortex chambers were centrally located at 90° to the exit flow, whereas the cylindrical chamber had both a central and a tangential inlet tube.
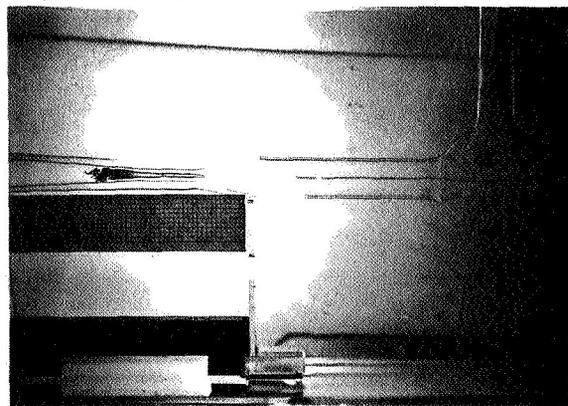

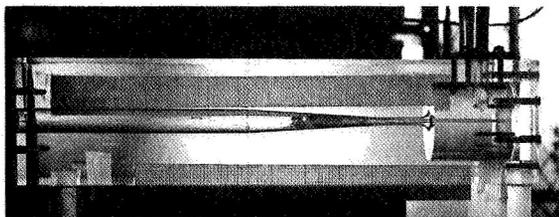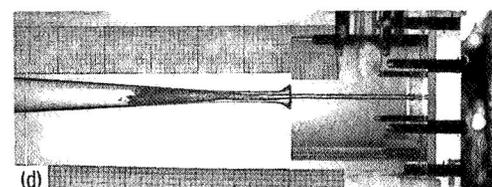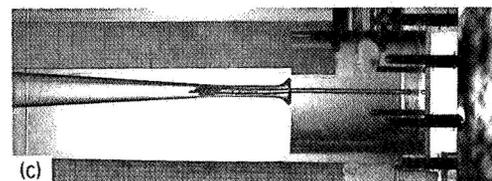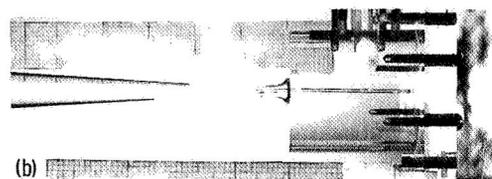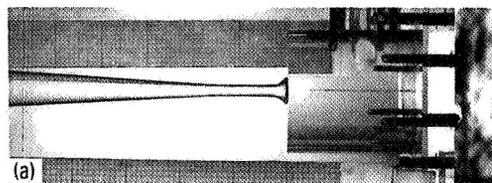Figure 95. Spherical chamber vortex inlet.

106

Figure 96. Cylindrical chamber vortex inlet.

Test Results

The series of photographs in figure 97 illustrates swirling and cavitating flows in the cylindrical chamber model with the tangential inlet feed tube in use. The test sequence is one of increasing chamber inlet pressure with a nearly constant pressure at the nozzle diffuser outlet of ~ 101 kN/m^2, as a consequence, the sequence also illustrates increasing flow rates. The fluid was demineralized water at about 346 K with a total dissolved gas content (mass fraction) of about 2.5 parts per million.

In figure 97(a), a small-diameter vortex filament can be seen at the chamber centerline, extending almost to the nozzle entrance. This gas-vapor core is hypothesized to be at or slightly above the saturation vapor pressure based on the temperature of the surrounding liquid. The interface is also conjectured to mark the radial location where free-vortex flow (velocity inversely proportional to radius) changes to wheel flow (velocity proportional to radius). Note that as the flow (and tangential velocity) increases, the diameter of the gas-vapor core increases.

In figure 97(b), the core has extended into the nozzle, and cavitation bubble formation and collapse in the central core region, associated with increased axial flow through the venturi, appears to be superimposed on the vortex flow. In figures 97(c) and (d), progressively more cavitation appears in the nozzle and the condensation interface is located further downstream in the diffuser A helical flow pattern through the nozzle throat can be visualized from the

(a) Gas-vapor core at chamber centerline.

(b) Gas-vapor core through nozzle throat.

(c) Moderate cavitation.

(d) Intense cavitation.

Figure 97 Swirling and cavitating flows in cylindrical chamber vortex inlet with tangential feed tube in use.

interface streaks in some of the photographs, and a thin annulus of clear liquid can generally be seen along the inside wall of the throat and diffuser This liquid annulus can be seen more clearly in the closeup photograph of the large spherical chamber model, figure 98, which illustrates colder water and lower exit pressure conditions than for the series shown in figure 97

Overall-pressure-drop data for the nozzle of the cylindrical chamber model are shown in figure 99, plotted as pressure-loss coefficient against the ratio of the gas-vapor core length downstream of the nozzle

107
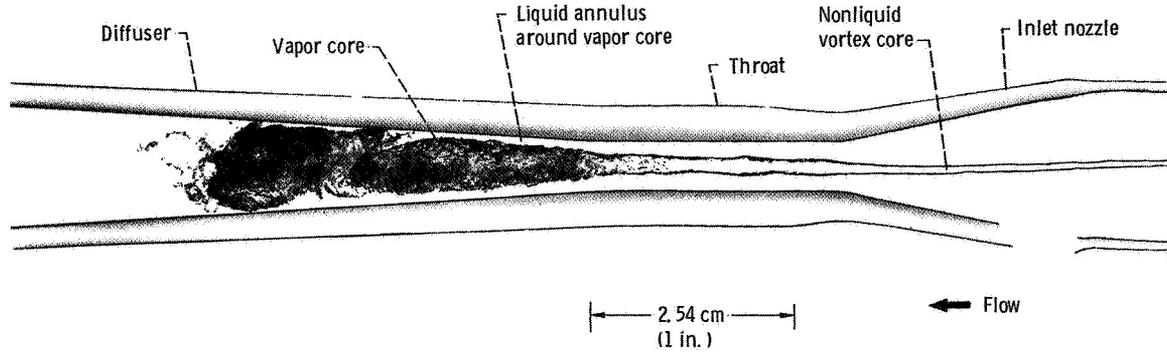
Figure 98. - Large spherical chamber vortex inlet. Vortex induced, flashing flow in venturi. Fluid, deaerated water; flow rate, 0.409 kg/sec (0.90 lbm/sec); temperature (corresponding to vapor pressure of 4.0 kN/m² abs (0.58 psia)), 302 K (84°F); inlet pressure, 207 kN/m² abs (30.1 psia); outlet pressure, 50 kN/m² abs (8.3 psia).

entrance to the nozzle throat diameter The nozzle pressure-loss coefficient is defined as the difference in nozzle inlet and exit static pressures divided by the nozzle-throat superficial axial velocity head Whereas all the

Figure 99. Cylindrical chamber vortex inlet pressure-loss coefficient as function of ratio of core length to throat diameter

coefficient data taken with the central inlet tube in use (axial flow) ranged between 0.3 and 0.45, the data with the tangential inlet ranged from 4.0 to 8.0. Thus, the vortex flow created 10 to 20 times the pressure drop of the axial flow. For most of the data with vortex flow, the minimum nozzle loss coefficient resulted when the gas-vapor core extended to the start of the diffuser The reasons for this behavior are not well understood, but it is significant that all-liquid vortex flow through the nozzle ($L_{cor}/D_t \leqslant 0$) can have pressure-loss coefficients as high as in cases with sizable extents of cavitation in the nozzle diffuser

Discussion of Vortex Inlets

The limited adiabatic-flow data presented here indicate that a sharp, stable liquid-vapor interface is formed when a vortex-chamber-with-nozzle boiler inlet is used. Additional research in this area appears warranted, especially in combination with heat addition along the nozzle to maintain the vapor core flow well into the boiler tube proper Although the vortex-induced helical flow of liquid along the tube wall persists for considerable distances, a helical insert may become necessary further downstream in a heated boiler tube. As mentioned before, the

108

vortex inlet allows a sizable pressure drop for control and stability, even with an advantageously large nozzle throat diameter. Also, the nozzle pressure-drop characteristics can be changed drastically for operation in off-design flows by externally modulating the proportions of axial and tangential flows into the vortex chamber. Thus, the control advantages of a fluidic valve technique can be combined with a large-throat-diameter flashing venturi, with the exiting liquid flowing along the heat-transfer wall.

REFERENCES

1 Lowdermilk, Warren H., Lanzo, Chester D., and Siegel, Byron L. Investigation of Boiling Burnout and Flow Stability for Water Flowing in Tubes. NACA TN 4382, 1958.

2 Aladyev, I T., Miropolsky, Z. L., Doroschchuk, V E., and Styrikovich, M. A. Boiling Crisis in Tubes. International Developments in Heat Transfer ASME, 1963, pp. 237-243.

3 Jeglic, Frank A. The Onset of Flow Oscillations in Forced-Flow Subcooled Boiling. Ph.D. Thesis, Univ Notre Dame, 1964.

4. Jeglic, Frank A., and Grace, Thomas M. Onset of Flow Oscillations in Forced-Flow Subcooled Boiling. NASA TN D-2821, 1965

5 Ledinegg, M. Unstabilitaet der Stroemung bei Natuerlichem und Zwangumlauf. Waerme, vol. 61, no. 48, Nov 26, 1938, pp. 891-898.

6. Dinos, Nicholas Pressure Drop for Flow of Boiling Water at High Pressure. Rep. DP-698, E. I DuPont de Nemours and Co., May 1962

7 Clark, J A., and Rohsenow, W M. Local Boiling Heat Transfer to Water at Low Reynolds Numbers and High Pressures. ASME Trans., vol. 76, no. 4, May 1954, pp. 553-562.

8. Jens, W H. Boiling Heat Transfer What Is Known About It J Mech. Eng., vol. 76, no. 12, Dec. 1954, pp. 981-986.

9 Grace, Thomas M., and Krejsa, Eugene A Analytical and Experimental Study of Boiler Instabilities Due to Feed-System-Subcooled Region Coupling. NASA TN D-3961, 1967

10. Krejsa, Eugene A., Goodykoontz, Jack H., and Stevens, Grady H. Frequency Response of Forced-Flow Single-Tube Boiler NASA TN D-4039, 1967

11 Goodykoontz, Jack H., Stevens, Grady H., and Krejsa, Eugene A Frequency Response of Forced-Flow Single-Tube Boiler with Inserts. NASA TN D-4189, 1967

12. Stevens, Grady H., Krejsa, Eugene A., and Goodykoontz, Jack H. Frequency Response of a Forced-Flow Single-Tube Boiler with Inserts and Exit Restriction NASA TN D-5023, 1969

13. Stevens, Grady H., Goodykoontz, Jack H., and Krejsa, Eugene A. Experimental Evaluation of Four Transfer Functions for a Single Tube Boiler Which Are Dynamically Independent of Exit Restrictions. NASA TM X-2247, 1971

14. Miles, Jeffrey H. Identification of Boiler Inlet Transfer Functions and Estimation of System Parameters. 1972 Joint Automatic Control Conference of the American Automatic Control Council, Palo Alto, Calif., Aug. 16-18, 1972, pp. 941-950.

15. Apfel, Robert E. The Tensile Strength of Liquids. Scientific American, vol. 227, no. 6, Dec. 1972, pp. 58-71

16. Hsu, Y Y. On the Size Range of Active Nucleation Cavities on a Heating Surface. J Heat Transfer, vol. 84, no. 3, Aug. 1962, pp. 207-216.

17 Bergles, A. E., and Rohsenow, W M. The Determination of Forced-Convection Surface-Boiling Heat Transfer J Heat Transfer, vol. 86, no. 3, Aug. 1964, pp. 365-372.

18. Davis, E. J., and Anderson, G. H. The Incipience of Nucleate Boiling in Forced Convection Flow AIChE J., vol. 12, no. 4, July 1966, pp. 774-780.

19 Bond, J A., and Converse, G L. Vaporization of High-Temperature Potassium in Forced Convection at Saturation Temperatures from 1800° to 2100° F NASA CR-843, 1967

20. Edwards, J A., and Hoffman, H W Superheat with Boiling Alkali Metals. Proceedings of the Conference on Application of High-Temperature Instrumentation to Liquid-Metal Experiments. Rep. ANL-7100, Argonne National Lab., 1965, pp. 515-534.

21 Hoffman, H W. Recent Experimental Results in ORNL Studies with Boiling Potassium. Proceedings of 1963 High-Temperature Liquid-Metal Heat Transfer Technology Meeting. Rep. ORNL-3605, vol. 1, Oak Ridge National Lab., Nov. 1964, pp. 334-350.

22. Holtz, Robert E Effect of the Pressure Temperature History upon Incipient-Boiling Superheats in Liquid Metals. Rep. ANL-7184, Argonne National Lab., June 1966.

23. Chen, J C. Incipient Boiling Superheats in Liquid Metals. J Heat Transfer, vol. 90, no. 3,

Aug. 1968, pp. 303-312.

24. Spiller, K.-H., Grass, G., and Perschke, D.. Superheating and Single Bubble Ejection in the Vaporization of Stagnating Liquid Metals. Rep. AERE-Trans-1078, United Kingdom Atomic Energy Authority, June 1967

25. Grass, G., Kottowski, H., and Warnsing, R.. Boiling of Liquid Alkali Metals. Rep. ANL-Trans-390, Argonne National Lab., Sept. 1966.

26. Ruggeri, Robert S., and Gelder, Thomas F.. Effects of Air Content and Water Purity on Liquid Tension at Incipient Cavitation in Venturi Flow. NASA TN D-1459, 1963.

27. Ruggeri, Robert S., and Gelder, Thomas F.. Cavitation and Effective Liquid Tension of Nitrogen in a Tunnel Venturi. NASA TN D-2088, 1964.

28. Gelder, Thomas F., Moore, Royce D., and Ruggeri, Robert S.. Incipient Cavitation of Freon-114 in a Tunnel Venturi. NASA TN D-2662, 1965.

29. Ruggeri, Robert S., Moore, Royce D., and Gelder, Thomas F.. Incipient Cavitation of Ethylene Glycol in a Tunnel Venturi. NASA TN D-2722, 1965.

30. Gelder, Thomas F., Ruggeri, Robert S., and Moore, Royce D.. Cavitation Similarity Considerations Based on Measured Pressure and Temperature Depressions in Cavitated Regions of Freon-114. NASA TN D-3509, 1966.

31. Moore, Royce D., Ruggeri, Robert S., and Gelder, Thomas F.. Effects of Wall Pressure and Liquid Temperature on Incipient Cavitation of Freon-114 and Water in Venturi Flow. NASA TN D-4340, 1968.

32. Blake, F G., Jr. The Tensile Strength of Liquids: A Review of the Literature. Tech. Memo 9, Harvard Univ., Acoustic Res. Lab., June 11, 1949

33. Briggs, Lyman J.. Limiting Negative Pressure of Water. J Appl. Phys., vol. 21, no. 7, July 1950, pp. 721-722.

34. Gavrilenko, T P., and Topchiyan, M. E.. Dynamic Tensile Strength of Water. J Appl. Mech. Tech. Phys., vol. 7, no. 4, July-Aug. 1966, pp. 128-129.

35. Briggs, Lyman J.. The Limiting Negative Pressure of Acetic Acid, Benzene, Aniline, Carbon Tetrachloride, and Chloroform, J

Chem. Phys., vol. 19, no. 7, July 1951, pp. 970-972.

36. Martinelli, R. C., and Nelson, D. B.. Prediction of Pressure Drop During Forced-Circulation Boiling of Water. ASME Trans., vol. 70, no. 6, Aug. 1948, pp. 695-702.

37 Baroczy, C. J.. Correlation of Liquid Fraction in Two-Phase Flow with Application to Liquid Metals. Chem. Eng. Progr. Symp. Ser., vol. 61, no. 57, 1965, pp. 179-191.

38. von Glahn, Uwe H., and Polcyn, Richard P.. On the Effect of Heat Addition in the Empirical Correlation of Void Fractions for Steam-Water Flow. NASA TN D-1440, 1962.

39 Kroeger, P G., and Zuber, N.. An Analysis of the Effects of Various Parameters on the Average Void Fraction in Subcooled Boiling. Int. J Heat Mass Transfer, vol. 11, no. 2, Feb. 1968, pp. 211-233.

40. Bowring, R. W.. Physical Model, Based on Bubble Detachment, and Calculation of Steam Voidage in the Subcooled Region of a Heated Channel Rep. HPR-10, Institute for Atomenergi, Halden, Norway, Dec. 1962.

41 Levy, S.. Forced Convection Subcooled Boiling – Prediction of Vapor Volumetric Fraction. Int. J Heat Mass Transfer, vol. 10, no. 7, July 1967, pp. 951-965

42 Rouhani, S. Z., and Axelsson, E.. Calculation of Void Volume Fraction in the Subcooled and Quality Boiling Regions. Int. J Heat Mass Transfer, vol. 13, no. 2, Feb. 1970, pp. 383-393.

43. Baker, O.. Multiphase Flow in Pipelines. Oil and Gas J., vol. 56, no. 45, Nov. 10, 1958, pp. 156-167

44. Baker, O. Design of Pipeline for the Simultaneous Flow of Oil and Gas. Oil and Gas J., vol. 53, 1954, pp. 185-190, 192, 194.

45 Kozlov, B. K.. Forms of Flow of Gas-Liquid Mixtures and Their Stability Limits in Vertical Tubes. Trans. RJ-418, Associated Technical Services, East Orange, N.J

46. Kosterin, S. I.. Investigation of the Effect of the Diameter and the Position of Pipe upon the Hydraulic Resistance and the Structure of the Flow of a Gas-Liquid Mixture. Trans. No. 3085, Henry Brutcher Technical Translation, Altadena, Calif

47 Govier, G. W., Radford, B. A., and Dunn, J S.

C.: The Upwards Vertical Flow of Air-Water Mixtures: I. Effect of Air and Water-Rates on Flow Pattern, Holdup and Pressure Drop. Can. J. Chem. Eng., vol. 35, no. 3, Aug. 1957, pp. 58-70.

48. Govier, G. W., Radford, B. A., and Dunn, J. S. C.: The Upward Vertical Flow of Air-Water Mixtures: II. Effect of Tubing Diameter on Flow Pattern, Holdup and Pressure Drop. Can. J. Chem. Eng., vol. 36, no. 5, Oct. 1958, pp. 195-202.

49. Krasiakova, L. I.: Some Characteristics of the Flow of a Two-Phase Mixture in a Horizontal Pipe. Rep. AERE-LIB/TRANS-695, Atomic Energy Research Establishment, Jan. 1957

50. Jakob, Max; Leppert, George; and Reynolds, J. B.: Pressure Drop During Forced-Circulation Boiling. Chem. Eng. Progr. Symp. Ser., vol. 52, no. 18, 1956, pp. 29-36.

51 Tippets, F. E.: Critical Heat Fluxes and Flow Patterns in High-Pressure Boiling Water Flows. J. Heat Transfer, vol. 86, no. 1, Feb. 1964, pp. 12-22.

52. Hosler, E. R.: Flow Patterns in High Pressure Two-Phase (Steam-Water) Flow with Heat Addition. Rep. WAPD-TM-658, Bettis Atomic Power Lab., June 1967

53. Janssen, E.: Two-Phase Flow Structure in a Nine-Rod Channel, Steam-Water at 1000 psia. Rep. GEAP-5480, General Electric Co., June 1967

54. Vohr, John H.: A Photographic Study of Boiling Flow Rep. NYO-9650, Columbia Univ., Oct. 25, 1963.

55. Johnson, H. A., Schrock, V. E., Selph, F. B., and Fabic, S.: Reactor Heat Transfer Research. Rep. SAN-1002, Univ. California, Nov. 1961

56. Martenson, Alfred J.: Transient Boiling in Small Rectangular Channels. Ph.D. Thesis, Univ Pittsburgh, 1962.

57 Dengler, Carl E.: Heat Transfer and Pressure Drop for Evaporation of Water in a Vertical Tube. Ph.D. Thesis, Massachusetts Inst. Tech., 1952.

58. Lockhart, R. W., and Martinelli, R. C.: Proposed Correlation of Data for Isothermal Two-Phase, Two-Component Flow in Pipes. Chem. Eng. Progr., vol. 45, no. 1, Jan 1949, pp. 39-48.

59. Schrock, V. E., and Grossman, L. M.: Local Pressure Gradients in Forced Convection Vaporization. Nucl. Sci. Eng., vol. 6, no. 3, Sept. 1959, pp. 245-250.

60. Levy, S.: Steam Slip – Theoretical Prediction from Momentum Model. J. Heat Transfer, vol. 82, no. 2, May 1960, pp. 113-124.

61. Thom, J. R. S.: Prediction of Pressure Drop During Forced Circulation Boiling of Water. Int. J. Heat Mass Transfer, vol. 7, no. 7, July 1964, pp. 709-724.

62. Rohsenow, Warren M.: Heat Transfer Associated with Nucleate Boiling. Proceedings of the 1963 Heat Transfer and Fluid Mechanics Institute. Stanford Univ. Press, 1963, pp. 123-141

63. Engelberg-Forster, Kurt, and Greif, R.: Heat Transfer to a Boiling Liquid – Mechanism and Correlations. J Heat Transfer, vol. 81, no. 1, Feb. 1959, pp. 43-53.

64. Forster, H. K., and Zuber, N.: Dynamics of Vapor Bubbles and Boiling Heat Transfer. AIChE J., vol. 1, no. 4, Dec. 1955, pp. 531-535.

65. Papell, S. Stephen: Subcooled Boiling Heat Transfer Under Forced Convection in a Heated Tube. NASA TN D-1583, 1963.

66. Dengler, C. E., and Addoms, J. N.: Heat Transfer Mechanism for Vaporization of Water in a Vertical Tube. Chem. Eng. Prog. Symp. Ser., vol. 52, no. 18, 1956, pp. 95-103.

67 Wright, Roger M Downflow Forced-Convection Boiling of Water in Uniformly Heated Tubes. Rep. UCRL-9744, Univ. California, Aug. 21, 1961

68. Schrock, V. E., and Grossman, L. M.: Forced Convection Boiling Studies. Rep. TID-14632, Univ. California, Lawrence Radiation Lab., Nov. 1, 1959.

69. Collier, J. G., and Pulling, D. J.: Heat Transfer to Two-Phase Gas-Liquid Systems, Part II. Further Data on Steam-Water Mixtures. Rep. AERE-R-3809, United Kingdom Atomic Energy Authority, 1962.

70. Chen, John C.: A Correlation for Boiling Heat Transfer to Saturated Fluids in Convective Flow. Paper 63-HT-34, ASME, 1963.

71 Mumm, J. F.: Heat Transfer to Boiling Water Forced Through a Uniformly Heated Tube. Rep. ANL-5276, Argonne National Lab., Nov 1954.

72. Altman, M., Norris, R. H., and Staub, F. W.. Local and Average Heat Transfer and Pressure Drop for Refrigerants Evaporating in Horizontal Tubes. J. Heat Transfer, vol. 82, no. 3, Aug. 1960, pp. 189-198.

73. Sachs, P., and Long, R. A. K. A Correlation of Heat Transfer in Stratified Two-Phase Flow with Vaporization. Int. J. Heat Mass Transfer, vol. 2, no. 3, Apr. 1961, pp. 222-230.

74. Wallerstedt, R. L., and Miller, D. B. Mercury Rankine Program Development Status and Multiple System Application. AIAA Specialists Conference on Rankine Space Power Systems. AEC Rep. CONF-651026, vol. 1, 1965, pp. 3-51.

75. Gresho, P. M., Poucher, F W., and Wimberly, F C.. Mercury Rankine Program Test Experience AIAA Specialists Conference on Rankine Space Power Systems. AEC Rep. CONF-651026, vol. 1, 1965, pp. 52-102.

76. Gordon, R., and Slone, H. O. SNAP-8 Development Status — September 1965 AEC Rep. CONF-651026, vol. 1, 1965, pp. 103-138.

77 Kreeger, A H., Hodgson, J N., and Sellers, A. J. Development of the SNAP-8 Boiler. AIAA Specialists Conference on Rankine Space Power Systems. AEC Rep. CONF-651026, vol. 1, 1965, pp. 285-306.

78. Owhadi, A. i. Boiling in Self-Induced Radial Acceleration Fields. Ph.D. Thesis, Oklahoma State Univ., 1966.

79. Gray, Vernon H., Marto, Paul J., and Joslyn, Allan W.. Boiling Heat-Transfer Coefficients, Interface Behavior, and Vapor Quality in Rotating Boiler Operating to 475 G's. NASA TN D-4136, 1968.

80. Marto, Paul J., and Gray, Vernon H.. Effects of High Accelerations and Heat Fluxes on Nucleate Boiling of Water in an Axisymmetric Rotating Boiler. NASA TN D-6307, 1971

81 Lawler, Martin T., and Ostrach, Simon: A Study of Cyclonic Two-Fluid Separation. Rep. FTAR-TR-65-2, Case Inst Tech (AFOSR-65-1523, AD-621524), June 1965

82. Kikin, Gerald M., Peelgren, Maurice L., Phillips, Wayne M., and Davis, Jerry P.. Shell Side Liquid Metal Boiler U.S. Patent 3,630,276, Dec. 28, 1971.

83. Lewis, James P., Groesbeck, Donald E., and Christenson, Harold H.. Tests of Sodium Boiling in a Single Tube-in-Shell Heat Exchanger Over the Range 1720° to 1980° F (1211 to 1355 K). NASA TN D-5323, 1969.

84. Groesbeck, Donald E.. Vacuum System for the Boiling Liquid-Metal Heat Transfer Facility. High Vacuum Technology, Testing, and Measurement Meeting — June 8-9, 1965. Compilation of Papers. NASA TM X-1268, 1966, pp. 37-45.

85. Stone, James R., and Damman, Thomas M.. An Experimental Investigation of Pressure Drop and Heat Transfer for Water Boiling in a Vertical-Upflow Single-Tube Heat Exchanger. NASA TN D-4057, 1967

86. Stone, James R., and Sekas, Nick J. Tests of a Single Tube-in-Shell Water-Boiling Heat Exchanger with a Helical-Wire Insert and Several Inlet Flow-Stabilizing Devices. NASA TN D-4767, 1968.

87 Stone, James R., and Sekas, Nick J. Tests of a Single Tube-in-Shell Water Boiler with Helical-Wire Insert, Inlet Nozzle, and Two Different Inlet-Region Plugs. NASA TN D-5644, 1970.

88. Sekas, Nick J., and Stone, James R.. Experimental Study of Blade-Type Helical Flow Inducers in a 5/8-Inch Electrically Heated Boiler Tube. NASA TM X-2001, 1970.

89 Jeglic, Frank A., Stone, James R., and Gray, Vernon H.. Experimental Study of Subcooled Nucleate Boiling of Water Flowing in 1/4-Inch-Diameter Tubes at Low Pressures. NASA TN D-2626, 1965

90. Stone, James R. Subcooled- and Net-Boiling Heat Transfer to Low-Pressure Water in Electrically Heated Tubes. NASA TN D-6402, 1971

91 Stone, James R.. Local Turbulent Heat Transfer for Water in Entrance Regions of Tubes with Various Unheated Starting Lengths. NASA TN D-3098, 1965.

92. Sekas, Nick J., and Stone, James R.. Local Heat Transfer for Water in Entrance Regions of Tubes with Tapered Flow Areas and Nonuniform Heat Fluxes. NASA TM X-1554, 1968.

93. Stone, James R.. A Method of Predicting Boiling Pressure Drop for Alkali Metals. AIChE J., vol. 14, no. 3, May 1968, pp. 507-508.

94. Peterson, J R High-Performance

"Once-Through" Boiling of Potassium in Single Tubes at Saturation Temperatures from 1500° to 1750° F NASA CR-842, 1967

95. Collins, R. A., Boppart, J A., and Berenson, P J Testing of Liquid-Metal Boilers for Rankine-Cycle Power Systems Rep. APS-5244-R, AiResearch Mfg. Co. (AFAPL-TR-67-10, vols. I and II), Apr 1967

96. Bond, J A. The Design of Components for an Advanced Rankine Cycle Test Facility Proceedings of Energy 70. Vol. 1 AIAA-SAE, 1970, pp. 7-66 to 7-71

97 Bond, J A., and Gutstein, M. U. Components and Overall Performance of an Advanced Rankine Cycle Test Rig. Proceedings of the Intersociety Energy Conversion Engineering Conference. SAE, 1971, pp. 464-471

98. Gutstein, Martin U., and Bond, James A. Preliminary Results of Testing a Single-Tube Potassium Boiler for the Advanced Rankine System. NASA TM X-52996, 1971.

99 Tong, L. S. Boiling Heat Transfer and Two-Phase Flow. John Wiley & Sons, Inc., 1965

100. Costello, C. P., and Adams, J. M. Burnout Heat Fluxes in Pool Boiling at High Accelerations. International Developments in Heat Transfer ASME, 1963, pp. 255-261.

101 Ivey, H. J. Preliminary Results on the Effect of Acceleration on Critical Heat Flux in Pool Boiling. Rep. AEEW-R-99, United Kingdom Atomic Energy Authority, 1961

102. Graham, Robert W., and Hendricks, Robert C. A Study of the Effect of Multi-G Accelerations on Nucleate-Boiling Ebullition NASA TN D-1196, 1963.

103. Kerr, S. L., and Leith, W C. A Review of Cavitation Damage by the Vibratory Method. Dominion Eng. Works, Ltd., Montreal, Canada, Nov. 1955

104. Stone, J P., et al. High-Temperature Properties of Sodium. Rep. NRL-6241, Naval Research Lab. (NASA CR-68286, AD-622191), Sept. 24, 1965.

105. Gutierrez, Orlando A., and Fenn, David B. Experimental Cavitation and Flashing of Potassium Flowing Adiabatically Through a Venturi Sized as a Boiler Inlet. NASA TN D-5738, 1970.

106. Fauske, Hans K. Liquid Metal Boiling in Relation to Liquid Metal Fast Breeder Reactor Safety Design. Chem. Eng. Progr. Symp. Ser., vol. 65, no. 92, 1969, pp. 138-149.

107 Fauske, Hans K. Contribution to the Theory of Two-Phase, One-Component Critical Flow. Rep. ANL-6633, Argonne National Lab., Oct. 1962.

108. Stone, James R. On the Effect of Helical-Flow Inserts on Boiling Pressure Drop. Heat Transfer 1970. Vol. 5 Elsevier Publ. Co., 1970, paper B5.1.

109. Stone, James R. A Correlation of Subcooled Boiling Pressure Drop for Low Pressure Water Flowing in Tubes With Constant Heat Flux. Chem. Eng. Progr. Symp. Ser., vol. 67, no. 113, 1971, pp. 57-63.

110. Reynolds, J B. Local Boiling Pressure Drop. Rep. ANL-5178, Argonne National Lab., Mar. 1954.

111 Owens, W L., and Schrock, V. E. Local Pressure Gradients for Subcooled Boiling of Water in Vertical Tubes. Paper 60-WA-249, ASME, 1960.

112. Thom, J R.S., Walker, W M., Fallon, T. A.; and Reising, G F S. Boiling in Sub-Cooled Water During Flow up Heated Tubes or Annuli. Proc. Inst. Mech. Eng., vol. 180, pt. 3C, 1965-1966, pp. 226-246.

113. Stone, James R., and Sekas, Nick J. Water Flow and Cavitation in Converging-Diverging Boiler-Inlet Nozzle. NASA TM X-1689, 1968.

114. Stein, R. P. A Method for the Determination of Local Heat Fluxes in Liquid-Metal Heat Exchangers. Proceedings of the Conference on Application of High-Temperature Instrumentation to Liquid-Metal Experiments. Rep. ANL-7100, Argonne National Lab., 1965, pp. 482-498.

115. Iida, Yoshihiro, and Kobayasi, Kiyosi: Distributions of Void Fraction Above a Horizontal Heating Surface in Pool Boiling. JSME Bull., vol. 12, no. 50, Apr. 1969, pp. 283-290.

BIBLIOGRAPHY

This bibliography includes the sources cited as references and is grouped alphabetically according to subject.

GENERAL

Benning, A. F., and McHarness, R. C. The Thermodynamic Properties of "FREON" 113 ($CCl_2F\text{-}CCOF_2$). Tech. Memo. T-113A, E. I Depont de Nemours Co., 1938.

Bergles, A. E., Bakhru, N., and Shires, J W., Jr. Cooling of High-Power-Density Computer Components. Rep. DSR-70712-60, Massachusetts Inst. Tech., Nov 1968.

Bergles, A. E., Brown, G. S., Jr., Lee, R. A., Simonds, R. R., and Snider, W D.. Investigation of Heat Transfer Augmentation Through Use of Internally Finned and Roughened Tubes. Rep DSR-70790-69, Massachusetts Inst Tech., Aug. 1970.

Bonilla, Charles F., ed. Nuclear Engineering. McGraw-Hill Cook Co., Inc., 1957

Bornhorst, W J., and Hatsopoulos, G. N Analysis of Liquid Vapor Phase Change by Methods of Irreversible Thermodynamics. Paper 67-WA/APM-35, ASME, 1967

Coe, Harold H. Summary of Thermophysical Properties of Potassium. NASA TN D-3120, 1965.

Cousins, L. B. Bibliography of Reports on Two-Phase Heat Transfer Issued by A.E.R.E., Harwell. AERE-Bib-150/Rev, Atomic Energy Research Establishment, June 1969

Eckert, E. R. G., Sparrow, E. M., Goldstein, R. J., Scott, C. J., and Ibele, W E. Heat Transfer Bibliography Int J Heat Mass Transfer, vol. 13, no. 3, Mar 1970, pp. 617-630.

Ewing, C P., et al. High Temperature Properties of Cesium. Rep. NRL-6246, Naval Research Lab. (NASA CR-68381, AD-622227), Sept. 24, 1965

Frost, W, and Dzakowic, G S.. Manual of Boiling Heat-Transfer Design Correlations. Rep. AEDC-TR-69-106, ARO, Inc. (AD 698323), Dec. 1969

Gouse, S. William, Jr. An Index to the Two-Phase Gas-Liquid Flow Literature – Part I Rep. DSR-8734-1, Massachusetts Inst. Tech., May 1963.

Gouse, S. William, Jr.. An Index to the Two-Phase Gas-Liquid Flow Literature – Part II Rep. DSR 8734-4, Massachusetts Inst.Tech., Sept. 1964.

Gouse, S. William, Jr. An Index to the Two-Phase Gas-Liquid Flow Literature – Part III. Rep. DSR-8734-6, Massachusetts Inst Tech. (AD-630295), Jan. 1966.

Graham, Robert W., and Hsu, Y Y. Research Efforts on Boiling and Two-Phase Flow in the Cryogenic Heat Transfer Section of NASA Lewis Research Center Proceedings of the Second Joint USAEC-EURATOM Two-Phase Flow Meetings. AEC Rep. CONF-640507, 1964, pp. 529-531

Gutstein, Martin U, Converse, George L., and Peterson, Jerry R.. Theoretical Analysis and Measurement of Single-Phase Pressure Losses and Heat Transfer for Helical Flow in a Tube. NASA TN D-6097, 1970.

Hobler, T.. Heat and Mass Transfer – Polish Works. Int. J Heat Mass Transfer, vol 13, no. 6, June 1970, pp. 1049-1055

Hsu, Y Y, and Stein, Ralph P., eds.. Convective and Interfacial Heat Transfer Chem. Eng. Progr. Symp. Ser., vol. 67, no. 113, 1971.

Keenan, Joseph H., and Keyes, Frederick G.. Thermodynamic Properties of Steam. John Wiley & Sons, Inc., 1965

Lee, Y.. Turbulent Heat Transfer from the Core Tube in Thermal Entrance Regions of Concentric Annuli. Int. J Heat Mass Transfer, vol. 11, no. 3, Mar 1968, pp. 509-522

Lopina, Robert F., and Bergles, Arthur E. Heat Transfer and Pressure Drop in Tape Generated Swirl Flow Rep. DSR 70281-47, Massachusetts Inst. Tech. (AD-654739), June 1967

Luikov, A V Heat and Mass Transfer Bibliography – Soviet Works. Int. J Heat Mass Transfer, vol. 13, no. 5, May 1970, pp. 911-923

Olsen, William A., Jr. Boiling Water Cooling of a Hypothetical Large Solid Rocket Nozzle Lined with a Porous Wall or a Melting Insulating Coating. NASA TM X-1952, 1970.

Peterson, Jerry R., Weltmann, Ruth N, and Gutstein, Martin U Thermal Design Procedures for Space

Rankine Cycle System Boilers. Intersociety Energy Conversion Engineering Conference. Vol. 1 IEEE, 1968, pp. 313-328.

Sams, E. W. Heat-Transfer and Pressure-Drop Characteristics of Wire-Coil-Type Turbulence Promoters. Reactor Heat Transfer Conference of 1956. John E. Viscardi, comp., AEC Rep. TID-7529, Pt 1, Bk. 2, Nov 1957

Sato, Takashi: Heat Transfer Bibliography – Japanese Works. Int J. Heat Mass Transfer, vol. 13, no. 5, May 1970, pp. 925-926.

Sekas, Nick J., and Stone, James R.. Local Heat Transfer for Water in Entrance Regions of Tubes with Tapered Flow Areas and Nonuniform Heat Fluxes. NASA TM X-1554, 1968.

Stone, James R.. Local Turbulent Heat Transfer for Water in Entrance Regions of Tubes with Various Unheated Starting Lengths. NASA TN D-3098, 1965

Strack, William C.. Condensers and Boilers for Steam-Powered Cars: A Parametric Analysis of Their Size, Weight and Required Fan Power NASA TN D-5813, 1970.

Tong, L. S.. Boiling Heat Transfer and Two-Phase Flow John Wiley & Sons, Inc., 1965

Wilson, N. W., and Medwell, J. O. An Analysis of Heat Transfer for Fully Developed Turbulent Flow in Concentric Annuli. J Heat Transfer, vol. 90, no. 1, Feb 1968, pp. 43-50.

ADIABATIC TWO-PHASE FLOW

Anderson, R. J., and Russell, T W F.. Film Formation in Two-Phase Annular Flow AIChE J., vol. 16, no. 4, July 1970, pp. 626-633.

Bailey, J F. Metastable Flow of Saturated Water ASME Trans., vol. 73, no. 8, Nov 1951, pp. 1109-1116.

Banerjee, Sanjoy, Rhodes, Edward, and Scott, D. S. Film Inversion of Cocurrent Two-Phase Flow in Helical Coils. AIChE J., vol. 13, no. 1, Jan. 1967, pp. 189-191

Batch, J. M. Critical Flow of Steam-Water Mixtures Through Short Pipes. Proceedings of the Second Joint USAEC-EURATOM Two-Phase Flow Meeting. Ronald M Scroggins, ed., AEC Rep. CONF-640507, Nov 1964, pp. 479-481

Benjamin, M. W, and Miller, J. G. The Flow of Saturated Water Through Throttling Orifices.

ASME Trans., vol. 63, no. 5, July 1941, pp. 419-429.

Bottomley, W T.. Flow of Boiling Water Through Orifices and Pipes. Trans. North-East Coast Inst. Eng. Shipbuilders (England), vol. 53, 1936-1937, pp. 65-100.

Burnell, J G.. Flow of Boiling Water Through Nozzles, Orifices, and Pipes. Engineering, vol. 164, Dec. 12, 1947, pp. 572-576.

Bursik, Joseph W.. Pseudo-Sonic Velocity and Pseudo-Mach-Number Concepts in Two-Phase Flows. NASA TN D-3734, 1966.

Butterworth, D.. Air-Water Climbing Film Flow in an Eccentric Annulus. Cocurrent Gas-Liquid Flow. Edward Rhodes and Donald Scott, eds., Plenum Press, 1969, pp. 145-201.

Butterworth, D.: Note on Fully-Developed, Horizontal, Annular Two-Phase Flow. Chem. Eng. Sci., vol. 24, no. 12, Dec. 1969, pp. 1832-1834.

Butterworth, D.. Air-Water, Annular Flow in a Horizontal Tube. Rep. AERE-R-6687, Atomic Energy Research Establishment, Feb. 1971

Chen, Ping Chien: Two-Phase Flow Through Apertures. Ph.D. Thesis, Univ. Minnesota, 1965

Chien, Sze-Foo, and Ibele, W. Pressure Drop and Liquid Film Thickness of Two-Phase Annular and Annular-Mist Flows. J Heat Transfer, vol. 86, no. 1, Feb. 1964, pp. 89-96.

Connelly, Robert E., Meng, Phillip R., and Urasek, Donald C.. Investigation of Two-Phase Hydrogen Flow in Pump Inlet Line. NASA TN D-5258, 1969.

Cruver, James E.. Metastable Critical Flow of Steam-Water Mixtures. Ph.D. Thesis, Univ. Washington, 1963.

Cruver, James E., and Moulton, R. W. Critical Flow of Liquid-Vapor Mixtures. AIChE J., vol. 13, no. 1, Jan. 1967, pp. 52-60.

Deich, M. E., Tsiklauri, G. V., Seleznev, L. I., Danilin, V S., and Shanin, V K.: Nonequilibrium Two-Phase Flows at High Velocities. Heat Transfer 1970. Vol. 5 Elsevier Publ. Co., 1970, paper B5.8.

Elliot, D.G., and Weinberg, E. Acceleration of Liquids in Two-Phase Nozzles. Rep. JPL-TR-32-987, Jet Propulsion Lab. (NASA CR-95146), July 1, 1968.

Evans, Rowland G., Gouse, S. William, Jr., and Bergles, Arthur E.. Pressure Wave Propagation in Adiabatic Slug-Annular-Mist Two-Phase Gas-Liquid Flow. Chem. Eng. Sci., vol. 25, no. 4, 1970, pp. 569-582.

Faletti, Duane W.. Two-Phase Critical Flow of Steam-Water Mixtures. Ph.D Thesis, Univ. Washington, 1959.

Faletti, Duane W., and Moulton, R. W. Two-Phase Critical Flow of Steam-Water Mixtures. AIChE J., vol. 9, no. 2, Mar 1963, pp. 247-253.

Fauske, H.. Critical Two-Phase, Steam-Water Flows. Proceedings of the 1961 Heat Transfer and Fluid Mechanics Institute, Stanford Univ. Press, 1961, pp. 79-89

Fauske, Hans K.. Contribution to the Theory of Two-Phase, One-Component Critical Flow Rep. ANL-6633, Argonne National Lab., Oct. 1962.

Fauske, Hans K.. Two-Phase Critical Flow with Application to Liquid-Metal Systems (Mercury, Cesium, Rubidium, Potassium, Sodium, and Lithium). Rep. ANL-6779, Argonne National Lab., Oct. 1963.

Fauske, H K Two-Phase, Two- and One-Component, Critical Flow Proceedings of Symposium on Two-Phase Flow, Exeter, 1966, pp. G101-G114.

Fauske, H. K., and Gromels, M. A. Modeling of Liquid-Vapor Metal Flows with Nonmetallic Fluids, Paper 70-HT-21, ASME, 1970.

Fauske, Hans K., and Min, Tony C.. A Study of the Flow of Saturated Freon-11 Through Apertures and Short Tubes. Rep. ANL-6667, Argonne National Lab., Jan. 1963.

Gelder, Thomas F., Moore, Royce D., and Ruggeri, Robert S.. Incipient Cavitation of Freon-114 in a Tunnel Venturi. NASA TN D-2662, 1965

Gelder, Thomas F., Ruggeri, Robert S., and Moore, Royce D.. Cavitation Similarity Considerations Based on Measured Pressure and Temperature Depressions in Cavitated Regions of Freon 114. NASA TN D-3509, 1966.

Gill, L.E., Hewitt, G. F., and Roberts, D. N. Studies of the Behavior of Disturbance Waves in Annular Flow in a Long Vertical Tube. Rep. AERE-R-6012, Atomic Energy Research Establishment, Mar 1969.

Gutierrez, Orlando A., and Fenn, David B.. Experimental Cavitation and Flashing of Potassium Flowing Through a Venturi Sized as a Boiler Inlet. NASA TN D-5738, 1970.

Hall Taylor, N. S.. Interfacial Wave Phenomena in Vertical Annular Two Phase Flow Ph.D. Thesis, Univ. Cambridge, 1968.

Henry, Robert E.. A Study of One- and Two-Component, Two-Phase Critical Flows at Low Qualities. Rep. ANL-7430, Argonne National Lab., Mar 1968.

Henry, Robert E.. Pressure Wave Propagation in Two-Phase Mixtures. NASA TM X-52593, 1969.

Henry, Robert E. Pressure Wave Propagation Through Annular and Mist Flows. Chem. Eng. Progr. Symp. Ser., vol. 67, no. 113, 1971, pp. 38-47

Hewitt, G. F. Photographic and Entrainment Studies in Two Phase Flow Systems. Rep. AERE-R-4683, Atomic Energy Research Establishment, 1964.

Hewitt, G. F., Hutchinson, P., Dukler, A. E.. A Random Walk Model for Drop Deposition in Two-Phase Flow AIChE Paper 12d presented at the 66th National Meeting, Aug. 1969.

Hewitt, G. F., King, R. D., and Lovegrove, P C.. Techniques for Liquid Film and Pressure Drop Studies in Annular Two-Phase Flow Rep. AERE-R-3921, Atomic Energy Research Establishment, Mar 1962.

Hodkinson, B.. The Flow of Hot Water Through a Nozzle. Engineering, vol. 143, 1937, pp. 629-630.

Hord, J., Anderson, L. M., and Hall, W J.. Cavitation in Liquid Cryogens. I – Venturi. NASA CR-2054, 1972.

Huey, C T., and Bryant, R. A A.. Isothermal Homogeneous Two-Phase Flow in Horizontal Pipes. AIChE J., vol. 13, no. 1, Jan 1967, pp. 70-77

Isbin, H S. Two-Phase Flow Through Apertures. Proceedings of the Second Joint USAEC-EURATOM Two-Phase Flow Meeting. Ronald M Scroggins, ed AEC Rep. CONF-640507, 1964, pp. 507-528.

Isbin, H. S. Comments on "Critical Flow of Liquid-Vapor Mixture." AIChE J., vol. 13, no. 2, Mar 1967, p. 392

Isbin, H. S., Fauske, H. K., Petrick, M., Robbings, C. H., Smith, R. V., Szawlewicz, S. A., and Zaloudek, F R. Critical Flow Phenomena in Two-Phase Mixtures and Their Relationships to Reactor Safety Presented at the Third United Nations Conference on the Peaceful Uses of Atomic Energy, Geneva, Switzerland, Aug. 31-Sept. 9, 1964.

Isbin, H S., and Gavalas, G R. Two-Phase Flow Through an Aperture. Proceedings of 1962 Heat Transfer and Fluid Mechanics Institute, Stanford Univ. Press, 1962, pp. 126-140.

Isbin, H. S., Moy, J. E., and DaCruz, A. J R.. Two-Phase, Steam-Water Critical Flow AIChE J.,

vol. 3, no. 3, Sept. 1957, pp. 361-365.

James, Russell: Steam-Water Critical Flow Through Pipes. Proc. Inst. Mech. Eng., vol. 176, no. 26, Dec. 1962, pp. 741 748.

Janssen, Earl: Two-Phase Pressure Loss Across Abrupt Contractions and Expansions, Steam-Water at 600 to 1,400 Psia. Proceedings of the Third International Heat Transfer Conference. Vol. 5. AIChE, 1966, pp. 13-23.

Janssen, E., and Kervinen, J A. Two-Phase Pressure Drop Across Contractions and Expansions: Water-Steam Mixtures at 600 to 1400 Psia. Rep. GEAP-4622, General Electric Co., June 1964.

Kling, Charles L.. A High Speed Photographic Study of Cavitation Bubble Collapse Ph.D Thesis, Univ Michigan, 1970.

Klingebiel, Ward J Critical Flow Slip Ratios of Steam-Water Mixtures. Ph.D Thesis, Univ Washington, 1964

Klingebiel, W J., and Moulton, R. W. Analysis of Flow Choking of Two-Phase, One-Component Mixtures. AIChE J., vol. 17, Mar 1971, pp. 383-390.

Leonov, E. G., Finatiev, Yu P., and Filatov, B S.. On the Hydraulic Resistance and Flow Structure of a Gas-Liquid Mixture in an Annular Passage with a Rotating Cylinder Inside. Int. J. Heat Mass Transfer, vol 9, no. 5, May 1966, pp. 427-432.

Levy, S. Prediction of Two-Phase Critical Flow Rate J Heat Transfer, vol. 87, no. 1, Feb 1965, pp. 53-58.

Matkin, John H. Determination of Aerosol Size and Velocity by Holography and Steam-Water Critical Flow Ph.D. Thesis, Univ Washington, 1968

McGee, John W Two-Phase Flow Through Abrupt Expansions and Contractions. Ph.D Thesis, North Carolina State Univ., 1966

Min, T C., Hoffman, H. W. and Peebles, F N.. Two-Phase Two-Component Annular Upward Flow Through a Concentric Annulus. Chem. Eng. Progr Symp Ser., vol. 67, no. 113, 1971, pp. 48-56.

Moeck, E. O.. Measurement of Liquid Film Flow and Wall Shear Stress in Two Phase Flow Two Phase Flow Instrumentation. ASME/AIChE, 1969, pp 39-46.

Moody, F J. Maximum Flow Rate of a Single Component, Two-Phase Mixture. J Heat Transfer, vol. 87, no. 1, Feb. 1965, pp. 134-142

Moore, Royce D.. Ruggeri, Robert S., and Gelder,

Thomas F. Effects of Wall Pressure and Liquid Temperature on Incipient Cavitation of Freon 114 and Water in Venturi Flow. NASA TN D-4340, 1968.

Nazarov, G. S. An Experimental Investigation of the Cavitational Characteristics of Converging Nozzles. J Eng. Phys., vol. 14, no. 3, Mar 1968, pp. 220-223

Neal, L. G. Local Parameters in Cocurrent Mercury-Nitrogen Flow. Rep. ANL-6625, Argonne National Lab., Jan. 1963.

Nedderman, R. M., and Shearer, C. J.. The Motion and Frequency of Large Disturbance Waves in Annular Two-Phase Flow of Air-Water Mixtures. Chem. Eng. Sci., vol. 18, no. 10, Oct. 1963, pp. 661-670.

Pasqua, P F. Metastable Flow of Freon-12. Refrigerating Eng., vol. 61, no. 10, Oct 1953, pp. 1084A-1088.

Peterson, Jerry R., Converse, George L., and Gutstein, Martin U. An Experimental Study of Pressure Loss and Phase Distribution for Air-Water Flow in a Tube Containing Swirl Generators. Presented at the 5th Intersociety Energy Conversion Conference, Las Vegas, Nev., Sept. 21-25, 1970.

Pogson, J T., Roberts, J H., and Waibler, P J. An Investigation of the Liquid Distribution in Annular Mist Flow. Paper 70-HT 11, ASME, 1970.

Rippel, G R., Eidt, C M., Jr, and Jordan, H. B., Jr.. Two-Phase Flow in a Coiled Tube. Ind Eng. Chem. Process Des. Dev., vol 5, no. 1, Jan. 1966, pp. 32-39

Rosenfeld, Robert T Measurement of Metastability in a Duct Containing a Flowing Steam-Water Mixture Under Choking Conditions. Ph.D. Thesis, Univ. Washington, 1969

Ruggeri, Robert S., and Gelder, Thomas F Effects of Air Content and Water Purity on Liquid Tension at Incipient Cavitation in Venturi Flow NASA TN D-1459, 1963.

Ruggeri, Robert S, and Gelder, Thomas F.. Cavitation and Effective Liquid Tension of Nitrogen in a Tunnel Venturi. NASA TN D-2088, 1964

Ruggeri, Robert S., and Gelder, Thomas F. Cavitation and Effective Liquid Tension of Nitrogen in a Hydrodynamic Cryogenic Tunnel. Advances in Cryogenic Engineering. Vol 9 K. D.

Timmerhaus, ed., Plenum Press, 1964, pp. 304-310.

Ruggeri, Robert S., Moore, Royce D., and Gelder, Thomas F. Incipient Cavitation of Ethylene Glycol in a Tunnel Venturi. NASA TN D-2722, 1965.

Ryley, D. J. Flow of Wet Steam. Engineer, vol. 193, 1952, pp. 323-363.

Ryley, D. J. Two-Phase Critical Mist Flow in Geothermal Wells. Symposium on Two-Phase Flow, Exeter, 1965, pp. G301-G317

Sanger, Nelson L. Noncavitating and Cavitating Performance of Two Low-Area-Ratio Water Jet Pumps with Throat Lengths of 5.66 Diameters. NASA TN D-4759, 1968.

Sanger, Nelson L. Cavitating Performance of Two Low-Area-Ratio Water Jet Pumps Having Throat Lengths of 7.25 Diameters. NASA TN D-4592, 1968

Sanger, Nelson L. A Jet Pump Cavitation Prediction Parameter NASA TM X-52417, 1968.

Sanger, Nelson L. Noncavitating and Cavitating Performance of Several Low Area Ratio Water Jet Pumps Having Throat Lengths of 3.54 Diameters. NASA TN D-5095, 1969

Sarma, G. S. R., Lu, Pau-Chang; and Ostrach, Simon Film-Stability in a Vertical Rotating Tube with a Core-Gas Flow. Rep. FTAS/TR-69-37, Case Western Reserve Univ (NASA CR-73716), Jan. 1969

Schraub, F A., Simpson, R. L., and Janssen, E. Two-Phase Flow and Heat Transfer in Multirod Geometries – Air-Water Flow Structure Data for a Round Tube, Concentric and Eccentric Annulus, and Nine-Rod Bundle. Rep. GEAP-5739, General Electric Co., Jan. 1969

Shearer, C. J., and Nedderman, R. M. Pressure Gradient of Liquid Film Thickness in Co-Current Upwards Flow of Gas/Liquid Mixtures: Application to Film-Cooler Design. Chem. Eng. Sci., vol. 20, no. 7, July 1965, pp. 671-683

Singer, Harvey A. Jet Mixing of a Two-Phase Stream with a Surrounding Fluid Stream. Ph.D. Thesis, Univ. Southern California, 1970.

Smith, R. V. Two-Phase Two-Component Critical Flow in a Venturi. Ph.D. Thesis, Oxford Univ., 1968.

Smith, R. V., Cousins, L. B., and Hewitt, G. F. Two-Phase Two-Component Critical Flow in a Venturi. Rep. AERE-R-5736, Atomic Energy

Research Establishment, Dec. 1968

Stone, James R., and Sekas, Nick J. Water Flow and Cavitation in Converging-Diverging Boiler-Inlet Nozzle. NASA TM X-1689, 1968.

Sutton, Richard F., Jr. Spreading of a Gas Stream in an Air-Water Cocurrent Bubbly Flow Ph.D. Thesis, Northwestern Univ., 1968.

Taylor, N. Hall, Hewitt, G F., and Lacey, P M C. The Motion and Frequency of Large Disturbance Waves in Annular Two-Phase Flow of Air-Water Mixtures. Chem. Eng. Sci., vol. 18, no. 8, Aug. 1963, pp. 537-552.

Taylor, N S. Hall; and Nedderman, R M. The Coalescence of Disturbance Waves in Annular Two Phase Flow. Chem. Eng. Sci., vol. 23, no. 6, Aug. 1968, pp. 551-564.

Telles, Alfonso C. da Silva: Liquid Film Characteristics in Vertical Two-Phase Flow Ph.D. Thesis, Univ Houston, 1968.

Telles, A. S., and Dukler, A E. Statistical Characterization of Thin, Vertical Wavy Liquid Films. Ind. Eng. Chem. Fundamentals, vol. 9, no. 3, 1970, pp. 412-421

Treaster, Allen L Cavitation Hysteresis. Pennsylvania State Univ. (NASA CR-62283), June 1964.

Uchida, Hideo, and Nariai, Hideki: Discharge of Saturated Water Through Pipes and Orifices. Proceedings of the Third International Heat Transfer Conference. Vol. 5 AIChE, 1966, pp. 1-12.

Webb, D. Studies of the Characteristics of Downward Annular Two Phase Flow Part 1 – The Effect of Length. Rep. AERE-R-6426, Pt. 1, Atomic Energy Research Establishment, 1970.

Webb, D. Studies of the Characteristics of Downward Annular Two Phase Flow Part 2 – Description of Experimental Apparatus and Its Calibration Rep. AERE-R-6426, Pt. 2, Atomic Energy Research Establishment, 1970.

Webb, D. Studies of the Characteristics of Downward Annular Two Phase Flow. Part 3: Measurements of Entrainment Rate, Pressure Gradient, Probability Distribution of Film Thickness and Disturbance Wave Inception. Rep. AERE-R-6426, Pt. 3, Atomic Energy Research Establishment, 1970.

Webb, D. Studies of the Characteristics of Downward Annular Two Phase Flow Part 4 Pressure Fluctuations. Rep. AERE-R-6426, Pt 4,

Atomic Energy Research Establishment, 1970.

Webb, D.. Studies of the Characteristics of Downward Annular Two Phase Flow. Part 5 Statistical Measurements of Wave Properties. Rep. AERE-R-6426, Pt. 5, Atomic Energy Research Establishment, 1970.

Woodmansee, Donald E.. Atomization from a Flowing Horizontal Water Film by a Parallel Air Flow. Ph.D. Thesis, Univ Illinois, 1968.

Woodmansee, Donald E., and Hanratty, Thomas J.. Base Film Over Which Roll Waves Propagate. AIChE J., vol. 15, no. 5, Sept. 1969, pp. 712-715.

Yershov, N. S., Borovskiy, B. I., Yakimov, V V. Experimental Study of the Effect of the Thermodynamic Properties of a Fluid on Cavitation Phenomena. NASA TT F-10, 913, 1967

Yu, H. S., and Sparrow, E. M.. Experiments on Two-Component Stratified Flow in a Horizontal Duct. Paper 68-HT-14, ASME, 1968

Zaloudek, F R.. The Low Pressure Critical Discharge of Steam-Water Mixtures from Pipes. Rep. HW-68934, Rev., General Electric Co., Mar 1961.

Zaloudek, F R. The Critical Flow of Hot Water Through Short Tubes. Rep. NW-77594, General Electric Co., May 1963.

Zarnett, G. D., and Charles, M E. Cocurrent Gas-Liquid Flow in Horizontal Tubes with Internal Spiral Ribs. Can. J Chem. Eng., vol. 47, no. 3, June 1969, pp. 238-241

Zivi, S. M.. Estimation of Steady-State Steam Void-Fraction by Means of the Principle of Minimum Entropy Production. J Heat Transfer, vol. 86, no. 2, May 1964, pp. 247-252.

BOILING HEAT TRANSFER

Altman, M., Norris, R. H., and Staub, F W.. Local and Average Heat Transfer and Pressure Drop for Refrigerants Evaporating in Horizontal Tubes. J Heat Transfer, vol. 82, no. 3, Aug. 1960, pp. 189-198.

Anderson, R. J., and Russell, T W F.. Designing for Two-Phase Flow – Part III Chem. Eng., vol. 73, no. 1, Jan.3, 1966, pp. 87-90.

Aydelott, John C., and Cochran, Thomas H.. Effects of Subcooling and Gravity Level on Boiling in the Discrete Bubble Region NASA TN D-3449, 1966.

Aydelott, John C., and Cochran, Thomas H.. Effects of Fluid Properties and Gravity Level on Boiling in the Discrete Bubble Region. NASA TN D-4070, 1967

Aydelott, John C., Cochran, Thomas H., and Spuckler, Charles M.. Experimental Investigation of Nucleate Boiling Bubble Dynamics in Normal and Zero Gravities. NASA TN D-4301, 1968.

Beaver, P R., and Hughmark, G. A.. Heat-Transfer Coefficients and Circulation Rates for Thermosiphon Reboilers. AIChE J., vol. 14, no. 5, 1968, pp. 746-749.

Bennett, A. W., Hewitt, G. F., Kearsey, H. A.; and Keeys, R. K. F.. Heat Transfer to Steam-Water Mixtures Flowing in Uniformly Heated Tubes in Which the Critical Heat Flux Has Been Exceeded. Inst. Mech. Eng. Thermodynamics and Fluid Mechanics Convention, Bristol, England, Paper 27, Mar 1968.

Bergles, A. E., and Rohsenow, W M.. The Determination of Forced-Convection Surface-Boiling Heat Transfer J Heat Transfer, vol. 86, no. 3, Aug. 1964, pp. 365-373.

Chawla, J M.. Correlation of Convective Heat Transfer Coefficient for Two-Phase Liquid-Vapor Flow. Heat Transfer 1970. Vol 5 Elsevier Publ. Co., 1970, paper B5.7

Chen, John C.. A Correlation for Boiling Heat Transfer to Saturated Fluids in Convective Flow. Paper 63-HT-34, ASME, 1963

Chen, John C. A Proposed Mechanism and Method of Correlation for Convective Boiling Heat Transfer with Liquid Metals. Proceedings of 1963 High-Temperature Liquid-Metal Heat Transfer Technology Meeting. Rep. ORNL-3605, vol. 2, Oak Ridge National Lab., Dec 1964, pp. 47-61

Chu, Shou-Chang: Problems on Heat Transfer to Slug Flow. Ph.D. Thesis, Northwestern Univ., 1963.

Chun, Kang Ryul: Evaporation from Thin Liquid Films. Ph.D. Thesis, Univ California, Berkeley, 1969.

Cochran, Thomas H.. Forced-Convection Boiling Near Inception in Zero Gravity NASA TN D-5612, 1970.

Cochran, Thomas H., Aydelott, John C., and Spuckler, Charles M An Experimental Investigation of Boiling in Normal and Zero Gravity NASA TM X-52264, 1967

Cole, Robert Bubble Dynamics in Boiling. Ph.D. Thesis, Clarkson College of Technology, 1966.

Collier, J G., and Pulling, D. J. Heat Transfer to Two-Phase Gas-Liquid Systems, Part II Further Data on Steam-Water Mixtures. Rep. AERE-R-3809, Atomic Energy Research Establishment, 1962.

Danilova, G. N.. The Effect of the Number of Active Nuclei on the Rate of Heat Transfer in Large-Volume Nucleate Boiling. NASA TT F-11305, 1967

Danilova, G. N.. Correlation of Boiling Heat Transfer Data for Freons. Heat Transfer – Soviet Res., vol. 2, no. 2, Mar 1970, pp. 73-78..

Deane, Charles W., IV, and Rohsenow, Warren M.. Mechanism of Nucleate Boiling Heat Transfer to the Alkali Liquid Metals. Rep. DSR 76303-65, TID-25294, Massachusetts Inst. Tech., Oct. 1969

Ebright, Frank E.. Effect of Depth on Film Boiling Heat Transfer in Liquid Helium II Ph.D Thesis, Univ Florida, 1969

Elrod, W C., Clark, J A., Lady, E. R., and Merte, H.. Boiling Heat-Transfer Data at Low Heat Flux. J Heat Transfer, vol. 89, no. 3, Aug. 1967, pp. 235-243.

Engelberg-Forster, Kurt, and Greif, R. Heat Transfer to a Boiling Liquid, Mechanism and Correlations. J. Heat Transfer, vol. 81, no. 1, Feb 1959, pp. 43-53.

Forster, H. K., and Zuber, N.. Dynamics of Vapor Bubbles and Boiling Heat Transfer AIChE J., vol. 1, no. 4, Dec. 1955, pp. 531-535

Graham, Robert W, and Hendricks, Robert C. Prerequisites for a Model of Nucleate Boiling. Presented at the 3rd National Conference on Heat Transfer, 1959.

Graham, Robert W, and Hendricks, Robert C. A Study of the Effect of Multi-G Accelerations on Nucleate-Boiling Ebullition. NASA TN D-1196, 1963.

Graham, Robert W, and Hendricks, Robert C.. Assessment of Convection, Conduction, and Evaporation in Nucleate Boiling. NASA TN D-3943, 1967

Hsu, Yih-Yun: Gradual Transition of Nucleate Boiling from Discrete-Bubble Regime to Multibubble Regime NASA TN D-2564, 1965

Hughmark, G A Designing Thermosiphon Reboilers. Chem. Eng. Progr., vol. 65, no. 7, July 1969, pp. 67-70.

Keshock, Edward G., and Siegel, Robert Forces Acting on Bubbles in Nucleate Boiling Under Normal and Reduced Gravity Conditions. NASA TN D-2299, 1964.

Keshock, Edward G., and Siegel, Robert Nucleate and Film Boiling in Reduced Gravity from Horizontal and Vertical Wires. NASA TR R-216, 1965.

Kosky, Philip G.. Studies in Boiling Heat Transfer to Cryogenic Liquids. Ph.D. Thesis, Univ California, Berkeley, 1966.

Kotake, Susumu. On the Mechanism of Nucleate Boiling. Int. J Heat Mass Transfer, vol. 9, no. 8, Aug. 1966, pp. 711-728

Kutateladze, S. S.. Problems of Heat Transfer and Hydraulics of Two-Phase Media. Pergamon Press, 1969.

Lovenguth, Ronald F.. Boiling Heat Transfer in the Presence of Electric Fields. Ph.D. Thesis, Newark College of Engineering, 1968.

Munn, J F. Heat Transfer to Boiling Water Forced Through a Uniformly Heated Tube. Rep. ANL-5276, Argonne National Lab., Nov. 1954.

Nagarajan, Ramanathan An Experimental Investigation of the Influence of the Surface Grain Size of the Metal on the Value of C_{sf} in the Rohsenow Equation for Boiling Heat Transfer Ph.D. Thesis, Univ Windsor, 1968.

Nangia, Krishan K. Convective and Boiling Heat Transfer From a Vibrating Surface Ph.D Thesis, McGill Univ., 1968.

Noel, M B. Experimental Investigation of Heat-Transfer Characteristics of Hydrazine and a Mixture of 90 Percent Hydrazine and 10 Percent Ethylenediamine Rep. JPL-TR-32-109, Jet Propulsion Lab. (NASA CR-60962), June 1961

Noel, M. B. Experimental Investigation of the Forced-Convection and Nucleate-Boiling Heat-Transfer Characteristics of Liquid Ammonia. Rep. JPL-TR-32-125, Jet Propulsion Lab. (NASA CR-79088), July 1961

Olinger, John L. A Study of Electrofluidmechanical Interactions in Boiling Heat Transfer Ph.D Thesis, Univ Oklahoma, 1969

Pujol, L., and Stenning, A H.. Effect of Flow Direction on the Boiling Heat Transfer Coefficient in Vertical Tubes. Cocurrent Gas-Liquid Flows, 1969, pp. 401-453.

Sachs, P., and Long, R. A. K.. A Correlation for Heat Transfer in Stratified Two-Phase Flow with Vaporization Int. J Heat Mass Transfer, vol. 2, no. 3, Apr 1961, pp. 222-230.

Schaefer, John W., and Jack, John R. Investigation of Forced-Convection Nucleate Boiling of Water for Nozzle Cooling at Very High Heat Fluxes. NASA TN D-1214, 1962.

Schrock, V E., and Grossman, L. M. Forced Convection Boiling Studies. Rep. TID-14632, California Univ., Nov. 1, 1959

Sciance, Carroll T. Pool Boiling Heat Transfer to Liquefied Hydrocarbon Gases. Ph.D. Thesis, Univ. Oklahoma, 1966.

Sharp, Robert R. The Nature of Liquid Film Evaporation During Nucleate Boiling. NASA TN D-1997, 1964.

Siegel, R., and Keshock, E. G. Effects of Reduced Gravity on Nucleate Boiling Bubble Dynamics in Saturated Water AIChE J., vol. 10, no. 4, July 1964, pp. 509-517

Stefanovic, M., Afgan, N., Pislar, V., and Jovanovic, Lj: Experimental Investigation of the Superheated Boundary Layer in Forced Convection Boiling. Heat Transfer 1970. Vol. 5. Elsevier Publ. Co., 1970, paper B4.12

Vos, A. S., and Van Stralen, J D. Heat Transfer to Boiling Water-Methylethylketone Mixtures. Chem. Eng. Sci., vol. 5, 1956, pp. 50-56.

Wright, Roger M. Downflow Forced-Convection Boiling of Water in Uniformly Heated Tubes. Rep. UCRL-9744, California Univ., Aug. 21, 1961

BOILING PRESSURE DROP

Anderson, R J., and Russell, T W F. Designing for Two-Phase Flow – Part II Chem. Eng., vol. 72, no. 26, Dec. 20, 1965, pp. 99-102, 104.

Banerjee, Sanjoy Mass Transfer, Interfacial Area, Pressure Drop, Hold-up and Axial Dispersion for Concurrent Gas-Liquid Flows in Centrifugal Fields, with Particular Reference to Turbulent Film Annular Flows. Ph.D. Thesis, Univ Waterloo, 1968

Costello, C. P. Aspects of Local Boiling Effects on Density and Pressure Drop. Paper 59-HT-18, ASME, 1959

Durkee, John B., II A Study Involving Flow-Boiling Peak Pressure Drops and Maximum Two-Phase Flow Ph.D. Thesis, Lehigh Univ., 1969

Gaspari, G P., Lombardi, C., and Peterlongo, G. Pressure Drops in Steam-Water Mixtures. Round Tubes – Vertical Upflow Rep. CISE-R-83, Centro Informagioni Studi Esperienze, Jan 1964.

Hewitt, G. F. Interpretation of Pressure Drop Data From an Annular Channel. Rep. AERE-R-4340, Atomic Energy Research Establishment, July 1964.

Hilding, W. E. Differential Equations for the Local Interfacial and Wall Shear Stresses for One-Dimensional Annular Two-Phase Flow. Proceedings of the Third International Heat Transfer Conference, Vol. 4. AIChE, 1966, pp. 167-177

Jacowitz, Laurence A. An Analysis of Geometry and Pressure Drop for the Annular Flow of Gas-Liquid Systems. Ph.D. Thesis, Ohio State Univ., 1962.

Jacowitz, L. A., and Brodkey, Robert S. An Analysis of Geometry and Pressure Drop for the Horizontal, Annular, Two-Phase Flow of Water and Air in the Entrance Region of a Pipe. Chem. Eng. Sci., vol. 19, no. 4, Apr 1964, pp. 261-274.

Janssen, E., and Kervinen, J A. Two-Phase Pressure Losses. Final Report 1 Pressure Losses Across Large Expansions and Contractions. 2. Pressure Drop with Heat Addition. 3 General Conclusions. Rep. GEAP-4634, General Electric Co., July 1964.

Kociscin, Joseph J. Pressure Drop, Heat Transfer, and Maximum Discharge in Forced-Convection, Horizontal Boiling. Ph.D. Thesis, Lehigh Univ., 1965

Lockhart, R. W., and Martinelli, R. C. Proposed Correlation of Data for Isothermal Two-Phase, Two-Component Flow in Pipes. Chem. Eng. Progr., vol. 45, no. 1, Jan. 1949, pp. 39-48.

Magiros, Peter G., and Dukler, A. E. Entrainment and Pressure Drop in Concurrent Gas-Liquid Flow II Liquid Properties and Momentum Effects. Developments in Mechanics. Vol. 1 Plenum Press, 1961, pp. 532-553

Martinelli, R. C., and Nelson, D. B. Prediction of Pressure Drop During Forced-Circulation Boiling of Water. ASME Trans., vol. 70, no. 6, Aug. 1948, pp. 695-702.

Owens, W L. Pressure Gradients in Forced Convection Boiling of a Subcooled Liquid. M.Sc. Thesis, Univ California, Berkeley, 1959.

Rogers, John D. Two Phase Friction Factor for Para-Hydrogen Between One Atmosphere and the Critical Pressure. AIChE J., vol 14, no. 6, Nov. 1968, pp. 895-902.

Rogers, John D., and Tietjen, Gary Two-Phase Friction Factor for Nitrogen Between One Atmosphere and the Critical Pressure. AIChE J.,

vol. 15, no. 1, Jan. 1969, pp. 144-146.

Schrock, V. E., and Grossman, L. M. Local Pressure Gradients in Forced Convection Vaporization. Nucl. Sci. Eng., vol. 6, no. 3, Sept. 1959, pp. 245-250.

Stone, James R. A Method of Predicting Boiling Pressure Drop for Alkali Metals. AIChE J., vol. 14, no. 3, May 1968, pp. 507-508.

Stone, James R. On the Effect of Helical-Flow Inserts on Boiling Pressure Drop. Heat Transfer, 1970. Vol. 5. Elsevier Publ. Co., 1970, paper B5 1

Stone, James R. A Correlation of Subcooled Boiling Pressure Drop for Low Pressure Water Flowing in Tubes With Constant Heat Flux. Chem. Eng. Progr. Symp. Ser., vol. 67, no. 113, 1971, pp. 57-63.

Tarasova, N. V., and Leontiev, A. I. Experimental Investigation of Some Characteristics for Non-Equilibrium Two-Phase Flow Heat Transfer 1970. Vol. 5. Elsevier Publ. Co., 1970, paper B5.13.

Tarasova, N. V., Leontiev, A. I., Hlopushin, V I., and Orlov, V M. Pressure Drop of Boiling Subcooled Water and Steam-Water Mixture Flowing in Heated Channels. Proceedings of the Third International Heat Transfer Conference. Vol. 4. AIChE, 1966, pp. 178-183

Thom, J. R. S. Prediction of Pressure Drop During Forced Circulation Boiling of Water Int. J. Heat Mass Transfer, vol. 7, no. 7, July 1964, pp. 709-724.

Wallis, G. B. Annular Two-Phase Flow Part 1 A Simple Theory J. Basic Eng., vol. 92, no. 1, Mar 1970, pp. 59-72.

Wallis, G. B. Annular Two-Phase Flow Part 2 Additional Effects. J. Basic Eng., vol. 92, no. 1, Mar 1970, pp. 73-82.

Wichner, Robert P., and Hoffman, Herbert W. Pressure Drop with Forced-Convection Boiling of Potassium. Rep. ORNL-P-1681, Oak Ridge National Lab., 1965.

DRYING OF VAPOR AND FILM BOILING

Baumeister, Kenneth J., and Hamill, Thomas D. Creeping Flow Solution of the Leidenfrost Phenomenon. NASA TN D-3133, 1965

Baumeister, Kenneth J., Hamill, Thomas D., and Hendricks, Robert C. Metastable Leidenfrost

States. NASA TN D-3226, 1966.

Baumeister, Kenneth J., and Hamill, Thomas D. Laminar Flow Analysis of Film Boiling from a Horizontal Wire. NASA TN D-4035, 1967

Baumeister, Kenneth J., and Hamill, Thomas D. Effect of Subcooling and Radiation on Film-Boiling Heat Transfer from a Flat Plate. NASA TN D-3925, 1967

Baumeister, Kenneth J., Hamill, Thomas D., Schoessow, Glen J., and Schwartz, F. L. Film Boiling Heat Transfer to Water Drops on a Flat Plate. NASA TM X-52103, 1965

Baumeister, Kenneth J., Hamill, Thomas D., and Schoessow, Glen J. A Generalized Correlation of Vaporization Times of Drops in Film Boiling on a Flat Plate. NASA TM X-52177, 1966.

Bell, K. J. The Leidenfrost Phenomenon. A Survey Chem. Eng. Progr Symp. Ser., vol. 63, no. 79, 1967, pp. 73-82.

Coury, Glenn E. A Study of Vertical Turbulent Film Boiling and Interfacial Effects. Ph.D. Thesis, Univ. Houston, 1968.

Coury, G. E., and Dukler, A. E. Turbulent Film Boiling on Vertical Surfaces – A Study Including the Influence of Interfacial Waves. Heat Transfer 1970. Vol. 5 Elsevier Publ. Co., 1970, paper B3.6.

Cumo, M., Farello, G. E., and Ferrari, G. Post Burnout Heat Transfer and Thermodynamic Disequilibrium up to the Critical Pressure. Heat Transfer 1970. Vol. 5 Elsevier Publ. Co., 1970, paper B3.5

Downing, Carl G. The Evaporation of Drops of Pure Liquids at Elevated Temperatures: Rates of Evaporation and Wet-Bulb Temperatures. AIChE J., vol. 12, no. 4, July 1966, pp. 760-766.

Forslund, Robert P., and Rohsenow, Warren M. Thermal Nonequilibrium in Dispersed Flow Film Boiling in a Vertical Tube. Rep. 75312-44, Massachusetts Inst. Tech., Nov 1966.

Forslund, R. P., and Rohsenow, W M. Dispersed Flow Film Boiling. Paper 68-HT-44, ASME, 1968.

Forslund, R. P., and Rohsenow, W M. Dispersed Flow Film Boiling. J. Heat Transfer, vol. 90, no. 4, Nov. 1968, pp. 399-407

Godleski, Edward S. The Leidenfrost Phenomenon for Binary Liquid Solutions. Ph.D. Thesis, Oklahoma State Univ., 1967

Gottfried, B S., Lee, C. J, and Bell, K. J. The Leidenfrost Phenomenon. Film Boiling of Liquid Droplets on a Flat Plate Int. J Heat Mass

Transfer, vol. 9, no. 11, Nov. 1966, pp. 1167-1188.

Hamill, Thomas D., and Baumeister, Kenneth J.. Film Boiling Heat Transfer From a Horizontal Surface as an Optimal Boundary Value Process. NASA TM X-52183, 1966.

Hendricks, Robert C., and Baumeister, Kenneth J.. Similarity and Curvature Effects in Pool Film Boiling. Heat Transfer 1970. Vol. 5. Elsevier Publ. Co., 1970, paper B3.7

Hsu, Yih-Yun, Hendricks, Robert C., and Cowgill, Glenn R.. Mist-Flow Heat Transfer Using Single-Phase Variable-Property Approach. NASA TN D-4149, 1967

Hucks, J. S., and Hall, V C., Jr.. Evaluation of Steam Separation Requirements for Large Integral Boiler-Superheater Reactors. Rep. CEND-116, Combustion Eng. Co., Dec. 1960.

Kalinin, E. K., Koshkin, V K., Yarkho, S. R., Berlin, I. I., Kochelaev, Y S., Kostyuk, V V., Korolev, A. L., and Sdobnov, G N. Investigation of Film Boiling in Tubes with Subcooled Nitrogen Flow Heat Transfer 1970. Vol. 5. Elsevier Publ. Co., 1970, paper B4.5

Kao, H. S., Morgan, C D., Crawford, M., and Jones, J. B.. Stability Analysis of Film Boiling on Vertical Surfaces as a Two-Phase Flow Problem. Paper AIChE 1, presented at the 12th National Heat Transfer Conference, Tulsa, Okla., Aug. 15-18, 1971

Keshock, Edward G.. Leidenfrost Film Boiling of Intermediate and Extended Bubbly Masses of Liquid Nitrogen. Ph.D Thesis, Oklahoma State Univ., 1968.

Lee, Kwan, and Ryley, D J. The Evaporation of Water Droplets in Superheated Steam. J Heat Transfer, vol. 90, no. 4, Nov. 1968, pp. 445-451

McGinnis, F K., III, and Holman, J P.. Individual Droplet Heat-Transfer Rates for Splattering on Hot Surfaces. Int. J Heat Mass Transfer, vol 12, no. 1, Jan. 1968, pp. 95-108.

Murphy, C D., Kermode, R. I., and Zahradnik, R. L.. Forced Convection Film Boiling Heat Transfer Heat Transfer 1970. Vol. 5. Elsevier Publ. Co., 1970, paper B4.8.

Papell, S. Stephen, Simon, Frederick F., and Simoneau, Robert J.. Minimum Film-Boiling Heat Flux in Vertical Flow of Liquid Nitrogen. NASA TN D-4307, 1968.

Parker, Jerald D., and Grosh, Richard J.. Heat Transfer to a Mist Flow. Rep. ANL-6291, Argonne National Lab., Jan. 1961.

Patterson, J. F., Grenda, R. J., and Wilson, J. F.. Performance Tests on a Mechanical Steam Dryer. Trans. ANS, vol. 5, no. 2, Nov. 1962, pp. 481-482.

Pennington, R. T.. Nuclear Superheat Project. Rep. GEAP-3785, General Electric Co., Mar 1962.

Ross, Lawrence L.. Forced Convection Evaporation of Droplets in a High Temperature Environment. Ph.D. Thesis, McMaster Univ., 1966.

Ross, L. L.; and Hoffman, T W.. Evaporation of Droplets in a High Temperature Environment. Proceedings of the Third International Heat Transfer Conference. Vol. 5. AIChE, 1966, pp. 50-59.

Ryley, D. J.. The Evaporation of Small Liquid Drops with Special Reference to Water Drops in Steam. J Liverpool Eng. Soc., vol. 7, no. 1, 1961-62, p. 1.

Savery, Clyde W.. Experimental Studies of the Vaporization of Droplets in Heated Air at High Pressures. Ph.D. Thesis, Univ Wisconsin, 1969.

Schoessow, G. J., and Baumeister, K. J.. Velocity Effects on Leidenfrost Boiling of Various Liquids. Heat Transfer 1970. Vol. 5 Elsevier Publ. Co., 1970, paper B3.11

Schoessow, Glen J., and Baumeister, Kenneth J.. Mass Diffusivity Effects on Droplets in Film Boiling. Paper AIChE 2, presented at the 12th National Heat Transfer Conference, Tulsa, Okla., Aug. 15-18, 1971

Short, William L. Some Properties of Sprays Formed by the Disintegration of a Superheated Liquid Jet. Ph.D. Thesis, Univ Michigan, 1963.

Trommelen, A. M., and Crosby, E. J.. Evaporation and Drying of Drops in Superheated Vapors. AIChE J., vol 16, no. 5, Sept. 1970, pp. 857-867

von Glahn, Uwe H.. A Correlation of Film-Boiling Heat-Transfer Coefficients Obtained with Hydrogen, Nitrogen, and Freon 113 in Forced Flow. NASA TN D-2294, 1964.

Wachters, L. H. J., and Westerling, N. A J.. The Heat Transfer from a Hot Wall to Impinging Water Drops in the Spheroidal State. Chem. Eng. Sci., vol. 21, no. 11, Nov 1966, pp. 1047-1056.

Wilson, J F., and Grenda, R. J. Removal of Entrained Moisture From Steam Using Natural Separation and Mechanical Dryers. Rep. ACNP-6105, Allis-Chalmers Mfg. Co., Apr 15, 1961

Wilson, John F., Grenda, Ronald J., and Yant,

Howard W. Separation of Water from Steam in a Boiling-Water Reactor Paper 63-WA-250, ASME, 1963.

ELECTRICALLY OR RADIATIVELY HEATED COILED TUBES OR TUBES WITH INSERTS

Bond, J. A., and Converse, G. L.. Vaporization of High-Temperature Potassium in Forced Convection at Saturation Temperatures from 1800° to 2100° F NASA CR-843, 1967

Carver, J R.. Kakarala, C R., and Slotnik, J S.. Heat Transfer in Coiled Tubes with Two-Phase Flow. Res. Rep. 4438, Babcock and Wilcox Co. (AEC Rep. TID-20983), July 31, 1964.

Crain, Berry, Jr., and Bell, K. J.. Forced Convection Heat Transfer to a Two-Phase Mixture of Water and Steam in a Helical Coil. Paper no. 27, AIChE 13th National Heat Transfer Conference, Denver, Colo., Aug. 6-9, 1972.

Fan, Y N. SNAP 50/SPUR Program Single-Tube Freon Boiling Experiments. Rep. 66-1429, APS 5248-R, AiResearch Mfg Co (AFAPL-TR-67-18), Mar 1967

Fisher, C R., Moskowitz, J H., and Clark, L. T. Alkali Metals Evaluation Program. Swirl Flow Boiling of Alkali Metals Heat Transfer and Pressure Drop Rep AGN-8127, Aerojet-General Nucleonics, Jan. 1965

Jones, J K. Boiling Heat Transfer Enhancement Using Integral Fins Inside Tubes. Paper 700115, SAE, Jan. 1970.

Jones, J K., MacPherson, R E., and Smith, A. M.. Development of Integrally Finned Dryer-Superheater Tubes for Potassium Rankine Cycle Boilers. Rep. ORNL-TM-3383, Oak Ridge National Lab., Apr 1971

Lavin, John G.. Heat Transfer to Refrigerants Boiling Inside Plain Tubes and Tubes with Internal Turbulators. Ph.D Thesis, Univ Michigan, 1964.

Owhadi, Ali: Boiling in Self-Induced Radial Acceleration Fields. Ph.D. Thesis, Oklahoma State Univ., 1966.

Parker, Jerald D., and Grosh, Richard J.. Heat Transfer to a Mist Flow Rep. ANL-6291, Argonne National Lab., Jan 1961

Poppendiek, H F., and Greene, N D.. Report on High Temperature Liquid Metal Heat Transfer

Research at Geoscience Ltd. Proceedings of 1963 High-Temperature Liquid-Metal Heat Transfer Technology Meeting. Rep. ORNL-3605, Vol. 1, Oak Ridge National Lab., Nov 1964, pp. 139-168.

Poppendiek, H F., Greene, N D., MacDonald, F R., Sabin, C. M., Livett, R. K., and Thompson, A. S.. High Acceleration Field Heat Transfer for Auxiliary Space Nuclear Power Systems. Rep. TID-19971, Geoscience, Ltd., 1963.

Sabin, C. M., Poppendiek, H. F., Mouritzen, G., Meckel, P T., and Cloakey, J. E. Liquid Metal Boiling Inception. NASA CR-2095, 1972.

Sekas, Nick J., and Stone, James R.. Experimental Study of Blade-Type Helical Flow Inducers in a 5/8-Inch Electrically Heated Boiler Tube. NASA TM X-2001, 1970.

Vary, Alex X-Ray Observations of Flow Patterns in a Mercury Boiler NASA TN D-5693, 1970.

ELECTRICALLY OR RADIATIVELY HEATED PLAIN, STRAIGHT TUBES

Aladyev, I T., Miropolsky, Z. L., Doroschchuk, V E., and Styrikovich, M A.. Boiling Crisis in Tubes. International Developments in Heat Transfer ASME, 1963, pp. 237-243.

Bergles, Arthur E., and Rohsenow, Warren M.. Forced-Convection Surface-Boiling Heat Transfer and Burnout in Tubes of Small Diameter Rep. 8767-21, Massachusetts Inst Tech., May 25, 1962.

Bijwaard, G., Staub, F W., and Zuber, N A Program of Two-Phase Flow Investigation. Rep. GEAP-4844, General Electric Co., Apr 10, 1965.

Buchberg, H., Romie, F., Lipkis, R., and Greenfield, M. Heat Transfer, Pressure Drop, and Burnout Studies With and Without Surface Boiling for De-Aerated and Gassed Water at Elevated Pressures in a Forced Flow System. 1951 Heat Transfer and Fluid Mechanics Institute. Stanford Univ. Press, 1951, pp. 177-191

Dinos, Nicholas: Pressure Drop for Flow of Boiling Water at High Pressure. Rep. DP-698, E. I DuPont de Nemours and Co., May 1962.

Dormer, Thomas, Jr., and Bergles, Arthur E.. Pressure Drop with Surface Boiling in Small-Diameter Tubes. Rep. 8767-31, Massachusetts Inst. Tech. (AD-461028), Sept. 1, 1964.

Dougall, R S., and Panian, D J.. Subcooled Forced Convection Boiling of R-113 (FREON). Pittsburgh

Univ. (Grant NGR 39-011-079), Aug. 31, 1970.

Fisher, C. R. Heat Transfer and Pressure Drop Characteristics for Boiling Rubidium in Forced Convection Proceedings of 1963 High-Temperature Liquid-Metal Heat Transfer Technology Meeting. Rep. ORNL-3605, Vol. 2, Oak Ridge National Lab., Dec. 1964, pp. 64-81

Fisher, C. R., Clark, L. T., and Moskowitz, J. H. Forced-Convection Boiling of Rubidium and Cesium Heat Transfer and Pressure Drop. Rep. AGN-8099, Aerojet-General Nucleonics, Feb. 28, 1964.

Grace, Thomas M., and Krejsa, Eugene A. Analytical and Experimental Study of Boiler Instabilities Due to Feed-System-Subcooled Region Coupling. NASA TN D-3961, 1967

Guerrieri, S. A., and Talty, R. D. A Study of Heat Transfer of Organic Liquids in Single-Tube, Natural Circulation, Vertical Tube Boilers. Chem. Eng. Progr., vol. 52, no. 18, 1956, pp. 69-77

Hoffman, H. W. Recent Experimental Results in ORNL Studies with Boiling Potassium Proceedings of 1963 High-Temperature Liquid-Metal Heat Transfer Technology Meeting. Rep. ORNL-3605, Vol 1, Oak Ridge National Lab., Nov 1964, pp. 334-348

Hoffman, Herbert W., and Krakoviak, A. I. Convective Boiling With Liquid Potassium. Proceedings of 1964 Heat Transfer and Fluid Mechanics Institute Stanford Univ Press, 1964, pp. 19-37

Hoffman, Herbert W., and Krakoviak, A. I. Studies in Boiling With Liquid Potassium. Proceedings of Second Joint USAEC-EURATOM Two-Phase Flow Meeting. Ronald M. Scroggins, ed., USAEC Rep. CONF-640507, Nov 1964.

Jeglic, Frank A. The Onset of Flow Oscillations in Forced Flow Subcooled Boiling. Ph.D Thesis, Univ. Notre Dame, 1964.

Jeglic, Frank A., and Grace, Thomas M. Onset of Flow Oscillations in Forced-Flow Subcooled Boiling. NASA TN D-2821, 1965

Jeglic, Frank A., Stone, James R., and Gray, Vernon H. Experimental Study of Subcooled Nucleate Boiling of Water Flowing in 1/4-Inch-Diameter Tubes at Low Pressures. NASA TN D-2626, 1965

Jeglic, Frank A., and Yang, Kwang-Tzu The Incipience of Flow Oscillations in Forced-Flow Subcooled Boiling. Proceedings of the 1965 Heat Transfer and Fluid Mechanics Institute Stanford

Univ Press, 1965, pp. 330-344.

Jens, W. H., and Lottes, P. A. Analysis of Heat Transfer, Burnout, Pressure Drop, and Density Data for High-Pressure Water Rep. ANL-4627, Argonne National Lab., May 1, 1951

Jicha, J. J., and Frank, S. An Experimental Local Boiling Heat-Transfer and Pressure-Drop Study of a Round Tube Paper 62-HT-48, ASME, 1962.

Jones, J. H., and Altman, Manfred Two-Phase Flow and Heat Transfer for Boiling Liquid Nitrogen in Horizontal Tubes. Chem. Eng. Progr Symp. Ser., vol 61, no. 57, 1965, pp. 205-212.

Keeys, R. K. F., Ralph, J. C., and Roberts, D. N. Post Burnout Heat Transfer in High Pressure Steam Water Mixtures in a Tube with Cosine Heat Flux Distribution Rep. AERE-R-6411, Atomic Energy Research Establishment, Jan 1971

Kennel, W. E. Local Boiling of Water and Superheating of High Pressure Steam in Annuli. Sc.D. Thesis in Chem. Eng., Massachusetts Inst Tech., 1948

Kreith, Frank, and Summerfield, Martin: Pressure Drop and Convective Heat Transfer With Surface Boiling at High Heat Flux. Proceedings of Heat Transfer and Fluid Mechanics Institute. Stanford Univ Press, 1949, pp. 127 138.

Kreith, Frank J., and Summerfield, Martin J. Heat Transfer to Water at High Flux Densities With and Without Surface Boiling. ASME Trans., vol. 71, no. 7, Oct 1949 pp. 805-815

Kreith, Frank J., and Summerfield, Martin J. Pressure Drop and Convective Heat Transfer With Surface Boiling at High Heat Flux, Data for Aniline and n-Butyl Alcohol. ASME Trans., vol. 72, no. 6, Aug. 1950, pp. 869-879

Kruger, R. A., and Rohsenow, W. M. Film Boiling Inside Horizontal Tubes. Proceedings of the Third International Heat Transfer Conference Vol. 5 AIChE, 1966, pp. 60-68

Lewis, James P., Goodykoontz, Jack H., and Kline, John F. Boiling Heat Transfer to Liquid Hydrogen and Nitrogen in Forced Flow NASA TN D-1314, 1962

Lis, J., and Strickland, J. A. Local Variations of Heat Transfer in a Horizontal Steam Evaporator Tube Heat Transfer 1970. Vol 5 Elsevier Publ. Co., 1970, paper B4.6.

Lowdermilk, Warren H., Lanzo, Chester D., and Siegel, Byron L. Investigation of Boiling Burnout and Flow Stability for Water Flowing in Tubes.

NACA TN 4382, 1958.

McAdams, W H., Addoms, J. N., and Kennel, W E.. Heat Transfer at High Rates to Water With Surface Boiling. Rep. ANL-4268, Argonne National Lab., Dec. 1948

Mendler, O. J., Rathbun, A. S., Van Huff, N E., and Weiss, A.. Natural-Circulation Tests With Water at 800 to 2000 Psia Under Nonboiling, Local Boiling, and Bulk Boiling Conditions. J Heat Transfer, vol. 83, no. 3, Aug. 1961, pp. 261-273.

Miller, M L. Pressure Drop in Forced-Circulation Flow of Subcooled Water With and Without Surface Boiling. S. M. Thesis in Mech. Eng., Massachusetts Inst. Tech., 1954

Noyes, R. C.. Boiling Studies for Sodium Reactor Safety Part I Experimental Apparatus and Results of Initial Tests and Analysis. Rep. NAA-SR-7909, North American Aviation, Inc., Aug. 30, 1963.

Owens, W L., and Schrock, V E. Local Pressure Gradients for Subcooled Boiling of Water in Vertical Tubes. Paper 60-WA-249, ASME, 1960.

Panian, D. J. Subcooled Forced Convection Boiling of R-113 (FREON). M S. Thesis, Univ Pittsburgh, 1970.

Papell, S. Stephen: Subcooled Boiling Heat Transfer Under Forced Convection in a Heated Tube NASA TN D-1583, 1963

Polomik, E. E., Levy, S., and Sawochka, S G. Film Boiling of Steam-Water Mixtures in Annular Flow at 800, 1100, and 1400 Psi. Paper 62-WA-136, ASME, 1962

Reynolds, J B. Local Boiling Pressure Drop. Rep ANL-5178, Argonne National Lab., Mar 1954.

Rohsenow, Warren M.., and Clark, John A. Heat Transfer and Pressure Drop Data for High Flux Densities to Water at High Sub Critical Pressures. 1951 Heat Transfer and Fluid Mechanics Institute Stanford Univ Press, 1951, pp. 193-207

Sabersky, R. H., and Mulligan, H E. On the Relationship Between Fluid Friction and Heat Transfer in Nucleate Boiling. Jet Propulsion, vol 25, no. 1, Jan. 1955 pp. 9-12

Staub, F W., Walmet, G E., and Niemi, R O. Heat Transfer and Hydraulics. The Effects of Subcooled Voids. Rep. NYO-3679-8, General Electric Co., May 1969

Stone, James R. Subcooled and Net-Boiling Heat Transfer to Low-Pressure Water in Electrically Heated Tubes. NASA TN D-6402, 1971

Tang, Y S., Smith, C. R., and Ross, P T.. Potassium-Mercury Amalgam Boiling Heat Transfer, Two-Phase Flow, and Properties Investigation Proceedings of 1963 High-Temperature Liquid-Metal Heat Transfer Technology Meeting. Rep. ORNL-3605, Vol. 2, Oak Ridge National Lab., Dec. 1964, pp. 110-127

Tarasova, N V., Khlopushin, V I., and Boronina, L. V. Local Fluid Friction in the Surface Boiling of Water in Tubes. High Temperature, vol. 5, no. 1, Jan.-Feb. 1967, pp. 111-116.

Thom, J R. S., Walker, W M., Fallon, T A., and Reising, G F S. Boiling in Sub-Cooled Water During Flow up Heated Tubes or Annuli. Proc. Inst. Mech. Eng., vol. 180, pt 3C, 1965-1966, pp. 226-246.

Tramontini, V N, et al. Final Report on Studies in Boiling Heat Transfer Rep. COO-24, Univ California, Mar 1951

Uchida, Hideo, and Yamaguchi, Susumu. Heat Transfer in Two-Phase Flow of Refrigerant 12 Through a Horizontal Tube Proceedings of the Third International Heat Transfer Conference. Vol. 5. AIChE, 1966, pp. 69-79

Weiss, D H. Pressure Drop in Two-Phase Flow Rep. ANL-4916, Argonne National Lab., Oct. 20, 1952.

HEAT-EXCHANGER BOILING

Albers, James A., Gorland, Sol H., and Wintucky, William T. Conditioning and Steady-State Performance of SNAP-8 Tube-in-Shell Mercury Boiler NASA TM X-1441, 1967

Albers, James A., Soeder, Ronald H., and Thollot, Pierre A. Design-Point Performance of a Double-Containment Tantalum-and-Stainless-Steel Mercury Boiler for SNAP-8. NASA TN D-4926, 1968.

Balzhiser, Richard E. Boiling Studies With Potassium. Proceedings of 1963 High-Temperature Liquid-Metal Heat Transfer Technology Meeting. Rep. ORNL-3605. Vol. 1, Oak Ridge National Lab., Nov 1964, pp. 351-369.

Balzhiser, Richard E., Barry, Robert E., Merte, Herman, Jr, Colver, C Phillip, Padilla, Andrew, Jr and Smith, Lowell R. Investigation of Liquid Metal Boiling Heat Transfer Michigan Univ (RTD-TDR-63-4130, AD-429182), Nov 1963

Berenson, P J., and Killackey, J J. An Experimental Investigation of Forced-Convection Vaporization of Potassium Proceedings of 1963 High-Temperature Liquid-Metal Heat Transfer Technology Meeting. Rep. ORNL-3605, Vol. 2. Oak Ridge National Lab., Dec. 1964, pp. 1-18.

Bond, J. A., and Gutstein, M. U.. Components and Overall Performance of an Advanced Rankine Cycle Test Rig. Proceedings of the Intersociety Energy Conversion Engineering Conference. SAE 1971, pp. 464-471

Collins, R. A., Boppart, J. A., and Berenson, P J.. Testing of Liquid-Metal Boilers for Rankine-Cycle Power Systems. Rep. APS-5244-R, AiResearch Mfg. Co. (AFAPL-TR-67-10, vols. I and II), Apr 1967

Davis, Jerry P., and Kikin, Gerald M. Lithium-Boiling Potassium Rankine Cycle Test Loop Operating Experience. Advances in Energy Conversion Engineering. ASME, 1967, pp. 87-95

Davis, J. P., Kikin, G. M., Phillips, W M., and Wolfson, L. S.. Lithium-Boiling Potassium Refractory Metal Loop Facility Rep. JPL-TR-32-508, Jet Propulsion Lab. (NASA CR-51236), Aug. 31, 1963.

Davis, Jerry P., Kikin, Gerald M., Phillips, Wayne M., and Wolfson, Lawrence S. Lithium-Boiling Potassium Refractory Metal Loop Facility Proceedings of 1963 High-Temperature Liquid-Metal Heat Transfer Technology Meeting. Rep. ORNL-3605, Vol. 1, Oak Ridge National Lab., Nov. 1964, pp. 171-193

Dengler, Carl E.. Heat Transfer and Pressure Drop for Evaporation of Water in a Vertical Tube. Ph.D Thesis, Massachusetts Inst. Tech., 1952.

Dengler, C. E., and Addoms, J. N. Heat Transfer Mechanism for Vaporization of Water in a Vertical Tube. Chem. Eng. Progr Symp. Ser., vol. 52, no. 18, 1956, pp. 95-103.

Gertsma, L. W., Thollot, P A., Medwid, D. W., and Sellers, A J. The Double Containment Tantalum-Stainless Steel SNAP-8 Boiler NASA TM X-52452, 1968.

Goodykoontz, Jack H., Stevens, Grady H., and Krejsa, Eugene A. Frequency Response of Forced-Flow Single-Tube Boiler with Inserts. NASA TN D-4189, 1967

Gordon, R., and Slone, H. O. SNAP-8 Development Status - September 1965 AIAA Specialists Conference on Rankine Space Power Systems.

Vol. 1 AEC Rep. CONF-651026, vol. 1, 1965, pp. 103-138.

Gresho, P M., Poucher, F W., and Wimberly, F C. Mercury Rankine Program Test Experience. AIAA Specialists Conference on Rankine Space Power Systems. Vol. 1 AEC Rep. CONF-651026, vol. 1, 1965, pp. 52-102.

Gutstein, Martin U., and Bond, James A. Preliminary Results of Testing a Single-Tube Potassium Boiler for the Advanced Rankine System. NASA TM X-52996, 1971

Israel, S. L., Nolan, D. J., and Malmborg, F B.. Performance Evaluation of Heat Exchangers for Sodium-Cooled Reactors. Rep. UNC-5213, United Nuclear Corp., Apr. 20, 1968.

Karig, H. E., Jackley, D. N., and Hidde, L. G.. Experimental Investigation of a Oncethrough Coaxial Steam Generator J. Spacecraft Rockets, vol. 2, no. 3, May-June 1965, pp. 405-410.

Kikin, Gerald M., Davis, Jerry P., Griffin, Daniel G., Pellgren, Maurice L., and Phillips, Wayne M.. Lithium-Boiling Potassium Test Loop. Rep. JPL-TR-32-1083, Jet Propulsion Lab. (NASA CR-84294), Sept 15, 1966.

Kreeger, A H., Hodgson, J N., and Sellers, A. J.. Development of the SNAP-8 Boiler AIAA Specialists Conference on Rankine Space Power Systems. Vol. 1 AEC Rep. CONF-651026, vol. 1, 1965, pp. 285-306.

Krejsa, Eugene A., Goodykoontz, Jack H., and Stevens, Grady H. Frequency Response of Forced-Flow Single-Tube Boiler NASA TN D-4039, 1967

Lewis, James P., Groesbeck, Donald E., and Christenson, Harold H. Tests of Sodium Boiling in a Single Tube-in-Shell Heat Exchanger Over the Range $1720°$ to $1980°$ F (1211 to 1355 K). NASA TN D-5323, 1969

Lottig, Roy A., and Soeder, Ronald H. Steady-State Performance of a SNAP-8 Double-Containment Tantalum-Stainless Steel Mercury Boiler. NASA TM X-52795, 1970.

McAdams, W H., Woods, W K., and Bryan, R L. Vaporization Inside Horizontal Tubes. ASME Trans., vol. 63, no. 6, Aug. 1941, pp. 545-552.

Peterson, J R. High-Performance "Once-Through" Boiling of Potassium in Single Tubes at Saturation Temperatures From $1500°$ to $1750°$ F NASA CR-842, 1967

Poppendiek, H. F. SNAP-8 Boiler Performance

Degradation and Two-Phase Flow Heat and Momentum Transfer Models. Rep. GLR-84, Geoscience, Ltd. (NASA CR-72759), Aug. 1970.

Soumerai, Henri: Single Component Two-Phase Annular-Dispersed Flow in Horizontal Tubes Without and With Heat Addition From a Constant or Variable Temperature Source. Ph.D. Thesis, Eidgenossische Technische Hochschule, Zurich, Switzerland, 1969

Stevens, Grady H., Goodykoontz, Jack H., and Krejsa, Eugene A. Experimental Evaluation of Four Transfer Functions for a Single Tube Boiler Which Are Dynamically Independent of Exit Restrictions. NASA TM X-2247, 1971

Stevens, Grady H., Krejsa, Eugene A., and Goodykoontz, Jack H. Frequency Response of a Forced-Flow Single-Tube Boiler with Inserts and Exit Restriction. NASA TN D-5023, 1969

Stone, James R., and Damman, Thomas M. An Experimental Investigation of Pressure Drop and Heat Transfer for Water Boiling in a Vertical-Upflow Single-Tube Heat Exchanger NASA TN D-4057, 1967

Stone, James R., and Sekas, Nick J. Tests of a Single Tube-in-Shell Water-Boiling Heat Exchanger with a Helical-Wire Insert and Several Inlet Flow-Stabilizing Devices. NASA TN D-4767, 1968.

Stone, James R., and Sekas, Nick J. Tests of a Single Tube-in-Shell Water Boiler with Helical-Wire Insert, Inlet Nozzle, and Two Different Inlet-Region Plugs NASA TN D-5644, 1970.

Wallerstedt, R. L., and Miller, D. B. Mercury Rankine Program Development Status and Multiple System Application. AIAA Specialists Conference on Rankine Space Power Systems. Vol. 1 AEC Rep. CONF-651026, vol. 1, 1965, pp. 3-51

Woods, W. K. Heat Transfer for Boiling Inside Horizontal Tubes. D.Sc Thesis, Massachusetts Inst Tech., 1940.

INITIATION OF VAPORIZATION

Apfel, Robert E. The Tensile Strength of Liquids. Scientific American, vol. 227, no. 6, Dec. 1972, pp. 58-71

Bergles, A. E., and Rohsenow, W. M. The Determination of Forced-Convection Surface-Boiling Heat Transfer J Heat Transfer,

vol. 86, no. 3, Aug. 1964, pp. 365-372

Blake, F G., Jr. The Tensile Strength of Liquids: A Review of the Literature. Tech. Memo 9, Harvard Univ., Acoustic Res. Lab., June 11, 1949.

Briggs, Lyman J. Limiting Negative Pressure of Water. J Appl. Phys., vol. 21, no. 7, July 1950, pp. 721-722.

Briggs, Lyman J. The Limiting Negative Pressure of Acetic Acid, Benzene, Aniline, Carbon Tetrachloride, and Chloroform. J Chem. Phys., vol. 19, no. 7, July 1951, pp. 970-972.

Davis, E. J., and Anderson, G H. The Incipience of Nucleate Boiling in Forced Convection Flow AIChE J., vol. 12, no. 4, July 1966, pp. 774-780.

Eisenberg, Phillip: On the Mechanism and Prevention of Cavitation. Rep. 712, David W Taylor Model Basin, July 1950.

Gaddis, E. S., and Hall, W B. Forced Convection Boiling from Prepared Nucleation Sites. Heat Transfer 1970. Vol. 5 Elsevier Publ. Co., 1970, paper B4.4

Gavrilenko, T P., and Topchiyan, M E. Dynamic Tensile Strength of Water J Appl. Mech. Tech Phys., vol. 7, no. 4, July-Aug. 1966, pp. 128-129

Hendricks, Robert C., and Sharp, Robert R. Initiation of Cooling Due to Bubble Growth on a Heated Surface. NASA TN D-2290, 1964.

Holtz, Robert E. A Study of Initiation of Nucleate Boiling in the Liquid Metals. Rep. ANL-6980, Argonne National Lab., Dec. 1964.

Holtz, Robert E. Effect of the Pressure-Temperature History Upon Incipient-Boiling Superheats in Liquid Metals. Rep. ANL-7184, Argonne National Lab., June 1966.

Holtz, Robert E., and Singer, Ralph M. Incipient Pool Boiling of Sodium. AIChE J., vol. 14, no. 4, July 1968, pp. 654-656.

Hooper, F C., and Abdelmessih, A H. The Flashing of Liquids at Higher Superheats. Proceedings of the Third International Heat Transfer Conference. Vol. 4 AIChE, 1966, pp. 44-50.

Howell, John R. and Siegel, Robert Activation, Growth, and Detachment of Boiling Bubbles in Water from Artificial Nucleation Sites of Known Geometry and Size. NASA TN D-4101, 1967

Howell, John R., and Siegel, Robert Incipience, Growth, and Detachment of Boiling Bubbles in Saturated Water from Artificial Nucleation Sites of Known Geometry and Size. NASA TM X-52179, 1966.

Hsu, Y. Y. On the Size Range of Active Nucleation Cavities on a Heating Surface. J Heat Transfer, vol. 84, no. 3, Aug. 1962, pp. 207-216.

Jiji, L. M., and Clark, J. A. Incipient Boiling in Forced-Convection Channel Flow Paper 62-WA-141, ASME, 1962.

Kenning, D. B. R., and Thirunavukkarasu, K. Bubble Nucleation Following a Sudden Pressure Reduction in Water Heat Transfer 1970. Vol. 5 Elsevier Publ. Co., 1970, paper B2.9

Krakoviak, A. I. Superheat Requirements with Boiling Liquid Metals. Proceedings of 1963 High-Temperature Liquid-Metal Heat Transfer Technology Meeting. Rep. ORNL-3605, Vol. 1, Oak Ridge National Lab., Nov 1964, pp. 310-322.

Logan, D., Baroczy, C. J., Landoni, J. A., and Morewitz, H. A. Studies of Boiling Initiation for Sodium Flowing in a Heat Channel. Rep. AI-AEC-12767, Atomics International, Sept 30, 1969

Mead, B. R., Romie, F. E., and Guibert, A. G. Liquid Superheat and Boiling Heat Transfer Proceedings of 1951 Heat Transfer and Fluid Mechanics Institute Stanford Univ Press, 1951, pp. 209-216.

Robb, William M., and Cole, Robert A Study of Incipient Vapor Nucleation Within Liquid Filled Conical Cavities. Heat Transfer 1970. Vol. 5 Elsevier Publ. Co., 1970, paper B2.7

Torikai, Kinichi; Shimamune, Hiroji; and Fujishiro, Toshio The Effect of the Dissolved Gas Content Upon Incipient Boiling Superheats. Heat Transfer 1970. Vol. 5 Elsevier Publ. Co., 1970, paper B2.11

Vohr, J H., and Chiang, T A Review of Criteria for Predicting Incipient Nucleation in Liquid Metals and Ordinary Fluids. Rep. MTI-69TR45, Mechanical Technology, Inc., (NASA CR-108896), Nov 1969

LIQUID FILM BREAKDOWN

Bärmann, D., Mayinger, F., and Weiss, E. Burnout Tests for Reactor Safety Studies, 1st Quarterly Report Rep 45 02 01, Maschenenfabrik Augsburg-Nurnberg A.G., Oct 1967

Barnett, P G. The Prediction of Burnout in Non-Uniformly Heated Rod Clusters from Burnout Data for Uniformly Heated Round Tubes. Rep. AEEW-R-362, Atomic Energy Establishment, Nov 1964.

Barnett, P G. A Correlation of Burnout Data for Uniformly Heated Annuli and Its Use for Predicting Burnout in Uniformly Heated Rod Bundles. Rep. AEEW-R-463, Atomic Energy Establishment, Sept 1966.

Becker, Kurt M. An Analytical and Experimental Study of Burnout Conditions in Vertical Round Ducts. Rep. AE-178, Aktiebolaget Atomenergi, Mar 1965

Bennett, A. W., Hewitt, G. F., Kearsey, H. A., and Keeys, R. K. F. Measurements of Burnout Heat Flux in Uniformly Heated Round Tubes at 1000 P.S.I.A. Rep. AERE-R-5055, Atomic Energy Research Establishment, Nov 1965.

Bennett, A. W., Hewitt, G. F., Kearsey, H A., Keeys, R. K. F., and Pulling, D. J. Studies of Burnout in Boiling Heat Transfer to Water in Round Tubes with non-Uniform Heating. Trans. Inst. Chem. Eng., vol. 45, 1967, pp. T319-T333.

Bergles, A. E. Subcooled Burnout in Tubes of Small Diameter Paper 63-WA-182, ASME, 1963.

Bergles, A E., Roos, J P., and Bourne, J G. Investigation of Boiling Flow Regimes and Critical Heat Flux Rep. 724, NYO-3304-10, Dynatech Corp., June 21, 1967

Bertoletti, S., Gaspari, G P, Lombardi, C., Peterlongo, G., Silvestri, M., and Tacconi, F A Heat Transfer Crisis with Steam-Water Mixtures. Energia Nucl., vol 12, no. 3, 1965, p. 121

Biancone, F, Campanile, A., Galimi, G., and Goffi, M Forced Convection Burnout and Hydrodynamic Instability Experiments for Water at High Pressure. Part I Presentation of Data for Round Tubes with Uniform and Non-Uniform Power Distribution. Rep. EUR-2490.e, Sezione Energia Nucleare, Aug 1965

Biasi, L., Clerici, G C., Garriba, S., Sala, R., and Tozzi, A. A New Correlation for Round Duct and Uniform Heating - Comparison with World Data EURAEC 1874, EUR-3376.e, Instituto di Recerche Breda, S P A., Sept 1967

Boure, J A. A Method to Develop Similarity Laws for Two-Phase Flows. Paper 70-HT-25, ASME, 1970.

Brown, Dwight D., Papell, S. Stephen, and Simoneau, Robert J. Buoyancy Effects on Critical Heat Flux of Forced Convective Boiling in Vertical Flow NASA TN D-3672, 1966.

Coffield, Ronald D., Jr., Rohrer, W M., Jr., and Tong, L. S. An Investigation of Departure from

Nucleate Boiling (DNB) in a Crossed-Rod Matrix with Normal Flow of Freon-113 Coolant. Nucl. Eng. Des., vol. 6, no. 2, Sept. 1967, pp. 147-154.

Coffield, R. D., Jr., Rohrer, W M., Jr., and Tong, L. S.. A Subcooled DNB Investigation of Freon-113 and Similarity to Subcooled Water DNB Data. Nucl. Eng. Des., vol. 11, no. 1, Feb. 1970., pp. 143-153.

Dean, Richard A.. Critical Heat Flux of R-113 with Vapor Injection at the Wall. Ph.D. Thesis, Univ Pittsburgh, 1970.

Dean, R. A., Dougall, R S., and Tong, L. S.. Critical Heat Flux in an Annular Test Section With and Without Vapor Injection. Res. Rep. No. 6, Mech. Eng. Department, Univ Pittsburgh, 1970.

Gambill, W R.. Generalized Prediction of Burnout Heat Flux for Flowing, Subcooled, Wetting Liquids. Preprint 17 presented at AIChE/ASME 5th National Heat Transfer Conf., Houston, Texas, Aug. 1962.

Gambill, W R.. Subcooled Swirl-Flow Boiling and Burnout with Electrically Heated Twisted Tapes and Zero Wall Flux. J Heat Transfer, vol. 87, no. 3, Aug. 1965, pp. 342-348.

Grace, Thomas M.. The Mechanism of Burnout in Initially Sub-Cooled Forced Convective Systems. Ph.D. Thesis, Univ Minnesota, 1964.

Henkel, D., Mayinger, F , Schad, O., and Weiss, E.. Research into the Critical Heat Flux (Burnout) in Boiling Water. Rep. 09.02.07, Maschinenfabrik Augsburg-Nurnberg A G., July 15, 1965.

Hewitt, G F.. A Method of Representing Burnout Data in Two-Phase Heat Transfer for Uniformly Heated Round Tubes. Rep. AERE-R-4613, Atomic Energy Research Establishment, Nov 1964.

Hewitt, G. F. Experimental Studies on the Mechanisms of Burnout in Heat Transfer to Steam-Water Mixtures. Heat Transfer 1970. Vol. 6. Elsevier Publ Co., 1970, paper B6.6.

Hewitt, G. F., Kearsey, H. A., and Collier, J. G.. Correlation of Critical Heat Flux for the Vertical Flow of Water in Uniformly Heated Channels. Rep. AERE-R-5590, Atomic Energy Research Establishment, Aug. 1970.

Hewitt, G, F , Kearsey, H A., Lacey, P M C, and Pulling, D. J.. Burnout and Nucleation in Climbing Film Flow Int. J Heat Mass Transfer, vol. 8, no. 5, May 1965, pp. 793-814.

Howell, John R., and Bell, Kenneth J. An Experimental Investigation of the Effect of Pressure Transients on Pool Boiling Burnout. Chem. Eng. Progr Symp. Ser., vol. 59, no. 41, 1963, pp. 88-95.

Howell, John R.; and Siegel, Robert: Critical Heat Flux for Saturated Pool Boiling from Horizontal and Vertical Wires in Reduced Gravity. NASA TN D-3123, 1965.

Hsu, Y Y., Simon, F F., and Lad, J. F.. Destruction of a Thin Liquid Film Flowing Over a Heating Surface. Chem. Eng. Progr. Symp. Ser., vol. 61, no. 57, 1965, pp. 139-152.

Jaikrishnan, K.: Study of the Effect of Pressure on the DNB in a Crossed-Rod Matrix with R-113 Coolant. M.S. Thesis, Univ Pittsburgh, 1970.

Janssen, E.. Multirod Burnout at Low Pressure. Paper 62-HT-26, ASME, 1962

Janssen, E., Levy, S., Kervinen, J A.. Investigations of Burnout in an Internally Heated Annulus Cooled by Water at 600 to 1450 Psia. Paper 63-WA-149, ASME, 1963.

Jones, J K., and Hoffman, H. W.. Critical Heat Flux for Boiling Water in a Rod Bundle as a Prelude to Boiling Potassium. Paper 70-HT-22, ASME, 1970.

Kirby, G. J. Model for Correlating Burnout in Round Tubes. Rep. AEEW-R-511, Atomic Energy Establishment, Sept 1966.

Kirby, G. B., and Westwater, J W. Bubble and Vapor Behavior on a Heated Horizontal Plate During Pool Boiling Near Burnout. Chem. Eng. Progr Symp. Ser., vol. 61, no. 57, 1965, pp. 238-248.

Kleeman, George E., III Critical Heat Flux in Two Phase Flow Ph.D. Thesis, Univ Minnesota, 1966.

Lee, D H.. An Experimental Investigation of Forced Convection Burnout in High Pressure Water Part 3. Long Tubes with Uniform and Non-Uniform Axial Heating. Rep. AEEW-R-355, Atomic Energy Establishment, 1965

Lee, D. H.. Burnout in a Channel with Non-Uniform Circumferential Heat Flux. Rep. AEEW-R-477, Atomic Energy Establishment, Mar 1966.

Mayinger, F., Schad, O., and Weiss, E. Investigations into the Critical Heat Flux in Boiling Water Rep. EUR-3347.e, Maschinenfabrik Augsburg-Nurnberg A. G., Aug. 1967

McPherson, G D.. The Mechanism of Film Dryout in Water-Steam Flow Ph.D. Thesis, Univ. London, England, 1966.

McPherson, G D. Axial Stability of the Dry Patch Formed in Dryout of a Two-Phase Annular Flow

131

Presented at the Canadian Congress of Applied Mechanics, University of Laval, Quebec, P Q., Canada, May 1967

McPherson, G D., and Murgatroyd, W. Film Breakdown and Dry-Out in Two-Phase Annular Flow. Proceedings of the Third International Heat Transfer Conference, Vol. 3, AIChE, 1966, pp. 111-122.

Moeck, E. O. Annular-Dispersed Two-Phase Flow and Critical Heat Flux. Rep. AECL-3656, Atomic Energy of Canada, Ltd., May 1970.

Moeck, E. O., Matzner, B., Casterline, J E., and Yuill, G. K. Critical Heat Fluxes in Internally Heated Annuli of Large Diameter Cooled by Boiling Water at 1000 Psia. Proceedings of the Third International Heat Transfer Conference, Vol. 3, AIChE, 1966, pp. 86-97

Newstadt, M L. Empirical Correlation for Subcooled DNB in a Cross Rod Matrix Flow with an Emphasis on Cooling Fluid Properties. M.S. Thesis, Univ Pittsburgh, 1968.

Pasint, D., and Pai, R. H. Empirical Correlation of Factors Influencing Departure from Nucleate Boiling in Steam-Water Mixtures Flowing in Vertical Round Tubes. Paper 65-WA/HT-24, ASME, 1965

Pickering, A., Shires, G. C., and Rounthwaite, C. Two-Phase Heat Transfer and Dry Out in a Thin Annular Channel. Proceedings of the Third International Heat Transfer Conference, Vol. 3, AIChE, 1966, pp. 98-110.

Ponter, A B., Davies, G. A., Ross, T K., and Thornley, P G. The Influence of Mass Transfer on Liquid Film Breakdown. Int J Heat Mass Transfer, vol. 10, no. 3, Mar 1967, pp. 349-359

Previti, G., and DeBernardi, M. An Investigation of Some Parameters Influencing Non-Uniform Heat Flux DNB Prediction. Rep. EUR-3114.e, Fiat S.P.A., Aug. 1966.

Sato, T , Hayashida, Y , and Motoda, T. The Effect of Flow Fluctuation on Critical Heat Flux. Proceedings of the Third International Heat Transfer Conference, Vol. 4, AIChE, 1966, pp. 226-233.

Shelef, Ginton. The Interplay of Surface Tension, Inertial and Gravitational Forces in the Nucleate Boiling "Burnout" Heat Flux. Ph.D. Thesis, Univ California, Berkeley, 1969

Skaug, J A. Down-Flow Burnout at a Uniformly Heated 20-mm Round Duct. Paper presented at European Two-Phase Flow Group Meeting, Karlshruhe, June 1969.

Smith, O Glenn; Tong, L. S., and Rohrer, W M., Jr. Burnout in Steam-Water Flows with Axially Nonuniform Heat Flux. Paper 65-WA/HT-33, ASME, 1965.

Staub, F W. Two-Phase Fluid Modeling – The Critical Heat Flux. Nucl. Sci. Eng., vol 35, no. 2, Feb. 1969, pp. 190-199

Stevens, G F , Elliott, D. G., and Wood, R. W. An Experimental Comparison Between Forced Convection Burn-Out in Freon 12 Flowing Vertically Upwards Through Uniformly and Non Uniformly Heated Round Tubes. Rep. AEEW-R-426, Atomic Energy Establishment, May 1965

Stevens, G. F., and Kirby, G J . A Quantitative Comparison Between Burn-Out Data for Water at 1000 lb/sq. in and Freon-12 at 155 lb/sq. in. (abs) Uniformly Heated Round Tubes, Vertical Up Flow Rep. AEEW-R-327, United Kingdom Atomic Energy Authority, 1964.

Stevens, G F , and Macbeth, R. V. The Use of Freon 12 to Model Forced Convection Burnout in Water· The Restriction on the Size of the Model. Paper 70-HT-20, ASME, 1970.

Stevens, G. F , Wood, R. W , and Pryzbylski, J. An Investigation into the Effects of the Cosine Heat Flux Distribution on Burnout in a 12 Ft. Long Annulus Using Freon-12 Rep. AEEW-R-609, Atomic Energy Establishment, Sept. 1968.

Thompson, B., and Macbeth, R. V Boiling Water Heat Transfer Burnout in Uniformly Heated Round Tubes: A Compilation of World Data with Accurate Correlations. Rep. AEEW-R-356, Atomic Energy Establishment, July 1964

Thompson, T S., and Murgatroyd, W Stability and Breakdown of Liquid Films in Steam Flow with Heat Transfer Heat Transfer 1970. Vol. 5 Elsevier Publ. Co., 1970, paper B5.2

Thorgerson, Eric J. Hydrodynamic Aspects of the Critical Heat Flux in Subcooled Convection Boiling. Ph.D. Thesis, Univ. of South Carolina, 1969

Todreas, N E., and Rohsenow, W M. The Effect of Axial Heat Flux Distribution on Critical Heat Flux in Annular, Two-Phase Flow Proceedings of the Third International Heat Transfer Conference, Vol. 3. AIChE, 1966, pp. 78-85

von Glahn, Uwe H. An Empirical Correlation of

Critical Boiling Heat Flux in Forced Flow Upward Through Uniformly Heated Tubes. NASA TN D-1285, 1962.

von Glahn, Uwe H. On the Empirical Correlation of Critical Boiling Heat Flux for Channels of Various Cross Sections and Orientations. NASA TN D-1656, 1963.

NOVEL GEOMETRIES

Gray, Vernon H. The Rotating Heat Pipe – A Wickless, Hollow Shaft for Transferring High Heat Fluxes. Paper 69-HT-19, ASME, Aug. 1969

Gray, Vernon H., Marto, Paul J., and Joslyn, Allan W. Boiling Heat-Transfer Coefficients, Interface Behavior, and Vapor Quality in Rotating Boiler Operating to 475 G's. NASA TN D-4136, 1968.

Homsy, George M. Centrifugally Driven Thermal Convection and Gravitational Instabilities in Bounded Rotating Fluids. Ph.D. Thesis, Univ. Illinois, 1969

Kikin, Gerald M., Peelgren, Maurice L., Phillips, Wayne M., and Davis, Jerry P. Shell Side Liquid Metal Boiler U.S. Patent 3,630,276, Dec. 28, 1971

Lawler, Martin T., and Ostrach, Simon: A Study of Cyclonic Two-Fluid Separation Rep FTAR-TR-65-2, Case Inst Tech (AFOSR-65-1523, AD-621524), June 1965

Marto, P J., Daley, T J., and Ballback, L. J. An Analytical and Experimental Investigation of Rotating, Non-Capillary Heat Pipes. Rep. NPS-59MX70061A, Naval Postgraduate School (NASA CR-109894), June 30, 1970.

Marto, Paul J., and Gray, Vernon H. Effects of High Accelerations and Heat Fluxes on Nucleate Boiling of Water in an Axisymmetric Rotating Boiler NASA TN D-6307, 1971

OTHER ELECTRICALLY OR RADIATIVELY HEATED CHANNEL GEOMETRIES

Bernath, Louis, and Begell, William Forced-Convection, Local-Boiling Heat Transfer in Narrow Annuli, Chem. Eng. Progr Symp. Ser., vol. 55, no. 29, 1959, pp. 59-65.

Bondurant, David L. Performance of Transverse Fins for Boiling Heat Transfer Ph.D. Thesis, Univ Illinois, 1970.

Bondurant, D. L., and Westwater, J W. Performance of Transverse Fins for Boiling Heat Transfer Chem. Eng. Progr Symp. Ser., vol. 67, no. 113, 1971, pp. 30-37

Bonilla, Charles F., Weiner, Mark M., Bilfinger, Hans: Pool Boiling of Potassium. Proceedings of 1963 High-Temperature Liquid-Metal Heat Transfer Technology Meeting. Rep. ORNL-3605, Vol. 1, Oak Ridge National Lab., Nov. 1964, pp. 286-307

Cobb, Calvin B. A Study of Surface and Geometric Effects on the Nucleate Boiling of Liquid Nitrogen and Liquid Argon from Atmospheric to the Critical Pressure. Ph.D. Thesis, Univ Missouri at Rolla, 1967

Hench, J E. Transition and Film Boiling Data at 600, 1000, 1400 Psia in Forced Circulation Heat Transfer to Water Rep. GEAP-4492, General Electric Co., Feb. 1964.

Hosler, E. R. Flow Patterns in High Pressure Two-Phase (Steam-Water) Flow with Heat Addition. Rep. WAPD-TM-658, Bettis Atomic Power Lab., June 1967

Hsu, Y Y. Analysis of Boiling on a Fin. NASA TN D-4797, 1968

Janssen, E. Two-Phase Flow Structure in a Nine-Rod Channel, Steam-Water at 1000 Psia Rep. GEAP-5480, General Electric Co., June 1967

Klein, George J. Heat Transfer from Multiple Fins to Boiling Liquids. Ph.D. Thesis, Univ Illinois, 1970.

Klein, G. J., Westwater, J W. Heat Transfer from Multiple Spines to Boiling Liquids. AIChE J., vol. 17, no. 5, Sept 1971, pp. 1050-1056.

Lahey, R. T., Jr., Shiralkar, B. S., and Radcliffe, D W. Two-Phase Flow and Heat Transfer in Multirod Geometries Subchannel and Pressure Drop Measurements in a Nine-Rod Bundle for Diabatic and Adiabatic Conditions. Rep. GEAP-13049, General Electric Co., Mar 1970.

Lai, Fang-Shyong; and Hsu, Yih-Yun: Temperature Distribution in a Fin Partially Cooled by Nucleate Boiling, AIChE J., vol 13, no. 4, July 1967, pp. 817-821

Lapin, Abraham: Heat Transfer Characteristics of Boiling Neon and Nitrogen in Narrow Annuli. Ph.D. Thesis, Lehigh Univ., 1963.

Marto, P J., and Rohsenow, W M. The Effect of Surface Conditions on Pool Boiling Heat Transfer of Sodium. Proceedings of 1963 High-Temperature Liquid-Metal Heat Transfer Technology Meeting.

Rep. ORNL-3605, Vol. 1, Oak Ridge National Lab., Nov. 1964, pp. 263-280.

McKee, Hugh R. Forced Convection Boiling from a Cylinder Normal to the Flow. Ph.D. Thesis, Oklahoma State Univ., 1967

Montgomery, Robert T. A Study of the Effect of Tube Bundle Geometry on the Nucleate Boiling Region of a Series of Hydrocarbon Liquids. Ph.D. Thesis, Univ. Missouri at Rolla, 1969

Murphy, Carl D. Forced Convection Film Boiling on a Horizontal Surface. Ph.D. Thesis, Carnegie-Mellon Univ., 1969

Noyes, R. C. Summary of Recent Results of Sodium Boiling Studies. Proceedings of 1963 High-Temperature Liquid-Metal Heat Transfer Technology Meeting. Rep. ORNL-3605, Vol. 2, Oak Ridge National Lab., Dec. 1964, pp. 24-44.

Noyes, R. C., and Lurie, H. Boiling Sodium Heat Transfer. Proceedings of the Third International Heat Transfer Conference. Vol. 5 AIChE, 1966, pp. 92-100.

Osmachkin, V. S., and Borisov, V. D. Pressure Drop and Heat Transfer for Flow of Boiling Water in Vertical Rod Bundles. Heat Transfer 1970. Vol. 5. Elsevier Publ. Co., 1970, paper B4.9

Padilla, Andrew, Jr. Film Boiling of Potassium on a Horizontal Plate. Ph.D. Thesis, Univ. Michigan, 1966.

Richards, Everett L. Transient Film Boiling in a Horizontal Annulus Filled With a Saturated Liquid. Ph.D. Thesis, Georgia Inst. Tech, 1969

Sher, N. C., and Green, S. J. Boiling Pressure Drop in Thin Rectangular Channels. Rep. WAPD-T-477, Westinghouse Electric Corp., 1958

Simon, Frederick F., and Simoneau, Robert J. A Visual Study of Velocity and Buoyancy Effects on Boiling Nitrogen. NASA TN D-3354, 1966.

Sowards, Jack W. Point Values for Boiling Heat Transfer for Liquid Nitrogen in a Vertical Cylinder. Ph.D. Thesis, Colorado School of Mines, 1966.

STABILITY

Berenson, P. J. An Experimental Investigation of Flow Stability in Multitube Forced-Convection Vaporizers. Paper 65-HT-61, ASME, 1965

Boure, J A., Bergles, A E., and Tong, L. S. Review of Two-Phase Flow Instability. Paper 71-HT-42, ASME, 1971

Chi, J. W. H., and Vetere, A. M. Two-Phase Flow During Transient Boiling of Hydrogen and Determination of Non-Equilibrium Vapor Fractions. Rep. WANL-SP-002, Westinghouse Electric Corp., June 1963.

Cho, S. M., Auge, L. J., Fenton, R. E., and Gardner, K. A. Performance Changes of a Sodium-Heated Steam Generator. Paper 71-HT-15, ASME, 1971.

Collins, D. B., Gacesa, M., and Parsons, C. B. Study of the Onset of Premature Heat-Transfer Crisis During Hydrodynamic Instability in a Full-Scale Reactor Channel. Paper 71-HT-11, ASME, 1971

Dijkman, Fred. Stability Aspects of a Boiling Channel with a Sine-Shaped Heatflux. Heat Transfer 1970. Vol. 5 Elsevier Publ. Co., 1970, paper B4.3.

Dorsch, Robert G. Frequency Response of a Forced-Flow Single-Tube Boiler. NASA TM X-60523, 1967

Fraas, A. P. Flow Stability in Heat Transfer Matrices Under Boiling Conditions. Rep. CF-59-11-1, Oak Ridge National Lab., 1959

Friedly, J C., and Krishnan, V S. Prediction of Nonlinear Flow Oscillations in Boiling Channels. Presented at the 12th National Heat Transfer Conference, Tulsa, Okla., Aug. 15-18, 1971

Graham, Robert W. Experimental Observations of Transient Boiling of Subcooled Water and Alcohol on a Horizontal Surface. NASA TN D-2507, 1965

Harden, Darrel G. Transient Behavior of a Natural-Circulation Loop Operating Near the Thermodynamic Critical Point. Rep. ANL-6710, Argonne National Lab., May 1963.

Hooper, J. R. Steady-State and Dynamic Operating Characteristics of Simulated Three-Loop Space Rankine Cycle Powerplant. NASA CR-625, 1966.

Hsu, Y Y., and Watts, R. G. Behavior of a Vapor Bubble in a Pulsating Pressure Field. Heat Transfer 1970. Vol. 5 Elsevier Publ. Co., 1970, paper B2.4.

Ishii, Mamoru, and Zuber, Novak. Thermally Induced Flow Instabilities in Two Phase Mixtures. Heat Transfer 1970. Vol. 5 Elsevier Publ. Co., 1970, paper B5 11

Jarvis, Stephen, Jr. Stability of Two-Phase Annular Flow in a Vertical Pipe. Tech. Note 314, National Bureau of Standards, June 7, 1965.

Johnson, H A. Transient Boiling Heat Transfer. Heat Transfer 1970. Vol. 5 Elsevier Publ. Co., 1970, paper B3.1

Kawamura, Hiroshi, Tachibana, Fujio, and Akiyama, Mamoru: Heat Transfer and DNB Heat Flux in

Transient Boiling. Heat Transfer 1970. Vol. 5. Elsevier Publ. Co., 1970, paper B3.3.

Krejsa,EugeneA.. Model for Frequency Response of a Forced Flow, Hollow, Single Tube Boiler NASA TM X-1528, 1968.

Levy, S., and Beckjord, E. S.. Hydraulic Instability in a Natural Circulation Loop with Net Steam Generation at 1000 Psia. Rep. GEAP-3215, General Electric Co., July 15, 1959.

Maulbetsch, John S., and Griffith, Peter A Study of System-Induced Instabilities in Forced-Convection Flows with Subcooled Boiling. Rep. TR-5382-35, Massachusetts Inst. Tech., (AD-619512), Apr 15, 1965.

Maulbetsch, J S , and Griffith, Peter System-Induced Instabilities in Forced Convection Flows with Subcooled Boiling. Proceedings of the Third International Heat Transfer Conference. Vol. 4. AIChE, 1966, pp. 247-257

Morin, R.. Wall-Temperature Fluctuations During Boiling in a Heating Tube. Chem. -Ing. Tech., vol. 38, no. 1, 1966, pp. 73-76.

Pan, C. H T., and Vohr, J H. Dynamical Analysis of Non-Equilibrium Forced Convective Boiling Flows. Rep MTI-70QTR16, Mechanical Technology, Inc. (NASA CR-117034), Dec. 1970.

Papell, S. Stephen. An Instability Effect on Two-Phase Heat Transfer for Subcooled Water Flowing Under Conditions of Zero Gravity NASA TN D-2259, 1964.

Poppendiek, H. F , Sabin, C M., Feigenbutz, L. V., Morton, W A., and Connely, D A. Dynamic Analysis of a Lithium-Boiling Potassium Refractory Metal Rankine Cycle Power System for the Jet Propulsion Laboratory Rep. GLR-39, Geoscience, Ltd. (NASA CR-70371), Nov 1965.

Redfield, J A., and Murphy, J H. Sectionalized Compressible and Momentum Integral Models for Channel Hydrodynamics. Paper 71-HT-14, ASME, 1971

Schoenberg, Andrew A., and Packe, Donald R. Analysis of Pressure-Drop Function in Rankine Space Power Boilers with Discussion of Flow Maldistribution Implications. NASA TN D-4498, 1968

Schuster, J R., and Berenson, P J. Flow Stability of a Five-Tube Forced-Convection Boiler Paper 67-WA/HT-20, ASME, 1967

Siegel, R., and Usiskin, C M.. A Photographic Study of Boiling in the Absence of Gravity NASA TM

X-56246, 1959.

Styrikivich, M. A., and Nevistrueva, E. I.. An Approximate Estimation of Circulation and Temperature Characteristics of Two-Phase Pulsation Flows with Surface Boiling. Proceedings of the Third International Heat Transfer Conference. Vol. 4. AIChE, 1966, pp. 207-215.

Veziroglu, T Nejat, and Lee, Samuel S.. Boiling-Flow Instabilities in a Cross-Connected Parallel-Channel Upflow System. Paper 71-HT-12, ASME, 1971.

Vild, Thomas J., and Sill, Donald E.. Stability of Parallel-Path Two-Phase Flow Proceedings of 1963 High-Temperature Liquid-Metal Heat Transfer Technology Meeting. Rep. ORNL-3605, vol. 2, Oak Ridge National Lab., Dec. 1964, pp. 293-313.

Westendorf, William H., and Brown, William F.. Stability of Intermixing of High-Velocity Vapor with Its Subcooled Liquid in Cocurrent Streams. NASA TN D-3553, 1966.

Westendorf, William H. A Model for Predicting the Onset of Oscillatory Instability Occurring with the Intermixing of High-Velocity Vapor with Its Subcooled Liquid in Cocurrent Streams. Heat Transfer 1970. Vol. 5 Elsevier Publ. Co., 1970, paper B5.4.

Yadigaroglu, G., and Bergles, A. E. Fundamental and Higher-Mode Density-Wave Oscillations in Two-Phase Flow The Importance of the Single-Phase Region. Paper 71-HT-13, ASME, 1971

Zuber, Novak Flow Excursions and Oscillations in Boiling, Two-Phase Flow Systems with Heat Addition. Symposium on Two-Phase Flow Dynamics. Vol. 1 EURATOM, Eindhoven, The Netherlands, 1967, p. 1071

VOID FRACTION

Anderson, Robert J. Interchange in Horizontal Annular Two-Phase Flow Ph.D. Thesis, Univ. Delaware, 1968.

Anderson, Robert J., and Russell, T W Fraser Circumferential Variation of Interchange in Horizontal Annular Two-Phase Flow Ind Eng. Chem. Fundamentals, vol. 9, no. 3, Aug. 1970, pp. 340-344.

Anderson, G H., and Minns, D E.. Nucleate Boiling in a Flowing Liquid Heat Transfer 1970. Vol. 5 Elsevier Publ. Co., 1970, paper B4.1

Asch, Victor The Effects of Uniform Electrostatic Fields on Bubble Behavior in Boiling "Freon-113." Ph.D Thesis, Lehigh Univ., 1968

Baroczy, C J. Comparison of Two-Phase Liquid Fraction Data for Potassium with Other Fluids. AIChE J., vol. 12, no. 5, Sept 1966, pp. 1028-1029

Bonnecaze, R H., Greskovich, E. J., and Erskine, W., Jr. Holdup and Pressure Drop for Two-Phase Slug Flow in Inclined Pipelines. AIChE J., vol. 17, no. 5, 1971, pp. 1109-1113.

Bowring, R. W. Physical Model, Based on Bubble Detachment, and Calculation of Steam Voidage in the Subcooled Region of a Heated Channel. Rep. HPR-10, Institutt for Atomenergi, Halden, Norway, Dec. 1962.

Brown, Francis C. A Model for the Prediction of Velocity and Void Fraction Profiles in Two-Phase Flow Ph.D. Thesis, Worcester Polytechnic Inst., 1966

Brown, F C., and Kranich, W L. A Model for the Prediction of Velocity and Void Fraction Profiles in Two-Phase Flow AIChE J., vol. 14, no. 5, Sept. 1968, pp. 750-758

Cimorelli, L., and Evangelisti, R. The Application of the Capacitance Method for Void Fraction Measurement in Bulk Boiling Conditions. Int J Heat Mass Transfer, vol. 10, no. 3, Mar 1967, pp. 277-288.

Cimorelli, L., and Evangelisti, R. Experimental Determination of the "Slip Ratio" in a Vertical Boiling Channel, Under Adiabatic Conditions at Atmospheric Pressure Int J Heat Mass Transfer, vol. 12, no. 6, June 1969, pp. 713-726.

Dorresteijn, W R. Experimental Study of Heat Transfer in Upward and Downward Two-Phase Flow of Air and Oil Through 70-mm Tubes. Heat Transfer 1970. Vol. 5 Elsevier Publ. Co., 1970, paper B5.9

Evangelisti, Roberto, and Lupoli, Paolo The Void Fraction in an Annular Channel at Atmospheric Pressure. Int J Heat Mass Transfer, vol. 12, no. 6, June 1969, pp. 699-711

Ford, William D. Bubble Growth and Collapse in Narrow Tubes with Nonuniform Initial Temperature Profiles. Rep. ANL-7746, Argonne National Lab., Dec. 1970.

Golan, L. P. On Void Fractions for Vertical Downward Flow Paper 22d presented at AIChE 67th National Meeting and Biennial Materials Sciences and Engineering Division Conf., Feb. 1970.

Gomezplata, A., and Brown, R. W. Axial Dispersion Coefficient Measurement in Two-Phase Flow AIChE J., vol. 14, no. 4, July 1968, pp. 657-658.

Griffith, P. The Prediction of Low-Quality Boiling Voids. Paper 63-HT-20, ASME, 1963.

Griffith, P., Clark, J A., and Rohsenow, W M. Void Volumes in Subcooled Boiling Systems. Paper 58-HT-19, ASME, 1958.

Hewitt, G. F. Analysis of Annular Two-Phase Flow Application of Dukler Analysis to Vertical Upward Flow in a Tube. Rep. AERE-R-3680, Atomic Energy Research Establishment, Jan. 1961

Hewitt, G. F., and Hall Taylor, N. S. Annular Two-Phase Flow Pergamon Press, 1970, ch. 6.

Hughmark, G. A. Holdup in Vertical Upward Slug Flow AIChE J., vol. 12, no. 5, Sept 1966, pp. 1023-1024.

Isbin, H. S., Sher, Neil C., and Eddy, K. C. Void Fractions in Two-Phase Steam-Water Flow AIChE J., vol. 3, no. 1, Mar 1957, pp. 136-142.

Kroeger, P G., and Zuber, N. An Analysis of the Effects of Various Parameters on the Average Void Fraction in Subcooled Boiling. Int J Heat Mass Transfer, vol. 11, no. 2, Feb. 1968, pp. 211-233.

Larsen, P S., and Tong, L. S. Void Fractions in Subcooled Flow Boiling. Paper 69-HT-5, ASME, 1969

Levy, S. Steam Slip-Theoretical Prediction from Momentum Model. J Heat Transfer, vol. 82, no. 2, May 1960, pp. 113-124.

Levy, S. Forced Convection Subcooled Boiling - Prediction of Vapor Volumetric Fraction. Int J Heat Mass Transfer, vol. 10, no. 7, July 1967, pp. 951-965

Madhaven, Srinivasa An Experimental and Mathematical Study of the Shapes of Bubbles Growing on Surfaces in an Isothermal Superheated Liquid Ph.D. Thesis, Univ Kansas, 1969

Marchaterre, J F. The Effect of Pressure on Boiling Density in Multiple Rectangular Channels. Rep. ANL-5522, Argonne National Lab., Feb. 1956.

McManus, H N., Jr. Film Characteristics and Dimensions in Annular Two-Phase Flow Int Rep. No. 2, Cornell Univ., Dec. 1959.

Miropol'skiy, Z. L., Shneyerova, R. I., and Karamysheva, A. I. Vapor Void Fraction in Steam-Fluid Mixtures Flowing in Heated and Unheated Channels. Heat Transfer 1970. Vol. 5

Elsevier Publ. Co., 1970, paper B4.7

Petrik, Michael, and Kudirka, A. A.. On the Relationship Between the Phase Distributions and Relative Velocities in Two-Phase Flow Proceedings of the Third International Heat Transfer Conference. Vol. 4. AIChE, 1966, pp. 184-192.

Rouhani, S. Z.. Void Measurements in the Region of Sub-Cooled and Low-Quality Boiling. Symposium on Two-Phase Flow Vol. 2, Exeter, June 1965, pp. E501-E526.

Rouhani, S. Z.. Void Measurements in Regions of Sub-Cooled and Low-Quality Boiling. Part I Low Mass Velocities. Rep. AE-238, Aktiebolaget Atomenergi, Stockholm, Sweden, July 1966.

Rouhani, S. Z., and Axelsson, E.. Calculation of Void Volume Fraction in the Subcooled and Quality Boiling Regions. Int. J Heat Mass Transfer, vol 13, no. 2, Feb. 1970, pp. 383-393.

Russell, T W F., and Lamb, D. E. Flow Mechanism of Two-Phase Annular Flow Can. J Chem. Eng., vol. 43, no. 5, Oct. 1965, pp. 237-245

Schrage, Dale L.. Isothermal Bubble Motion Under the Influence of Varying Body Forces. Ph.D. Thesis, Univ Arizona, 1970.

Shekriladze, I. G.. Mechanism of Steam Bubble Formation. NASA TM X-59398, 1967

Singh, Kuldip; St Pierre, C C., Crago, W A., and Moeck, E. O.. Liquid Film Flow-Rates in Two-Phase Flow of Steam and Water at 1000 Lb./Sq. In. Abs. AIChE J., vol. 15, no. 1, Jan. 1969, pp. 51-56.

Staub, F W.. Prediction of the Void Fraction in Subcooled Boiling, Annular Flow, and Ideal Bubbly Flow Rep. GEAP-5414, General Electric Co., Jan. 1967

Staub, F W.. The Void Fraction in Subcooled Boiling – Prediction of the Initial Point of Net Vapor Generation. J Heat Transfer, vol. 90, no. 1, Feb. 1968, pp. 151-157

Staub, F W., and Walmet, G. E.. The Void Fraction and Pressure Drop in Subcooled Flow Boiling. Heat Transfer 1970. Vol. 5 Elsevier Publ. Co.,

1970, paper B4.11

Styushin, N. G., and Dvorina, G. M.. Slip Effect and Flow Friction in an Adiabatic Vapour-Liquid Mixture Flowing in Tubes. Int J. Heat Mass Transfer, vol. 9, no. 11, Nov 1966, pp. 1227-1232

Vance, William H.. A Study of Slip Ratios for the Flow of Steam-Water Mixtures at High Void Fractions. Ph.D Thesis, Univ Washington, 1962

Wallis, G B., Steen, D A.. and Turner, J M. Two-Phase Flow and Boiling Heat Transfer Rep. NYO-3114/3, Dartmouth Coll., June 1964

Wichner, Robert P., and Hoffman, H. W. Vapor-Bubble-Growth Rates in Superheated Liquid Metals. Rep. ORNL-TM-1413, Oak Ridge National Lab., July 1966.

Yates, Robert A.. The Motion of Spherical-Cap Bubbles in Superheated Liquids. Ph.D. Thesis, Univ Delaware, 1966.

Zakharova, E. A., Kolchugin, B. A., Korniukhin, I P., Labuntsov, D A., and Lobachiov, A G. Vapor Void Fraction in Annular Channels at Separated and Joint Heat Supplied. Heat Transfer 1970. Vol. 5 Elsevier Publ. Co., 1970, paper B5.5

Zuber, N., and Findlay, J A The Effects of Non-Uniform Flow and Concentration Distributions and the Effect of the Local Relative Velocity on the Average Volumetric Concentration in Two-Phase Flow Rep. GEAP-4595, General Electric Co., Apr 1964.

Zuber, N., and Findlay, J A. Average Volumetric Concentration in Two-Phase Flow Systems. J Heat Transfer, vol. 86, no. 4, Nov 1965. pp 453-468.

Zuber, N., Staub, F W., and Bijwaard, G. Vapor Void Fraction in Subcooled Boiling and in Saturated Boiling Systems. Proceedings of the Third International Heat Transfer Conference. Vol. 5 AIChE, 1966, pp. 24-38

Zuber, N., Staub, F W, Bijwaard, G., and Kroeger, P G. Steady State and Transient Void Fraction in Two-Phase Flow Systems. Rep GEAP-5417 General Electric Co., Jan. 1967

"The aeronautical and space activities of the United States shall be conducted so as to contribute   to the expansion of human knowledge of phenomena in the atmosphere and space. The Administration shall provide for the widest practicable and appropriate dissemination of information concerning its activities and the results thereof"

—NATIONAL AERONAUTICS AND SPACE ACT OF 1958

NASA SCIENTIFIC AND TECHNICAL PUBLICATIONS

TECHNICAL REPORTS Scientific and technical information considered important, complete, and a lasting contribution to existing knowledge.

TECHNICAL NOTES Information less broad in scope but nevertheless of importance as a contribution to existing knowledge.

TECHNICAL MEMORANDUMS Information receiving limited distribution because of preliminary data, security classification, or other reasons. Also includes conference proceedings with either limited or unlimited distribution.

CONTRACTOR REPORTS Scientific and technical information generated under a NASA contract or grant and considered an important contribution to existing knowledge.

TECHNICAL TRANSLATIONS Information published in a foreign language considered to merit NASA distribution in English.

SPECIAL PUBLICATIONS Information derived from or of value to NASA activities. Publications include final reports of major projects, monographs, data compilations, handbooks, sourcebooks, and special bibliographies.

TECHNOLOGY UTILIZATION PUBLICATIONS Information on technology used by NASA that may be of particular interest in commercial and other non-aerospace applications. Publications include Tech Briefs, Technology Utilization Reports and Technology Surveys.

Details on the availability of these publications may be obtained from:

SCIENTIFIC AND TECHNICAL INFORMATION OFFICE

NATIONAL AERONAUTICS AND SPACE ADMINISTRATION
Washington, D.C. 20546